UNIVERSIDADE DE BRASÍLIA
FACULDADE DE MEDICINA
PROGRAMA DE PÓS-GRADUAÇÃO EM
PATOLOGIA MOLECULAR

TESE DE DOUTORADO

ANÁLISE PROTEÔMICA E FOSFOPROTEÔMICA DURANTE TRANSIÇÃO DIMÓRFICA EM *Paracoccidioides brasiliensis* .

CANDIDATA: DANIELLE SILVA ARAÚJO
ORIENTADORA: CÉLIA MARIA DE ALMEIDA SOARES

Universidade de Brasília – UNB

Faculdade de Medicina – FM

Pós-Graduação em Patologia Molecular

ANÁLISE PROTEÔMICA E FOSFOPROTEÔMICA DURANTE TRANSIÇÃO DIMÓRFICA EM *Paracoccidioides brasiliensis*

Tese apresentada ao programa de Pós-graduação em Patologia Molecular da Universidade de Brasília como requisito para obtenção do Título de doutor em Patologia Molecular.

Orientadora: Profa. Dra. Célia Maria de Almeida Soares

Brasília, DF

Julho de 2018

Banca examinadora

Titulares:

Dra. Célia Maria de Almeida Soares- Presidente da banca
Instituto de Ciências Biológicas-UFG

Dr. Carlos André Ornelas Ricart
Universidade de Brasília-UnB

Dr. Juliano Domiraci Paccez
Instituto de Ciências Biológicas-UFG

Dr. Clayton Luiz Borges
Instituto de Ciências Biológicas-UFG

Suplente: Dra. Patrícia de Souza Lima
Universidade Estadual de Goiás-UFG

Data: 23/07/2018

AGRADECIMENTOS

À Deus, porque tem sido tudo em minha vida. Por todas as bênçãos concedidas, por todos os milagres realizados. Por iluminar o meu caminho. Por sempre estar comigo, me ajudando a subir cada degrau da vida. Por ser minha inspiração ao prosseguir.

Aos meus pais, Ivani e Joaquim, a vocês que me fizeram acreditar na realização dos meus sonhos e trabalharam muito para que eu pudesse realizá-los.

A minha irmã, Helen, pelo apoio, amizade e companheirismo. Por sempre me ajudar quando eu mais preciso.

Reconheço que sem o apoio e investimento afetivo da família que tanto amo, em especial da tia Nilda, não teria chegado até aqui.

À Profa. Dra. Célia Maria de Almeida Soares, pela orientação, paciência e confiança. Admiro sua competência e profissionalismo.

Aos professores, Alexandre, Clayton, Juliana, Maristela, Mirelle, Silvia, Wagner Fontes, Carlos André por todos os auxílios e preciosos ensinamentos, que foram muito valiosos.

Aos professores Carlos André, Wagner Fontes e Laurine pela contribuição no exame de qualificação. Por expandirem meu conhecimento, importante ferramenta para a minha formação acadêmica e científica.

Aos Professores, Juliano, Clayton e Carlos André por aceitarem participar da banca de defesa da tese de doutorado.

Ao programa de Pós-graduação em Patologia Molecular, coordenação, secretaria e corpo docente.

Ao auxílio financeiro, Coordenação de Aperfeiçoamento de Pessoal de Nível Superior (CAPES), pela concessão da bolsa de estudo.

Ao Paulo Henrique, pela sua amizade. Por sempre estar ao meu lado.

Aos meus amigos, Igor, Juliana de Curcio, Lucas Nojosa e Marielle pela infinita ajuda, amizade, companheirismo e incentivo em todos os momentos.

Aos meus amigos Leandro de Prado, Amanda, Sam, Kleber, Marta, Lívia, Raisa, Lana, Karla, Kassyo, Luiz Paulo, Mariana Pedrosa, Denner, Moises e Ayda.

Aos companheiros de convivência e aprendizado em Brasília, Agenor, Guilherme Petito, Reinaldo, Arthur.

Aos colegas do laboratório Andrea, Aparecido, Gabriel, André, Lorena, Bianca, Mariana Tomazett, Vanessa, Lucas Weba pelo convívio, experiências compartilhadas, por participarem direta ou indiretamente para o desenvolvimento deste trabalho.

Aos funcionários da limpeza, pela dedicação de todos os dias.

A todos que fizeram desses quatro anos e meio, anos mais alegres.

Resumo

Paracoccidioidomicose (PCM) é uma micose sistêmica de alta incidência na América Latina, atribuída aos fungos termodimórficos do gênero *Paracoccidioides*. O contato com o hospedeiro ocorre através da inalação de conídios, que alcançam os alvéolos pulmonares e se diferenciam em leveduras. Esta etapa de transição é considerada vital na patogênese da PCM, permitindo a sobrevivência do fungo no hospedeiro. Assim, este estudo procurou identificar proteínas envolvidas nas fases miceliana e leveduriforme e na transição morfológica micélio-levedura de *Paracoccidioides brasiliensis*. Os peptídeos marcados com iTRAQ foram identificados por LC-MS / MS. Esta abordagem permitiu a identificação de 312 proteínas diferencialmente expressas em micélio, levedura e transição micélio-levedura. Na batalha contra o fungo, o hospedeiro desenvolve várias estratégias para eliminar o patógeno e o fungo por sua vez, reprograma seu metabolismo para subverter as estratégias de defesa do hospedeiro. A fase parasitária de *P. brasiliensis* utiliza as vias de beta-oxidação, TCA e cadeia transportadora de elétrons e fosforilação oxidativa para a produção de ATP. Na fase leveduriforme há a indução de fatores de virulência e proteínas de choque térmico que permitem que o fungo se adapte ao aumento na temperatura. Por outro lado, as enzimas reguladas positivamente da fase miceliana se relacionam com a fermentação alcoólica. Além disso, vias como o ciclo celular, a transcrição e o metabolismo da parede celular foram regulados em micélio. Após marcação com iTRAQ, uma alíquota foi submetida a enriquecimento dos fosfopeptídeos com TiO_2, seguido da identificação das proteínas por LC-MS / MS. O total de 72 e 23 fosfoproteínas foi identificado na fração enriquecida com TiO_2 e fração global, respectivamente. Fosfoproteínas foram diferencialmente acumuladas nas fases do fungo.

Abstract

Paracoccidioidomycosis (PCM) is a systemic mycosis with a high incidence in Latin America, attributed to the thermodimorphic fungi of the *Paracoccidioides* genus. The contact with host occurs through the inhalation of conidia, where once that this reach the pulmonary alveoli differentiate into yeast. This transition stage is considered vital in the pathogenesis of PCM allowing the survival of the fungus in the host. Thus, this study sought to identify proteins involved in the mycelium and yeast phases and in the mycelium-to-yeast transition of *Paracoccidioides brasiliensis*. This approach allowed the identification of 312 differentially expressed proteins in mycelium, yeast, and mycelial-yeast transition. In the battle against the fungus, the host develops several strategies to eliminate the pathogen and the fungus in turn reprogramme its metabolism to subvert the strategies of defense of the host. The parasitic phase of *P. brasiliensis* uses the beta-oxidation pathways, TCA and electron transport chain and oxidative phosphorylation for the production of ATP. In the yeast phase there is the induction of virulence factors and heat shock proteins that allow the fungus to adapt to the increase in temperature. On the other hand, the positively regulated enzymes of the mycelial phase are related to alcoholic fermentation. In addition, pathways such as the cell cycle, transcription, and cell wall metabolism were regulated in mycelium. After labeling with iTRAQ, an aliquot was submitted to enrichment of the phosphopeptides with TiO2, followed by identification of the proteins by LC-MS / MS. The total of 72 and 23 phosphoproteins were identified in the fraction enriched with TiO2 and overall fraction, respectively. Phosphoproteins were differentially accumulated in the fungus phases.

Sumário

Lista de Figuras e Tabelas

CAPÍTULO I

CAPÍTULO II

ABREVIATURAS

4-HPPD: 4-hidro-fenil-piruvato desidrogenase

2-DE: eletroforese bidimensional

ATP: adenosina trifosfato

cAMP: adenosina monofosfato cíclico

$CaCl_{2:}$ cloreto de cálcio

GAPDH: gliceraldeído-3-fosfato desidrogenase

GPI: glicosil-fosfatidilinositol

H_2O_2: peroxido de hidrogênio

IFNγ: interferon gama

IL: interleucina

IMAC: immobilized metal affinity chromatography ou cromatografia de afinidade de íons metais imobilizados

iTRAQ: *Isobaric tag for relative and quantitation*

LC-MS/MS: espectrometria de massas acoplada à nano-cromatografia líquida de alta eficiência

NO: óxido nítrico

O^{-2}: aníon superóxido

$ONOO^-$: peroxinitrito

PAMP: padrões moleculares associados ao patógeno

PRRs: receptores de reconhecimento do padrão

PCM: Paracoccidioidomicose

TFA: ácido trifluoroacético

TEAB: tampão bicarbonato de trieltilamônico

TGF-β: fator de crescimento tumoral beta

Th1: resposta imune T auxiliar do tipo 1

Th2: resposta imune T auxiliar do tipo 2

TiO_2: dióxido de titânio

TNF-α: fator de necrose tumoral alfa

Capítulo I

1. Introdução

1.1. Aspectos gerais de membros do gênero *Paracoccidioides*

Os fungos termodimórficos do gênero *Paracoccidioides* representados pelas espécies *P. brasiliensis, P. americana, P. restrepiensis, P. venezuelensis* e *P. lutzii* causam a micose denominada Paracoccidioidomicose (PCM) (BRUMMER et., 1993). Em 1908 Adolpho Lutz, foi o primeiro pesquisador a descrever o micro-organismo isolado de lesões orais de dois pacientes, o qual diferia do fungo já conhecido na Argentina, denominado *Coccidioides immitis.* Em seus achados Lutz enfatiza a ausência de esférulas com esporos no seu interior, o que foi visualizado através de exames histológicos realizados em suas amostras, assumindo que o fungo encontrado era diferente do *C. immitis* (Lutz, 1945). Inicialmente o fungo *P. brasiliensis* era conhecido por ser o único agente etiológico da micose, e a priori foi denominado *Zymonema brasiliensis* por Splendore em 1912. Floriano de Almeida propôs o nome *Paracoccidioides brasiliensis*, sendo em 1930 o nome do agente causador da PCM. Em 1971 em um encontro de micologistas o termo paracoccidioidomicose foi então reconhecido (Lacaz, 1994).

Uma nova espécie do gênero *Paracoccidioides* foi definida, por meio de estudos de sequenciamento de multilocus. Essa nova espécie foi denominada *Paracoccidioides lutzii* em homenagem a Adolpho Lutz (CARRERO et al., 2008; TEIXEIRA et al., 2009).

O complexo *brasiliensis* era composto por quatro diferentes espécies crípticas, como a seguir designado: PS1 (amplamente distribuída na América do Sul),

PS2 (isolada apenas no Brasil e Venezuela), PS3 (restrita à Colômbia) e PS4 (limitada à Venezuela) (Matute et al., 2006; Salgado-Salazar, Jones, Restrepo, & McEwen, 2010; Theodoro et al., 2012) e *P. lutzii* distribuída nas regiões central, oeste e noroeste do Brasil e Equador (TEIXEIRA et al., 2013; TEIXEIRA et al., 2009; THEODORO et al., 2012). Contudo essa classificação sofreu uma atualização recentemente. Um estudo realizado em 2017 propôs uma nova nomenclatura para o complexo *brasiliensis*, pois através das análises morfológicas e moleculares verificou-se que as espécies de *Paracoccidioides brasiliensis* apresentavam divergências entre si. Os autores do estudo sugeriram três novas espécies filogenéticas do gênero: *P. americana* para PS2, *P. restrepiensis* para PS3, *P. venezuelensis* para PS4. Já o termo *P. brasiliensis* refere-se apenas ao grupo monofilético S1 (Turissini, Gomez, Teixeira, McEwen, & Matute, 2017).

O genoma completo de três diferentes espécies filogenéticas do complexo *Paracoccidioides* (*Pb*01, *Pb*03 e *Pb*18) foi descrito (https://www.broadinstitute.org/fungal-genome-initiative/paracoccidioides-genome-project). O genoma do isolado *Pb*01 apresenta o maior número de bases representando 32,94 Mb, com um total de 9.132 genes. Os isolados *Pb*03 e *Pb*18 apresentam genomas com tamanho de 29,06 e 29,95 Mb, com 7.875 e 8.741 genes, respectivamente (Desjardins et al., 2011). Recentemente os genomas de *P. restrepiensis* (*Pb*Cnh) e *P. venezuelensis* (*Pb*300) foram descritos, os quais apresentaram 8.324 e 8.070 genes, respectivamente (Muñoz et al., 2016).

1.2. Aspectos morfológicos de *Paracoccidioides* spp.

Uma peculiaridade que os fungos dimórficos pertencentes à família Ajellomycetaceae, ordem Onygenales apresentam é a alteração morfológica associada à temperatura (DESJARDINS *et al.*, 2011; MCEWEN et al., 1987). Em condições ambientais ou durante o cultivo *in vitro*, a 22-25ºC, o fungo *Paracoccidioides* apresenta-se como micélio, com hifas finas e septadas, com vários núcleos produzindo clamidósporos ou conídios; macroscopicamente o fungo apresenta aspecto algodonoso (BRUMMER et al., 1993). Nos tecidos do hospedeiro ou quando do cultivo a 36ºC, *Paracoccidioides* é caracterizado por múltiplos brotamentos com morfologia oval ou alongada, contendo múltiplos núcleos e brotamentos, o que confere aspecto de "roda de leme" à forma leveduriforme (BRUMMER et al., 1993) (**Figura 1**).

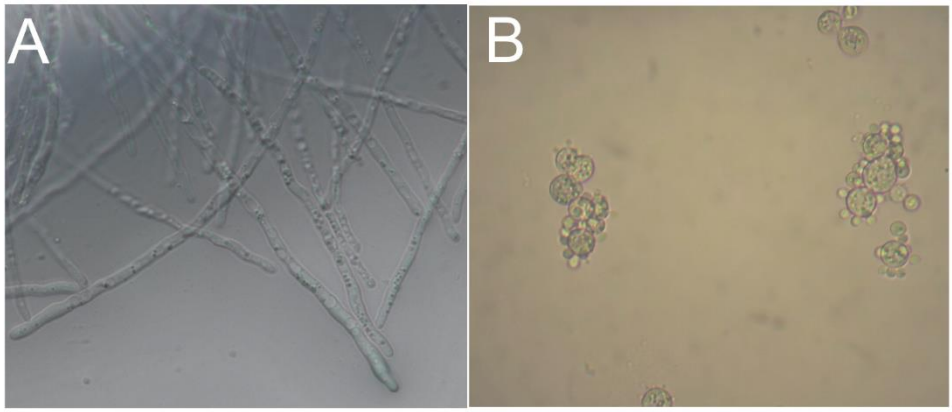

Figura 1. Morfologia *de Paracoccidioides brasiliensis*. (A) micélio sob temperatura de 22ºC (Aumento 100x), **(B)** levedura sob temperatura 36ºC (Aumento 40x).

Quando se compara a morfologia de diferentes espécies de *Paracoccidioides* torna-se evidente que a morfologia/fisiologia conidial produzida por alguns isolados é um possível marcador para diferenciar espécies do gênero *Paracoccidioides*. Isolados como T5LN1, T10B1 e BT84, não produzem qualquer conídio; em paralelo, em isolados como T9B1, BT85 e D01 (pertencentes a espécies do grupo S1) a produção de conídio é alta,

quando os fungos são cultivados com substâncias contendo extratos do solo (TERÇARIOLI et al., 2007). Além disso, a morfologia conidial um pouco mais alongada em *P. lutzii* permite distingui-lo das outras espécies de *Paracoccidioides*. Entretanto, observa-se que as diferenças morfológicas da fase de levedura entre as espécies de *Paracoccidioides* são discretas; *Pb*01 apresenta leveduras maiores, quando comparado a outras espécies como *P. brasiliensis*, *P. americana*, *P. restrepiensis* (Theodoro et al., 2012)(TEIXEIRA et al., 2009). Nesse mesmo contexto a maioria dos isolados de *P. americana* com exceção de *Pb*dog e *Pb*927, apresentam leveduras alongadas similares a pseudohifas (Theodoro et al., 2008). Destaca-se ainda o fato que a espécie *P. venezuelensis* produz menos brotamentos a partir da célula mãe que as outras espécies, sendo esse aspecto considerado um constituinte de diagnóstico (Turissini et al., 2017). Ressalte-se que conhecer as divergências morfológicas e fisiológicas de cada espécie pode ser importante para o diagnóstico e tratamento da PCM (Batista et al., 2010; Taylor et al., 2000). Por exemplo, tem sido mostrado que isolados de *P. lutzii* são mais susceptíveis a sulfametoxazol-trimetroprim em comparação a outros isolados (Hahn et al., 2003).

1.3. Biologia de *Paracoccidioides* spp.

No que tange à biologia do fungo a dificuldade em predizer sua exata localização e o micro nicho está associada à escassez do isolamento da forma saprofítica na natureza (Franco, Bagagli, Scapolio, & da Silva Lacaz, 2000). Sabe-se que o fungo possui uma fase miceliana encontrada no solo, mas sua interação com fatores bióticos e abióticos do ambiente não tem sido completamente determinada (BAGAGLI et al., 2008). Pode-se supor, com base em dados na literatura, que o habitat da forma miceliana ocorre

em locais úmidos, pluviosidade média para alta, temperaturas médias e com a presença de rios e florestas (RESTREPO; MCEWEN, 2001). Tem sido proposto também que regiões agrícolas constituem um ambiente com condições necessárias para o desenvolvimento do fungo; por exemplo, o solo argiloso poder reter mais água e nutrientes (BELLISSIMO-RODRIGUES et al., 2011; CADAVID; RESTREPO, 1993; SIMÕES et al., 2004). Além disso, a presença de tatus infectados com o fungo em áreas com solo arenoso e ácido sugere que ambientes similares podem ser o habitat para este patógeno (E Bagagli et al., 2003). Nota-se que a umidade é um aspecto importante para manutenção do fungo, tanto no solo argiloso quanto para o solo arenoso (TERÇARIOLI *et al*., 2007).

Através da detecção do fungo em amostras provenientes da toca de tatus, especula-se que esse ambiente fornece condições satisfatórias para o fungo, entre elas umidade, temperatura (RESTREPO et al., 2001). Além disso, o hábito de escavar túneis contribui para a dispersão fúngica. Ademais, a temperatura corporal e a baixa imunidade celular dos tatus, sugerem que tais animais forneçam um importante reservatório para *Paracoccidioides* (TERÇARIOLI *et al.*, 2007; THEODORO et al., 2005). Vale ressaltar que o fungo tem sido frequentemente isolado em tatus tais como *Dasypus novemcinctus* e ocasionalmente em *Cabassus centralis*. O fungo pode causar infecção e doença em animais domésticos como tem sido relatado em cachorros. Esporadicamente tem sido isolado de fezes de morcegos e pinguins e comida de cachorros (BAGAGLI, E *et al.*, 2003; CORREDOR et al., 2005; FERREIRA et al., 1990; GROSE E, 1965; GARCIAI et al., 1993; RICCI et al., 2004).

Na tentativa de mapear a distribuição geográfica das espécies do gênero *Paracoccidioides* em áreas endêmicas da PCM no Brasil, Arantes e colaboradores (2016) utilizaram amostras provenientes do solo e aerossol, como representado na **Figura 2**.

Corroborando com dados anteriores, ficou evidente que o crescimento e dispersão do fungo são influenciados pelo clima. A alta umidade propicia o crescimento fúngico e a sua manutenção no solo. Já períodos de seca promove uma dispersão mais fácil e intensa dos aerossóis (BARROZO et al., 2010, 2009; YAMAMOTO et al., 2012). Nesse sentido, quando avaliado o estado de Rondônia, a detecção de *Paracoccidioides* em amostras de aerossóis mostrou-se negativa e em contrapartida nas amostras do solo foram positivas. Os autores explicam que as coletas das amostras nessa região foram realizadas em período de chuva, o que pode favorecer a manutenção do fungo no solo (Arantes, Theodoro, Teixeira, Bosco, & Bagagli, 2016). Como ressaltado pelos autores esse fato também corrobora com o crescente número de casos após os períodos de chuvas em regiões endêmicas e o aumento de novos casos em áreas do Norte do Brasil (BARROZO et al., 2010, 2009; VIEIRA et al., 2014). Além disso, os estados de Rondônia e Goiás apresentam uma grande indecência de casos de PCM, possivelmente devido ao aumento da atividade agrícola nessas regiões (FERREIRA et al., 2012; GEGEMBAUER et al., 2014; VIEIRA et al., 2014).

No que se refere à distribuição das espécies filogenéticas no Brasil, *P. lutzii* e *P. brasiliensis* foram encontrados em todas as quatro regiões analisadas (Arantes et al., 2016). Acredita-se que tal fato está relacionado à capacidade de cada espécie produzir propágulos infectivos em áreas distintas. Com base na literatura, sugere-se que *P. brasiliensis* produza uma maior quantidade de conídios que as outras espécies, o que explicaria o alto índice de isolamento de *P. brasiliensis* em áreas endêmicas (MOLINARI-MADLUM et al., 1999; TERÇARIOLI et al., 2007). Ressalte-se que à época de publicação do trabalho citado, a espécie *P. brasiliensis* ainda comportava vários grupos filogenéticos.

Como abordado acima a produção de esporos assexuais dos fungos é importante para a disseminação destes na natureza (TERÇARIOLI et al., 2007). Evidências tem mostrado a expressão de genes relacionados à maquinaria sexual, sugerindo que reprodução sexual possa ocorrer durante o ciclo de vida de *P. brasiliensis* (TEIXEIRA et al., 2014).

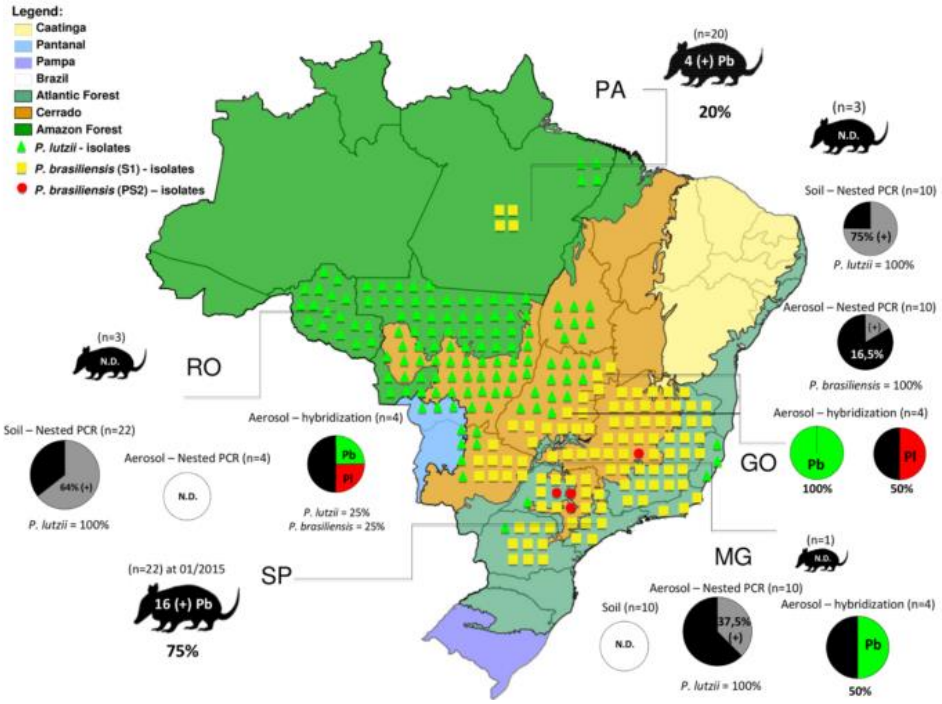

Figura 2. Distribuição biogeográfica no território brasileiro onde a detecção ambiental (do solo, aerossol e tatus) de *Paracoccidioides* spp. foi realizada. As áreas de coleta abrangem os Estados de Minas Gerais (MG), Goiás (GO), Rondônia (RO), São Paulo (SP) e Pará (PA). Círculos fora do mapa indicam a porcentagem de positividade em cada área para *P. brasiliensis* (verde) e *P. lutzii* (vermelho) por hibridização *in situ* para amostras de aerossol. Os círculos fora do mapa em preto e cinza indicam a porcentagem de positividade em cada área para *P. brasiliensis* e *P. lutzii* por Nested PCR para amostras de solo e aerossol. O círculo branco indica a detecção negativa nas áreas avaliadas (N.D = Não detectado). Os tatus indicam o número de animais coletados e a positividade para isolamento de *P. brasiliensis* (*Pb*) em cada localidade (em RO, GO, MG, SP e PA). Os triângulos (verde), quadrados (amarelo) e círculos (vermelho) mostram a distribuição dos isolados clínicos para espécies crípticas (S1, PS2 e *P. lutzii*) Adaptado de Arantes (2016).

1.4. Interação com o hospedeiro

A interação do *Paracoccidioides spp.* com as células do hospedeiro é um evento chave na patogênese da PCM. Macrófagos alveolares e células epiteliais alveolares são as primeiras linhas de defesa que o fungo encontra. Uma vez no hospedeiro, o fungo pode ser completamente destruído, ou então persistir e se multiplicar (BORGES *et al.*, 2002; GONZALEZ *et al.*, 2005; MENDES-GIANNINI et al., 2005; MENDES-GIANNINI et al., 2000).

Durante a interação com as células do hospedeiro, tem sido demonstrado que o fungo consegue aderir e invadir células não fagocíticas como as células epiteliais e endoteliais (Filler & Sheppard, 2006). Esse processo de invasão permite que o fungo alcance a corrente sanguínea e se dissemine para outros tecidos (MENDES-GIANNINI et al., 2004; MENDES-GIANNINI et al., 2008). Tais células fornecem uma proteção para o fungo contra os macrófagos, permitindo sua evasão da resposta microbicida desses fagócitos, embora o fungo não seja um parasita intracelular obrigatório (FILLER; SHEPPARD, 2006; MENDES-GIANNINI et al., 2005; MENDES-GIANNINI et al., 2000; TUDER et al., 1985). Especula-se que para o sucesso da infecção o fungo deve primeiro aderir às células do hospedeiro podendo elas serem fagocíticas ou não; após essa etapa há a translocação do fungo para o citoplasma, seguida pela multiplicação da célula fúngica (MENDES-GIANNINI et. al, 2008). Sugere-se que o fungo induz sua própria endocitose, por desencadear sinais extracelulares específicos que culminam no rearranjamento do citoesqueleto, no ponto de contato fungo-célula (Swanson et al., 1995a; Swanson et al., 1995b). Uma vez que as células epiteliais não possuem receptores do tipo CR3, acredita-se que esse processo envolva integrinas e o rearranjamento do

citoesqueleto (HAYWARD; KORONAKIS, 1999; MB; PJ, 1993; ROSENSHINE et al., 1992). Infere-se que *P. brasiliensis* possui dois mecanismos diferentes de invasão; um dependente de microfilamentos como actina e outro dependente de microtúbulos de tubulina, pois o tratamento com citocalasina D e colchicina reduzem a invasão das células fúngicas (MENDES-GIANNINI et. al, 2004).

Tem sido proposto que durante o processo de replicação, alguns patógenos empregam estratégias para impedir a morte da célula do hospedeiro, mas para que consiga escapar e disseminar para uma nova célula é preciso que haja destruição da célula infectada. Nesse sentido, o processo apoptótico tem sido destacado, pois a morte da célula do hospedeiro com o fungo dentro fornece uma rota de disseminação para sítios distantes. Outra hipótese sugere que células apoptóticas com o fungo dentro servem como um veículo para entrada em macrófagos, sem estimular sua atividade microbicida (MENDES-GIANNINI et.al, 2008). A apoptose de uma célula fagocítica como os macrófagos, permite que o fungo obtenha dois objetivos: o fungo promove a morte de uma célula microbicida para ele, impedindo assim sua própria morte, bem como promove a resposta inflamatória, que por sua vez pode propiciar a invasão fúngica aos tecidos, devido ao dano que esta resposta causa (Bayles et al., 1998; Lewis, 2000).

Por outro lado, as células do sistema imune do hospedeiro podem apresentar um arsenal capaz de eliminar o fungo. Assim, durante a batalha contra o fungo, as células do hospedeiro polarizam uma resposta imune T auxiliar do tipo 1 (Th1), caraterizada pela produção de interferon gama (IFN-ɣ), que culmina na ativação da atividade microbicida dos macrófagos (MENDES et al., 2017; SA et. al, 2003). A atividade microbicida dessas células está relacionada com a produção de produtos derivados de oxigênio, como peróxido de hidrogênio (H_2O_2) e aníon superóxido (O^-_2) e principalmente, de óxido nítrico (NO) e seus metabólitos. Outra importante espécie reativa é o peroxinitrito

($ONOO^-$), gerado a partir da interação de NO com superóxido (O^-_2); este composto subsequentemente decompõe-se em outras moléculas reativas. Essas espécies reativas causam uma variedade de alterações no DNA incluindo quebras das fitas e desaminação, enquanto que em proteínas causam modificações que envolvem nitrosilação de resíduos de cisteína e tirosina, além da inativação de enzimas com núcleo de ferro-enxofre (PINA, et. al, 2013; FANG , 2004; D & Ehrt S et. al, 2003; C; MU, 2000).

A defesa do hospedeiro é mediada pelas seguintes etapas: a fagocitose entre a célula fagocítica e o patógeno, que ocorre por meio da ligação dos receptores de reconhecimento do padrão (PRRs- "*patterns recognizing receptors*") dos fagócitos às estruturas moleculares conservadas dos micro-organismos conhecidas como padrões moleculares associados aos patógenos (PAMPs- "*pattern associated molecular pathogens*") (CHAI et al., 2009; WHEELER et al., 2008). Nesta etapa, os macrófagos e as células dendríticas fazem a apresentação de antígenos fúngicos para linfócitos T, sendo que posteriormente tem-se uma resposta imune adaptativa que produzirá citocinas, que incluem fator de necrose tumoral (TNF-α) e IFN-γ, que induzirão os macrófagos a produzir espécies reativas de oxigênio e nitrogênio, que matam o fungo ou inibem seu crescimento (Gauthier & Klein, 2010).

Dessa maneira a resposta imune adaptativa é orquestrada pela interação entre as células imunes, anticorpos e citocinas e antígenos fúngicos, como representado na **Figura 3** (Mendes et al., 2017). Assim, indivíduos que entraram em contato com o fungo, mas não desenvolveram a doença, exibem uma resposta imune Th1, resultando na formação de um granuloma compacto capaz de controlar a replicação fúngica, embora ainda existam formas latentes do fungo dentro do granuloma (ROMANO et al., 2001; SHIKANAI-YASUDA *et al.*, 2017; SJ et al., 2002). Do outro lado temos os indivíduos que manifestam as formas aguda e crônica da PCM. Nesses indivíduos tem sido

observado um padrão de resposta Th2 e Th9, onde não há formação de granulomas compactos, mas sim uma atividade de linfócitos B, que produzem altos níveis de anticorpos específicos, por exemplo IgE, cujo perfil do indivíduo com as formas aguda e crônica é caracterizado por hipergamaglobulinemia e eosinofilia (de Castro et. al, 2013).

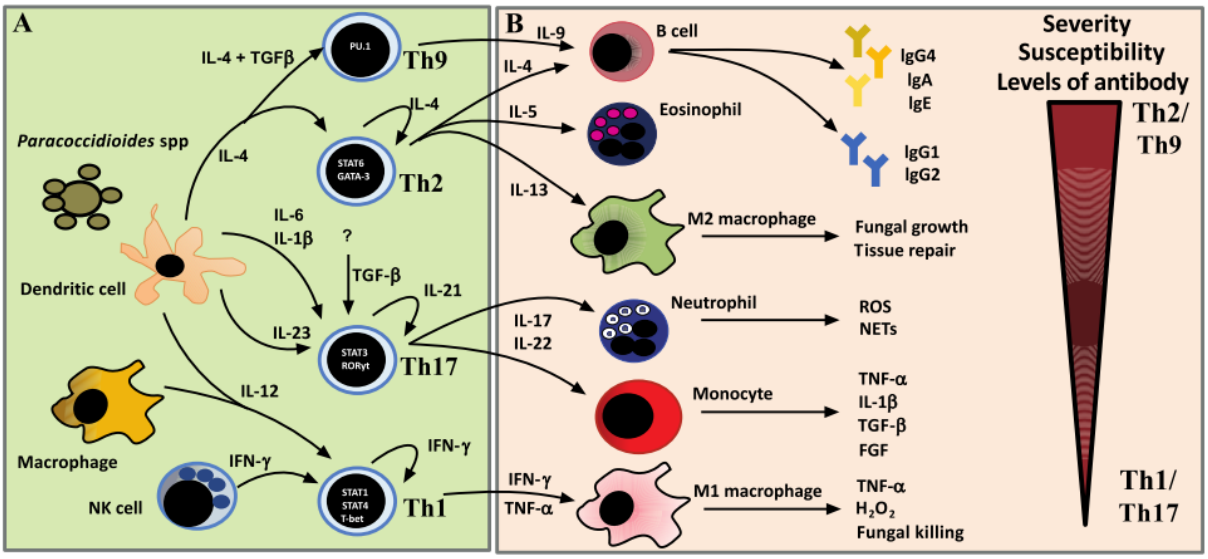

Figura 3. Resposta imune adaptativa na PCM. (A) Ativação de subgrupos T auxiliar (Th). Células dendríticas (DCs) induzidas por moléculas antigênicas do fungo migram para o linfonodo onde apresentam antígenos processados para células Th virgens que se diferenciam em um dos subgrupos de linfócitos Th (Th1, Th2, Th9 e Th17), dependendo principalmente de citocinas presentes no ambiente extracelular. Para polarização Th1, IL-12 de DCs e macrófagos, e IFNɣ de células NK ativam a sinalização STAT1 / STAT4 para induzir a expressão do fator de transcrição especifico de Th1, T-bet. Para polarização Th17, IL-6, IL-1β, TGF-β e IL-23 são necessárias para induzir a expressão do fator de transcrição específico para Th17, RORβτ, através da sinalização STAT3. Para a polarização Th2, a IL-4 das DCs ativa a sinalização STAT6 para induzir a expressão do fator de transcrição específico para Th2, GATA-3. Para a polarização Th9, IL-4 e TGF-β são necessários para induzir a expressão do fator de transcrição específico de Th9, PU.1. **(B)** Fases efetoras das respostas das células T. Os clones Th1, Th17, Th2 e Th9 podem ser distinguidos principalmente pelas citocinas produzidas pelas células. As células Th1 liberam altas quantidades de IFN-γ e TNF-α que classicamente ativam os macrófagos (M1) resultando na eliminação dos fungos. Células Th17 secretam IL-17 e IL-22 que recrutam neutrófilos e monócitos. Os neutrófilos atuam gerando espécies reativas de oxigênio (ROS) que resultam na eliminação de fungos. Os monócitos têm sido estudados na

PCM por induzir altos níveis de citocinas inflamatórias, como TNF-α e IL-1β, e fatores de crescimento, como TGF-β e fator de crescimento de fibroblastos (FGF). Th2 apresenta várias funções que dependem de cada citocina secretada. A IL-4 induz a ativação de células B e subsequente produção de imunoglobulinas; A IL-5 desencadeia o recrutamento de eosinófilos; a IL-13 está envolvida na desativação de macrófagos denominados "macrófagos ativados alternativamente" (M2), que resultam em crescimento fúngico e também no reparo tecidual. Th9 libera IL-9 e IL-21 que atuam em sinergia com Th2 para produzir anticorpos. Adaptado de Mendes (2017).

Apesar do arsenal microbicida dos fagócitos, o fungo apresenta estratégias para escapar da destruição e sobreviver no interior dos macrófagos como parasitas intracelulares dessas células (BRUMMER et al., 1989, 1990; FAN et al., 2005). Como abordado acima, tem sido notado que em macrófagos não ativados as células fúngicas conseguem sobreviver e replicar, uma vez que há falhas na indução de espécies reativas de oxigênio (Gauthier & Klein, 2010). Assim, o macrófago não ativado fornece um ambiente favorável à multiplicação e também um mecanismo de transporte para as células de *Paracoccidioides* spp. via corrente sanguínea ou linfática. Desta forma, os macrófagos podem representar um papel importante na disseminação do fungo a partir do foco primário de infecção (JP, 2003; TAVARES et al., 2007).

Uma vez fagocitado, o patógeno exibe uma dramática reprogramação transcricional e traducional refletindo estratégias de adaptação ao ambiente hostil do fagócito (FAN et al., 2005; FERNANDES et al., 2008). Mudanças na parede celular contribuem para virulência e evasão imune da fase patogênica, as quais incluem o aumento de α-glicana. A α-glicana contribui para latência do fungo, protegendo a β-glicana do reconhecimento das células do sistema imune inato, além de reduzir a produção de TNF-α pelas células infectadas. A β-glicana é um importante imunomodulador na resposta contra infecções fúngicas, induzindo a secreção de TNF-α que potencializa a resposta inflamatória e eliminação do patógeno (LEMUS et. al, 2014).

Em *Paracoccidioides* o transcrito do gene codificante para β-glicana sintase, fks, foi suprimido em resposta ao ambiente intracelular do macrófago, o que sugere ser um importante mecanismo adaptativo que o fungo utiliza com o objetivo de reduzir a resposta inflamatória desencadeada pela β-glicana (TAVARES et al., 2007).

O fagossomo, presente no macrófago, é uma organela que apresenta um ambiente com limitações nutricionais, sendo pobre em fontes de glicose e aminoácidos e com pH extremamente baixo, assim como é um ambiente rico em espécies reativas de oxigênio (FERNANDES et al., 2008; SILVA et al., 2008). Neste contexto, em resposta ao microambiente hostil do macrófago, o fungo induz a expressão de genes relacionados ao processo de detoxificação de espécies reativas de oxigênio e biossíntese de aminoácidos, além de reprimir a expressão de genes codificantes de enzimas da via glicolítica (TAVARES et al., 2007).

Derengowski e colaboradores (2008) observaram a indução de genes que codificam para enzimas do ciclo do glioxalato (*icl* e *mls*) em leveduras recuperadas da internalização por macrófagos em um período de 9 horas, sugerindo que o patógeno é capaz de utilizar compostos de 2 carbonos para a síntese de glicose (Derengowski et. al, 2008). Voltan e colaboradores (2013) verificaram que em macrófagos infectados com *P. brasiliensis* ocorre diminuição na expressão de EEA1. Essa proteína é um marcador de fagossomo precoce, inferindo-se que possivelmente o fungo é capaz de modular o tráfego fagossomal (Voltan et al., 2013). A análise proteômica de *P. brasiliensis* sob interação com macrófagos revelou a indução de proteínas e enzimas relacionadas com a detoxificação de ROS, como a citocromo c peroxidase que protege o fungo contra o estresse nitrosativo. Ademais, o catabolismo de aminoácidos fornece percussores de glicose para a gliconeogênese, uma vez que há a mudança metabólica da glicólise para gliconeogênese (PARENTE et al., 2015).

Um recente trabalho foi publicado em nosso laboratório, buscando compreender a interação de *P. brasiliensis* com o hospedeiro. Um modelo de infecção intranasal foi realizado, o lavado broncoalveolar obtido foi analisado por abordagens transcricional e proteômica. A infecção das células pulmonares por um período de 6h, e posterior análise de RNAs e proteínas, demonstraram que as células leveduriformes mudam seu perfil metabólico, usando lipídios como fonte de energia durante a infecção. Ademais a resposta adaptativa inclui o aumento de vias relacionadas com a resposta protetiva contra ROS e inibição do metabolismo da parede celular (Lacerda Pigosso et al., 2017).

1.5. Paracoccidioidomicose

Por não ser uma doença de notificação compulsória, a prevalência da PCM é estimada com base em casos reportados, dados de hospitalização e morte. Presume-se que vários casos de PCM sejam diagnosticados por ano (Martinez, 2017). No Brasil esta taxa varia entre 3360 a 5600 casos por ano (Prado, da Silva, Laurenti, Travassos, & Taborda, 2009). Estima-se que a ocorrência da PCM em áreas endêmicas seja de 1 a 4 casos por 100.000 habitantes, por ano. Destaca-se que em regiões de elevada endemia, como Rondônia e região Oeste do Amazonas, esta média alcance 9.4 casos/100.000 habitantes/ano. Durante períodos de surto alguns municípios do Sudeste já registraram 40 casos/100.000 habitantes/ano (VIEIRA et al., 2014). Nota-se que a taxa de mortalidade por essa micose é em torno de 3% a 5%. No período de 1986 a 2006 um total de 1853 mortes foram registradas no Brasil, representando 51% do número de mortes por infecções fúngicas (Prado et al., 2009). As regiões Centro-Oeste e Norte do Brasil mostraram ter altas taxas de hospitalização e morte, ressaltando-se que a região Centro-Oeste do Brasil é uma importante área endêmica da PCM (Martinez, 2017).

A micose afeta principalmente indivíduos que desempenham atividades relacionadas com agricultura e a incidência da PCM após a puberdade é maior no sexo masculino; cerca de 75% a 95% são pacientes homens (Franco et al., 2000; Shikanai-Yasuda, Telles Filho, Mendes, Colombo, & Moretti, 2006) A capacidade que o estrógeno possui em inibir a transição micélio para levedura pode explicar essa diferença (Shankar, Restrepo, Clemons, & Stevens, 2011). A transmissão de uma pessoa para outra não tem sido relatada. Entre os fatores de risco para PCM estão o uso de álcool e tabaco (Santos, Silva, Passos, Zandonade, & Falqueto, 2003). Tem sido mostrado que neoplasias, tuberculose, chagas, leishmaniose, lepra, estrongiloidíase podem ocorrer, antes, após ou simultaneamente com a PCM (Bellissimo-Rodrigues et. al., 2011).

A PCM é uma micose que pode acometer qualquer órgão, aparelho ou sistema. Assim as formas clínicas da doença são classificadas de acordo com o *International Colloquium on Paracoccidioidomycosis*, realizado em Medelín, Colômbia no ano de 1986 (BELLISSIMO-RODRIGUES et al., 2013; FRANCO et al., 1987; FRANCO et al., 1989) A doença é classificada em infecção Paracoccidioidomicose, Paracoccidioidomicose aguda/subaguda, forma crônica e forma residual ou sequelar (FRANCO et. al., 1987). A infecção Paracoccidioidomicose é caracterizada quando o indivíduo saudável entra em contato com o fungo e a infecção é diagnosticada por teste intradermo positivo para antígenos específicos do fungo (MONTENEGRO, 1994).

A forma aguda/subaguda corresponde a 5-25% dos casos. Nos estados do Maranhão, Minas Gerais, Pará, Goiás e São Paulo, essa forma da doença é comumente observada, por ser tratar de regiões endêmicas (Shikanai-yasuda et al., 2017). Crianças, adolescentes e jovens adultos entre 30 a 40 anos, são mais susceptíveis a desenvolver a PCM aguda/subaguda. Com relação ao gênero, nessa forma da PCM a distribuição tende a ser uniforme, principalmente na população adolescente (BELLISSIMO-RODRIGUES

et al., 2013; FABRIS et al., 2014; SHIKANAI-YASUDA et al., 2006). Nas manifestações clínicas da forma aguda é observado o envolvimento do sistema mononuclear fagocítico, com linfadenomegalia localizada ou geral, podendo ocorrer supuração, fistulas e hepatoesplêniomegalia. Há o envolvimento dos sistemas digestivo, cutâneo, osteoarticular e raramente há comprometimento pulmonar. Frequentemente estão associados a essa forma febre, perda de peso e anorexia. Uma massa tumoral resultante da linfadenomegalia intra-abdominal, pode comprimir vários órgãos (BARBOSA; DAHER, 1968; SHIKANAI-YASUDA et al., 2017)

A forma crônica da micose, ocorre em 74 a 96% dos casos, frequentemente acomete indivíduos entre faixa etária de 30 a 60 anos que trabalharam em atividades relacionadas com a agricultura. Indivíduos do sexo masculino são mais comumente afetados com uma proporção de 22 homens do sexo masculino, para 1 mulher. O desenvolvimento da PCM crônica é lento, os sintomas persistem entre 4 a 6 meses ou por um ano. Em alguns casos a doença pode apresentar-se assintomática. Em 90% dos casos há um comprometimento pulmonar, mas pode acometer outros órgãos como mucosa, via aero digestiva e pele (COSTA et al., 2013; RP, 1994; SHIKANAI-YASUDA et al., 2017). Nos casos graves da PCM crônica observa-se uma perda de peso superior a 10%, intenso envolvimento pulmonar, assim como de outros órgãos como glândulas adrenais, sistema nervoso central, medula e linfonodos. Em casos mais leves da PCM crônica, existe uma perda de peso entre 5% com envolvimento de um ou poucos órgãos ou tecido (Shikanai-yasuda et al., 2017). A forma residual é caracterizada pelas mudanças anatômicas e funcionais após o tratamento da PCM. Essa forma pode acontecer em vários órgãos, mas frequentemente acomete pulmão, pele, laringe, traqueia, adrenais, sistema linfático, sistema nervoso e mucosa do trato superior aero digestivo (MACHADO FILHO, 1965; TOBÓN et al., 2003; VALLE et al., 1995).

Para o tratamento da PCM medicamentos como itraconazol, cotrimoxazol (combinação de sulfametoxazol/trimetropim) e anfotericina B estão entre as principais escolhas de tratamentos praticados na clínica. Contudo a interação dos medicamentos, efeitos adversos e a terapia de longa duração são fatores que devem ser levados em consideração na escolha de tratamento da PCM (Shikanai-yasuda et al., 2017).

1.6 Dimorfismo de *Paracoccidioides* spp.

Como já abordado acima, *Paracoccidioides* é um fungo saprofítico, onde o contato com solo contaminado pelo fungo, pode ocasionar inalação dos propágulos infectivos (BRUMMER et al., 1993; LACAZ; PORTO, 1984). Assim, o ambiente fornecido pelo hospedeiro induz o fungo a desenvolver estratégias ou fatores de virulência para adaptar-se ao novo ambiente encontrado (DERENGOWSKI et al., 2008; FELIPE et al., 2003; FELIPE et al., 2005; PARENTE et al., 2015; TAVARES et al., 2005). Entre esses fatores de virulência está a transição morfológica para a forma parasitária caracterizada por leveduras com múltiplos brotamentos (BRUMMER et al., 1993). As leveduras de *Paracoccidioides* exibem um repertório de proteínas que permitem ao fungo se adaptar com essa mudança na temperatura como, por exemplo, proteínas do choque térmico (HSPs) como a hsp70 (Nunes, Costa de Oliveira, et al., 2005; Theodoro et al., 2008) Dessa maneira, a mudança morfológica que o fungo sofre é essencial para a patogenicidade de *Paracoccidioides*; concordando com tal fato, assume-se que linhagens incapazes de transitar para levedura não são virulentas (Nemecek, 2006). Além da temperatura, fatores nutricionais, como a adição de soro fetal podem desencadear a transição dirmórfica do fungo para a fase leveduriforme, a 25ºC (VILLAR; SALAZAR, 1988). Por outro lado, fatores hormonais podem inibir a transição micélio para levedura (Shankar et al., 2011). Com base em dados epidemiológicos, mulheres são mais

resistentes ao desenvolvimento da PCM. Acredita-se que a presença do hormônio 17-β-estradiol associado a EBP (Estradiol Binding Protein) iniba a transição micélio para levedura, explicando a baixa incidência da PCM em mulheres (FELIPE et al., 2005; LOOSE et al., 1983; SHIKANAI-YASUDA et al., 2017).

A adaptação ao aumento da temperatura requer mudanças morfológicas e bioquímicas orquestradas pela modulação da expressão de genes e proteínas (NUNES et al., 2005; REZENDE et al., 2011; TAVARES et al., 2015) Entre os genes identificados durante transição micélio-levedura incluem-se aqueles codificantes para proteínas envolvidas no metabolismo da parede celular (Nunes, Costa de Oliveira, et al., 2005). A parede celular de *Paracoccidioides* é composta por quitinas, glicanas, lipídeos e proteínas que podem ser cobertas por carboidratos (SAN-BLAS, 1982; SAN-BLAS; NIÑO-VEGA, 2008) Durante a transição morfológica para a fase de levedura, há uma migração e reorganização dos lipídeos, como glicoesfingolipídeos e alteração dos carboidratos da parede celular (Levery, Toledo, Straus, & Takahashi, 1998). Notavelmente há um aumento no conteúdo de quitina, além da mudança no polímero de β-1,3-glicana para α-1,3-glicana, que fornece proteção contra o reconhecimento das células do sistema imune inato, consequentemente reduzindo a produção de TNF-α pelas células infectadas (SAN-BLAS, 1982). Em concordância com esse dado, a analise transcricional de *P. lutzii* durante transição revelou a indução de vários genes relacionados com a síntese de carboidratos da parede. Entre eles incluem genes codificantes das enzimas fosfoglicomutase, UDP-glicose pirofosforilase e α-1,3-glicana sintase, permitindo o aumento da síntese de α-1,3-glicana na forma leveduriforme (BASTOS et al. 2007). Além disso, há uma maior expressão de genes que codificam quitina sintases; em contrapartida quitinases e endoquitinases foram reprimidas (Nunes, Costa de Oliveira, et al., 2005).

Oliveira e colaboradores (2017), verificaram que o transcrito correspondente a uma proteína que interage com a quitina denominada paracoccina (PCN), é mais expressa nas fases de micélio e transição de levedura-para-micélio, comparado à forma leveduriforme. Segundo os autores, sua localização na ponta das hifas sugere participação no crescimento do micélio, contribuindo para degradação de quitina e prolongamento da hifa devido à atividade de NAGase (N-acetil-β-D-glicosaminidase) dessa proteína. Os autores concluem que envolvimento da PCN é importante no processo de transição morfológica e consequentemente no remodelamento da parede celular, contribuindo para patogênese do fungo (OLIVEIRA et al. 2017). Um fato importante que deve ser ressaltado refere-se à resposta transcricional de *P. brasiliensis* para o hormônio estradiol. Durante transição por 2 e 6 horas com diferentes concentrações de estradiol, buscando representar níveis encontrados fisiologicamente, o gene que codifica quitina sintase 1 (CHS) foi menos expresso em ambos os pontos de transição analisados, corroborando com a inibição da transição micélio-levedura promovido por estradiol, já que as leveduras requerem um maior conteúdo de quitina (TAVARES *et al.*, 2015). Duas quitinases foram descritas em *P. lutzii*. A *Pb*CTS1 foi detectada em micélio, transição e levedura. Para levedura, quando comparados os extratos da fração de parede celular e a fração secretada, a quitinase *Pb*CTS1 foi detectada apenas na fração secretada. Já a quitinase, de peso molecular 39 kDa, denominada *Pb*CTS2, foi detectada principalmente durante transição micélio-levedura e levedura. Sua presença na parede celular e meio extracelular sugere que tal proteína esteja relacionada com biossíntese da parede celular (SANTANA et al., 2012).

A proteína CDC42 é importante para o controle da transição dimórfica atuando na manutenção dos sinais intracelulares (SU et al., 2007; VANDENBERG et al., 2004). Em *P. brasiliensis* o silenciamento do gene codificante de *Pb*CDC42 em leveduras, produziu

linhagens com morfologia alterada, com redução no tamanho das células mãe e de brotamentos. Em modelo de infecção animal, essas células leveduriformes, com morfologia alterada devido ao silenciamento de cdc42, eram menos virulentas e apresentaram maior susceptibilidade à fagocitose (Almeida et al., 2009).

O papel das vias de sinalização que controlam a transição morfológica em *P. brasiliensis* ainda não é bem esclarecido. O híbrido histidina quinase (DRK1), é um sistema de sinalização de dois componentes, envolvido na transição dimórfica e virulência de fungos como *Blastomyces dermatidis* e *Histoplasma capsulatum*. Através do uso da técnica de RNA de interferência para o gene drk1, foi possível observar -se mudanças na parede celular de *B. dermatidis*, por redução da expressão do gene que codifica α-1,3-glicana sintase. Esse sistema, propicia a adaptação do fungo durante a transição bem como estimula o fungo a expressar fatores de virulência (Nemecek, 2006). Em *P. brasiliensis* o gene drk1 é induzido na transição dimórfica e linhagens que foram crescidas com inibidor para drk1 mostraram um atraso na diferenciação morfológica micélio-levedura (CHAVES et al., 2016).

A expressão de genes codificantes de calmodulina e da subunidade regulatória de calcineurina estão aumentadas durante a transição morfológica, sugerindo papel chave dessa via de transdução sinal na morfogênese (Nunes, Costa de Oliveira, et al., 2005). Além disso, drogas que bloqueiam cinases dependentes de Ca^{2+}/calmodulina inibem a diferenciação de micélio para levedura (de Carvalho et al., 2003). Genes que codificam proteínas RAS1 e RAS2 estão envolvidos no dimorfismo de *P. lutzii*. Nesse mesmo estudo foi observado que o uso de inibidor para farnesilação durante a transição levedura-micélio, induziu aumento na filamentação, de maneira dose dependente (FERNANDES et al., 2008).

Avaliando processos biológicos importantes para *P. lutzii* sugeriu-se que enzimas relacionadas ao metabolismo de enxofre foram induzidas em levedura durante a transição, sugerindo relevância do metabolismo de enxofre para o processo de diferenciação celular (Andrade et al., 2006). Além disso, membros do complexo induzem a proteína ubiquinol oxidase alternativa, nos estágios iniciais da diferenciação micélio-levedura na tentativa de controlar os níveis de ROS (HERNÁNDEZ et al., 2015; MARTINS et al., 2011). Durante a transição de *P. lutzii*, catalases como *Pb*CatA, *Pb*CatP apresentaram expressão diferencial em resposta ao estresse oxidativo. A *Pb*CatA foi mais expressa em micélio, já a *Pb*CatP é mais expressa em levedura (CHAGAS et al., 2008; MOREIRA et al., 2004). Sugere-se que a *Pb*CatA está associada à proteção contra estresse oxidativo endógeno e *Pb*CatP contra a produção exógena de peróxido de hidrogênio (CHAGAS et al., 2008;GROSSKLAUS et al., 2013).

1.7. Análises transcricionais e proteômicas durante transição morfológica em membros do complexo *Paracoccidioides*

O perfil transcricional descrito para as fases miceliana e leveduriforme de *P. lutzii*, isolado *Pb*01, obtido através da abordagem de ESTs, resultou em 6.022 expressed sequenced tags (ESTs). Felipe e colaboradores (2005) propõem que a produção de ATP ocorra preferencialmente através da fermentação alcoólica em células levefuriformes e que micélio apresenta metabolismo mais aeróbico. Esse aspecto seria decorrente do fato que enzimas chaves do ciclo ácido-cítrico foram induzidas em micélio, tais como isocitrato desidrogenase e succinil-CoA sintetase e em contrapartida genes que codificam álcool desidrogenase I foram induzidos em levedura (FELIPE et al., 2005). Ainda em *P.lutzzi*, Rezende e colaboradores (2011) avaliaram a expressão diferencial, no nível de proteoma, para as fases de micélio, transição micélio-levedura e levedura. Um total de 18

proteínas foram diferencialmente expressas na fase de micélio, nas quais se incluem peroxiredoxina mitocondrial PRX1, Mn superóxido dismutase e aldeído desidrogenase. Em transição micélio para levedura 30 proteínas foram diferencialmente expressas tais como enolase, fosfoglicomutase, transaldolase e transcetolase. Na fase leveduriforme, 33 proteínas foram diferencialmente expressas como fosfoglicerato quinase, frutose-1,6-bifosfato aldolase, gliceraldeído-3-fosfato desidrogenase, isocitrato liase, enoil-CoA hidratase e metilcitrato desidratase. Os autores propõem um perfil metabólico durante a morfogênese do fungo. Dessa maneira, em leveduras a via glicolítica é induzida, sendo que algumas enzimas dessa via se acumulam durante a transição micélio-levedura. A via das pentoses fosfato é induzida na transição podendo fornecer substratos para a glicólise. No repertório de proteínas expressas em micélio estão aquelas envolvidas na manutenção do potencial redox intracelular, fosforilação oxidativa e proteção contra o estresse oxidativo (REZENDE et al. 2011).

A temperatura é o principal fator que governa a transição morfológica. Dessa maneira, compatível com o aumento na temperatura de crescimento da levedura (37ºC), o número de chaperonas e co-chaperonas foi 38% maior na forma leveduriforme, do que em micélio. Fatores de virulência também foram identificados em levedura, entre os quais se incluem quitina desacetilase, isocitrato liase (FELIPE et al. 2005). De modo similar Goldman e colaboradores (2003), obtiveram as sequencias de 4.692 genes através da análise de ESTs de *P. brasiliensis* e identificaram homólogos à *C. albicans*. Entre os genes identificados, notam-se alguns relacionados com vias de transdução sinal tais como CST20, CPP1, CEK, PKA, CDC42 e GEF, atribuindo a participação desses genes para controlar a mudança morfológica. Ubiquitinas e proteínas de choque térmico como HSP70, HSP82 e HSP140 mostraram um perfil de expressão aumentado na transição

dimórfica de micélio para leveduras, sugerindo que há um maior controle de qualidade das proteínas durante a transição (Goldman et al., 2003).

Nunes e colaboradores (2005), realizaram microarranjos de DNA durante a transição morfológica de micélio para levedura nos tempos de 0, 5, 10, 24, 120 h pós-alteração de temperatura. Essa abordagem permitiu aos autores identificar 2.583 genes diferencialmente expressos na transição micélio-leveduras. A inibição da enzima 4-hidroxil-fenil piruvato dioxigenase (4-HPPD) pelo uso de NTBC [2-(2-nito-4-trifluorometilbenzoil)-ciclohexano-1,3,-dione] afetou a transição dimórfica de maneira dose dependente; além disso sua expressão foi aumentada cerca de 15 vezes durante a transição.

A análise do transcriptoma de *P. lutzii* durante diferenciação morfológica de micélio para levedura foi realizado por Bastos e colaboradores (2007), como anteriormente citado. Entre os transcritos que tiveram expressão aumentada destacam-se aqueles relacionados com síntese de membrana e parede celulares. Um gene que codifica uma α-glicosidase, envolvido no processamento de β-1,6-glicana, bem como genes para quitinase 1 (CTS1) e 3 (CTS3) foram induzidos durante a transição micélio-levedura, sugerindo o processamento de quitina (BASTOS et al. 2007). Durante a transição morfológica foram identificados genes envolvidos em vias de transdução de sinais tais como MAPK (proteína cinase ativada por mitógeno), serina/treonina cinase e histidina cinase, sugerindo que a morfogênese em *Paracoccidioides* é mediada por vias de transdução de sinais que controlam a adaptação ao ambiente para sobrevivência do fungo no hospedeiro (BASTOS et al. 2007).

2. Fosfoproteoma

2.1. Fosforilação de proteínas

Dentre os eventos de modificações pós-traducionais inclui-se a fosforilação. A fosforilação é um evento chave para diversos processos biológicos como diferenciação, sinalização e metabolismo celulares, apoptose, degradação de proteínas, ciclo, homeostase, comunicação, proliferação e sobrevivência celulares entre outros (Delom & Chevet, 2006; Jensen & Larsen, 2007; Thingholm, Jensen, & Larsen, 2009). Esta modificação pós-traducional é caracterizada por ser um processo transitório e reversível, que desencadeia uma mudança na conformação, na atividade e interação de uma proteína, que culmina em uma resposta para o estímulo celular. Proteínas que mantém o controle dessa modificação pós-traducional são denominadas, cinases e fosfatases, responsáveis pelas atividades de fosforilação e defosforilação respectivamente (Thingholm et al., 2009). Estima-se que 2-3% dos genes de eucariotos são constituídos por proteínas cinases. Já no que tange a fosfatases cerca de 100 proteínas ou mais tem sido preditas em humanos (ALONSO et al., 2004; DE SOUZA et al., 2013; LAM; GERIK; LODGE, 2013; SELVAN et al., 2014).

A fosforilação é um evento enzimático onde proteínas específicas são responsáveis por fosforilar resíduos de aminoácidos específicos (BURNETT G, 1954). Em eucariotos a fosforilação ocorre nos resíduos de serina, treonina, tirosina e histidina sendo que esse último, por ser a fosforilação altamente lábil, raramente são identificados em estudos abrangendo análises fosfoproteômicas (Puttick, Baker, & Delbaere, 2008). Anteriormente especulava-se que a fosforilação em resíduos de Ser, Thr, Tyr predominava em eucariotos. Sabe-se atualmente que fosforilação desses resíduos também ocorre em Archea e bactérias (CHAO et al., 2014; KENNELLY, 2014) Nota-se também

que uma proteína pode ser composta por múltiplos sítios de fosforilação permitindo assim que ela possa se adaptar a diferentes funções (Thingholm et al., 2009).

Fosfoproteínas apresentam baixa abundância, assumindo-se que algumas dessas são constitutivamente fosforiladas, enquanto outras são transitoriamente fosforiladas; ainda a forma fosforilada de uma determinada proteína pode apresentar-se em menor quantidade do que sua forma nativa (Reinders & Sickmann, 2005; Zolnierowicz & Bollen, 2000) Com o intuito de melhorar a detecção dessas proteínas, diversos métodos analíticos que propõem abordagens mais sensíveis e especificas têm sido empregadas. Essas abordagens abrangem o uso de tampões com inibidores de proteases e fosfatases, permitindo que o isolamento dessas proteínas apresente uma qualidade de amostra sem degradação e perda de grupos fosfatos.

Várias estratégias estão disponíveis para a detecção de fosfoproteínas, como eletroforese em gel bidimensional (2-DE) que permite separar proteínas de uma amostra complexa através do seu p*I* e peso molecular. Tais fosfoproteínas quando coradas com corantes como coomassie blue e prata apresentam diferentes isoformas em decorrência da modificação do seu p*I*, resultado da adição ou subtração de um grupo químico (Baik, Joo, Kim, & Lee, 2008; Cole et al., 2007; Masaki, Yamada, Hirasawa, Todaka, & Kanekatsu, 2008; Park et al., 2006; Thingholm et al., 2009) Outra metodologia é a marcação radioativa com ^{32}P ou ^{33}P detectada por autorradiografia (EYMANN et al., 2007; REINDERS; SICKMANN, 2005; SU et al., 2007). Outra metodologia disponível é o uso de anticorpos anti-fosfoserina, anti-fosfotreonina e anti-fosfotirosina; contudo pode ocorrer co-migração de proteínas não permitindo identificar-se sítios específicos de fosforilação (Kaufmann, Bailey, & Fussenegger, 2001; Thingholm et al., 2009).

Diversos estudos de fosfoproteoma usam métodos de espectrometria de massa (MS), após processamento proteolítico, para caracterizar fosfoproteínas. Entretanto, a

análise por esse método torna-se um processo difícil por fatores como presença de peptídeos não modificados, baixa eficiência de ionização de peptídeos fosforilados resultando em baixos sinais de intensidades comparado com íons de peptídeos não fosforilados. Nesse sentido para aumentar a eficiência e sensibilidade de identificação dessas fosfoproteínas, estratégias de enriquecimento de fosfopeptídeos tem sido empregadas (Thingholm et al., 2009). Entre os métodos de enriquecimento, destacam-se a imunopreciptação, onde uma única fosfoproteína, a partir de um lisado celular, pode ser detectada por uso de anticorpos (Xu & Yu, 2007). Para enriquecimento de fosfopeptídeos a técnica de cromatografia de afinidade de íons metais imobilizados-IMAC (Immobilized Metal Affinity Chromatography) tem sido amplamente usada. Esta técnica de afinidade sofreu diversos ajustes buscando um melhor enriquecimento de fosfopeptídeos. Íons metais como Fe^{3+}, Al^{3+}, Ga^{3+} ou Co^{2+} são quelados por ácido nitrilotriacético ou ácido iminodiacético formando uma fase estacionária onde fosfopeptídeos carregados negativamente em uma fase móvel podem se ligar (Chaga, Hopp, & Nelson, 1999; Ficarro et al., 2002; Porath, Carlsson, Olsson, & Belfrage, 1975; Posewitz & Tempst, 1999). Em estudos de fosfoproteoma, em larga escala, a cromatografia com TiO_2 tem sido bastante usada, visto que o fosfato apresenta a capacidade para ligar a metais tais como TiO_2 e ZrO_2 na forma de óxidos covalentes. A base da interação consiste na troca de íons e interações de ácido e base de Lewis (Leitner, 2016). Uma notável vantagem de utilizar TiO_2 é a sua sensibilidade e a compatibilidade com diversos tampões e sais usados em laboratórios de biologia celular e bioquímica (Benschop et al., 2007; Jensen & Larsen, 2007; Leitner, Sturm, & Lindner, 2011; Olsen et al., 2006, 2007; Wilson-Grady, Villén, & Gygi, 2008). Técnicas de pré-fracionamento tem sido aplicadas para amostras complexas, antes do enriquecimento de fosfopeptídeos tais como, cromatografia de troca de íons que incluem SAX (troca intensa de ânions) e

SCX (troca intensa de cátions) e a cromatografia de interação hidrofílica (HILIC) (Thingholm et al., 2009). Todas essas metodologias têm sido desenvolvidas visando melhorar o estudo de fosfoproteínas.

2.2. Fosfoproteoma em micro-organismos

Durante seu ciclo de vida os fungos precisam detectar e responder a sinais como condições ambientais e estresse imposto a eles durante interação com o hospedeiro (Kosti, Mandel-Gutfreund, Glaser, & Horwitz, 2010). Avaliando artigos que estudam fosfoproteoma em micro-organismos, esses apresentam resultados que ressaltam a importância de se estudar tais proteínas. Um estudo enfatiza a importância de cinases na patogênese de *Aspergillus fumigatus*, mencionando a participação da fosforilação de calcineurina em uma região rica em prolina e serina. Tal proteína se localiza nas pontas das hifas e permite que esse fungo filamentoso invada o tecido afetado. No estudo, os autores notaram que quando há um bloqueio da fosforilação em resíduos específicos de serina, houve um significante defeito de crescimento e virulência (Juvvadi et al., 2013). Como drogas antifúngicas que atuam diretamente na calcinerina causam imunossupressão, estudos têm focado em buscar proteínas reguladoras associadas a calcinerina como alvo para novas drogas (Juvvadi et al., 2015).

Um estudo de fosfoproteoma em *Saccharomyces cerevisiae* durante sua transição para sua forma filamentosa, mostrou uma maior anotação de proteínas para o metabolismo de glicose. Embora o mecanismo que liga a via de sinalização e o crescimento da pseudohifa não seja claro, foi encontrada uma proteína cinase responsiva à glicose, SKs1p, a qual contribui para a morfogênese da levedura durante privação de glicose, sendo requerida para o crescimento da pseudohifa (Johnson et al., 2014). Em estudo avaliando fosfoproteínas do fungo *Aspergillus nidulans*, foi possível notar uma

maior anotação, segundo os termos GO, de proteínas em categorias como sítio de crescimento polar. No que tange a processos biológicos houve uma maior anotação para transporte mediado por vesículas e organização do citoesqueleto (Ramsubramaniam, Harris, & Marten, 2014). *A. nidulans* é um fungo filamentoso que durante o processo de crescimento polar, uma maquinaria de proteínas do citoesqueleto como actina, microtúbulos e septinas e transporte mediado por vesículas se interconectam e atuam como um importante mecanismo para a morfogênese do fungo e secreção para as pontas das hifas (Riquelme, 2013), evidenciando assim a participação de fosfoproteínas durante processos de morfogênese em fungos.

Estudo avaliando o perfil de fosforilação de proteínas durante a resposta da levedura de *P. brasiliensis* ao estresse oxidativo, evidenciou que há uma ativação de diferentes sítios de fosforilação a esse estresse. Isso pode ser explicado pelo fato que ROS atua como um segundo mensageiro na via de sinalização celular induzindo a fosforilação. Como mencionado no estudo, foi possível verificar que existem diferentes vias que regulam os eventos de fosforilação, em diferentes condições de estresse oxidativo. Sugere-se que *P. brasiliensis* consiga proliferar em baixas concentrações de peróxido de hidrogênio, onde enzimas como ser/thr cinases são importantes reguladoras na capacidade de proliferação do fungo. Por sua vez, fosfatases regulam a redução da fosforilação em condições como resistência ao estresse oxidativo e morte celular (CHAVES et al., 2016). Um resultado interessante obtido pelos autores foi a descrição de sistemas de transdução sinal de dois componentes (TCST) (CHAVES et al., 2016). O mecanismo de ação desse sistema se dá através de um estímulo onde a proteína histidina cinase se autofosforila em um resíduo conservado de histidina, seguido pela transferência de um grupo fosforil para um resíduo de asparagina presente em uma proteína reguladora de resposta. Esse sistema tem sido descrito na patogênese de diversos fungos como

Candida albicans, Cryptococcus neoformans, B. dermatitidis e H. capsulatum, e uma vez que é ausente em mamíferos torna-se um alvo atrativo para terapias antifúngicas (Capra & Laub, 2012; Fassler & West, 2013).

Evento regulatório de enzimas produzido por fosforilação em *P. lutzii* foi descrito anteriormente para uma enzima chave do ciclo do glioxalato, a isocitrato liase (ICL). Essa capacidade regulatória mediada por fosforilação é explicada pelo fato que a desfosforilação *in vitro* da *Pb*ICL aumenta sua atividade em meio com glicose. os autores concluem que a regulação do ciclo do glioxilato é independe de regulação transcricional, mas controlado por modificação pós transcricional (CRUZ et al., 2011).

Em estudo proteômico quantitativo realizado pelo grupo do Laboratório de Biologia Molecular, UFG, utilizando-se 2-DE durante transição de *P. lutzii* foi possível identificar proteínas que apresentavam modificações pós-traducionais e entre as mais comuns foram a fosforilação (REZENDE et al. 2011). Entre as proteínas identificadas como fosforiladas incluem-se a enolase, gliceraldeído-3-fosfato desidrogenase, HSP70 e a fosfoglicerato cinase. A enolase é uma proteína que tem sido identificada em diferentes compartimentos celulares; em *P. lutzii* ela é localizada tanto no citosol, como na parede celular (Nogueira et al., 2010). Além disso, como elucidado por Rezende e colaboradores, (2011), 4 isoformas da enolase, com modificação por fosforilação, foram detectadas durante a transição micélio-levedura. Os dados sugerem que a enzima pode desempenhar diversas funções não só na via glicolítica, como também na virulência, através de processos como adesão, colonização e invasão (Donofrio et al., 2009; Nogueira et al., 2010). A gliceraldeído-3-fosfato desidrogenase é mais expressa em levedura de *P. lutzii;* os autores do trabalho ressaltam que sua localização na parede celular possibilita que a proteína se ligue à laminina, colágeno I e fibronectina, sugerindo seu papel na adesão do fungo à matriz extracelular do hospedeiro (Barbosa et al., 2006; Rezende et al., 2011).

Todos os estudos citados acima mostram a importância de se conhecer melhor os eventos de fosforilação e como eles podem afetar nos mecanismos de morfogênese, virulência, patogênese, entre outros, para os fungos.

Assim o estudo de proteínas, enzimas e eventos de fosforilação e as vias de sinalização que ocorrem durante as fases morfológicas de *Paracoccidioides*, pode fornecer uma melhor compreensão da biologia do fungo, possibilitando a identificação de vias e proteínas chave que podem ser, posteriormente, novos alvos para antifúngicos.

3. Justificativa

A paracoccidioidomicose é uma importante micose sistêmica, com alta incidência em países como Brasil, Venezuela, Equador e Colômbia. Para o sucesso da infecção os fungos termodimórficos do gênero *Paracoccidioides*, sofrem uma mudança na sua morfologia sob influência da temperatura. Inicialmente quando encontrado em

condições ambientais ou durante o cultivo *in vitro* a 22-25ºC manifesta-se como micélio. Nos tecidos do hospedeiro ou quando do cultivo a 36ºC, membros do complexo *Paracoccidioides* são caracterizados na forma de levedura. A identificação de genes e proteínas especificamente envolvidos na transição dimórfica micélio-levedura têm sido objeto de grande interesse, uma vez que a patogenicidade está intimamente ligada à transição dimórfica, pois isolados que não são capazes de diferenciar para levedura não são virulentos.

Diversos estudos transcricionais tem descrito genes relacionados com o dimorfismo do complexo *Paracoccidioides*. Contudo, apenas um estudo em nível de proteínas foi realizado para descrever o perfil proteômico durante a transição, em *P. lutzii*. O conhecimento dos mecanismos moleculares, em nível de proteínas, que governam a transição de *P. brasiliensis* requer investigação. Este é o primeiro estudo que investiga o perfil proteômico durante a transição micélio-para-levedura em *P. brasiliensis*, através da marcação iTRAQ, permitindo a quantificação relativa das amostras, além de complementar os dados transcricionais, já descritos (Nunes, Costa de Oliveira, et al., 2005). Assim, compreender os mecanismos envolvidos no processo de transição, olhando para os eventos de fosforilação de proteínas, representa parte da estratégia o entendimento de como os fungos patogênicos se adaptam às condições ambientais e do hospedeiro que são impostos a eles, uma vez que a atividade de muitas proteínas é regulada por modificações como as fosforilações. Além disso, as fosfoproteínas tem se tornado um alvo promissor para novas drogas, pois suas funções são amplamente diversas e estão envolvidas em funções chave para os patógenos. Vale ressaltar que a abordagem proposta para o presente estudo deverá possibilitar um avanço no conhecimento do processo de diferenciação celular de *P. brasiliensis.*

4. Objetivos

4.1. Objetivo Geral

Identificar e comparar as proteínas e fosfoproteínas expressas no fungo patogênico humano *Paracoccidioides brasiliensis* nas formas micélio e levedura e durante a transição dimórfica micélio -levedura.

4.2. Objetivos Específicos

4.2.1. Realizar marcação das amostras com iTRAQ (isobaric tag for relative and absolute quantitation-iTRAQ)

4.2.2. Realizar o enriquecimento das amostras com $TiO_{2;}$

4.2.3. Realizar a identificação de proteínas por espectrometria de massas;

4.2.4. Descrever e comparar perfis de acúmulo das proteínas nas fases de micélio, transição micélio- levedura e levedura;

4.2.5. Descrever mudanças metabólicas por meio de fosforilação de proteínas nas fases de micélio, transição micélio -levedura e levedura;

4.2.6. Realizar teste confirmatórios para o perfil metabólico encontrado.

Capítulo II

Conclusão

Nossos resultados descrevem que durante a transição morfológica de micélio para levedura, *P. brasiliensis* sofre uma reorganização metabólica para se adaptar ao aumento da temperatura no hospedeiro. Este estudo evidência que o fungo favorece um metabolismo mais aeróbico através das vias de beta-oxidação e TCA para a produção de ATP na fase parasitária. Esse aspecto contrasta ao que foi descrito para outra espécie do complexo *Paracoccidioides*, onde a fase leveduriforme tem a glicólise e a fermentação alcoólica como principais vias de produção de energia. Surpreendentemente, aqui nesse estudo observamos que enzimas reguladas positivamente na fase micelial relacionam à fermentação alcoólica da glicose. Além disso, alguns fatores de virulência foram encontrados nas células em transição micélio para levedura e nas leveduras como Hsps e proteínas associadas à adesão celular. Esses fatores de virulência podem ser relevantes para que o fungo estabeleça a infecção no hospedeiro.

Os dados obtidos representam parte da estratégia para entender como os fungos patogênicos se adaptam às condições ambientais e do hospedeiro, observando os eventos de fosforilação proteica, uma vez que a fosforilação controla os principais eventos na biologia das células fúngicas. Assim descrevemos, pela primeira vez, as fosfoproteínas presentes em micélio, transição de micélio-para-levedura e levedura. Este estudo permitiu avaliar que processos biológicos como metabolismo de aminoácidos, nitrogênio e carboidratos, tradução, transporte celular, podem ser regulados por fosfoproteínas em *P. brasiliensis*. Além disso, as proteínas relacionadas na transcrição e no ciclo celular foram acumuladas em micélio e levedura, mostrando a importância da fosforilação para a transcrição modulada nestas fases morfológicas.

Capítulo III

Elsevier Editorial System(tm) for Journal of Proteomics

Manuscript Draft

Manuscript Number:

Title: Proteomic and phosphoproteomic analysis during dimorphic transition of Paracoccidioides brasiliensis

Article Type: Full Length Article

Section/Category: Original Article

Keywords: iTRAQ; proteomics; phosphoproteomics; neglected disease; paracoccidioidomycosis; dimorphism.

Corresponding Author: Professor Celia Maria de Almeida Soares, PhD

Corresponding Author's Institution: Universidade Federal de Goias

First Author: Danielle S Araújo, PhD

Order of Authors: Danielle S Araújo, PhD; Maristela Pereira, PhD; Igor G Portis, PhD student; Agenor C Junior, PhD; Wagner Fontes, PhD; Marcelo V de Sousa, PhD;

Leandro P Assunção, PhD student; Lilian C Baeza, PhD; Alexandre M Bailão, PhD; Carlos A Ricart, PhD; Matthias Brock, PhD; Celia Maria de Almeida Soares, PhD

Abstract: Paracoccidioidomycosis (PCM) is a systemic mycosis, caused by thermodimorphic fungi of the genus Paracoccidioides. The transition process is vital in the pathogenesis of PCM allowing the survival of the fungus in the host. Thus, the present work performed a comparative proteome analysis of mycelia, mycelia to yeast- transition and yeast cells of Paracoccidioides brasiliensis. For that, tryptic peptides were labeled with iTRAQ and identified by LC-MS/MS and computational data analysis. This approach allowed the identification of 312 proteins differentially expressed in mycelia, mycelia-to-yeast transition and yeast cells. Data showed that P. brasiliensis yeast cells utilize aerobic beta-oxidation and the tricarboxylic acid cycle accompanied by oxidative phosphorylation for ATP production. Furthermore, yeast cells show a metabolic reprogramming in amino acid metabolism and in the induction of virulence determinants and heat shock proteins allowing adaptation to environmental conditions as the temperature increases. Interestingly, mycelium showed an up-regulation of enzymes related to alcoholic fermentation of glucose. Enrichment of phosphopeptides using TiO2 followed by their identification by LC-MS/MS was performed. Evaluation revealed 72 proteins with modification by phosphorylation. It was possible to describe some biological processes putatively regulated by phosphorylation in the fungus phases.

Suggested Reviewers: Joshua D Nosanchuk's PhD

josh.nosanchuk@einstein.yu.edu

Dr. Nosnchuk’s research has focus on the pathogenesis of human pathogenic

fungi, especially Histoplasma capsulatum, Candida parapsilosis, Paracoccidioides and Cryptococcus neoformans.

Marcio L Rodrigues

marciolr@cdts.fiocruz.br

Dr. Rodrigues is an expertise in cell biology and microbiology. Recently, he published about proteomics and cellular events involving fungal vesicles.

Gregory M Gauthier
gmg@medicine.wisc.edu

Dr. Gauthier’s research seeks to understand the pathogenesis of the thermally dimorphic fungi at the molecular level using Blastomyces dermatitidis as a model organism.

Carlos P Taborda
tabordausp@gmail.com

Dr. Taborda is an expert in Paracoccidioides brasiliensis. His work focus on the biology and immunology of this pathogenic fungus.

Opposed Reviewers:

Cover Letter

To the
Editor
Journal of Proteomics
Juan Calvete

Goiânia, October _9_th, 2018.

Dear Editor,

It is our pleasure to submit our article entitled "**Proteomic and phosphoproteomic analysis during dimorphic transition of *Paracoccidioides brasiliensis***" to the Journal of Proteomics editorial board.

In dimorphic pathogenic fungi, transition process from mycelium to the yeast phase is essential to establish the disease, since strains that are unable to differentiate into yeast cells are avirulent. Therefore, identification of genes and proteins specifically involved in the mycelia-to-yeast transition has been subject of interest. The thermodymorphic fungi of the genus *Paracoccidioides* represented by the species *P. brasiliensis*, *P. americana*, *P. restrepiensis*, *P. venezuelensis* and *P. lutzii* cause mycosis called Paracoccidioidomycosis (PCM). Because it is not a compulsory notified disease, it is estimated 3360 to 5600 cases per year, in Brazil, the country with higher prevalence of the disease. The present work performed a comparative proteome analysis of, mycelia, mycelia-to-yeast transition and yeast cells of *Paracoccidioides brasiliensis*. For that,

tryptic peptides were labeled with iTRAQ and identified by LC-MS/MS and computational data analysis. This approach allowed the identification of 312 proteins differentially expressed in mycelia, mycelia-to-yeast transition and yeast cells.

Data showed that *P. brasiliensis* yeast cells utilize aerobic beta-oxidation and the tricarboxylic acid cycle accompanied by oxidative phosphorylation for ATP production. This was a surprising result, as metabolism adapts in opposite of that found to *P. lutzii* another species in the complex. Furthermore, yeast cells show a metabolic reprogramming in amino acid metabolism and in the induction of virulence determinants and heat shock proteins. The data obtained here reinforce that during the morphological transition of mycelium-to-yeast cells, *P. brasiliensis* undergoes a metabolic reorganization for adapting to the increased temperature and nutritional environment in the host. Interestingly, mycelium showed an up-regulation of enzymes related to alcoholic fermentation of glucose, which was significantly less pronounced in the transition phase and in yeast cells. Moreover, some virulence determinants were found to be upregulated mainly in the mycelium-to-yeast transition phase and yeast

cells.

We also describe, for the first time, the phosphoproteins present in mycelia, mycelia-to-yeast transition and yeast cells. Enrichment of phosphopeptides using TiO_2 followed by their identification by LC-MS/MS was performed. Evaluation revealed 72 proteins with modification by phosphorylation. It was possible to describe some biological processes putatively regulated by phosphorylation in the fungus phases. Between

them, proteins related to transcription and cell cycle were up-regulated in mycelium and yeast cells, showing the importance phosphorylation for modulating the transcriptionl in these morphological phases.

We believe that this article represents a great contribution for those involved in this area.

We hope to hear from you soon

Sincerely,

Célia Maria de Almeida Soares, PhD
Laboratório de Biologia Molecular
Instituto de Ciências Biológicas Universidade Federal de Goiás, 74001-970, Goiânia, Goiás, Brazil.
Tel/Fax:55-6235211736
e-mail:<cmasoares@gmail.com >

***Significance**

Significance

Members of the *Paracoccidioides* genus cause Paracoccidioidomycosis (PCM), the most prevalent systemic mycosis in Latin America. Here, we report and compare the proteomes of morphological stages of *Paracoccidioides brasiliensis*, one of the most investigated species in the genus. By quantitative proteomic analysis, we report that yeast parasitic cells utilize aerobic beta-oxidation and tricarboxylic acid cycle accompanied by oxidative phosphorylation, for ATP production, in opposite of that found to *Paracoccidioides lutzii*. Furthermore, yeast cells show a metabolic reprogramming in amino acid metabolism and in the induction of virulence determinants and heat shock proteins. The data obtained here reinforce that during the morphological transition of mycelium-to-yeast cells, *P. brasiliensis* undergoes a metabolic reorganization for adapting to the increased temperature and nutritional environment in the host. Interestingly, mycelium showed an up-regulation of enzymes related to alcoholic fermentation of glucose, which was significantly less pronounced in the transition phase and in yeast cells. In addition to describing metabolic peculiarities in the fungus phases, which may be related to the fungus adaptation to the host, we also describe, the phosphoproteins present the different fungus phases.

***Graphical Abstract**

Click here to download high resolution image

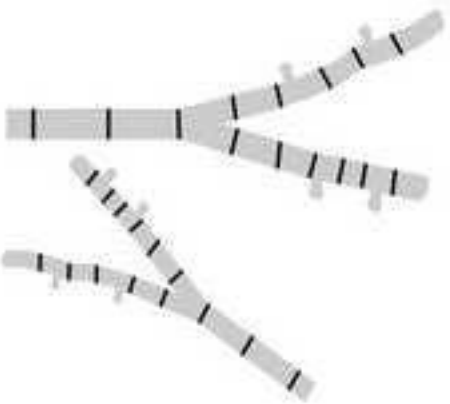

Mycelium

Glycolysis
glucose

Fermentation

pyruvate → ethanol

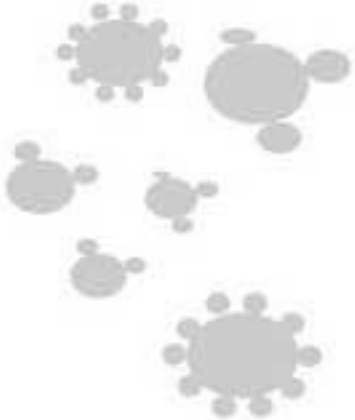

Yeast

Beta-oxidation

Methycitrate Cycle

Citric Acid Cycle

***Highlights (for review)**

Highlights

1. The pathogenicity of *Paracoccidioides* is linked to the dimorphic transition.
2. A proteomic approach compared mycelia, mycelia-to-yeast transition and yeast.
3. The proteomic profile of mycelium suggested anaerobic metabolism.
4. The proteomic profile of yeast cells suggested aerobic metabolism.
5. Biological processes are regulated by phosphorylation in the fungus phases.

Proteomic and phosphoproteomic analysis during dimorphic transition of *Paracoccidioides brasiliensis*

Danielle Silva Araújo [1,2], Maristela Pereira[1], Igor Godinho Portis[1], Agenor de Castro Moreira dos Santos Junior[2], Wagner Fontes[2], Marcelo Valle de Sousa[2], Leandro do Prado Assunção[1], Lilian Cristiane Baeza[3]; Alexandre Mello Bailão[1], Carlos André Ornelas Ricart[2], Matthias Brock[3], Célia Maria de Almeida Soares [1*]

[1] Laboratório de Biologia Molecular, Instituto de Ciências Biológicas, ICB II, Campus 10 II, Universidade Federal de Goiás, 74690-900, Goiânia, Goiás, Brazil;

[2] Laboratório de Bioquímica e Química de Proteínas, Instituto de Ciências Biológicas, Universidade de Brasília, 70910-900, Brasília, DF- Brasil;

[3] University of Nottingham, Fungal Biology and Genetics Group

[*] Corresponding author
Célia Maria de Almeida Soares
Laboratório de Biologia Molecular
Instituto de Ciências Biológicas II
Campus Samambaia
Universidade Federal de Goiás
74690-900, Goiânia, Goiás-Brazil
Tel: +55 62 3521-1736
E-mail address corresponding author: cmasoares@gmail.com (C.M.A Soares)

23

24 **Key Words**: iTRAQ, proteomics, phosphoproteomics, neglected disease, 25 paracoccidioidomycosis, dimorphism.

26

Abstract

Paracoccidioidomycosis (PCM) is a systemic mycosis, caused by thermodimorphic fungi of the genus *Paracoccidioides*. The transition process is vital in the pathogenesis of PCM allowing the survival of the fungus in the host. Thus, a comparative proteome analysis was performed on mycelia, mycelia-to yeast transition and yeast cells of *Paracoccidioides brasiliensis*. Tryptic peptides were labeled with iTRAQ and identified by LC-MS/MS and computational data analysis, which allowed the identification of 312 proteins differentially expressed in different morphological stages. Data showed that *P. brasiliensis* yeast cells utilize aerobic beta-oxidation and the tricarboxylic acid cycle accompanied by oxidative phosphorylation for ATP production. Furthermore, yeast cells show a metabolic reprogramming in amino acid metabolism and in the induction of virulence determinants and heat shock proteins allowing adaptation to environmental conditions during the increase of the temperature. Interestingly, mycelium showed an up-regulation of enzymes related to alcoholic fermentation of glucose. Enrichment of phosphopeptides using TiO_2 followed by their identification by LC-MS/MS was performed. Evaluation revealed 72 proteins with modification by phosphorylation. It was possible to describe some biological processes putatively regulated by phosphorylation in the fungus phases.

Significance

Members of the *Paracoccidioides* genus cause Paracoccidioidomycosis (PCM), the most prevalent systemic mycosis in Latin America. Here, we report and compare for the first time, the proteomes of morphological stages of *Paracoccidioides brasiliensis*, one of the most investigated species in the genus. By quantitative proteomic analysis, we report that yeast parasitic cells utilize aerobic beta-oxidation and tricarboxylic acid cycle accompanied by oxidative phosphorylation, for ATP production, in opposite of that found to *Paracoccidioides*

lutzii. Furthermore, yeast cells show a metabolic reprogramming in amino acid metabolism and in the induction of virulence determinants and heat shock proteins. The data obtained here reinforce that during the morphological transition of mycelium-to-yeast cells, *P. brasiliensis* undergoes a metabolic reorganization for adapting to the increased temperature and nutritional environment in the host. Interestingly, mycelium showed an up-regulation of enzymes related to alcoholic fermentation of glucose, which was significantly less pronounced in the transition phase and in yeast cells. In addition to describing metabolic peculiarities in the fungus phases, which may be related to the fungus adaptation to the host, we also describe, the phosphoproteins present in the different fungus phases.

Introduction

Dimorphic fungi of the *Paracoccidioides* genus cause a systemic mycosis called Paracoccidioidomycosis (PCM) [1,2]. The genus *Paracoccidioides*, was previously described to comprise a single species but more recent classifications divided the genus, in five species: *P. brasiliensis*, *P. americana*, *P. restrepiensis*, *P. venezuelensis* and *P. lutzii* [3,4].

Under free environmental conditions or during *in vitro* cultivation at 22-25ºC, members of this genus develop hyphae and form a mycelium. However, in host tissue or when cultivated at 36°C, these organisms display a yeast cell morphology [1]. The mycelium generally decomposes organic matter in soil that is necessary for environmental survival. Moreover, mycelia can respond to different environmental conditions such as changes in temperature and humidity and competition with other microorganisms [5]. Human infection initiates through the inhalation of conidia or hyphal fragments , which reach the pulmonary alveoli and transit to the yeast form in response to the increased temperature in the body [6,7].

The transition from mycelium into the yeast phase is essential for members of the *Paracoccidioides* complex to establish the disease, since strains that are unable to

differentiate into yeast cells are avirulent [8]. Therefore, identification of genes and proteins specifically involved in the mycelia-to-yeast transition has been subject of interest, since pathogenicity is intimately linked to the dimorphic transition [9]. In previous studies the transcriptome of *Paracoccidioides lutzii* mycelium and yeast cells have been investigated and provided insights into metabolism in the different fungal phases [10]. The transcription profile of mycelium suggested the shunting of pyruvate into aerobic metabolism, whereas in yeast cells pyruvate produced by glycolysis undergoes a fermentative metabolism [10].

Transcriptomic analysis of *P. brasiliensis* yeast cells deriving from a myceliumto-yeast transition was performed by monitoring the expression of 4,692 genes at several time points of the transition period by using microarray analyses [11]. The results revealed a total of 2,583 genes differentially expressed during transition, which were involved in several cellular processes such as cell wall metabolism, signal transduction, and oxidative stress response. The transcriptome analysis of early morphogenesis in *P. lutzii* mycelium undergoing transition to yeast cells, performed at our laboratory, revealed 179 genes that were positively modulated during the early transition process when compared to mycelia [12]. Of special note, genes related to fungal cell wall and membrane remodeling were positively regulated during mycelium to yeast transition, including those related to the cell wall carbohydrates biosynthesis and degradation, transporters of the precursors for the synthesis of those molecules, enzymes related to protein glycosylation and to the synthesis of membrane lipids. Notably, 34 expressed sequenced tags (ESTS) were significantly induced, whose cognate proteins were supposed to work in cell wall/membrane remodeling in the 22 initial hours of the transition from mycelia to yeast cells. The data strongly suggest that *P. lutzii* favors the membrane and cell wall remodeling in the early stages of the transition from mycelium to yeast cells [12].

In a pioneering quantitative 2-D electrophoresis based (2-DE) proteomic study of the morphological phases of *P. lutzii*, Rezende and colleagues (2011), detected changes in the relative abundance of the components of the proteome in mycelia, mycelia-to-yeast transition and yeast cells. This resulted in detailed 2-DE reference maps of proteins in the mycelia, yeast cells and mycelia to yeast transition and revealed a global reorganization of the *P. lutzii* metabolism during transition from mycelia to yeast cells [13]. A major change was detected in the accumulation of glycolytic enzymes and of alcohol dehydrogenase starting at 22 hours after the mycelium to yeast transition, consistent with transcriptional studies that have shown a shift toward anaerobic metabolism in the yeast phase of *P. lutzii* [10].

Proteomics can offer unique large-scale data on cellular differentiation, as we had previously described [13]. However, measurements of protein abundances alone may be insufficient to understand the regulation of the differentiation process since the activities of many eukaryotic proteins are modulated at post-translational levels. For instance, phosphorylation events may affect mechanisms of morphogenesis, virulence, pathogenesis and others processes in fungi [14–21]. In this respect, we have previously identified a phosphorylation dependent activation/inactivation cycle for isocitrate lyase, in *P. brasiliensis* yeast cells that appears to dominate the regulation of glyoxylate cycle activity, rather than the carbon source dependent gene expression [22].

Therefore, the study presented here also aimed at analyzing the phosphoproteome in the specific morphological phases and during the dimorphic transition. Integration of proteomic and phosphoproteomic data demonstrated that in the yeast phase a metabolic reprogramming occurs in pathways such as beta-oxidation, methylcitrate cycle and amino acid metabolism. Furthermore, induction of virulence factors and heat shock proteins that allow the fungus to adapt to the environmental conditions were observed. The alcoholic fermentation appears more abundant in mycelium of *P. brasiliensis* as compared to the yeast

form. Proteins related to β-1,3glucan synthesis required for the mycelium to construct a cell wall enriched in β-glucan polymers were annotated. In addition, SODs and thioredoxins important for the mycelial phase to increase protection against oxidative stress were also found to be differentially regulated.

It was possible to observe that biological processes regulated by phosphoproteins during the transition were distributed in functional categories such as amino acids, nitrogen, carbohydrate metabolism, translation, cellular transport, transcription and cell cycle. In the metabolism of nitrogen, formamidase was upregulated in mycelium. In addition, two ribose-phosphate pyrophosphokinases, previously described as required in the growth and maintenance of cell integrity were found in mycelium. Phosphorylation is also required for governing biological processes as cell cycle and transcription. Among the cell cycle several proteins that were modified by phosphorylation were up-regulated in mycelium and yeast cells. Phosphoproteins related to transcription were detected reinforcing the importance of phosphorylation for modulating transcriptional response in *P. brasiliensis*.

Material and Methods

Microorganisms and culture conditions

Paracoccidioides brasiliensis, *Pb*18, was used in all the experiments of this study. The mycelium and yeast phases were maintained in vitro in solid BHI medium with 4% (w/v) glucose at 22°C and 36°C for 15 and 7 days, respectively. The mycelium and yeast cells were inoculated in liquid BHI with glucose, 4% (w/v) at 22°C and 36°C under constant agitation (150 rpm) for 72 hours. The mycelium-to-yeast transition was also performed in liquid BHI medium. The fungus was initially incubated at 22ºC for 18 hours and after this period, the temperature was shifted to 36ºC, for 22 hours. The whole procedure of sample preparation and analysis is schematically depicted in **Fig.**

S1.

Extraction of proteins

Mycelia, mycelia in transition to yeast and yeast cells, were harvested by centrifugation at 1200 × g for 10 min at 4°C, washed three times with PBS and resuspended in lysis buffer [8 M Urea, 75 mM NaCl, 50 mM Tris, pH 8.2, 50 mM βglycerol phosphate, 1 mM sodium orthovonadate, 10 mM sodium pyrophosphate, 1 mM PMSF]. After addition of glass beads cells were mechanically lysed by vigorous shaking using a mini bead beater (Bio- Spec). Cell debris were removed by centrifugation at 10,000 × g for 15 min at 4°C. Proteins contents were estimated using the Qubit protein assay kit (Thermo Scientific, Bremen, Germany) and confirmed on

12% SDS-PAGE gel. The supernatants were stored at -80°C.

Acetone Precipitation of Proteins

Before performing protein digestion, an acetone precipitation step was performed on the cell extracts [23]. A total of 150 µg of protein sample was mixed with ice-cold acetone at 1:5 volume ratio and incubated for 16 h at -20°C. Subsequently, the samples were centrifuged at 1500 □ g, for 5 min, followed by removal of the supernatant. The pellet was resuspended in lysis buffer [8 M urea, 0.05 M triethylammonium bicarbonate buffer (TEAB), pH 7.9].

Sample preparation for LC-MS/MS

A trypsin digestion was performed on the acetone-precipitated and resuspended proteins. The sample in lysis buffer was maintained at 4°C and sonicated for 60 seconds. Subsequently a reduction step was performed for 25 min at 55°C by the addition of 0.005 M dithiothreitol. Iodoacetamide (0.014 M) was added and the samples were held for 40 min at room temperature in the dark. Soon after, DTT was added to the sample to give a final concentration of 0.005 M. To this sample 0.025 M TEAB, pH 7.9, 0.001 M $CaCl_2$, was added at a volume ratio of 1:5. Digestion was then performed by addition of trypsin (Promega) at the

enzyme:substrate ratio of 1:50, with incubation at 37°C for 12 h. The peptide samples were acidified with 0.1% TFA (v/v). Then, 50 µg of the sample was desalted in a StageTip on the low-binding P-200 tip with a C18 disc, and the rest of the sample was stored at -80°C. The eluate resulting from desalting was collected and dried in vacuum.

iTRAQ labeling

For iTRAQ labeling of protein samples of biological triplicates from each cultivation condition, the manufacturer's specifications were followed with some modifications. A total of 50 µg desalted and dried peptide was resuspended in 17 µl of 300 mM TEAB. Then iTRAQ reagent, which was resuspended in 70 µl of ethanol, was added. The solution was mixed and incubated at room temperature for 2 h, followed by mixing all the labeled samples in equal proportion (mycelium 114; transition 116; yeast 115). Samples were desalted with a StageTip on the low-binding P-200 tip with C18 matrix, and dried under vacuum. **Phosphopeptide enrichment**

The labeled samples were enriched with TiO_2, according to standard protocols [24], with some modifications. Briefly, iTRAQ-labeled multiplexed samples (100 µg for each replicate) were suspended in 1 M glycolic acid in 80% acetonitrile/5% TFA (v/v), and 0.6 mg of TiO_2 beads were added per 100 µg of peptide, followed by incubation under shaking (200 rpm) for 15 min. Beads were spun down, and the supernatant was transferred to microtubes. Addition of TiO_2 beads to the supernatants (using 0.3 mg TiO_2 per 100 µg of peptide) was repeated twice. The TiO_2 beads from the three rounds of enrichment were combined and washed first with 80% acetonitrile/1% TFA (v/v) and then with 10% acetonitrile/0.1% TFA (v/v) to remove non-phosphorylated peptides bound to TiO_2 in StageTip on the low-binding P-200 tip with a C18. Phosphopeptides were then eluted with 1.5% (v/v) ammonia solution, pH 11.5, and dried in vacuum.

Data acquisition by LC/MS-MS

The tryptic peptides were separated using a capillary column chromatography system (nano-UHPLC Dionex Ultimante 3000) coupled to a hybrid ion trap-orbitrap mass spectrometer, Orbitrap Elite ™ (Thermo Scientific). The first chromatography was carried out on a pre-column with internal diameter of 100 µm x 200 mm in length, packed in-house with silica spherical particles coated with C18 ReprosilPur of 5 µm with 120 Å pores (Dr. Maisch GmbH, Ammerbuch, Germany). The second

chromatography was carried out using an analytical column of internal diameter of 75 µm and 350 mm in length, also packed in-house with C18 Reprosil of particles 3µm with 120 Å pores (Dr. Maisch GmbH, Ammerbuch, Germany). The gradient for sample elution followed from 100% phase A (0.1% formic acid) to 26% phase B (0.1% formic acid, 95% ACN) for 180 min, 26% to 100% phase B for 5 min and 100% B phase for 8 min (a total of 193 min at 200 nL / min). After each run, the column was washed with

90% B-phase and re-equilibrated with phase A.

The spectra were acquired in positive mode by applying data-dependent automatic MS scan and acquisition of mass spectra in tandem (MS/MS). All MS scans in the orbitrap (mass amplitude: m/z 350-1800 and resolution: 120000) were followed by MS/MS of the fifteen most intense ions in the LTQ. Fragmentation in LTQ occurred by high-energy collision-induced dissociation (HCD) and selected ion sequences were dynamically deleted every 15 sec. The search and identification of proteins used Proteome Discoverer v.1.3 beta software (Thermo Scientific) with Mascot algorithm v.2.3 against *P. brasiliensis* database installed on the lab server and generated using the

Database on Demand tool containing the proteins found in UniProt/SWISS-PROT, UniProt/TrEMBL. The searches were made with the following parameters: MS precision of 10 ppm, MS/MS of 0.05 Da, until 2 cleavage sites lost;

carbamidomethylation of cysteines as modification and oxidation of methionine and Nterminal acetylation of the protein as variable modifications. The number of proteins, the group of proteins and the number of peptides were filtered with a false positive detection rate (FDR) of less than 1% and peptides with a rank of 1 and a minimum of 2 peptides per protein were accepted for identification with Proteome Discoverer. The Protein Center software (Thermo Scientific) was used to interpret the identified proteins.

Statistical analysis

The differences in protein expression levels among the three conditions were tested using the ANOVA and Tukey's test; the latter was applied after statistically significant results were obtained by ANOVA and was used to compare the differences among the means in analyzed groups. The statistical analyses were performed using R software (http://www.r-project.org/). A p-value ≤ 0.05 was considered statistically significant. For this analysis, only proteins detected in at least two replicates were evaluated.

Bioinformatics analysis

For the identified proteins we performed a search using the Blast2GO (https://www.blast2go.com/). Thus, the annotations of the identified proteins were assessed using the BLASTP algorithm with a BLAST Expect value of 10^{-3} and a maximum number of 30 hits in a non-redundant protein sequence database. After these analyses the mapping and annotation steps were performed [25]. The Motif-X algorithm (http://motif-x.med.harvard.edu/) was used to build motif enrichment and phosphorylation sites [26][27]. The reference database used in this search was the SGD

Yeast Proteome, and the central characters were Ser, Thr or Tyr with windows of 13, 15, and 17 amino acids. In addition, the identified proteins were sorted into functional categories based on the MIPS Functional categories database (Funcat 2.0) (http://mips.helmholtz-muenchen), available in pedant (http://pedant.gsf.de/). For cellular localization prediction, the

WoLF PSORT bioinformatics tool was used (https://wolfpsort.hgc.jp/). The heat maps were generated using the package *heatmap.plus* of software R [28].

Determination of ethanol concentrations in fungal lysates

A total of 2 g of yeast cells, mycelium and mycelium-to-yeast cells in transition were used to perform the assay. Briefly, the cells were lysed using glass beads and mini bead beater apparatus (Bio- Spec) in 4 cycles of 30 sec, keeping the samples on ice in the interval of each cycle. The cell lysates were centrifuged at 10,000 × g for 15 min at 4°C and the supernatant was used for the enzymatic assay. The concentration of ethanol was quantified by using an enzymatic detection kit according to the manufacturer's instruction (UV-test for ethanol, RBiopharm, Darmstadt, Germany). In the presence of the enzyme alcohol dehydrogenase, ethanol is oxidized to acetaldehyde by nicotinamide-adenine dinucleotide (NAD^+). Subsequently the acetaldehyde is quantitatively oxidized to acetic acid in the presence of aldehyde dehydrogenase and NAD^+, releasing NADH, which is determined by means of its absorbance at 340 nm.

Concentrations of ethanol were determined in biological triplicates.

Evaluation of reduced thiol level

Concentrations of thiol were determined in biological triplicates. Briefly, a total of 2g of mycelium, yeast cells and mycelium-to-yeast cells in transition were used to perform the assay. The cells were disrupted in lysis buffer (50 mM Tris-Cl, 150 mM NaCl, 50 mM ethylenediamine tetraacetic acid [EDTA], pH 7.2), using glass beads and a mini bead beater apparatus (Bio- Spec) in 4 cycles of 30 sec, keeping the samples on ice in the interval of each cycle. The cell lysates were centrifuged at 10,000 □ g for 15 min at 4°C and the supernatant was used for enzymatic assay. Thereafter, 100 µL of supernatant was combined with 100 µL of 500 mM sodium phosphate buffer, pH 7.5 and transferred in a microtiter well, followed by the addition of 20 µL of 1 mM DTNB (2-nitrobenzoic acid). Absorbance was measured at 412 nm using a plate

reader. The reaction principle is based on the fact that thioredoxin (Trx) is reduced to dithiol T(SH)2 by thioredoxin reductase (TR), in the thioredoxin system. The inhibition of TR decreases the amount of total reduced thiol [29]. Free thiol levels were determined using Ellman's reagent, 5, 50- dithio-bis-(2-nitrobenzoic acid), DTNB (Sigma Aldrich, Co).

RNA extraction, cDNA synthesis and real-time RT-PCR

RNAs obtained by using Trizol were treated with DNase (RQ1 RNase-free DNase, Promega). Then, the cDNAs were prepared using Superscript II reverse transcriptase (Invitrogen™, Life Technologies, Carlsbad, CA) and oligo (dT)15 primer. Quantitative real-time PCR reactions were performed in a StepOnePlus™ real-time PCR system (Applied Biosystems, Foster City, CA) using the SYBR green PCR master mix (Applied Biosystems). The genes encoding chitinase II (PADG_00994), pyruvate decarboxylase (PADG_00714) and the antigen gp43 (PADG_07615), were selected for analysis. Constitutively expressed alpha tubulin and L34 was selected to normalize the samples [30]. An aliquot of cDNA from each sample, serially diluted 1:5 was mixed and used to generate a relative standard curve. The relative expression levels of selected genes were calculated using the standard curve method for relative quantification [31].

Statistical analysis was performed by the student's t-test where p-values ≤ 0.05 were considered statistically significant.

Mitochondrial activity assay

Mycelia, transition mycelia-to-yeast and yeast cells of *P. brasiliensis*, were grown in biological triplicates. After, cells were harvested by centrifugation at 2,000 x g for 5 min at 4°C and diluted in PBS buffer at 10^6cells/ml. Then, the cells were stained with Rhodamine 123 (1.2 mM) (Sigma Aldrich) according to the manufacturer's protocol and following washed twice with 1X PBS. Stained cells were observed under a fluorescence microscope (AxioScope A1, Carl

Zeiss) and analyzed with the 546–512 nm filter. The imagens were acquired using the AxioVision Software (Carl Zeiss).

Results and Discussion

Analysis of proteins in mycelium, mycelium-to-yeast transition and yeast cells

A large-scale proteome analysis was performed for mycelium, mycelium-toyeast transition and yeast cells, in which an isobaric tag to proteins from each condition allowed relative quantification of the expressed proteins. A flow chart of the experimental steps is shown in **Fig. S1**.

Proteins with high FDR confidence and found in at least 2 replicates were selected for further analysis as depicted in **Fig. S2**. A total of 1008 proteins were identified through mass spectrometry. In **Table S1** the protein accession number and description, the coverage of proteins, the number of peptides, unique peptides, groups of proteins, number of amino acids identified, protein molecular mass (kDa) and isoelectric point are presented. In addition, **Table S1** also depicts the post translational modifications found for each protein, the protein abundance and the protein score.

Statistical analysis, ANOVA ($p \leq 0.05$) and Tukey's test, determined 312 differentially regulated *P. brasiliensis* proteins. **Table S2** summarizes all differentially expressed proteins from the three morphological phases; whereby the accession number and description of the protein, p-value determined by the ANOVA test, and average abundance obtained in the Tukey's test is given. Furthermore, the identified proteins were sorted into functional categories by the functional catalog (Funcat 2.0) or KEGG terms and depicts the score of the proteins obtained from the MS Amanda 2.0 and pvalue (≤ 0.05, ANOVA). Several proteins have been grouped as unclassified, since their biological function is still unknown. Most of these unclassified proteins are hypothetical (even after Blast2GO search), which may explain why no term can be assigned

to most of these proteins (**Fig. S3, panel A**). **Figure S3, panel B** depicted top-hit of species in the genus *Paracoccidioides* that were homologous for proteins found using Blast2GO.

Metabolic changes in the mycelium

At first, we compared the differentially expressed proteins in mycelium to the transition state and to yeast cells. In the metabolism category, mycelium presented upregulation of proteins related to nucleotide/nucleoside/nucleobase, carbohydrate metabolism, phosphate metabolism, and secondary metabolism (**Table S3**). We first focused on the category of genes encoding for proteins related to energy production. Mycelium presented a high number of up-regulated enzymes related to glycolysis and fermentation than the transition phase and yeast cells. For example, fructose-1,6bisphosphate aldolase, class 2 (PADG_00852), hexokinase (PADG_07950), triosephosphate isomerase (PADG_06906) and 2,3-bisphosphoglycerate-independent phosphoglycerate mutase (PADG_05109) were up-regulated in mycelium. In respect to enzymes related to alcoholic fermentation, two alcohol dehydrogenases (PADG_11405) and (PADG_04701) were induced in comparison to the other two developmental stages. This fact caught our attention since it had been previously described that *P. lutzii* presents a more anaerobic metabolism in yeast cells, when compared to mycelia [10,13]. Therefore, we studied ethanol accumulation by comparing mycelium, transition of mycelium-to-yeast and yeast phases, as shown in **Fig. 1, panel A**. In agreement to the proteomic data, the mycelium showed a higher accumulation of ethanol than the other phases. In addition, analysis of the level of expression of alcohol dehydrogenase (PADG_11405) from proteomic analysis confirmed that the abundance of this enzyme was significantly higher in mycelium (**Table S3**). Pyruvate decarboxylase (PADG_00714) is required to shunt pyruvate from glycolysis into the fermentative pathway of ethanol production by converting pyruvate into acetaldehyde. Therefore, we performed expression analyses on the respective transcript by real time PCR (**Fig. 1B**) demonstrating a 6 times higher expression in mycelium. This

reinforces that in contrast to *P. lutzii* the mycelium from *P. brasiliensis* is dominated by a fermentative metabolism producing ethanol from pyruvate. This is also in line with a high activity of glycolysis since enzymes of the glycolytic pathway are induced in the mycelium (**Table S3**).

While our data strongly suggest that *P. brasiliensis* presents a more anaerobic metabolism in the mycelium compared to mycelia-to-yeast transition phase and yeast cells, previous transcriptional studies with *P. brasiliensis* undergoing mycelia-to-yeast transition using a biochip detected an induction of transcripts encoding alcohol dehydrogenase I and pyruvate decarboxylase during the dimorphic transition from mycelia to yeast cells. However, the latter data were obtained at last 120 h after dimorphic transition, which could explain the difference in the transcript levels compared to the protocol used here [11].

Besides an increased fermentation capacity, proteins related to the maintenance of the intracellular redox state and protection against oxidative stress such as glutathione S-transferase Gst3 (PADG_03423), two thioredoxins (PADG_02764, PADG_05504), mitochondrial peroxiredoxin PRX1 (PADG_03095), superoxide dismutase [Cu-Zn] SOD1 (PADG_07418), Fe-Mn family superoxide dismutase SOD2 (PADG_01755) were up regulated in mycelium (**Table S3**). In agreement with these proteomic data, evaluation of the enzymatic activity of thioredoxin by measuring the thiol dosage revealed that mycelium produces more thiols than the other two morphological phases (**Fig. 2A**). The thiol levels also correlated with the expression of thioredoxins that were up-regulated in mycelium (**Fig. 2B**). This suggests a need for increased protection against reactive oxygen species in mycelia compared to the other phases.

An accumulation of Rad23 also caught our attention. Rad23 is an important protein involved in nucleotide excision repair (NER) and *Saccharomyces cerevisiae rad*23 deletion mutants show increased sensitivity to DNA-damaging agents as Rad23 has been assumed to protect Rad4 from degradation by the proteasome in cells [32].

Similarly in plants ultraviolet light causes DNA damage and the proteins RAD4 and RAD23 are required for UV tolerance [33]. As the mycelium is the major morphology in the free saprobiotic phase, those proteins could be of special importance to provide protection against DNA damage from conditions found in the environment.

We also detected major differences in the abundance of enzymes involved in cell wall biosynthesis and degradation. A chitinase class II (PADG_00994) showed an accumulation in mycelium (**Table S3**). Additionally, other enzymes such as β-1,3exoglucanase (PADG_03691), cell wall protein ECM33 precursor (PADG_04499) and β-1,3-glucosidase (PADG_02862) were more abundant in mycelium compared to the mycelium to yeast transition and yeast cells (**Table S3**). Of special note, β-1,3glucosidase (PADG_02862), and β-1,3-exoglucanase (PADG_03691) cleave β-1,3 glucan polymers that predominate in mycelia and consequently may be relevant for cell wall maintenance [34]. A diagram depicting the processes potentially induced and repressed in the *P. brasiliensis* cell wall mycelia and yeast cells is shown in Supplementary **Fig. 4**.

Table S4 depicts the down regulated proteins in mycelia compared to the other analyzed phases. Amino acid metabolism was down-regulated in mycelium compared to yeast cells, which is consistent with transcriptional data, in which *P. brasiliensis* revealed a predominance of up regulated transcripts related to the amino acid metabolism in yeast cells [11]. Furthermore, most enzymes of the tricarboxylic acid cycle, electron transport and oxidative phosphorylation were repressed in mycelium compared to mycelium-to-yeast transition and yeast cells (**Table S4**). Most strikingly, all enzymes involved in beta-oxidation of fatty acids were down regulated (**Table S4**). Those data reinforce the presence of a more anaerobic metabolism in the mycelium phase, compared to transition phase and yeast cells. These data demonstrate significant metabolic differences among members of the

Paracoccidioides genus. While metabolism of mycelium from *P. brasiliensis* seems to follow a fermentative pathway, transcriptomic and proteomic analyses of the different morphological phases of *P. lutzzi* demonstrated a more anaerobic metabolism for yeast cells [10, 13]. A heat map and the related metabolic pathways that are induced and repressed in *P. brasiliensis* mycelia compared to mycelia-to-yeast transition and yeast cells is shown in **Fig. 4**.

Interestingly, differences were also observed in proteins related to ribosome biogenesis, protein synthesis, protein folding and stabilization (**Table S4**). Here these data indicate a decreased turnover of proteins in mycelium compared to mycelium-toyeast transition and yeast cells.

Metabolic changes during the mycelium-to-yeast transition phase

Metabolic processes that predominate during the mycelium-to-yeast transition compared to mycelium and yeast cells are depicted in **Supplementary Table 5**. The accumulation of phosphoenolpyruvate carboxykinase (PADG_08503) suggests a shift of metabolism to gluconeogenesis at 22 h after entering the transition phase. This enzyme produces phosphoenolpyruvate, a precursor of glucose synthesis. In *P. brasiliensis* the enzyme phosphoenolpyruvate carboxykinase has been described as relevant for metabolic adaptation within macrophages [35]. Additionally, the exoantigen Gp43 (PADG_07615) accumulates during transition. However, despite significant changes on the transcript level [11], overall only 19 proteins accumulated at the 22 h transition phase, which could be explained by the time required to translate a protein from a transcript.

Besides proteins strongly upregulated, the 22 h temperature shift period resulted in a reduction of several proteins that are involved in different metabolic processes (**Supplementary Table 6**). Proteins involved in amino acid metabolism were strongly down

regulated. Similarly, the TCA, glycolysis, alcoholic fermentation, electron transport and oxidative phosphorylation were repressed at this cellular stage, strongly suggesting a major repression of the overall cellular metabolism at this early time of transition. According to Medoff and collaborators (1987), immediately after the temperature shift, the metabolism of *Paracoccidioides* is characterized by partial or complete uncoupling of oxidative phosphorylation and immediate decline in ATP levels. Subsequently, there is a dormant period of 4 to 6 days that is characterized by absent or low rates of respiration and inhibition of protein synthesis [36]. Our proteomic data showing a high number of repressed proteins corroborate with the description of the metabolic changes described above.

Metabolic changes in the established yeast phase

In yeast cells several enzymes of amino acid metabolism were more abundant than in mycelium and during the transition phase (**Supplementary Table 7).** In particular**,** the accumulation of 4-hydroxyphenylpyruvate dioxygenase (PADG_08468) an enzyme essential for tyrosine metabolism, was observed in yeast cells. This is in agreement with previous microarray analyses and it had been shown that inhibition of this enzyme inhibits the dimorphic transition in *P. brasiliensis* [11].

Furthermore, 24 ribosomal proteins showed an accumulation in yeast cells (**Supplementary Table 7**), which indicates an increased requirement for *de novo* protein biosynthesis in this morphological state. In terms of metabolic physiology proteins related to the tricarboxylic-acid cycle (TCA), such as pyruvate dehydrogenase

(PADG_00246), ATP-citrate synthase (PADG_04993), succinyl-CoA ligase (PADG_02260 and PADG_00317) and aconitate hydratase (PADG_11845), were more abundant in yeast cells compared to transition phase and mycelium. Also, proteins involved in the electron transport

chain and ATP synthase complex also were predominantly induced in yeast cells (PADG_07813, PADG_05402, PADG_08349, PADG_07042, PADG_02561), which agrees with an increased metabolite flux through the TCA cycle accompanied by aerobic respiration. The Supplementary **Fig. 5** depicts activity assays from mycelia, transition phase and yeast cells where it was possible to observe an increased aerobic respiration in yeast cells compared to mycelia and transition phase. This is also in accordance with biochemical data published for *Paracoccidioides* sp. in which Medoff and collaborators (1986) described increasing concentrations of cytochrome components and resumption of the normal respiration in yeast cells five days after transition [36]. Interestingly, our data indicate that metabolism appears not to be directly dependent on glucose utilization, as all enzymes involved in beta-oxidation of fatty acids were highly abundant in yeast cells compared to the mycelia-to-yeast transition and mycelia (**Supplementary Table 7)**. In agreement, during in vivo infection of lungs by *P. brasiliensis*, enzymes related to lipid degradation were up-regulated in yeast cells [37].

In fungi, regulation of production of heat shock proteins (HSPs) is modulated in response to various stimuli, including temperature. As the process of cell differentiation in *Paracoccidioides* spp. to the parasitic phase requires an increase of the temperature, HSPs are expected to accumulate during the morphological transition [38]. However, our data indicate that accumulation of HSPs does not immediately take place at 22 h after temperature shift but is slightly delayed with seven more abundant HSPs (PADG_01711, PADG_02785, PADG_07715, PADG_00430, PADG_08369, PADG_02761) in the yeast phase. **Fig. 5** depicts a heat map the HSPs induced and repressed in yeast cells compared to mycelia and mycelia-to-yeast transition.

Besides HSPs, cytochrome c peroxidase, which is an important cell-rescue related protein, accumulated in yeast cells compared to the other phases. This enzyme is involved in *P. brasiliensis* in the response to oxidative and nitrosative stresses and mutants with low

expression of the gene were more sensitive to nitrosative stress [39]. Furthermore, these antisense knockdown mutants of *P. brasiliensis* revealed a decreased survival inside macrophages and in a murine model of infection [39]. The higher expression in yeast cells added of the previous data, corroborate the protein to be designated as a virulence factor.

Evaluation of proteins at the yeast phase revealed down regulation of enzymes involved in ethanol production such as the alcohol dehydrogenases Adh1 and Adh2 (PADG_11405 and PADG_04701) (**Supplementary Table 8**). Of special note six enzymes of the glycolysis, including hexokinase, were down regulated in yeast cells compared to mycelia and mycelia-to yeast transition. These data strongly support the observed metabolic preference for the TCA cycle and respiration and is in agreement with similar observations in *Talaromyces marneffei* [40].

We also observed a dramatic change in the composition of cell wall related enzymes. The chitinase class II (PADG_00994), β-1,3-glucosidase (PADG_02862) and β-1,3-exoglucanase (PADG_03691) showed a significant decrease (**Supplementary Table 8)**. Especially the decrease in the amount of chitinase correlates to the high amount of chitin found in yeast cells [41].

Summary of metabolic pathways in *P. brasiliensis* in the different morphological phases

Proteomic analysis of the three morphological phases of *P. brasiliensis* revealed unexpected data related to carbon source utilization and energy production. While yeast cells of *P. lutzii* use glycolysis and fermentation as main energy production pathways, *P. brasiliensis* yeast cells rely on the aerobic beta-oxidation and the TCA cycle for ATP production, as depicted

in **Fig. 6**. This observation is sustained by the accumulation of enzymes such as acyl-CoA dehydrogenase (EC 1.3.8.1), enoyl-CoA hydratase, (EC:4.2.1.17), aconitate hydratase (EC:4.2.1.3), thiolase (EC:2.3.1.16), citrate synthase (EC:2.3.3.1), succinyl-CoA transferase (EC:2.8.3.5) and others that were highly present in yeast cells. In addition, eight proteins of oxidative phosphorylation were induced in the yeast form. Furthermore, besides an accumulation of enzymes involved in betaoxidation of fatty acids, an accumulation of methylcitrate synthase and methylcitrate dehydratase was observed. These enzymes play an essential role in the methylcitrate cycle and convert propionyl-CoA into pyruvate. As propionyl-CoA can derive from the beta-oxidation of odd-chain fatty acids and from degradation of amino acids, this metabolic pathway may be essential for increasing the nutritional status of yeast cells by simultaneously preventing the accumulation of toxic propionyl-CoA that may derive the degradation pf amino acids [42].

In contrast, alcoholic fermentation of glucose was found to be up-regulated in mycelium. This is supported by the accumulation of glycolytic enzymes such as the glycolysis specific enzyme hexokinase (EC:2.7.1.1), fructose 1,6-biphosphate aldolase (EC:4.1.2.13), triose phosphate isomerase (EC:5.3.1.1), and phosphoglycerate mutase (EC:5.3.1.1), as well as two alcohol dehydrogenases (EC:1.1.1.1), (**Fig. 4)**. Although a dominant fermentative metabolism of *P. brasiliensis* mycelium was not expected, this data agrees with the dimorphic fungus *T. marneffei* in which hyphae also predominantly exhibit a fermentative metabolism with the production of ethanol and a minimum flow of pyruvate through the citric acid cycle. On the contrary, yeast cells of both, *P. brasiliensis* and *T. marneffei*, display increased use of shunting metabolites through the TCA cycle [40].

In agreement with a limited glucose supply during the parasitic phase, the metabolism of amino acids seems important for adaptation to the host environment. This may explain the increased abundance of proteins involved in amino acid metabolism in yeast cells of *P.*

brasiliensis [43,44]. The highly abundant protein 4HPPD (EC:1.13.11.27) is related to tyrosine degradation and had been described as a new potential drug target, since the use of the specific 4-HPPD inhibitor NTBC [2-(2nitro-4trifluoromethyl-benzoyl)-cyclohexane-1,3-dione] prevents the dimorphic transition in a dose-dependent manner [11]. Studies on *T. marneffei* yeast cells revealed a lower consumption rate of glucose in yeast cells compared to hyphae accompanied by the utilization of several amino acids that are likely to undergo deamination and fuel the TCA cycle. This shift to a more efficient energy metabolism reduces the requirement for exogenous glucose, allowing for an optimization of nutrient utilization in the limited environment of macrophages [40]. We also observed an accumulation of the enzyme adenosylhomocysteinase (EC:3.3.1.1) in yeast cells of *P. brasiliensis*. This enzyme degrades S-adenosylhomocysteine, which is a strong inhibitor of S-adenosyl methionine-dependent methyltransferases, which is essential for the synthesis of the phospholipid phosphatidylcholine, preferentially found in yeast cells [45,46].

Besides the carbon flux through metabolic pathways, remodeling of the cell wall during the transition from mycelium to yeast cells is vital. As with other fungi, the cell wall of *P. brasiliensis* is a network of glycoproteins and polysaccharides that protects the fungal cell from environmental stress [47] and confers virulence to the fungus. Compared to mycelium, an increase in chitin levels in parasitic phases was detected in *P. brasiliensis* [48], which defines the cell wall thickness [48]. Furthermore, the chitin degrading chitinase CTS2 was accumulated in mycelium and decreased in the yeast phase. Moreover, glucans account for approximately 40% of the cell wall components in mycelium and yeast cells of *P. brasiliensis* [48]. α-glucan is the major cell wall glucan of the yeast form, whereas the mycelial form contains larger amounts of βglucan [49,50]. An α-glucan layer is essential for avoiding dectin-1-mediated phagocytosis of yeast cells by macrophages, by masking the β-1,3-glucan layer, as shown for *Histoplasma capsulatum* chemotype II cells [51]. Therefore, variations in cell wall glucans may play a key role in the dimorphism of the fungus and, thus, its pathogenesis. For a remodeling of

the glucan structure, β-(1,3)-glucanase plays a key role in morphogenetic-morpholytic processes by hydrolyzing the β-glucan chain, which is largely predominant in mycelial phase [34]. In agreement with an alteration of the glucan structure, a β-(1,3)-exoglucanase was up regulated in mycelium and transition of mycelium-to-yeast cells. Furthermore, other cell wall related proteins such as Ecm33 were differentially produced in mycelia (Supplementary **Fig.4**). Ecm33 is a GPI-linked cell wall protein that plays an important role for cell wall integrity and architecture in *C. albicans* [52][53]. In *P. lutzii* this protein occurs in the mycelium cell wall, in agreement to the data here presented [54].

Phosphoproteins identified in the three morphological phases of *Paracoccidioides brasiliensis*

Similarly, to the filter applied to proteins found in global fraction of the different morphological phases of the fungus, the fraction of proteins enriched with TiO_2 was composed of those that presented high and medium FDR confidence and were found in at least 2 replicates, resulting in identification of a total of 195 proteins, as depicted in **Table S9**. The table shows the protein accession number and description, the coverage of proteins, the number of peptides, unique peptides, groups of proteins, number of identified amino acids, molecular weight (kDa), isoelectric point of proteins. In addition, it shows the modifications found for each protein, the protein abundance and the protein *score*. After this selection, we searched proteins that showed phosphorylation modification, both in the global fraction and in the TiO_2 enriched fraction. It was possible to find 72 proteins in the enriched TiO_2 fraction and 23 proteins in the global fraction, which presented phosphorylation, as shown in **Tables S10 and 11,** respectively. By using TiO_2 enrichment, phosphoproteins that are less abundant in complex samples, can be isolated by the ability of the phosphate group to bind metals such as

TiO_2 in the form of covalent oxides, allowing an enriched fraction of phosphoproteins (Supplementary **Fig. S6**) [55].

When evaluating the phosphoproteins, our proteomic analyzes resulted in a total of 178 and 40 phosphopeptides for the enriched TiO_2 and global, fractions, respectively and 220 and 51 phosphosites respectively (**Fig. 6A**). Of the total of 178 phosphopeptides, 140 had one phosphorylation, 34 had two phosphorylations and 4 contained three phosphorylations for the enriched TiO_2 fraction. The proportion for global fraction corresponded to 30:9:1 for one, two and three phosphorylations of the total of 40 phosphopeptides. Therefore, we were able to verify multiple phosphorylation events in the different morphological phases (**Tables S10-11**).

Moreover, when we evaluated the residues that comprise phosphosites, the proportion of 160:31:1 for Ser/Thr/Tyr were identified in enriched TiO_2 fraction (**Fig. 6B**). For the global fraction this proportion corresponded to 34:17:5 Ser/Thr/Tyr residues (**Fig. 6B**). It is known that protein kinases are the key enzymes for phosphorylation of Ser/Thr/Tyr residues. This event depends on the recognition of a consensus sequence (phosphorylation motif), represented by amino acids that surround the phosphorylation sites. To search for these consensus sequences in the identified proteins, we used the Motif-X algorithm, which allows the enrichment of such motifs.

Fig. 6C shows the result of these analyzes where the proportion of enriched motifs were 21:13:1 Ser/Thr/Tyr residues in TiO_2 enriched fraction and 6:3 Ser/Thr residues in global fraction.

Supplementary **Fig. 7** shows the functional classification of phosphoproteins found for the three phases of *P. brasiliensis*, obtained by the functional catalog (Funcat 2.0) or KEGG terms, for both TiO_2 enriched and global fraction (**Tables S10 and S11**). Proteins were distributed in several functional categories such as, metabolism (8%), energy (3%), cell

cycle and DNA processing (8%), transcription (23%), protein synthesis (8%), protein folding (8%). The categories of cellular transport (12%), cellular communication (3%), cell rescue (2%), biogenesis of cellular components (1%), cell fate (1%) and unclassified proteins (23%) were also included.

Supplementary Figure 8 depicts the distributions of terms obtained from Gene Ontology (Blast2GO) for categories, to obtain more information about those proteins. Regarding to cell localization, the proteins were mainly distributed in nucleus (49%), followed by cytoplasm (14%), mitochondrion (13%), membrane (11%), ribosome (4%), and peroxisome (2%). In agreement to our results, the analysis of phosphoproteins from *C. albicans* and *Aspergillus nidulans*, revealed a predominant localization in cytoplasm and nucleus as deduced from the GO terms of cellular components [20,21]. According to the annotation for molecular function, proteins with RNA binding (8,1%), protein binding (6%), nucleotide binding (3.5%), DNA binding (3.5%), catalytic activity (3.5%) were observed.

Profile of phosphoproteins differentially accumulated in the three morphological phases of *Paracoccidioides*

Due to our focus on differentially regulated proteins in phases of *P. brasiliensis*, we gave attention to the phosphoproteins up and down regulated in the different morphological phases as shown in **Table S12**. We considered phosphopeptides that differed in relative abundance among the individual phases and a difference was considered as significant if $p \leq 0.05$ as determined by the *t* test.

At first, we directed our attention to the phosphoproteins regulated in yeast cells. 18 and 4 phosphoproteins were down and up regulated, respectively, in yeast cells compared to

623 the other fungus phases, as depicted in **Table S12.** The down regulated phosphoproteins
624 belong to the functional categories of carbohydrate and amino acid metabolism, transcription,
625 protein synthesis and 4 were unclassified. Regarding to the up regulated phosphoproteins in
626 the yeast phase, they were classified as members of the metabolism of amino acids, cell cycle
627 and DNA processing and protein synthesis and folding. Regarding to mycelium only a single
628 phosphoprotein was decreased in comparison to the two other analyzed phases and no
629 phosphoprotein was up regulated in mycelium. 20 phosphoproteins shared an increase in two
630 phases and 4 shared a decrease, as depicted in **Table S12**. Regarding to mycelia-to-yeast
631 transition only one phosphoprotein was decreased in comparison to the two other analyzed
632 phases and no phosphoprotein was up regulated; 18 phosphoproteins shared increase in two
633 morphological phases and 4 shared a decrease as depicted in **Table S12**. Therefore, it can be
634 concluded that an increase of phosphoproteins is most frequently occurring in yeast cells.

635 However, ribose-phosphate pyrophosphokinase (PADG_00780) was down-
636 regulated in yeast cells. This protein plays a role in a diverse range of functions such as the
637 pentose phosphate pathway, nucleotide metabolism, in the biosynthesis of nucleotides and
638 coenzymes, and biosynthesis of the amino acids histidine and tryptophan [56]. In *S. cerevisiae*
639 its presence is related to maintenance of cell integrity [57]. One member of this family in *S.*
640 *cerevisiae*, Prs5 is a protein kinase, donating a phosphate group to ribose-5-phosphate to yield
641 PRPP [58]. Mutation of three phosphosites in the protein compromised the expression of the
642 gene encoding the stressactivated β-1,3 glucan synthase, Fks2 [59]. In *P. brasiliensis* β-1,3
643 glucan predominates in the mycelia phase, in agreement to the up regulation of ribose-
644 phosphate pyrophosphokinase in mycelia and transition from mycelia to the yeast phase.

645 CCR4-Not complex is a multifunctional regulator that plays important roles in multiple
646 cellular processes in eukaryotes. In the present study, a protein homologue accumulates in

yeast cells. FonNot2, a core subunit of the CCR4-Not complex, plays a critical role in regulating virulence in the water melon wilt pathogen *Fusarium oxysporum* f. sp. *niveum* [60].

Conclusion

In this work we have studied the transition process of *P. brasiliensis*, one of the most studied members of the *Paracoccidioides* complex, by proteomic, biochemical and molecular analyses. Results revealed that yeast cells of *P. brasiliensis* compared to mycelium display a more aerobic metabolism. This was a surprising result, as metabolism adapts in opposite of that found to *P. lutzii*. The data obtained here reinforce that during the morphological transition of mycelium-to-yeast cells, *P. brasiliensis* undergoes a metabolic reorganization for adapting to the increased temperature and nutritional environment in the host. This study provides evidence that *P. brasiliensis* favors beta-oxidation, methylcitrate cycle, electron transfer and oxidative phosphorylation in the parasitic phase. Even more surprising, alcoholic fermentation, at least under laboratory conditions, is strongly favored in mycelium compared to yeast cells. Some virulence determinants were found to be upregulated mainly in the mycelium-to-yeast transition phase and yeast cells, with a special importance of HSPs, proteins associated to cell adhesion, and cytochrome c peroxidase. Those virulence determinants can be assumed to be relevant for the fungus to establish an infection. We also investigated the phosphoproteome of the three morphological phases. As a result, this study implicates that biological processes such as amino acid, nitrogen and carbon metabolism, translation and cellular transport might be regulated by phosphorylation events in *P. brasiliensis*. In addition, proteins related to transcription and cell cycle were up-regulated in mycelium and yeast cells, indicating the importance of phosphorylation for modulating the transcription in these morphological phases. The in silico analysis of the phosphopeptides additionally allowed the characterization of putative phosphorylation motifs in *P. brasiliensis*.

Acknowldegments

This work at Universidade Federal de Goiás was supported by grants from Conselho Nacional de Desenvolvimento Científico e Tecnológico (CNPq) and Fundação de Amparo à Pesquisa do Estado de Goiás (FAPEG) and the Medical Research Council (MRC). This work is part of the National Institute of Science and Technology of the Strategies of Host-Pathogen Interaction (HPI).

REFERENCE

[1] E. Brummer, E. Castaneda, A. Restrepo, Paracoccidioidomycosis: an update., Clin. Microbiol. Rev. 6 (1993) 89–117. http://www.ncbi.nlm.nih.gov/pubmed/8472249.

[2] S.H. Marques-da-Silva, A.M. Rodrigues, G.S. De Hoog, F. Silveira-Gomes, Z.P. De Camargo, Case report: Occurrence of Paracoccidioides lutzii in the Amazon Region: Description of two cases, Am. J. Trop. Med. Hyg. 87 (2012) 710–714. doi:10.4269/ajtmh.2012.12-0340.

[3] M.M. Teixeira, R.C. Theodoro, M.J.A. de Carvalho, L. Fernandes, H.C. Paes, R.C. Hahn, L. Mendoza, E. Bagagli, G. San-Blas, M.S.S. Felipe, Phylogenetic analysis reveals a high level of speciation in the Paracoccidioides genus, Mol. Phylogenet. Evol. 52 (2009) 273–283. doi:10.1016/j.ympev.2009.04.005.

[4] D.A. Turissini, O.M. Gomez, M.M. Teixeira, J.G. McEwen, D.R. Matute, Species boundaries in the human pathogen Paracoccidioides, Fungal Genet. Biol. 106 (2017) 9–25. doi:10.1016/j.fgb.2017.05.007.

[5] L. V Barrozo, R.P. Mendes, S.A. Marques, G. Benard, M.E.S. Silva, E. Bagagli, Climate and acute/subacute paracoccidioidomycosis in a hyper-endemic area in Brazil, Int. J. Epidemiol. 38 (2009) 1642–1649. doi:10.1093/ije/dyp207.

[6] R. Buccheri, Z. Khoury, L.C.B. Barata, G. Benard, Incubation Period and Early Natural History Events of the Acute Form of Paracoccidioidomycosis: Lessons from Patients with a Single Paracoccidioides spp. Exposure, Mycopathologia. 181 (2016) 435–439. doi:10.1007/s11046-015-9976-0.

[7] J.A. Smith, C.A. Kauffman, Pulmonary fungal infections, Respirology. 17 (2012) 913–926. doi:10.1111/j.1440-1843.2012.02150.x.

[8] J.C. Nemecek, Global Control of Dimorphism and Virulence in Fungi, Science (80-.). 312 (2006) 583–588. doi:10.1126/science.1124105.

[9] P.J. Rooney, B.S. Klein, Linking fungal morphogenesis with virulence, Cell. Microbiol. 4 (2002) 127–137.

[10] M.S.S. Felipe, Transcriptional Profiles of the Human Pathogenic Fungus Paracoccidioides brasiliensis in Mycelium and Yeast Cells, J. Biol. Chem. 280 (2005) 24706–24714. doi:10.1074/jbc.M500625200.

[11] L.R. Nunes, R. Costa de Oliveira, D.B. Leite, V.S. da Silva, E. dos Reis Marques, M.E. da Silva Ferreira, D.C.D. Ribeiro, L.A. de Souza Bernardes, M.H.S. Goldman, R. Puccia, L.R. Travassos, W.L. Batista, M.P. Nóbrega, F.G. Nobrega, D. Yang, C.A. de Bragança Pereira, G.H. Goldman, Transcriptome analysis of Paracoccidioides brasiliensis cells undergoing mycelium-to-yeast transition., Eukaryot. Cell. 4 (2005) 2115–28. doi:10.1128/EC.4.12.2115-2128.2005.

[12] K.P. Bastos, A.M. Bailão, C.L. Borges, F.P. Faria, M.S.S. Felipe, M.G. Silva, W.S. Martins, R.B. Fiúza, M. Pereira, C.M. a Soares, The transcriptome analysis of early morphogenesis in Paracoccidioides brasiliensis mycelium reveals novel and induced genes potentially associated to the dimorphic process., BMC

722 Microbiol. 7 (2007) 29. doi:10.1186/1471-2180-7-29.
723 [13] T.C. V Rezende, C.L. Borges, A.D. Magalhães, M.V. de Sousa, C.A.O. Ricart,
724 A.M. Bailão, C.M.A. Soares, A quantitative view of the morphological phases of
725 Paracoccidioides brasiliensis using proteomics, J. Proteomics. 75 (2011) 572– 587.
726 doi:10.1016/j.jprot.2011.08.020.
727 [14] M.R. Flory, H. Lee, R. Bonneau, P. Mallick, K. Serikawa, D.R. Morris, R.
728 Aebersold, Quantitative proteomic analysis of the budding yeast cell cycle using acid-
729 cleavable isotope-coded affinity tag reagents, Proteomics. 6 (2006) 6146– 6157.
730 doi:10.1002/pmic.200600159.
731 [15] S.B. Ficarro, M.L. McCleland, P.T. Stukenberg, D.J. Burke, M.M. Ross, J. Shabanowitz, D.F.
732 Hunt, F.M. White, Phosphoproteome analysis by mass spectrometry and its application
733 to Saccharomyces cerevisiae., Nat. Biotechnol.
734 20 (2002) 301–305. doi:10.1038/nbt0302-301.
735 [16] A. Carpy, K. Krug, S. Graf, A. Koch, S. Popic, S. Hauf, B. Macek, Absolute
736 Proteome and Phosphoproteome Dynamics during the Cell Cycle of
737 *Schizosaccharomyces pombe* (Fission Yeast), Mol. Cell. Proteomics. 13 (2014) 1925–
738 1936. doi:10.1074/mcp.M113.035824.
739 [17] L.D.N. Selvan, S. Renuse, J.E. Kaviyil, J. Sharma, S.M. Pinto, S.D. Yelamanchi,
740 V.N. Puttamallesh, R. Ravikumar, A. Pandey, T.S.K. Prasad, H.C. Harsha,
741 Phosphoproteome of Cryptococcus neoformans, J. Proteomics. 97 (2014) 287– 295.
742 doi:10.1016/j.jprot.2013.06.029.
743 [18] P.R. Kraus, D.S. Fox, G.M. Cox, J. Heitman, The Cryptococcus neoformans MAP kinase
744 Mpk1 regulates cell integrity in response to antifungal drugs and loss of calcineurin
745 function, Mol. Microbiol. 48 (2003) 1377–1387.
746 doi:10.1046/j.1365-2958.2003.03508.x.

[19] J.J. Benschop, S. Mohammed, M. O'flaherty, A.J.R. Heck, M. Slijper, F.L.H. Menke, Quantitative Phosphoproteomics of Early Elicitor Signaling in Arabidopsis, Mol. Cell. Proteomics. 6.7 (2007) 1198–1214. doi:10.1074/mcp.M600429-MCP200.

[20] N. Ramsubramaniam, S.D. Harris, M.R. Marten, The phosphoproteome of Aspergillus nidulans reveals functional association with cellular processes involved in morphology and secretion, Proteomics. 14 (2014) 2454–2459. doi:10.1002/pmic.201400063.

[21] S.D. Willger, Z. Liu, R.A. Olarte, M.E. Adamo, J.E. Stajich, L.C. Myers, A.N. Kettenbach, D.A. Hogan, Analysis of the Candida albicans phosphoproteome, Eukaryot. Cell. 14 (2015) 474–485. doi:10.1128/EC.00011-15.

[22] A.H. Da Silva Cruz, M. Brock, P.F. Zambuzzi-Carvalho, L.K. Santos-Silva, R.F. Troian, A.M. Gões, C.M. De Almeida Soares, M. Pereira, Phosphorylation is the major mechanism regulating isocitrate lyase activity in Paracoccidioides brasiliensis yeast cells, FEBS J. 278 (2011) 2318–2332. doi:10.1111/j.17424658.2011.08150.x.

[23] M.-H. Lin, N. Sugiyama, Y. Ishihama, Systematic profiling of the bacterial phosphoproteome reveals bacterium-specific features of phosphorylation, Sci. Signal. 8 (2015) rs10-rs10. doi:10.1126/scisignal.aaa3117.

[24] S.S. Jensen, M.R. Larsen, Evaluation of the impact of some experimental procedures on different phosphopeptide enrichment techniques., Rapid Commun. Mass Spectrom. 21 (2007) 3635–45. doi:10.1002/rcm.3254.

[25] A. Conesa, S. Götz, J.M. García-Gómez, J. Terol, M. Talón, M. Robles, Blast2GO: A universal tool for annotation, visualization and analysis in functional genomics research, Bioinformatics. 21 (2005) 3674–3676. doi:10.1093/bioinformatics/bti610.

[26] M.F. Chou, D. Schwartz, Biological Sequence Motif Discovery Using *motif-x*,

772 Curr. Protoc. Bioinforma. (2011) 1–52. doi:10.1002/0471250953.bi1315s35.

773 [27] D. Schwartz, S.P. Gygi, An iterative statistical approach to the identification of protein
774 phosphorylation motifs from large-scale data sets, Nat. Biotechnol. 23
775 (2005) 1391–1398. doi:10.1038/nbt1146.

776 [28] R.C. Team, R: A language and environment for statistical computing. R Foundation for
777 Statistical Computing, Vienna, Austria., (2018).

778 [29] P. De Souza Bonfim-Mendonça, B.A. Ratti, J. Da Silva Ribeiro Godoy, M.
779 Negri, N.C.A. De Lima, A. Fiorini, E. Hatanaka, M.E.L. Consolaro, S. De Oliveira Silva,
780 T.I.E. Svidzinski, β-Glucan induces reactive oxygen species production in human
781 neutrophils to improve the killing of Candida albicans and Candida glabrata isolates
782 from vulvovaginal candidiasis, PLoS One. 9 (2014) 1– 14.
783 doi:10.1371/journal.pone.0107805.

784 [30] C.L. Borges, A.M. Bailão, S.N. Báo, M. Pereira, J.A. Parente, C.M. de Almeida Soares,
785 Genes Potentially Relevant in the Parasitic Phase of the Fungal Pathogen
786 Paracoccidioides brasiliensis, Mycopathologia. 171 (2011) 1–9.
787 doi:10.1007/s11046-010-9349-7.

788 [31] A.L. Bookout, C.L. Cummins, D.J. Mangelsdorf, J.M. Pesola, M.F. Kramer, High-throughput
789 real-time quantitative reverse transcription PCR., Curr. Protoc.
790 Mol. Biol. Chapter 15 (2006) Unit 15.8. doi:10.1002/0471142727.mb1508s73.

791 [32] Z. Xie, S. Liu, Y. Zhang, Z. Wang, Roles of Rad23 protein in yeast nucleotide excision repair,
792 Nucleic Acids Res. 32 (2004) 5981–5990.
793 doi:10.1093/nar/gkh934.

794 [33] T. Lahari, J. Lazaro, D.F. Schroeder, RAD4 and RAD23/HMR contribute to arabidopsis UV
795 tolerance, Genes (Basel). 9 (2018) 1–12.
796 doi:10.3390/genes9010008.

797 [34] D.J. Adams, Fungal cell wall chitinases and glucanases, Microbiology. 150

(2004) 2029–2035. doi:10.1099/mic.0.26980-0.

[35] L.S. Derengowski, A.H. Tavares, S. Silva, L.S. Procópio, M.S.S. Felipe, I. Silva-Pereira, S.-P.I. Derengowski LS, Tavares AH, Silva S, Procópio LS, Felipe MS, Upregulation of glyoxylate cycle genes upon Paracoccidioides brasiliensis internalization by murine macrophages and in vitro nutritional stress condition., Med. Mycol. 46 (2008) 125–34. doi:10.1080/13693780701670509.

[36] G. Medoff, A. Painter, G.S. Kobayashi, Mycelial- to Yeast-phase transitions of the dimorphic fungi Blastomyces dermatitidis and Paracoccidioides brasiliensis, J. Bacteriol. 169 (1987) 4055–4060. doi:10.1128/jb.169.9.4055-4060.1987.

[37] L. Lacerda Pigosso, L.C. Baeza, M. Vieira Tomazett, M. Batista Rodrigues Faleiro, V.M. Brianezi Dignani de Moura, A. Melo Bailão, C.L. Borges, J. Alves Parente Rocha, G. Rocha Fernandes, G.M. Gauthier, C.M. de A. Soares, Paracoccidioides brasiliensis presents metabolic reprogramming and secretes a serine proteinase during murine infection, Virulence. 8 (2017) 1417–1434. doi:10.1080/21505594.2017.1355660.

[38] C.A. Rappleye, W.E. Goldman, Defining virulence genes in the dimorphic fungi., Annu. Rev. Microbiol. 60 (2006) 281–303. doi:10.1146/annurev.micro.59.030804.121055.

[39] J.A. Parente-Rocha, A.F.A. Parente, L.C. Baeza, S.M.R.C. Bonfim, O. Hernandez, J.G. McEwen, A.M. Bailão, C.P. Taborda, C.L. Borges, C.M. De Almeida Soares, Macrophage interaction with *Paracoccidioides brasiliensis* yeast cells modulates fungal metabolism and generates a response to oxidative stress, PLoS One. 10 (2015) 1–18. doi:10.1371/journal.pone.0137619.

821 [40] S. Pasricha, J.I. MacRae, H.H. Chua, J. Chambers, K.J. Boyce, M.J. McConville, A.
822 Andrianopoulos, Extensive Metabolic Remodeling Differentiates Nonpathogenic and
823 Pathogenic Growth Forms of the Dimorphic Pathogen
824 Talaromyces marneffei, Front. Cell. Infect. Microbiol. 7 (2017) 1–12.
825 doi:10.3389/fcimb.2017.00368.
826 [41] G. San-Blas, The cell wall of fungal human pathogens: its possible role in hostparasite
827 relationships., Mycopathologia. 79 (1982) 159–84.
828 http://www.ncbi.nlm.nih.gov/pubmed/6755258.
829 [42] M. Brock, W. Buckel, On the mechanism of action of the antifungal agent propionate.
830 Propionyl-CoA inhibits glucose metabolism in Aspergillus nidulans,
831 Eur. J. Biochem. 271 (2004) 3227–3241. doi:10.1111/j.1432-1033.2004.04255.x.
832 [43] Y.J. Zhang, E.J. Rubin, Feast or famine: The host-pathogen battle over amino acids, Cell.
833 Microbiol. 15 (2013) 1079–1087. doi:10.1111/cmi.12140.
834 [44] M. Costa, C.L. Borges, A.M. Bailão, G. V. Meirelles, Y.A. Mendonça, S.F.I.M.
835 Dantas, F.P. de Faria, M.S.S. Felipe, E.E.W.I. Molinari-Madlum, M.J.S. MendesGiannini,
836 R.B. Fiuza, W.S. Martins, M. Pereira, C.M.A. Soares, Transcriptome profiling of
837 Paracoccidioides brasiliensis yeast-phase cells recovered from infected mice brings new
838 insights into fungal response upon host interaction, Microbiology. 153 (2007) 4194–
839 4207. doi:10.1099/mic.0.2007/009332-0.
840 [45] N. Malanovic, I. Streith, H. Wolinski, G. Rechberger, S.D. Kohlwein, O. Tehlivets, S-
841 adenosyl-L-homocysteine hydrolase, key enzyme of methylation metabolism, regulates
842 phosphatidylcholine synthesis and triacylglycerol homeostasis in yeast: Implications for
843 homocysteine as a risk factor of atherosclerosis, J. Biol. Chem. 283 (2008) 23989–23999.
844 doi:10.1074/jbc.M800830200.
845 [46] M. Manocha, Lipid composition of Paracoccidioides brasiliensis: comparison between
846 the yeast and mycelial forms., Sabouraudia. 18 (1980) 281–6.

847 [47] P.W.J. De Groot, A.F. Ram, F.M. Klis, Features and functions of covalently linked proteins
848 in fungal cell walls, Fungal Genet. Biol. 42 (2005) 657–675.
849 doi:10.1016/j.fgb.2005.04.002.
850 [48] F. Kanetsuna, L.M. Carbonell, R.E. Moreno, J. Rodriguez, Cell wall composition of the
851 yeast and mycelial forms of Paracoccidioides brasiliensis., J. Bacteriol. 97 (1969) 1036–
852 41. http://www.ncbi.nlm.nih.gov/pubmed/5776517.
853 [49] F. Kanetsuna, L.M. Carbonell, Cell wall glucans of the yeast and mycelial forms of
854 Paracoccidioides brasiliensis., J. Bacteriol. 101 (1970) 675–680.
855 [50] G. San-Blas, F. San-Blas, *Paracoccidioides brasiliensis*: cell wall structure and virulence.
856 A review., Mycopathologia. 62 (1977) 77–86.
857 http://www.ncbi.nlm.nih.gov/pubmed/340954.
858 [51] J.A. Edwards, E.A. Alore, C.A. Rappleye, The yeast-phase virulence requirement for α-
859 glucan synthase differs among histoplasma capsulatum chemotypes, Eukaryot. Cell. 10
860 (2011) 87–97. doi:10.1128/EC.00214-10.
861 [52] R. Martinez-Lopez, L. Monteoliva, R. Diez-Orejas, C. Nombela, C. Gil, The GPI-anchored
862 protein CaEcm33p is required for cell wall integrity, morphogenesis and virulence in
863 *Candida albicans*, Microbiology. 150 (2004) 3341–3354. doi:10.1099/mic.0.27320-0.
864 [53] R. Martinez-Lopez, H. Park, C.L. Myers, C. Gil, S.G. Filler, *Candida albicans* Ecm33p is
865 important for normal cell wall architecture and interactions with host cells., Eukaryot.
866 Cell. 5 (2006) 140–7. doi:10.1128/EC.5.1.140-147.2006.
867 [54] D.S. Araújo, P. de Sousa Lima, L.C. Baeza, A.F.A. Parente, A. Melo Bailão, C.L.
868 Borges, C.M. de Almeida Soares, Employing proteomic analysis to compare
869 Paracoccidioides lutzii yeast and mycelium cell wall proteins, Biochim. Biophys.
870 Acta - Proteins Proteomics. 1865 (2017) 1304–1314.
871 doi:10.1016/j.bbapap.2017.08.016.

[55] A. Leitner, Phospho-Proteomics, Springer New York, New York, NY, 2016. doi:10.1007/978-1-4939-3049-4.

[56] P. Jiang, W.F. Wei, G.W. Zhong, X.G. Zhou, W.R. Qiao, R. Fisher, L. Lu, The function of the three phosphoribosyl pyrophosphate synthetase (Prs) genes in hyphal growth and conidiation in Aspergillus nidulans, Microbiol. (United Kingdom). 163 (2017) 218–232. doi:10.1099/mic.0.000427.

[57] R. Schneiter, A.T. Carter, Y. Hernando, G. Zellnig, L.M. Schweizer, M. Schweizer, The importance of the five phosphoribosyl-pyrophosphate synthetase (Prs) gene products of Saccharomyces cerevisiae in the maintenance of cell integrity and the subcellular localization of Prs1p, Microbiology. 146 (2000) 3269–3278. doi:10.1099/00221287-146-12-3269.

[58] J. Fasol, P.M. Kim, A. Sboner, M. Gerst, F. Sun, R. Chen, D. Sharon, Divers protein kinase interac o s ident f by protein microa ys rev al novel con e ti s betw n cel u ar proces, Genes Dev. (2010) 767–778. doi:10.1101/gad.1998811.Freely.

[59] E.A. Ugbogu, K. Wang, L.M. Schweizer, M. Schweizer, Metabolic gene products have evolved to interact with the cell wall integrity pathway in Saccharomyces cerevisiae, FEMS Yeast Res. 16 (2016) 1–10. doi:10.1093/femsyr/fow092.

[60] Y. Dai, Z. Cao, L. Huang, S. Liu, Z. Shen, Y. Wang, H. Wang, H. Zhang, D. Li, F. Song, CCR4-not complex subunit Not2 plays critical roles in vegetative growth, conidiation and virulence in watermelon fusarium wilt pathogen Fusarium oxysporum f. sp. niveum, Front. Microbiol. 7 (2016) 1–20. doi:10.3389/fmicb.2016.01449.

Figure legends

Figure 1. Ethanol measurements in protein extracts of mycelium, mycelium-toyeast transition and yeast cells and analysis of the transcript encoding pyruvate decarboxylase by qRT-PCR. (A) Measurement of ethanol accumulation in *P. brasiliensis* morphological phases*:* M: mycelium; T: transition mycelium-to-yeast cells; Y: yeast cells; **(B)** Analysis of the abundance of the transcript encoding pyruvate decarboxylase. *Asterisks evidence statistical differences observed by the Student T test presenting *p* value ≤ 0.05 considered significant.

Figure 2. Thiol measurements in protein extracts of mycelium, mycelium-to-yeast transition and yeast cells. **(A)** Increased production of thiol in *P. brasiliensis* morphological phases*:* M: mycelium; T: transition mycelium-to-yeast cells; Y: yeast cells; **(B)** Expression levels of the proteins for PADG_05504/ thioredoxin; PADG_02764/ thioredoxin, from proteomic analysis [fmol/µL (log2]). *Asterisks evidence statistical differences observed by the Student T test presenting *p* value ≤ 0.05 considered significant.

Figure 3. Schematic diagram of the metabolic processes differentially expressed in mycelia compared to yeast cells and transition mycelia-to-yeast (A). The figure summarizes the data obtained from proteomic analysis; enzymes are listed as follows: HK: hexokinase; FBA: fructose-1,6-bisphosphate aldolase; TPI: triosephosphate isomerase; PGM: phosphoglycerate mutase; ADH 1 and 2: Alcohol dehydrogenase; MTAP: methylthioadenosine phosphorylase; SRM: spermidine synthase; MTCBP: 1,2dihydroxy-3-keto-5-methylthiopentene dioxygenase. **(B) Heat map of proteins in mycelium compared to mycelium-to-yeast transition and yeast cells.** The color scale shows the mean of abundance of proteins obtained that were differentially expressed by the ANOVA test (p-value ≤0.05). Functional categories were obtained by manual search in the annotation database Pedant (http://pedant.gsf.de/) on MIPS that provides a tool to search the Functional Categories (Funcat 2.0). Red represents significantly higher expression and green represents a significantly low level of expression.

Figure 4. Heat map of HSPs induced and repressed in yeast cells compared to mycelia and mycelia-to-yeast transition. The color scale shows the mean of abundance of differentially expressed proteins (p-value ≤0.05). Functional categories were obtained by manual search in the annotation database Pedant (http://pedant.gsf.de/) on MIPS that provides a tool to search

the Functional Categories (Funcat 2.0). Red represents significantly higher expression and green represents a significantly low level of expression.

Figure 5. Schematic diagram of the metabolic processes differentially expressed in yeast cells compared to mycelia-to-yeast transition and mycelia. (A) The figure summarizes the data obtained from proteomic analysis; enzymes are listed as follows: Acad: acyl-CoA dehydrogenase; ECH: enoyl-CoA hydratase; ACAT: ketoacyl-CoA thiolase; MCS: methylcitrate synthase; MCD: methylcitrate dehydrogenase; ACO: aconitase; CS: citrate synthase; SUCLA: succinyl-CoA ligase; PDH: pyruvate dehydrogenase; ATPase: ATP synthase, ANT: aspartate aminotransferase; HPPD: hydroxyphenylpyruvate dioxygenase; FAH: fumarylacetoacetase; CRAT: carnitine acetyltrasnferase; SRM: spermidine synthase; MTAP: methylthioadenosine phosphorylase; MTCBP: 1,2-dihydroxy-3-keto-5-methylthiopentene dioxygenase. **(B) Heat map of proteins in mycelium, mycelium-to-yeast transition and yeast.** The color scale shows the mean of abundance of differentially expressed proteins (p-value ≤0.05). Functional categories were obtained by manual search in the annotation database Pedant (http://pedant.gsf.de/) on MIPS that provides a tool to search the Functional Categories (Funcat 2.0). Red represents significantly higher expression and green represents a significantly low level of expression.

Figure 6. Number of phosphoproteins, phosphopeptides and phosphosites detected in *P. brasiliensis*, mycelium, mycelium-to-yeast cells transition and yeast cells. The proteins were analyzed by LC-MS-MS before and after enrichment with TiO_2. **(A)** Number of phosphoproteins, phosphopeptides and phosphosites from protein extracts of mycelia, mycelium-to-yeast transition and yeast; **(B)** distribution of the phosphorylation sites on the amino acid residues serine, threonine and tyrosine; **(C)** Motifs found using the Motif-X algorithm (http://motif-x.med.harvard.edu/); as central characters were selected the residues of Ser, Thr or Tyr. The gray bar corresponds to the total fraction and the black bar corresponds to the enriched fraction.

Supplementary Figure 1. Schematic overview of performed experiments. Nine cultures were prepared with *P. brasiliensis*, grown as mycelium, mycelium to-yeast and yeast cells. After 72 h of growth for mycelium and yeast and 22 h for transition, the cultures were

collected and the proteins extracted and digested in peptides. The threecondition samples (mycelium, transition and yeast) from each replicate were labeled with iTRAQ (114,116 and 115 tag).

Supplementary Figure 2. Flowchart of the filters applied to the identified proteins during mycelium, mycelium-to-yeast transition and yeast cells. It was considered those proteins with high or medium FDR confidence and those that were found in at least 2 replicates.

Supplementary Figure 3. Proteins identified in *P. brasiliensis* that were annotated by Blast2GO. (A) Number of sequences analyzed and that had annotation; **(B)** Top-hit of species that were homologous to proteins found using Blast2GO.

Supplementary Figure 4. Schematic diagram of the metabolic processes in cell wall differentially expressed in mycelia and yeast cells. The figure summarizes the data obtained from proteomic analysis; enzymes are listed as follows: CTS2: chitinase; ECM33; β-1,3-exoglucanase; 1,3- β-glucosidade; β-1,6 glucan synthase (Knh1). M: mycelium; T: transition from mycelium to yeast cells; Y: yeast cells.

Supplementary Figure 5. Mitochondrial activity assay in mycelia, transition mycelia-to-yeast, yeast cells. The images were acquired to mycelia, transition myceliato-yeast and yeast cells (magnification x 400) in the Microscope Axio Scope A1 (Zeiss), using the AxioVision Software (Carl Zeiss).

Supplementary Figure 6. Schematic overview of experiments performed for enrichment with TiO_2. Phosphopeptides were enriched with TiO_2 and subjected to MS/ MS analysis.

Supplementary Figure 7. Distribution of phosphoproteins identified in *P. brasiliensis*, according to FunCat 2.0 categories. The categories were generated by manual search based on FunCat 2.0 functional annotation (http://pedant.gsf.de/).

Supplementary Figure 8. Functional annotations of phosphoproteins identified during transition of *Pb*18 obtained from GO slim terms. Cellular component.

Figure

Click here to download high resolution image

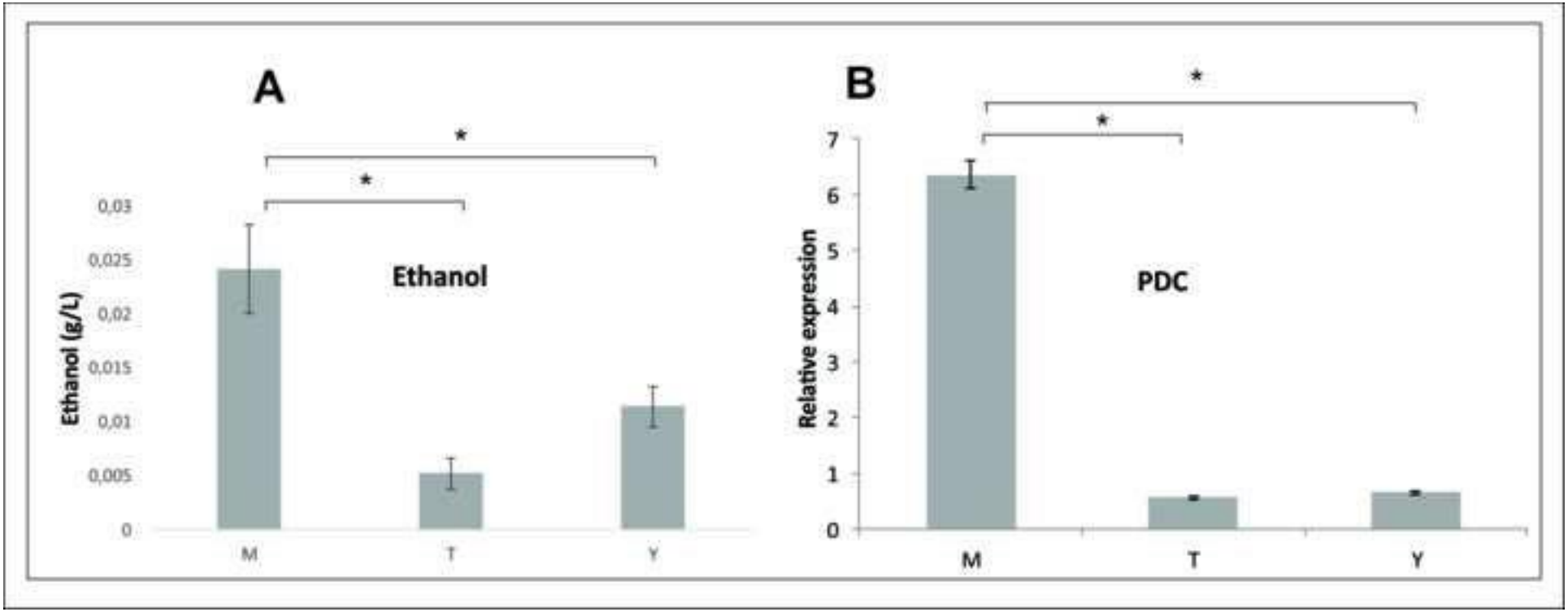

Figure

Click here to download high resolution image

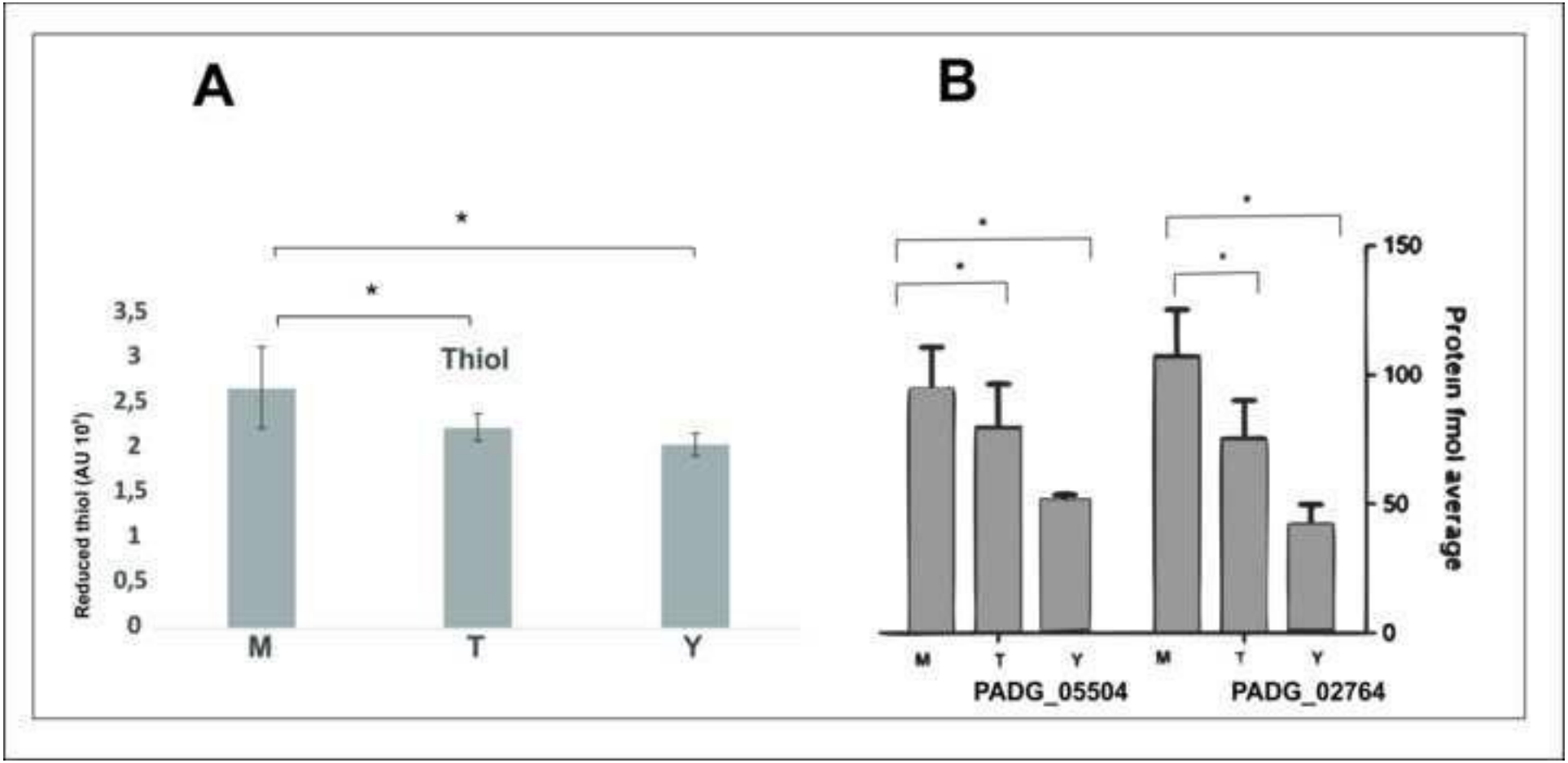

Figure

Click here to download high resolution image

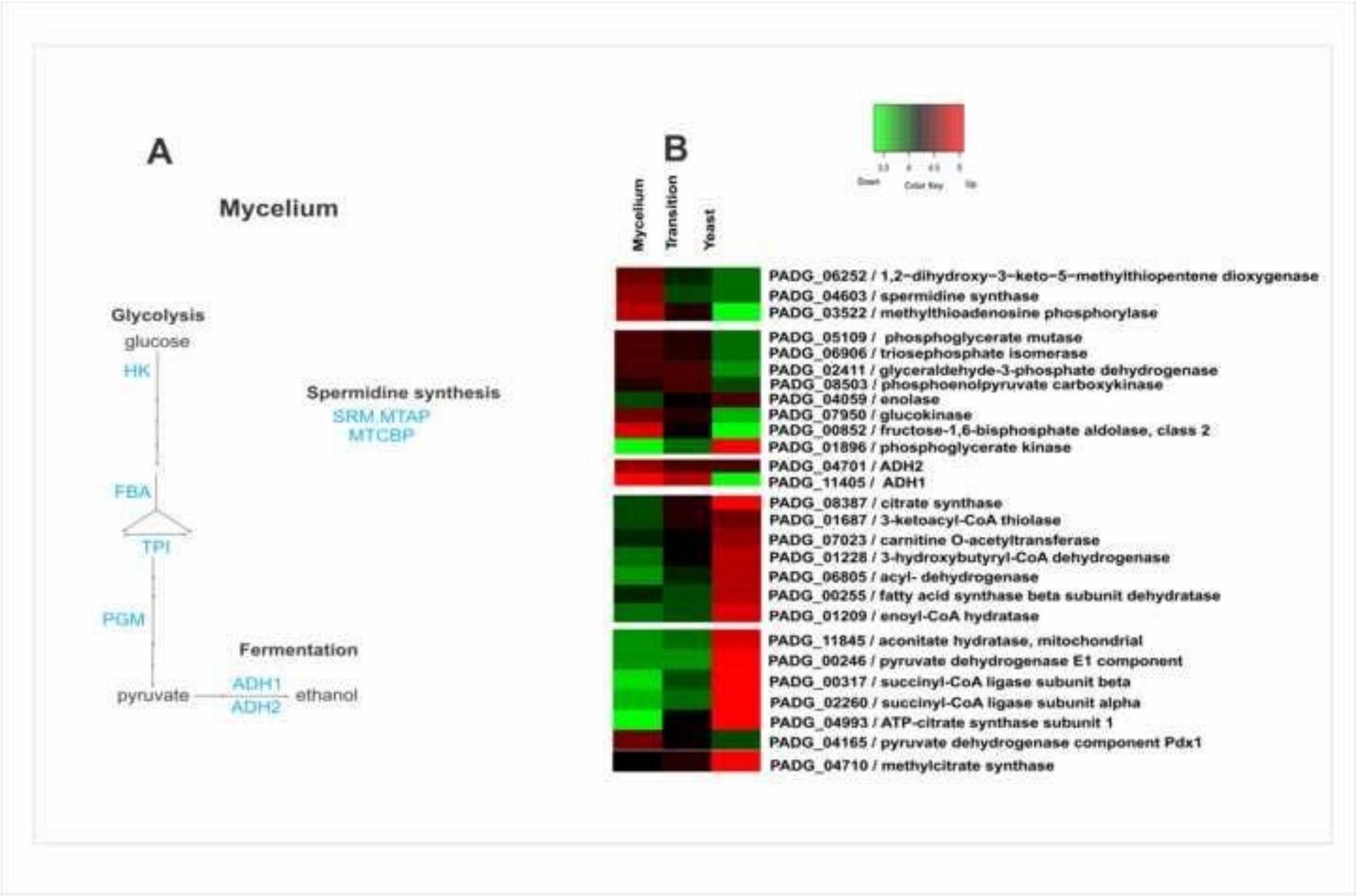

Figure

Click here to download high resolution image

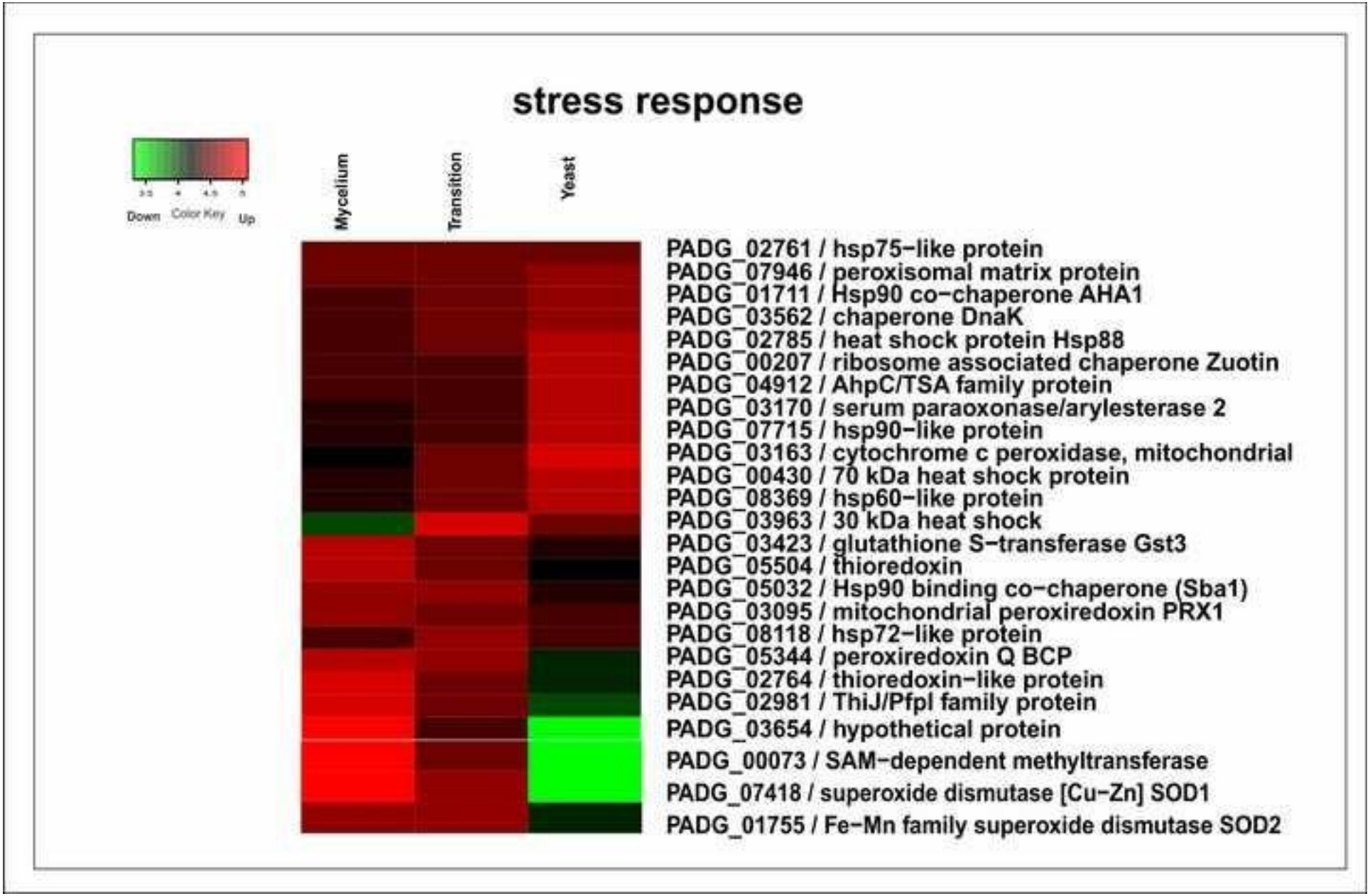

Figure

Click here to download high resolution image

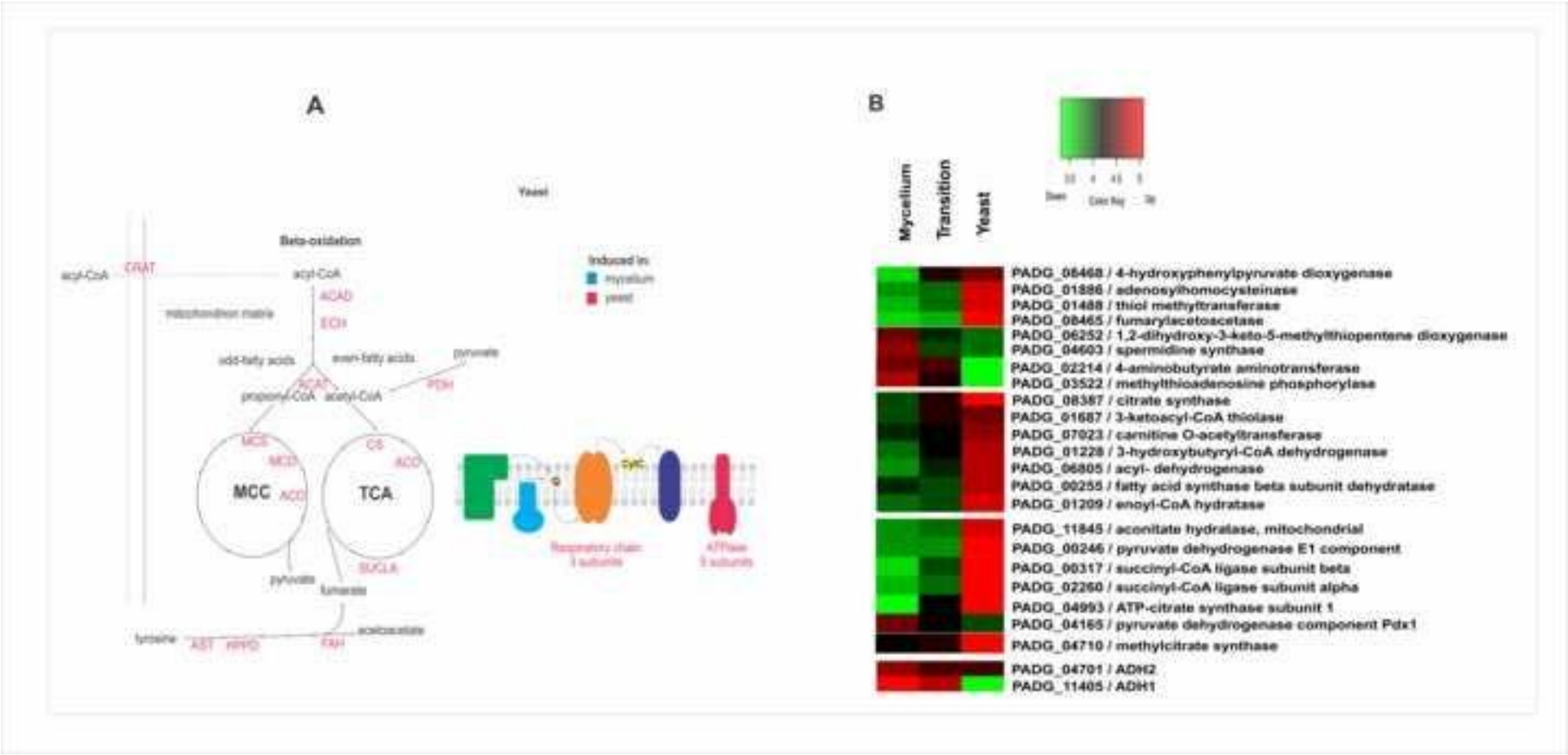

Figure

Click here to download high resolution image

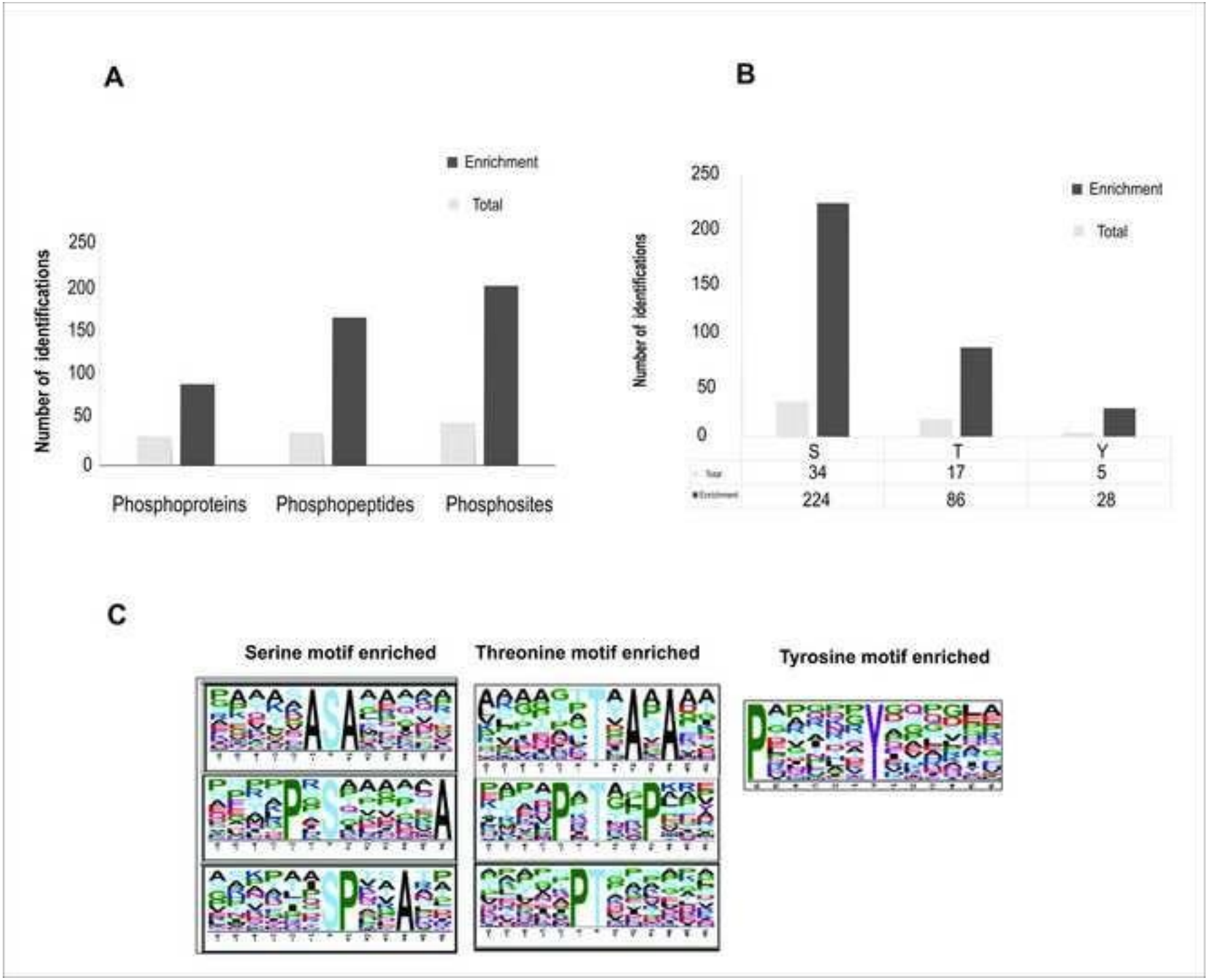

Click here to download Supplementary material: Supplementary tables.xlsx

Click here to download Supplementary material: Fig. S1.jpg

Click here to download Supplementary material: Fig. S2.jpg

Click here to download Supplementary material: Fig. S3.jpg

Click here to download Supplementary material: Fig. S4.jpg

Click here to download Supplementary material: Fig. S5.jpg

Click here to download Supplementary material: Fig. S6.jpg

Click here to download Supplementary material: Fig. S7.jpg

Click here to download Supplementary material: Fig. S8.jpg

Click here to download Conflict of Interest: coi_disclosure (4)CMAS.pdf

Click here to download Conflict of Interest: coi_disclosure Agenor.pdf

Click here to download Conflict of Interest: coi_disclosure Carlos Andr.pdf

Click here to download Conflict of Interest: coi_disclosure Danielle.pdf

Click here to download Conflict of Interest: coi_disclosure Igor.pdf

Click here to download Conflict of Interest: coi_disclosure_ALEX.pdf

Click here to download Conflict of Interest: coi_disclosure_Maristela (1).pdf

Click here to download Conflict of Interest: coi_disclosureCristiane.pdf

Click here to download Conflict of Interest: coi_disclosureFontes.pdf

Click here to download Conflict of Interest: coi_disclosuremathias.pdf

Click here to download Conflict of Interest: coi_disclosureSouza.pdf

Click here to download Conflict of Interest: Conflito de interesse Leandro.pdf

Supplementary Tables

Table S2. Identified proteins from *Paracoccidioides brasiliensis* regulated in mycelia phase, mycelia-to-yeast transition and yeast phases (312 proteins)

Acession number[a]	Protein description[b]	(ANOVA) p-value[c]	Tukey's test[d]		
Functional categories[e]					
METABOLISM			Mycelium	Transition	Yeast
Amino acid metabolism					
PADG_01488	thiol methyltransferase	0.00859584687713703	4,357395921	4,457967301	4,930534141
PADG_02214	4-aminobutyrate aminotransferase	0.000473697117025741	4,774082039	4,742095318	4,259441682
PADG_01621	aspartate aminotransferase	0.000603223867301128	4,338645698	4,386894559	4,988491176
PADG_05277	Serine hydroxymethyltransferase	0.00298066391122739	4,313434112	4,537809004	4,907056998
PADG_03627	2-oxoisovalerate dehydrogenase subunit beta	0.0373648418664289	4,532748713	4,496012916	4,792385261
PADG_08262	asparagine synthase (glutamine-hydrolyzing)	0.0374351680322741	4,484731825	4,298103427	4,932595586
PADG_03522	methylthioadenosine phosphorylase	0.00188671139057892	4,859110833	4,651349554	4,247099542
PADG_00888	Argininosuccinate synthase	0.0283905003634937	4,512792078	4,386215185	4,874246012
PADG_06252	1,2-dihydroxy-3-keto-5-methylthiopentene dioxygenase	0.00701338481935753	4,772594359	4,587661184	4,470433667
PADG_06144	saccharopine dehydrogenase	0.00527529557636022	4,823341923	4,603325863	4,374084022
PADG_01718	Saccharopine dehydrogenase [NADP+, L-glutamate-forming]	0.0221450392480064	4,780448166	4,602597515	4,437593924
PADG_08021	phospho-2-dehydro-3-deoxyheptonate aldolase	0.00034871632473159	4,877840236	4,532623342	4,37805998
PADG_05058	chorismate mutase	0.0226842449859004	4,452149194	4,573981509	4,793085575
PADG_04487	chorismate synthase	0.0314909968419182	4,476966948	4,68357954	4,679151712
PADG_01886	adenosylhomocysteinase	0.02113109868656	4,409869706	4,450179505	4,901358859
PADG_04603	spermidine synthase	0.0432103775062461	4,796966216	4,528418021	4,492998824
PADG_00210	glycine dehydrogenase	0.0105405077270114	4,432687389	4,551247093	4,824906144
PADG_08468	4-hydroxyphenylpyruvate dioxygenase	0.00549013636700336	4,33976034	4,690252318	4,76955878
PADG_08465	fumarylacetoacetase	0.0108038616369285	4,331202389	4,367229714	4,990015745

PADG_07366	methylcrotonoyl-CoA carboxylase subunit alpha	0.0509066885694793	4,446444661	4,49685016	4,845850704
Nucleotide/nucleoside/nucleobase metabolism					
PADG_00780	ribose-phosphate pyrophosphokinase II	0.00949990061787514	4,726349088	4,629276735	4,483911142
PADG_08066	purine nucleoside phosphorylase I, inosine and guanosine-specific	0.00427473565670872	4,865537705	4,602304101	4,301426508
PADG_00322	xanthine-guanine phosphoribosyl transferase	0.00126429186045653	4,922411517	4,728670169	3,954547923
PADG_00621	Hydroxyisourate hydrolase	0.0195414250770774	4,722482955	4,591608884	4,531697027
PADG_04099	phosphoribosylaminoimidazolecarboxamide formyltransferase/IMP cyclohydrolase	0.0290343921451513	4,483577849	4,595723993	4,754511436
PADG_07970	dihydroorotase, homodimeric	0.000601494528361185	4,991544911	4,497471404	4,198579474
PADG_01100	uracil phosphoribosyltransferase	0.00342045544824264	4,85832049	4,669313701	4,213034304
PADG_07782	Deoxyuridine 5'-triphosphate nucleotidohydrolase	0.00385911777105953	4,779608694	4,655545988	4,375951356
PADG_01159	Uridylate kinase	0.0225226043444458	4,444078824	4,600156216	4,777968858
PADG_06054	deoxyribose-phosphate aldolase	0.0359382344610037	4,791283412	4,628635869	4,381937664
PADG_05321	DNA RNA non-specific nuclease	0.0499799223721024	4,489899421	4,538990484	4,791304551
PADG_02658	nucleoside-diphosphate-sugar epimerase	0.000440673349932956	4,990042242	4,693718456	3,852417285
Phosphate metabolism					
PADG_0417	Inorganic pyrophosphatase	0.00039648057603618	4,782424549	4,670177805	4,356346182
C-compound and carbohydrate metabolism					
PADG_03118	aldose 1-epimerase family	0.0473203607543561	4,37165452	4,493943291	4,887357209
PADG_00649	alcohol oxidase	0.000210018090153545	4,962803672	4,744007286	3,802490419
PADG_04687	short-chain dehydrogenase reductase family	0.00109994176880593	4,794811557	4,650258297	4,36161594
PADG_03859	NADP-dependent mannitol dehydrogenase	0.0016711614063246	4,86517442	4,804952725	3,916394521
PADG_00735	Lactam utilization protein lamB	0.00269083936760223	4,842857422	4,56686141	4,389733319
PADG_01372	mannitol-1-phosphate 5-dehydrogenase	0.00320014525763444	4,898708002	4,60128546	4,241112488
PADG_05855	lactonohydrolase	0.00734969612425638	4,724017248	4,617268936	4,50241177
PADG_00912	UDP-galactopyranose mutase	0.00775039746204842	4,408709844	4,395977585	4,937538497
PADG_07606	2,5-diketo-D-gluconic acid reductase A	0.010818881866288	4,81211545	4,621084036	4,364412925
PADG_06740	betaine aldehyde dehydrogenase	0.0325496051578872	4,909650786	4,627054209	4,122307349

PADG_04710	2-methylcitrate mitochondrial	0.00129368626044376	4,324990832	4,45976783	4,951290254
PADG_01677	acetyl-coenzyme A synthetase	0.0413980013723899	4,695949428	4,740065239	4,3677976
PADG_05081	Aldehyde dehydrogenase	0.000318428299089706	4,865377473	4,807954631	3,935349485
Lipid, fatty acid and isoprenoid metabolism					
PADG_12025	glutaryl- CoA dehydrogenase	0.0378176148991082	4,434739438	4,417009061	4,898457292
PADG_03492	phosphatidylserine decarboxylase	0.00185747080872941	4,983469681	4,625121469	3,994671637
PADG_01228	3-hydroxybutyryl-CoA dehydrogenase	0.00942493695792639	4,354421308	4,520679397	4,892191139
PADG_03449	Isopentenyl-diphosphate delta-isomerase	0.0209229087713661	4,938486367	4,570222911	4,168964753
PADG_00255	fatty acid synthase beta subunit dehydratase	0.0372553299870248	4,445759947	4,363560056	4,922206428
PADG_04718	2-methylcitrate dehydratase	0.000131666517534101	4,053654335	4,403710395	5,100529262
Metabolism of vitamins, cofactors, and prosthetic groups					
PADG_00443	Dihydropteroate synthase	0.00123800894548555	4,216512814	4,535664446	4,95778356
PADG_05822	Pyridoxine biosynthesis protein pyroA	0.00277034051507976	4,262083878	4,623090523	4,871129629
PADG_08457	biotin synthase	0.0395889417320599	4,498044895	4,582941514	4,75345774
Secondary metabolism					
PADG_08034	dienelactone hydrolase family protein	0.00108007819663931	5,000018595	4,627709395	3,942709651
PADG_01052	3-demethylubiquinone-9 3-methyltransferase	0.00572417440168868	4,928667501	4,619226437	4,132627594
PADG_00312	cytochrome c heme lyase	0.0179304699139903	4,82805197	4,673890027	4,249379481
ENERGY					
Glycolysis and gluconeogenesis					
PADG_00852	fructose-1,6-bisphosphate aldolase, class 2	0.0321261222174796	4,883148515	4,598238224	4,245067703
PADG_07950	glucokinase	0.0269789169774159	4,767477211	4,666734275	4,37011628
PADG_08503	Phosphoenolpyruvate carboxykinase	0.0115249761276736	4,634733167	4,696117599	4,51720421
PADG_01896	Phosphoglycerate kinase	0.000712735140039373	4,282905818	4,480390608	4,962068686
PADG_06906	Triosephosphate isomerase	0.00153813947318225	4,72253189	4,64278566	4,475694292
PADG_04059	Enolase	0.00541040257511781	4,526980304	4,62178786	4,700181624
PADG_05109	2,3-bisphosphoglycerate-independent phosphoglycerate mutase	0.0117496849150458	4,697818777	4,661476065	4,483192077
PADG_02411	Glyceraldehyde-3-phosphate dehydrogenase	0.0492052726676888	4,691169819	4,711898586	4,417702937
Tricarboxylic-acid pathway (citrate cycle, Krebs cycle, TCA cycle)					

PADG_00246	pyruvate dehydrogenase E1 component subunit beta	0.0014620825618247	4,467508969	4,476987844	4,85747928
PADG_04993	ATP-citrate synthase subunit 1	0.0215948774017605	4,357064943	4,595652482	4,834104584
PADG_04165	pyruvate dehydrogenase complex component Pdx1	0.00131307433739174	4,699334268	4,619484707	4,53142248
PADG_07213	pyruvate dehydrogenase complex dihydrolipoamide acetyltransferase	0.006306183339428	4,434292544	4,606149474	4,782783259
PADG_11845	Aconitate hydratase, mitochondrial	0.0302112190508672	4,483588291	4,519733136	4,810778766
PADG_00317	succinyl-CoA ligase subunit beta	0.0126837599715285	4,411623854	4,540414639	4,846019033
PADG_02260	succinyl-CoA ligase subunit alpha	0.0326252304957893	4,432012377	4,516637915	4,843352517
PADG_04939	Succinyl-CoA:3-ketoacid-coenzyme A transferase	58,28	0.0201943831690541	0,52	0,34
PADG_08387	Citrate synthase	76,95	0.00379083047685583	1,21	0,8
PADG_01797	Dihydrolipoamide acetyltransferase component of pyruvate dehydrogenase	57,76	0.0128389547829813	0,83	0,42
Electron transport and membrane-associated energy conservation					
PADG_02561	ATP synthase subunit alpha, mitochondrial	0.00099703997320092	4,514311737	4,54718815	4,774140041
PADG_05436	Cytochrome b-c1 complex subunit Rieske	0.00954500862971618	4,315058774	4,601035599	4,8553777
PADG_06196	12-oxophytodienoate reductase	0.000130524968963367	4,221724966	4,958880373	4,535806942
PADG_03516	NADH-ubiquinone oxidoreductase 30.4 kDa subunit	0.00859471577854355	4,413920482	4,598805445	4,80183725
PADG_07749	NAD(P)H:quinone oxidoreductase, type IV	0.0488987573295302	4,764273976	4,673423235	4,358226487
Respiration					
PADG_05750	cytochrome c oxidase polypeptide VI	0.000329872995986405	4,327414272	4,583503177	4,870384569
PADG_07081	electron transfer flavo alpha subunit	0.0265951000485402	4,467574541	4,594267781	4,766509434
PADG_03039	MICOS complex subunit MIC60	0.0458991211511605	4,614707509	4,538443978	4,695847586
PADG_03872	mitochondrial import inner membrane translocase subunit tim1	0.0280037026658489	4,512346768	4,509263593	4,798797544
PADG_07042	ATP synthase F1, delta subunit	0.0514263542897544	4,467080817	4,578621275	4,776631304
PADG_07813	ATP synthase F1, gamma subunit	0.00320229579998738	4,412755298	4,534006308	4,852687023
PADG_08349	ATP synthase subunit beta, mitochondrial	0.0091913956997716	4,464996516	4,593674453	4,771136879
PADG_05403	NADH-ubiquinone oxidoreductase 21 kDa subunit	0.0252028231260988	4,716340303	4,697210773	4,407618916
PADG_02454	NADH-ubiquinone oxidoreductase	0.0505489922010667	4,506005914	4,491903257	4,811385388

PADG_05402	mitochondrial F1F0 ATP synthase subunit	0.0128065223457609	4,423523411	4,510957779	4,857985376
Fermentation					
PADG_11405	Alcohol dehydrogenase 1	0.000117667332982207	4,952888704	4,747259161	3,846698619
PADG_04701	Alcohol dehydrogenase	0.0398751128886334	4,729114784	4,583255636	4,53121067
Oxidation of fatty acids					
PADG_06805	acyl- dehydrogenase	93,54	0.00228164549110767	0,93	0,63
PADG_01209	enoyl-CoA hydratase	75,09	0.0158508402126517	0,9	0,82
PADG_07023	carnitine O-acetyltransferase	23,7	0.0299195036063134	0,52	0,42
PADG_01687	3-ketoacyl-CoA thiolase	148,38	0.000606823603773545	0,59	0,27
CELL CYCLE AND DNA PROCESSING					
DNA processing					
PADG_03459	replication factor-A protein	0.0149027131920101	4,803611291	4,631925045	4,364286479
PADG_05818	HLH DNA binding	0.0230078557563301	4,79948516	4,634164835	4,363756203
PADG_00656	Non-histone chromosomal protein 6	0.00349912944508594	4,906250412	4,600075027	4,221520091
PADG_02683	UV excision repair protein Rad23	0.0101122103649832	4,856812725	4,58476368	4,335095591
PADG_05709	histone acetyltransferase type B subunit 2	0.00164234466516168	4,872207824	4,608112384	4,287139498
Cell cycle					
PADG_04795	deubiquitination-protection protein dph1	0.00011583181867771	4,943714372	4,668528478	4,042339871
PADG_05683	cell division control protein 48	0.000330152297791995	4,728360485	4,570125724	4,549182823
PADG_07319	septin-1	0.000818895717889287	4,943927683	4,618243319	4,123545495
PADG_07515	NSFL1 cofactor p47	0.0143456926429943	4,751931979	4,70872448	4,337770908
TRANSCRIPTION					
RNA synthesis					
PADG_00814	branchpoint-bridging protein	0.000361519806372817	5,047732467	4,673468071	3,675357801
PADG_04307	mRNA binding post-transcriptional regulator	0.00322339287702619	4,751796253	4,575249434	4,513237913
PADG_02555	nucleic acid-binding protein	0.0101850714020848	4,302673113	4,686218094	4,794858851
PADG_01508	U1 small nuclear ribonucleoprotein C	0.0268581913593662	4,846954785	4,609097493	4,314940715
PADG_01455	KH domain RNA-binding protein	0.000544832339699319	4,883202937	4,59033517	4,29517172
PADG_08081	zinc knuckle domain	0.000727891867202843	5,145549837	4,598537389	3,374465368
PADG_00220	class 2 transcription repressor NC2	0.00304321420966517	4,715661439	4,703197836	4,406054885
PADG_04311	cellular nucleic acid-binding protein	0.0115271319353104	4,755938062	4,680801878	4,374570008

PADG_03869	HMG box	0.0149326260057446	4,777629973	4,647394631	4,38649155
PADG_00872	histone H4	0.0252015733715969	4,094860492	4,597863514	4,949826114
PADG_06182	transcriptional repressor	0.0323405291079937	4,750188446	4,576900111	4,510062701
RNA processing					
PADG_02783	RNA-binding La domain-containing protein	0.0252707765390186	4,806173642	4,608765672	4,386423159
PADG_07689	transformer-SR ribonucleoprotein	0.00285515817257463	4,806471097	4,711771461	4,245265591
PADG_00044	28 kDa ribonucleoprotein	0.0311052414112992	4,826318919	4,603172713	4,356169393
PADG_00576	RNA recognition domain-containing protein containing protein, variant	0.000366474914980045	5,069074064	4,60559948	3,780682898
PADG_05340	pre-mrna splicing factor	0.00567170230733727	4,732043744	4,598566473	4,513185844
PADG_04369	splicing factor U2AF 23 kDa subunit	0.0093556652043975	4,83916269	4,756474346	4,084939571
PADG_04301	WD repeat-containing protein	0.0304988927372442	4,818757102	4,627822306	4,336149519
PROTEIN SYNTHESIS					
Ribosome biogenesis					
PADG_11904	Ribosomal protein L1	0.0547556214196747	4,333029061	4,397187409	4,952762219
PADG_03856	60S ribosomal protein L15	0.000948265034607996	4,189422544	4,40680774	5,043969711
PADG_01026	60S ribosomal protein L43	0.00189393950236822	4,809348217	4,580571089	4,427329649
PADG_04848	60S ribosomal protein L8-B	0.00391393542396789	4,365212074	4,453111871	4,930933449
PADG_04862	50S ribosomal protein Mrp49	0.0046969426014565	4,418086256	4,682786869	4,726134701
PADG_05686	ribosome biogenesis protein	0.0171919284417786	4,801621339	4,659351825	4,326989436
PADG_05721	60S ribosomal protein L4	0.031687423620715	4,404223676	4,500729435	4,870044136
PADG_00784	40S ribosomal protein S0	0.038488765469723	4,369239676	4,469794223	4,907728943
PADG_00335	40S ribosomal protein S14	0.0009283171462339	4,793071291	4,647424884	4,369497964
PADG_02056	ribosomal protein L7	0.00101174747252608	4,307582955	4,474848419	4,952560187
PADG_01654	40S ribosomal protein S6-A	0.00128612006836141	4,427246586	4,569962116	4,817963337
PADG_07583	40S ribosomal protein S21	0.00321015987134523	4,864587041	4,561849834	4,358935866
PADG_00354	40S ribosomal protein S17	0.00512401922994533	4,640741634	4,534444795	4,676807142
PADG_01914	60S ribosomal protein L35	0.00595985342101163	4,443572878	4,494247565	4,859613758
PADG_00627	mitochondrial large ribosomal subunit L49, variant	0.00635571801442804	4,177210626	4,685931824	4,857318127
PADG_01387	60S ribosomal protein L7	0.00676476492288821	4,478819934	4,458638854	4,859308418
PADG_03781	60S ribosomal protein L30	0.00769160773234302	4,801662368	4,485606126	4,536244441

PADG_03778	60S ribosomal protein L10-A	0.0128434095495006	4,391561477	4,364361928	4,959189085
PADG_00995	ubiquitin-40S ribosomal protein S27a	0.0155770103199853	4,753200876	4,706126019	4,334911423
PADG_04106	60S ribosomal protein L11	0.0202870981819721	4,464415059	4,419543415	4,887507806
PADG_03873	60S ribosomal protein L20	0.0326173334051663	4,397480509	4,4764334	4,888334657
PADG_02249	60S ribosomal protein L2	0.049831342606761	4,6721549	4,634018134	4,545273527
PADG_06525	40S ribosomal protein S1	0.0498924638228775	4,511865866	4,5150257	4,793093079
PADG_05939	60S ribosomal protein L27a	0.00976778835723734	4,253816826	4,43760718	4,986899377
PADG_03326	40S ribosomal protein S9	0.0516200825998414	4,466153191	4,623416439	4,741101244
PADG_01427	40S ribosomal protein S12	0.00188255977619058	4,780783503	4,590982975	4,457546658
PADG_03315	40S ribosomal protein S4	0.00145057927925207	4,5444158	4,45935618	4,816455562
PADG_02888	60S ribosomal protein L6 O	0.00058696534564495	4,397019825	4,458751242	4,914581945
PADG_06838	40S ribosomal protein S5	0.0280593514265553	4,43905201	4,507306026	4,848014728
PADG_02828	Ribosomal protein	0.0319912825552141	4,218909607	4,385583492	5,01356461
PADG_06048	40S ribosomal protein S27	0.0441806922768012	4,239394371	4,339910872	5,023802484
PADG_11379	60S ribosomal protein L5	0.00947872658438146	4,424046408	4,528604172	4,846860462
Translation					
PADG_02759	ribosome recycling factor domain-containing protein	0.00717309135667122	4,028680901	4,733512273	4,880313615
PADG_02896	elongation factor 1-beta	0.000328396134515179	4,367074803	4,505714536	4,902468013
PADG_00692	elongation factor 1-alpha	0.0033049385655597	4,297478086	4,440733419	4,973961821
PADG_01079	translation initiation factor 4B	0.0305078072836169	4,808578979	4,628513924	4,353437358
PADG_07356	woronin body major protein	0.00055674974717756	4,949665607	4,74902932	3,823345641
PADG_01865	Eukaryotic translation initiation factor 3	0.00217169449999158	4,802673995	4,563534348	4,457022653
PADG_00457	translation initiation factor 4G	0.0127112389368946	4,717625813	4,623735614	4,502564617
PADG_06110	translation initiation factor SUI1	0.0258640355371289	4,901266984	4,565821794	4,249253249
PADG_02691	eukaryotic translation initiation factor 6	0.0525198964080063	4,744329655	4,583201125	4,509362113
PADG_08125	Elongation factor 2	0.00977484226145031	4,359842122	4,404776422	4,956060943
PADG_06265	elongation factor 1-gamma	0.00245190358187735	4,306685534	4,471280725	4,953718586
Aminoacyl-tRNA-synthetases					
PADG_05848	glycine-tRNA ligase	0.0284549763738526	4,399126604	4,572192477	4,826642684
PROTEIN FOLDING AND STABILIZATION					
Protein folding and stabilization					

PADG_12323	peptidyl-prolyl cis-trans isomerase	0.000811310718754342	4,269159364	4,619869091	4,872745703
PADG_12329	prefoldin subunit 2	0.00122708938870604	4,854558774	4,658516886	4,244446155
PADG_08587	Peptidylprolyl isomerase	0.000635200628117717	4,729995443	4,766144736	4,293032079
PADG_02895	ATP-dependent Clp protease ATP-binding subunit ClpB	0.00276781772538938	4,309112753	4,586539333	4,874189192
PADG_07815	disulfide-isomerase domain	0.00378267127358446	4,427835248	4,609493963	4,785028387
PADG_04092	peptidyl-prolyl cis-trans isomerase B	0.00718691945820977	4,45601706	4,503789035	4,845143342
PADG_05628	Protein disulfide-isomerase domain	0.0189209329424933	4,383572565	4,585127806	4,82622498
PADG_01852	small glutamine-rich tetratricopeptide repeat-containing protein	0.0194408966072878	4,797137292	4,629881365	4,376494646
PADG_06488	peptidyl-prolyl cis-trans isomerase D	0.0284592321370524	4,359952662	4,664029466	4,775411091
PADG_05203	Peptidyl-prolyl cis-trans isomerase	0.028957954112554	4,919547485	4,596710017	4,167124876
PADG_08048	T-complex protein 1 subunit beta	0.0435867936243462	4,572410426	4,567250563	4,709244123
PADG_01565	calnexin	0.0476035441549569	4,444980406	4,69442803	4,689870869
PADG_07953	Peptidyl-prolyl cis-trans isomerase	0.00239744249348738	4,787055659	4,584064055	4,455706867
PADG_04034	Chaperone DnaJ	0.0070692227624351	4,558610158	4,758515213	4,521182693
PADG_02206	DnaJ domain protein Psi	0.0474842422073504	4,552133162	4,807494028	4,449863068
PADG_05229	chaperone protein dnaJ 3	0.00851844162738829	4,458411173	4,80311525	4,559839006
Protein targeting, sorting and translocation					
PADG_02619	F-box domain-containing	0.0017688464217684	4,884213308	4,619984634	4,245578509
PADG_08188	vacuolar-sorting protein snf7	0.00562474527488371	4,924496022	4,629892113	4,119413712
PADG_08646	class E vacuolar -sorting machinery HSE1	0.0176936537439237	4,842217291	4,681826504	4,204193377
PADG_03274	mitochondrial import inner membrane translocase subunit tim9	0.0226626979060814	4,78379858	4,581068394	4,458070753
PADG_00240	SNF7 family protein Fti1/Did2	0.00561971799727414	4,922978229	4,715685856	3,959057129
Protein modification					
PADG_00809	ubiquitin-conjugating enzyme	0.00179716781257883	4,851076997	4,737854341	4,109317376
PADG_07925	ubiquitin-conjugating enzyme E2 N	0.00217641874973217	4,778034896	4,60878509	4,43966477
PADG_00569	5'/3'-nucleotidase SurE	0.0203490779710472	4,814937844	4,595744091	4,391319978
PADG_05929	protein-L-isoaspartate O-methyltransferase	0.000104293058688337	5,015705218	4,715644074	3,704689037
Protein/peptide degradation					
PADG_04167	aspartyl aminopeptidase	0.000221830754827111	4,711707982	4,761664746	4,32935125
PADG_02637	ubiquitin-conjugating enzyme	0.00552046595228165	4,872792902	4,74713498	4,027498635

PADG_06290	proteasome component PRE5	0.0119003210880048	4,766307346	4,669917249	4,373567455
PADG_03221	thimet oligopeptidase	0.0152211653648595	4,80783707	4,592539483	4,408436623
PADG_05922	glutamate carboxypeptidase	0.018794315888034	4,73451406	4,71895508	4,348713572
PADG_05820	xaa-Pro aminopeptidase	0.0537361658754471	4,727833223	4,664197629	4,432840532
PADG_05160	Dipeptidyl peptidase 3	0.000553026709381306	4,873587688	4,631341491	4,253430698
PADG_08442	Proteasome subunit alpha type	0.00644585367629858	4,755281119	4,638679663	4,433031534
PADG_03967	proteasome component C5	0.012833799267322	4,786024043	4,639418991	4,383072309
PADG_00599	26S protease regulatory subunit 6A	0.0340488792956519	4,595244231	4,576041291	4,681882584
PADG_07190	Proteasome endopeptidase complex	0.0500129362578737	4,685808127	4,644370537	4,516694831
PADG_00634	vacuolar protease A	0.00276331930081985	4,968790506	4,530863777	4,194408176
PADG_06546	Aminopeptidase	0.018748446410497	4,830794751	4,571297209	4,395915568
CELLULAR TRANSPORT					
Transported compounds (substrates)					
PADG_07964	V-type proton ATPase subunit E	0.00770764690084264	4,729775199	4,646047625	4,460493418
PADG_06692	mitochondrial phosphate carrier protein	0.028478971205458	4,39420673	4,490605834	4,882011935
PADG_08176	phosphatidylinositol-phosphatidylcholine transfer protein	0.0103878866021587	4,784662539	4,635754975	4,392693401
PADG_01363	diazepam-binding inhibitor (GABA receptor acyl- -binding)	0.0170201896661536	4,92734214	4,669880198	3,987396721
PADG_03559	Cytochrome b5	0.0428430530059768	4,522398224	4,667890812	4,658478151
PADG_01440	ADP,ATP carrier protein	0.00222386670540909	4,098809904	4,459730894	5,045813264
Transport facilities					
PADG_08263	mitochondrial outer membrane protein porin	0.00119131447896499	4,366925706	4,526098105	4,887228756
Transport routes					
PADG_02022	clathrin light chain	0.00526327780889446	4,816200246	4,626926026	4,354178111
PADG_02924	G2/M phase checkpoint control protein Sum2	0.000640360610487575	4,825499055	4,681949322	4,265576511
PADG_07014	vesicular-fusion sec17	0.0410862235352565	4,746350966	4,585578765	4,504549974
CELLULAR COMMUNICATION					
Cellular signalling					
PADG_08191	cAMP-dependent kinase regulatory subunit	0.000153652216039725	4,905139026	4,724698939	4,024461135
PADG_02845	CORD and CS domain-containing	0.000230062222189261	4,42651858	4,702698151	4,703069903

PADG_04383	tricalbin-3	0.00157729548942107	4,833496334	4,683724573	4,245252584
PADG_08342	GTP-binding protein ypt1	0.0262887200043236	4,373899747	4,617449581	4,805830969
PADG_07652	CAMK/CAMK1/CAMK1-CMK protein k	0.00982473505840494	4,617217107	4,739956467	4,481243158
PADG_07287	WD repeat	0.0424886349236938	4,778071968	4,624811589	4,407390063
PADG_03219	myosin regulatory light chain cdc4	0.00245254380627877	4,856051855	4,638140556	4,269488836
CELL RESCUE					
Stress response					
PADG_02981	ThiJ/PfpI family protein	0.0202700356111835	4,969158895	4,653292207	3,862802668
PADG_03170	serum paraoxonase/arylesterase 2	0.0049738065878992	4,263271672	4,534383093	4,930269596
PADG_01711	Hsp90 co-chaperone AHA1	0.00381621468774507	4,418910947	4,665225748	4,742829359
PADG_07715	hsp90-like protein	0.00592148500579047	4,272601712	4,506756175	4,944427698
PADG_02761	hsp75-like protein	0.0479601189854827	4,625108398	4,555358538	4,672132226
PADG_08369	hsp60-like protein	0.00127751244263923	4,269861989	4,623919284	4,868828951
PADG_03562	chaperone DnaK	0.00874116932727769	4,416981747	4,670109878	4,737873104
PADG_00430	70 kDa heat shock protein	0.00660782723481957	4,277611741	4,636715823	4,848676144
PADG_02785	heat shock protein Hsp88	0.0223062727662165	4,421970281	4,566846133	4,818361241
PADG_08118	hsp72-like protein	0.00757422338032652	4,503971072	4,807084211	4,510914648
PADG_03963	30 kDa heat shock	0.000805454890924632	3,907234604	5,040011608	4,593466774
PADG_05032	Hsp90 binding co-chaperone (Sba1)	0.0317768742306163	4,760075651	4,723692703	4,287059782
PADG_03163	cytochrome c peroxidase, mitochondrial	0.000593374880337985	4,149460697	4,552686262	4,97892349
PADG_04912	AhpC/TSA family protein	0.0170318717607415	4,422928572	4,43992092	4,900662484
PADG_07946	peroxisomal matrix protein	0.0297718977714577	4,603479545	4,547338774	4,699472102
PADG_00207	ribosome associated chaperone Zuotin	0.0439051277963011	4,487465531	4,493959266	4,822791798
PADG_03654	hypothetical protein	0.000102412429082015	5,232858129	4,510580278	3,142854946
PADG_03423	glutathione S-transferase Gst3	0.000573696552796715	4,861451528	4,642080797	4,260052768
PADG_02764	thioredoxin-like protein	0.00495776661632139	4,970281957	4,613656546	4,028733488
PADG_05504	thioredoxin	0.0208911445460205	4,839752856	4,666219097	4,227951953
PADG_05344	peroxiredoxin Q BCP	0.00309586826577796	4,908836395	4,675628207	4,091123767
PADG_03095	mitochondrial peroxiredoxin PRX1	0.0351949640957963	4,770536689	4,57017366	4,488509141
Virulence, disease factors					
PADG_07422	serine proteinase	0.00264817902949662	5,023466375	4,4580047	4,164800203
Detoxification					

PADG_00073	SAM-dependent methyltransferase COQ5 family	0.000874824117092326	5,02377962	4,673354018	3,778110074
PADG_07418	superoxide dismutase [Cu-Zn] SOD1	0.00119250240482325	5,002572022	4,694157826	3,748331219
PADG_01755	Fe-Mn family superoxide dismutase SOD2	0.0191136606558536	4,747140254	4,730220693	4,308531933
CELL FATE					
Cell growth / morphogenesis					
PADG_05517	rho-gdp dissociation inhibitor	0.019945607030085	4,695970017	4,674661965	4,467466281
PADG_04559	progesterone binding	0.0378473693930494	4,890078931	4,554044211	4,289504007
Cell death					
PADG_06087	hypothetical protein	0.000495869192119841	5,057736394	4,505364369	4,013416318
INTERACTION WITH THE ENVIRONMENT					
Cell adhesion					
PADG_04440	14-3-3-like protein	0.0115304629233556	4,474747759	4,558294872	4,792281251
PADG_07615	immunodominant antigen Gp43	0.00164042968040959	4,666062545	5,03618576	3,737957307
BIOGENESIS OF CELLULAR COMPONENTS					
Cell wall					
PADG_00994	chitinase class II	0.000152810421803673	5,076451382	4,682857856	3,526148881
PADG_03691	cell wall glucanase	0.000192529842468642	5,034906222	4,798688942	3,309820744
PADG_04499	cell wall protein ECM33 precursor	0.000415316082694873	5,013609023	4,588094308	4,000958064
PADG_05303	beta-1,6-glucan biosynthesis (Knh1)	0.013018510681609	4,176862126	4,450846863	5,014504656
PADG_02862	1,3-beta-glucosidase	0.0194863299097851	4,967639252	4,671081374	3,875321475
CELL TYPE DIFFERENTIATON					
Fungal/microorganismic cell type differentiation					
PADG_04260	NIMA-interacting protein TinC	0.000707300897920691	4,902369826	4,716769921	4,038720453
PADG_08091	cell polarity (Alp11)	0.0208774113534429	4,819567617	4,640531791	4,314261242
UNCLASSIFIED PROTEINS					
PADG_02604	hypothetical protein	0.00015844299425143	3,233564568	5,086561244	4,737180078
PADG_02181	HAD-superfamily hydrolase	0.000200997050975056	4,053767528	5,043066536	4,510838058
PADG_12447	hypothetical protein	0.000252966887635888	3,859343	4,914596903	4,786711526
PADG_04907	hypothetical protein	0.000318705002215328	2,79302038	5,255516879	4,500497277
PADG_05157	cell surface protein, putative	0.000347601158886615	3,342738381	5,159512053	4,584087403

PADG_04343	short chain dehydrogenase/reductase	0.000645592053848837	3,885565792	4,943943662	4,739162014
PADG_01857	Uncharacterized protein	0.000735739746029736	3,475920184	5,210426343	4,449778533
PADG_02967	Uncharacterized protein	0.000954103076199105	3,980577659	4,913308671	4,729137937
PADG_06021	hypothetical protein	0.000987328858139613	3,812707863	5,038164044	4,628818149
PADG_06202	Arp2 3 complex subunit Arc16	0.00132807191136456	4,115747717	4,883504224	4,697949964
PADG_07670	SAP domain-containing protein	0.0013911862778064	4,09916138	4,898914551	4,68836461
PADG_11347	hypothetical protein	0.00197211084602885	4,241811493	4,847036187	4,669120514
PADG_00422	actin cytoskeleton protein (VIP1)	0.00207529238829785	4,090794531	4,863618806	4,730589951
PADG_04205	hypothetical protein	0.00267855755722755	3,67182148	5,11971357	4,547409828
PADG_01002	erythrocyte band 7 integral membrane protein	0.00271552290942387	4,109788027	4,892394591	4,689302311
PADG_02858	hypothetical protein	0.00310539167374307	3,98101627	4,984665705	4,619603997
PADG_11101	hypothetical protein	0.00317627875002816	4,250211253	4,855392875	4,652679694
PADG_12152	hypothetical protein	0.00345282888989835	5,054402241	4,032047001	4,484611312
PADG_00674	hypothetical protein	0.00394824311127837	3,434948878	5,07839186	4,66710289
PADG_02909	Uncharacterized protein	0.00455833380773627	4,278707126	4,681344705	4,8137992
PADG_11424	hypothetical protein	0.00515308641760238	4,349022319	4,808892077	4,640147015
PADG_02338	Uncharacterized protein	0.00599800759227989	4,442172881	4,882050852	4,461177222
PADG_12252	hypothetical protein	0.00737286242790404	4,120546287	4,922314886	4,639368701
PADG_08152	hypothetical protein	0.00772151473816209	4,232944489	4,867997096	4,64225325
PADG_08270	UBX domain-containing protein	0.00779498683485196	4,283499377	4,761452674	4,733948994
PADG_02944	hypothetical protein	0.00846113292689915	3,941461494	4,922342363	4,717490349
PADG_05356	isochorismatase domain-containing protein	0.00876062721083998	4,809702986	4,411124649	4,591003962
PADG_00921	Uncharacterized protein	0.00965739615783812	4,287608501	4,773037508	4,718379986
PADG_11487	hypothetical protein	0.0106368435907347	3,670316578	5,027612697	4,671415452
PADG_07225	Uncharacterized protein	0.0107115482507958	4,054135489	4,924010107	4,66342363
PADG_11950	hypothetical protein	0.0114196399407177	4,330746747	4,818522183	4,637288403
PADG_06136	related to mismatched base pair and cruciform dna recognition	0.0130031745279776	3,61461079	5,16149797	4,452555837
PADG_07506	hypothetical protein	0.0146863742665499	4,230198937	4,766928354	4,754791959
PADG_02118	Uncharacterized protein	0.016955093392485	3,90669173	4,980449614	4,62905153
PADG_04818	hypothetical protein	0.0170034848346801	4,166392385	4,801772905	4,747415906

PADG_00676	hypothetical protein	0.0225015189702146	4,372216502	4,787850896	4,642178096
PADG_04685	Uncharacterized protein	0.0233426763011714	4,515853332	4,695951088	4,635245877
PADG_03203	BAR domain-containing protein	0.0256785799658214	4,519041996	4,715698997	4,610822345
PADG_04215	DUF124 domain-containing protein	0.026961653931293	3,977082861	4,895178906	4,719112589
PADG_01688	DlpA domain-containing protein	0.030468175182578	4,437803058	4,793920884	4,582297304
PADG_02709	hypothetical protein	0.0373430897201166	4,314839579	4,774355705	4,68820212
PADG_05584	hypothetical protein	0.0507774717047346	4,318844881	4,816236545	4,63363081
PADG_02307	CUE domain-containing	0.052604670310913	4,379546441	4,815450114	4,595509363
PADG_04806	hypothetical protein	0.0526341547562164	4,304262402	4,855251489	4,589656491
PADG_06945	GYF domain-containing protein	0.0535146776162895	4,351586581	4,811209957	4,620114275
PADG_06080	hypothetical protein	0.00220468098930026	4,946386859	4,250591833	4,525162759
PADG_06699	Uncharacterized protein	0.000786530106643649	3,644784847	4,550367318	5,134387548
PADG_11413	hypothetical protein	0.0184217228588476	4,887682067	4,415166133	4,467751787
PADG_11832	hypothetical protein	0.0233063048763567	4,790666354	4,618384776	4,399943327
PADG_01128	hypothetical protein	0.0298111381892491	4,732805598	4,420444995	4,669133595
PADG_04439	Uncharacterized protein	0.054953798716532	4,948640174	4,227123579	4,482777612

[a]Acession number - acession number of matched protein from *Paracoccidioides brasiliensis* Uniprot database

[b]Protein description - proteins annotation from *Paracoccidioides brasiliensis* database or by homology in Blast2GO or NCBI

[c]p-value - statistically significant differences are considered with ≤ 0.05 (ANOVA)

[d]Tukey's test- average of the Tukey test (of mycelia, mycelia-to-yeast transition and yeast) used for statistical

[e] Biological process of differentially expressed proteins from MIPS (http://mips.helmholtz-muenchen.de/funcatDB) and Uniprot databases (http://www.uniprot.org/)

Table S3. Identified proteins from *Paracoccidioides brasiliensis* up-regulated in the mycelia phase compared to the mycelia-to-yeast transition and yeast cells

Acession number[a]	**Protein description[b]**	**Score[c]**	**p-value[d]**
Functional categories[e]			

METABOLISM			
Amino acid metabolism			
PADG_02214	4-aminobutyrate aminotransferase	146,62	0.000473697117025741
PADG_03522	methylthioadenosine phosphorylase	61,07	0.00188671139057892
PADG_06252	1,2-dihydroxy-3-keto-5-methylthiopentene dioxygenase	29,88	0.00701338481935753
PADG_06144	saccharopine dehydrogenase	25,89	0.00527529557636022
PADG_01718	Saccharopine dehydrogenase [NADP+, L-glutamate-forming]	25,07	0.0221450392480064
PADG_08021	phospho-2-dehydro-3-deoxyheptonate aldolase	35,26	0.00034871632473159
PADG_04603	spermidine synthase	34,69	0.0432103775062461
Nucleotide/nucleoside/nucleobase metabolism			
PADG_00780	ribose-phosphate pyrophosphokinase II	65,5	0.00949990061787514
PADG_04869	HIT domain-containing	27,59	0.00214233464281135
PADG_08066	purine nucleoside phosphorylase I, inosine and guanosine-specific	14,82	0.00427473565670872
PADG_00322	xanthine-guanine phosphoribosyl transferase	29,21	0.00126429186045653
PADG_00621	Hydroxyisourate hydrolase	5,54	0.0195414250770774
PADG_07970	dihydroorotase, homodimeric	36,69	0.000601494528361185
PADG_01100	uracil phosphoribosyltransferase	22,47	0.00342045544824264
PADG_07782	Deoxyuridine 5'-triphosphate nucleotidohydrolase	81,69	0.00385911777105953
PADG_06054	deoxyribose-phosphate aldolase	14,93	0.0359382344610037
PADG_02658	nucleoside-diphosphate-sugar epimerase	26,88	0.000440673349932956
Phosphate metabolism			
PADG_0417	Inorganic pyrophosphatase	101,62	0.00039648057603618
C-compound and carbohydrate metabolism			
PADG_00649	alcohol oxidase	99,63	0.000210018090153545
PADG_04687	short-chain dehydrogenase reductase family	63,12	0.00109994176880593
PADG_03859	NADP-dependent mannitol dehydrogenase	37,32	0.0016711614063246
PADG_00735	Lactam utilization protein lamB	19,26	0.00269083936760223
PADG_01372	mannitol-1-phosphate 5-dehydrogenase	98,2	0.00320014525763444
PADG_05855	lactonohydrolase	38,03	0.00734969612425638
PADG_07606	2,5-diketo-D-gluconic acid reductase A	77,45	0.010818881866288
PADG_06740	betaine aldehyde dehydrogenase	60,37	0.0325496051578872
PADG_05081	Aldehyde dehydrogenase	222,22	0.000318428299089706

Lipid, fatty acid and isoprenoid metabolism			
PADG_03492	phosphatidylserine decarboxylase	29,91	0.00185747080872941
PADG_03449	Isopentenyl-diphosphate delta-isomerase	20,95	0.0209229087713661
Secondary metabolism			
PADG_08034	dienelactone hydrolase family protein	107,18	0.00108007819663931
PADG_01052	3-demethylubiquinone-9 3-methyltransferase	20,31	0.00572417440168868
PADG_00312	cytochrome c heme lyase	15,03	0.0179304699139903
ENERGY			
Glycolysis and gluconeogenesis			
PADG_00852	fructose-1,6-bisphosphate aldolase, class 2	18,6	0.0321261222174796
PADG_07950	glucokinase	34,61	0.0269789169774159
PADG_06906	Triosephosphate isomerase	155,73	0.00153813947318225
PADG_05109	2,3-bisphosphoglycerate-independent phosphoglycerate mutase	62,5	0.0117496849150458
Tricarboxylic-acid pathway (citrate cycle, Krebs cycle, TCA cycle)			
PADG_04165	pyruvate dehydrogenase complex component Pdx1	38,2	0.00131307433739174
Respiration			
PADG_05403	NADH-ubiquinone oxidoreductase 21 kDa subunit	61,24	0.0252028231260988
PADG_07749	NAD(P)H:quinone oxidoreductase, type IV	209,82	0.0488987573295302
Fermentation			
PADG_11405	Alcohol dehydrogenase 1	181,54	0.000117667332982207
PADG_04701	Alcohol dehydrogenase	19,87	0.0398751128886334
CELL CYCLE AND DNA PROCESSING			
DNA processing			
PADG_03459	replication factor-A protein	33,18	0.0149027131920101
PADG_05818	HLH DNA binding	11,19	0.0230078557563301
PADG_02683	UV excision repair protein Rad23	95,32	0.0101122103649832
PADG_05709	histone acetyltransferase type B subunit 2	27,36	0.00164234466516168
PADG_00656	Non-histone chromosomal protein 6	49,18	0.00349912944508594
Cell cycle			
PADG_04795	deubiquitination-protection protein dph1	66,45	0.00011583181867771
PADG_05683	cell division control protein 48	276,29	0.000330152297791995
PADG_07319	septin-1	30,11	0.000818895717889287

PADG_07515	NSFL1 cofactor p47	31,97	0.0143456926429943
TRANSCRIPTION			
RNA synthesis			
PADG_00814	branchpoint-bridging protein	22,78	0.000361519806372817
PADG_04307	mRNA binding post-transcriptional regulator	149,3	0.00322339287702619
PADG_01508	U1 small nuclear ribonucleoprotein C	9,16	0.0268581913593662
PADG_01455	KH domain RNA-binding protein	177,31	0.000544832339699319
PADG_08081	zinc knuckle domain	30,31	0.000727891867202843
PADG_00220	class 2 transcription repressor NC2	9,43	0.00304321420966517
PADG_04311	cellular nucleic acid-binding protein	21,89	0.0115271319353104
PADG_03869	HMG box	37,81	0.0149326260057446
PADG_06182	Glucose repression regulatory protein TUP1	130,91	0.0323405291079937
RNA processing			
PADG_02783	RNA-binding La domain-containing protein	35,41	0.0252707765390186
PADG_07689	transformer-SR ribonucleoprotein	63,33	0.00285515817257463
PADG_00044	28 kDa ribonucleoprotein	51,51	0.0311052414112992
PADG_00576	RNA recognition domain-containing protein containing protein, variant	43,25	0.000366474914980045
PADG_05340	pre-mrna splicing factor	73,65	0.00567170230733727
PADG_04369	splicing factor U2AF 23 kDa subunit	7,35	0.0093556652043975
PADG_04301	WD repeat-containing protein	33,57	0.0304988927372442
PROTEIN SYNTHESIS			
Ribosome biogenesis			
PADG_01026	60S ribosomal protein L43	48,71	0.00189393950236822
PADG_05686	ribosome biogenesis protein	19,52	0.0171919284417786
PADG_00335	40S ribosomal protein S14	150,13	0.0009283171462339
PADG_07583	40S ribosomal protein S21	54,68	0.00321015987134523
PADG_03781	60S ribosomal protein L30	65,22	0.00769160773234302
PADG_00995	ubiquitin-40S ribosomal protein S27a	80,68	0.0155770103199853
PADG_02249	60S ribosomal protein L2	50,71	0.049831342606761
PADG_01427	40S ribosomal protein S12	55,94	0.00188255977619058
Translation			
PADG_01079	translation initiation factor 4B	132,46	0.0305078072836169

PADG_07356	woronin body major protein	79,11	0.00055674974717756
PADG_01865	Eukaryotic translation initiation factor 3 subunit H	84,83	0.00217169449999158
PADG_00457	translation initiation factor 4G	97,39	0.0127112389368946
PADG_06110	translation initiation factor SUI1	25,21	0.0258640355371289
PADG_02691	eukaryotic translation initiation factor 6	19,22	0.0525198964080063
PROTEIN FOLDING AND STABILIZATION			
Protein folding and stabilization			
PADG_12329	prefoldin subunit 2	15,08	0.00122708938870604
PADG_01852	small glutamine-rich tetratricopeptide repeat-containing protein	61,51	0.0194408966072878
PADG_05203	Peptidyl-prolyl cis-trans isomerase	49,8	0.028957954112554
PADG_07953	Peptidyl-prolyl cis-trans isomerase	32,66	0.00239744249348738
Protein targeting, sorting and translocation			
PADG_02619	F-box domain-containing	45,73	0.0017688464217684
PADG_08188	vacuolar-sorting protein snf7	23,85	0.00562474527488371
PADG_08646	class E vacuolar -sorting machinery HSE1	22,48	0.0176936537439237
PADG_03274	mitochondrial import inner membrane translocase subunit tim9	36,03	0.0226626979060814
PADG_00240	SNF7 family protein Fti1/Did2	20,82	0.00561971799727414
Protein modification			
PADG_00809	ubiquitin-conjugating enzyme	17,71	0.00179716781257883
PADG_07925	ubiquitin-conjugating enzyme E2 N	24,77	0.00217641874973217
PADG_00569	5'/3'-nucleotidase SurE	7,3	0.0203490779710472
PADG_05929	protein-L-isoaspartate O-methyltransferase	8,5	0.000104293058688337
Protein/peptide degradation			
PADG_02637	ubiquitin-conjugating enzyme	47,99	0.00552046595228165
PADG_06290	proteasome component PRE5	48,18	0.0119003210880048
PADG_03221	thimet oligopeptidase	44,01	0.0152211653648595
PADG_05922	glutamate carboxypeptidase	62,82	0.018794315888034
PADG_05820	xaa-Pro aminopeptidase	60,96	0.0537361658754471
PADG_05160	Dipeptidyl peptidase 3	42,94	0.000553026709381306
PADG_08442	Proteasome subunit alpha type	30,72	0.00644585367629858
PADG_03967	proteasome component C5	45,24	0.012833799267322
PADG_07190	Proteasome endopeptidase complex	37,56	0.0500129362578737

PADG_00634	vacuolar protease A	25,22	0.00276331930081985
PADG_06546	Aminopeptidase	59,91	0.018748446410497
CELLULAR TRANSPORT			
Transported compounds (substrates)			
PADG_07964	V-type proton ATPase subunit E	83,38	0.00770764690084264
PADG_08176	phosphatidylinositol-phosphatidylcholine transfer protein	31,56	0.0103878866021587
PADG_01363	diazepam-binding inhibitor (GABA receptor acyl- -binding)	84,2	0.0170201896661536
Transport routes			
PADG_02022	clathrin light chain	84,07	0.00526327780889446
PADG_02924	G2/M phase checkpoint control protein Sum2	24,09	0.000640360610487575
PADG_07014	vesicular-fusion sec17	58,84	0.0410862235352565
CELLULAR COMMUNICATION			
Cellular signalling			
PADG_08191	cAMP-dependent kinase regulatory subunit	15,37	0.000153652216039725
PADG_04383	tricalbin-3	25,57	0.00157729548942107
PADG_07287	WD repeat	13,98	0.0424886349236938
PADG_03219	myosin regulatory light chain cdc4	34,13	0.00245254380627877
CELL RESCUE			
Stress response			
PADG_02981	ThiJ/PfpI family protein	71,14	0.0202700356111835
PADG_05032	Hsp90 binding co-chaperone (Sba1)	39,31	0.0317768742306163
PADG_03423	glutathione S-transferase Gst3	28,83	0.000573696552796715
PADG_02764	thioredoxin-like protein	76,21	0.00495776661632139
PADG_05344	peroxiredoxin Q BCP	15,93	0.00309586826577796
PADG_05504	thioredoxin	106,67	0.0208911445460205
Virulence, disease factors			
PADG_07422	serine proteinase	29,51	0.00264817902949662
Detoxification			
PADG_03095	mitochondrial peroxiredoxin PRX1	33,08	0.0351949640957963
PADG_00073	SAM-dependent methyltransferase COQ5 family	35,14	0.000874824117092326
PADG_07418	superoxide dismutase [Cu-Zn] SOD1	101,1	0.00119250240482325
PADG_01755	Fe-Mn family superoxide dismutase SOD2	40,2	0.0191136606558536

CELL FATE			
Cell growth / morphogenesis			
PADG_05517	rho-gdp dissociation inhibitor	21,41	0.019945607030085
PADG_04559	progesterone binding	16,55	0.0378473693930494
Cell death			
PADG_06087	hypothetical protein	15,32	0.000495869192119841
BIOGENESIS OF CELLULAR COMPONENTS			
Cell wall			
PADG_00994	chitinase class II	236,68	0.000152810421803673
PADG_03691	cell wall glucanase	9,66	0.000192529842468642
PADG_04499	cell wall protein ECM33 precursor	22,82	0.000415316082694873
PADG_02862	1,3-beta-glucosidase	9,17	0.0194863299097851
CELL TYPE DIFFERENTIATON			
Fungal/microorganismic cell type differentiation			
PADG_04260	NIMA-interacting protein TinC	29,3	0.000707300897920691
PADG_08091	cell polarity (Alp11)	11,88	0.0208774113534429
UNCLASSIFIED PROTEINS			
PADG_02604	hypothetical protein	33,89	0.00015844299425143
PADG_02181	HAD-superfamily hydrolase	36,51	0.000200997050975056
PADG_12447	hypothetical protein	102,27	0.000252966887635888
PADG_04907	hypothetical protein	47,96	0.000318705002215328
PADG_05157	cell surface protein, putative	27,81	0.000347601158886615
PADG_04343	short chain dehydrogenase/reductase	21,75	0.000645592053848837
PADG_01857	Uncharacterized protein	41,39	0.000735739746029736
PADG_02967	Uncharacterized protein	111,93	0.000954103076199105
PADG_06021	hypothetical protein	32,74	0.000987328858139613
PADG_06202	Arp2 3 complex subunit Arc16	66,98	0.00132807191136456
PADG_07670	SAP domain-containing protein	30,66	0.0013911862778064
PADG_11347	hypothetical protein	33,49	0.00197211084602885
PADG_00422	actin cytoskeleton protein (VIP1)	162,78	0.00207529238829785
PADG_04205	hypothetical protein	39,47	0.00267855755722755
PADG_01002	erythrocyte band 7 integral membrane protein	17,5	0.00271552290942387

PADG_02858	hypothetical protein	37,78	0.00310539167374307
PADG_11101	hypothetical protein	41,61	0.00317627875002816
PADG_00674	hypothetical protein	13,05	0.00394824311127837
PADG_11424	hypothetical protein	41,88	0.00515308641760238
PADG_02338	Uncharacterized protein	19,47	0.00599800759227989
PADG_12252	hypothetical protein	8,88	0.00737286242790404
PADG_08152	hypothetical protein	13,17	0.00772151473816209
PADG_08270	UBX domain-containing protein	8,33	0.00779498683485196
PADG_02944	hypothetical protein	23,01	0.00846113292689915
PADG_00921	Uncharacterized protein	35,19	0.00965739615783812
PADG_11487	hypothetical protein	17,57	0.0106368435907347
PADG_07225	Uncharacterized protein	24,59	0.0107115482507958
PADG_11950	hypothetical protein	122,48	0.0114196399407177
PADG_06136	related to mismatched base pair and cruciform dna recognition	21,36	0.0130031745279776
PADG_07506	hypothetical protein	44,27	0.0146863742665499
PADG_02118	Uncharacterized protein	16,96	0.016955093392485
PADG_04818	hypothetical protein	5,42	0.0170034848346801
PADG_00676	hypothetical protein	128,58	0.0225015189702146
PADG_04685	Uncharacterized protein	15,49	0.0233426763011714
PADG_03203	BAR domain-containing protein	88,17	0.0256785799658214
PADG_04215	DUF124 domain-containing protein	21,2	0.026961653931293
PADG_01688	DlpA domain-containing protein	12,4	0.030468175182578
PADG_02709	hypothetical protein	17,25	0.0373430897201166
PADG_05584	hypothetical protein	13,06	0.0507774717047346
PADG_02307	CUE domain-containing	12,64	0.052604670310913
PADG_04806	hypothetical protein	14,14	0.0526341547562164
PADG_06945	GYF domain-containing protein	26,02	0.0535146776162895

[a]Acession number - acession number of matched protein from *Paracoccidioides brasiliensis* Uniprot database

[b]Protein description - proteins annotation from *Paracoccidioides brasiliensis* database or by homology in Blast2GO or NCBI

[c]Score - score obtained from the MS Amanda 2.0

[d]p-value - statistically significant differences are considered with ≤ 0.05 (ANOVA)
[e]Biological process of differentially expressed proteins from MIPS (http://mips.helmholtz-muenchen.de/funcatDB) and Uniprot databases (http://www.uniprot.org/).

Table S4. Identified proteins from *Paracoccidioides brasiliensis* down-regulated in the mycelia phase compared to the mycelia-to-yeast transition and yeast cells

Acession number[a]	Protein description[b]	Score[c]	p-value[d]
Functional categories[e]			
METABOLISM			
Amino acid metabolism			
PADG_01488	thiol methyltransferase	16,36	0.00859584687713703
PADG_01621	aspartate aminotransferase	76,22	0.000603223867301128
PADG_05277	Serine hydroxymethyltransferase	84,56	0.00298066391122739
PADG_03627	2-oxoisovalerate dehydrogenase subunit beta	40,81	0.0373648418664289
PADG_08262	asparagine synthase (glutamine-hydrolyzing)	7,22	0.0374351680322741
PADG_00888	Argininosuccinate synthase	54,79	0.0283905003634937
PADG_05058	chorismate mutase	36,37	0.0226842449859004
PADG_01886	adenosylhomocysteinase	101,7	0.02113109868656
PADG_00210	glycine dehydrogenase	39,27	0.0105405077270114
PADG_08468	4-hydroxyphenylpyruvate dioxygenase	60,91	0.00549013636700336
PADG_08465	fumarylacetoacetase	57,67	0.0108038616369285
PADG_07366	methylcrotonoyl-CoA carboxylase subunit alpha	32,16	0.0509066885694793
PADG_04487	chorismate synthase	22,9	0.0314909968419182
Nucleotide/nucleoside/nucleobase metabolism			
PADG_04099	phosphoribosylaminoimidazolecarboxamide formyltransferase/IMP cyclohydrolase	105,74	0.0290343921451513
PADG_01159	Uridylate kinase	25,89	0.0225226043444458
PADG_05321	DNA RNA non-specific nuclease	31,72	0.0499799223721024
C-compound and carbohydrate metabolism			
PADG_03118	aldose 1-epimerase family	20,92	0.0473203607543561
PADG_00912	UDP-galactopyranose mutase	49,9	0.00775039746204842
PADG_01677	acetyl-coenzyme A synthetase	23,94	0.0413980013723899
PADG_04710	2-methylcitrate mitochondrial	179,9	0.00129368626044376

Lipid, fatty acid and isoprenoid metabolism			
PADG_12025	glutaryl- CoA dehydrogenase	11,75	0.0378176148991082
PADG_01228	3-hydroxybutyryl-CoA dehydrogenase	26,98	0.00942493695792639
PADG_00255	fatty acid synthase beta subunit dehydratase	97,69	0.0372553299870248
PADG_04718	2-methylcitrate dehydratase	162,21	0.000131666517534101
Metabolism of vitamins, cofactors, and prosthetic groups			
PADG_00443	Dihydropteroate synthase	75,47	0.00123800894548555
PADG_05822	Pyridoxine biosynthesis protein pyroA	89,63	0.00277034051507976
PADG_08457	biotin synthase	6,95	0.0395889417320599
ENERGY			
Glycolysis and gluconeogenesis			
PADG_01896	Phosphoglycerate kinase	134,19	0.000712735140039373
PADG_08503	Phosphoenolpyruvate carboxykinase	71,43	0.0115249761276736
PADG_02411	Glyceraldehyde-3-phosphate dehydrogenase	554,25	0.0492052726676888
PADG_04059	Enolase	350,01	0.00541040257511781
Tricarboxylic-acid pathway (citrate cycle, Krebs cycle, TCA cycle)			
PADG_00246	pyruvate dehydrogenase E1 component subunit beta	71,06	0.0014620825618247
PADG_04993	ATP-citrate synthase subunit 1	69,17	0.0215948774017605
PADG_07213	pyruvate dehydrogenase complex dihydrolipoamide acetyltransferase	103,07	0.006306183339428
PADG_11845	Aconitate hydratase, mitochondrial	207,07	0.0302112190508672
PADG_00317	succinyl-CoA ligase subunit beta	48,46	0.0126837599715285
PADG_02260	succinyl-CoA ligase subunit alpha	74,34	0.0326252304957893
PADG_04939	Succinyl-CoA:3-ketoacid-coenzyme A transferase	58,28	0.0201943831690541
PADG_08387	Citrate synthase	76,95	0.00379083047685583
PADG_01797	Dihydrolipoamide acetyltransferase component of pyruvate dehydrogenase	57,76	0.0128389547829813
Electron transport and membrane-associated energy conservation			
PADG_02561	ATP synthase subunit alpha, mitochondrial	327,16	0.00099703997320092
PADG_05436	Cytochrome b-c1 complex subunit Rieske	13,56	0.00954500862971618
PADG_03516	NADH-ubiquinone oxidoreductase 30.4 kDa subunit	15,29	0.00859471577854355
PADG_06196	12-oxophytodienoate reductase	53,59	0.000130524968963367
Respiration			
PADG_05750	cytochrome c oxidase polypeptide VI	57,71	0.000329872995986405

PADG_07081	electron transfer flavo alpha subunit	85,34	0.0265951000485402
PADG_03039	MICOS complex subunit MIC60	52,1	0.0458991211511605
PADG_03872	mitochondrial import inner membrane translocase subunit tim1	28,08	0.0280037026658489
PADG_07042	ATP synthase F1, delta subunit	73,15	0.0514263542897544
PADG_07813	ATP synthase F1, gamma subunit	94,65	0.00320229579998738
PADG_08349	ATP synthase subunit beta, mitochondrial	526,17	0.0091913956997716
PADG_05402	mitochondrial F1F0 ATP synthase subunit	32,02	0.0128065223457609
Oxidation of fatty acids			
PADG_06805	acyl- dehydrogenase	93,54	0.00228164549110767
PADG_01209	enoyl-CoA hydratase	75,09	0.0158508402126517
PADG_07023	carnitine O-acetyltransferase	23,7	0.0299195036063134
PADG_01687	3-ketoacyl-CoA thiolase	148,38	0.000606823603773545
TRANSCRIPTION			
RNA synthesis			
PADG_02555	nucleic acid-binding protein	62,4	0.0101850714020848
PADG_00872	histone H4	71,3	0.0252015733715969
PROTEIN SYNTHESIS			
Ribosome biogenesis			
PADG_11904	Ribosomal protein L1	36,56	0.0547556214196747
PADG_03856	60S ribosomal protein L15	31,71	0.000948265034607996
PADG_04848	60S ribosomal protein L8-B	58,13	0.00391393542396789
PADG_04862	50S ribosomal protein Mrp49	12,73	0.0046969426014565
PADG_05721	60S ribosomal protein L4	139	0.031687423620715
PADG_00784	40S ribosomal protein S0	43,43	0.038488765469723
PADG_02056	ribosomal protein L7	39,41	0.00101174747252608
PADG_01654	40S ribosomal protein S6-A	84,13	0.00128612006836141
PADG_00354	40S ribosomal protein S17	91,49	0.00512401922994533
PADG_01914	60S ribosomal protein L35	36,39	0.00595985342101163
PADG_00627	mitochondrial large ribosomal subunit L49, variant	5,15	0.00635571801442804
PADG_01387	60S ribosomal protein L7	35,88	0.00676476492288821
PADG_03778	60S ribosomal protein L10-A	56,25	0.0128434095495006
PADG_04106	60S ribosomal protein L11	47,97	0.0202870981819721

PADG_03873	60S ribosomal protein L20	18,21	0.0326173334051663
PADG_06525	40S ribosomal protein S1	78,17	0.0498924638228775
PADG_05939	60S ribosomal protein L27a	92,23	0.00976778835723734
PADG_03326	40S ribosomal protein S9	28,36	0.0516200825998414
PADG_03315	40S ribosomal protein S4	84,65	0.00145057927925207
PADG_02888	60S ribosomal protein L6 O	64,61	0.00058696534564495
PADG_06838	40S ribosomal protein S5	81,11	0.0280593514265553
PADG_02828	Ribosomal protein	35,23	0.0319912825552141
PADG_06048	40S ribosomal protein S27	16,06	0.0441806922768012
PADG_11379	60S ribosomal protein L5	90,99	0.00947872658438146
Translation			
PADG_02759	ribosome recycling factor domain-containing protein	14,85	0.00717309135667122
PADG_02896	elongation factor 1-beta	55,72	0.000328396134515179
PADG_00692	elongation factor 1-alpha	229,91	0.0033049385655597
PADG_08125	Elongation factor 2	258,41	0.00977484226145031
PADG_06265	elongation factor 1-gamma	94,06	0.00245190358187735
Aminoacyl-tRNA-synthetases			
PADG_05848	glycine-tRNA ligase	29,33	0.0284549763738526
PROTEIN FOLDING AND STABILIZATION			
Protein folding and stabilization			
PADG_12323	peptidyl-prolyl cis-trans isomerase	46,01	0.000811310718754342
PADG_02895	ATP-dependent Clp protease ATP-binding subunit ClpB	62,13	0.00276781772538938
PADG_07815	disulfide-isomerase domain	37,88	0.00378267127358446
PADG_04092	peptidyl-prolyl cis-trans isomerase B	109,77	0.00718691945820977
PADG_05628	Protein disulfide-isomerase domain	65,37	0.0189209329424933
PADG_06488	peptidyl-prolyl cis-trans isomerase D	139,23	0.0284592321370524
PADG_08048	T-complex protein 1 subunit beta	88,82	0.0435867936243462
PADG_08587	Peptidylprolyl isomerase	24,02	0.000635200628117717
PADG_01565	calnexin	82,6	0.0476035441549569
PADG_04034	Chaperone DnaJ	148,98	0.0070692227624351
PADG_02206	DnaJ domain protein Psi	62,1	0.0474842422073504
PADG_05229	chaperone protein dnaJ 3	20,67	0.00851844162738829

Protein/peptide degradation			
PADG_00599	26S protease regulatory subunit 6A	58,13	0.0340488792956519
PADG_04167	aspartyl aminopeptidase	86,75	0.000221830754827111
CELLULAR TRANSPORT			
transported compounds (substrates)			
PADG_06692	mitochondrial phosphate carrier protein	49,55	0.028478971205458
PADG_01440	ADP,ATP carrier protein	185,6	0.00222386670540909
PADG_03559	Cytochrome b5	28,87	0.0428430530059768
Transport facilities			
PADG_08263	mitochondrial outer membrane protein porin	144,86	0.00119131447896499
CELLULAR COMMUNICATION			
Cellular signalling			
PADG_02845	CORD and CS domain-containing	36,07	0.000230062222189261
PADG_08342	GTP-binding protein ypt1	36,58	0.0262887200043236
PADG_07652	CAMK/CAMK1/CAMK1-CMK protein k	16,53	0.00982473505840494
CELL RESCUE			
Stress response			
PADG_03170	serum paraoxonase/arylesterase 2	8,91	0.0049738065878992
PADG_01711	Hsp90 co-chaperone AHA1	85,65	0.00381621468774507
PADG_07715	hsp90-like protein	342,67	0.00592148500579047
PADG_02761	hsp75-like protein	294,38	0.0479601189854827
PADG_08369	hsp60-like protein	831,65	0.00127751244263923
PADG_03562	chaperone DnaK	355,03	0.00874116932727769
PADG_03163	cytochrome c peroxidase, mitochondrial	109,64	0.000593374880337985
PADG_04912	AhpC/TSA family protein	50,22	0.0170318717607415
PADG_07946	peroxisomal matrix protein	44,1	0.0297718977714577
PADG_00430	70 kDa heat shock protein	484,2	0.00660782723481957
PADG_02785	heat shock protein Hsp88	152,1	0.0223062727662165
PADG_00207	ribosome associated chaperone Zuotin	60,82	0.0439051277963011
PADG_08118	hsp72-like protein	959,26	0.00757422338032652
PADG_03963	30 kDa heat shock	138,26	0.000805454890924632
PADG_03654	hypothetical protein	19,31	0.000102412429082015

INTERACTION WITH THE ENVIRONMENT			
Cell adhesion			
PADG_04440	14-3-3-like protein	109,53	0.0115304629233556
PADG_07615	immunodominant antigen Gp43	22,2	0.00164042968040959
BIOGENESIS OF CELLULAR COMPONENTS			
Cell wall			
PADG_05303	beta-1,6-glucan biosynthesis (Knh1)	5,13	0.013018510681609
UNCLASSIFIED PROTEINS			
PADG_12152	hypothetical protein	10,19	0.00345282888989835
PADG_05356	isochorismatase domain-containing protein	80,89	0.00876062721083998
PADG_06080	hypothetical protein	17,63	0.00220468098930026
PADG_11413	hypothetical protein	19,14	0.0184217228588476
PADG_11832	hypothetical protein	18,79	0.0233063048763567
PADG_01128	hypothetical protein	11,22	0.0298111381892491
PADG_04439	Uncharacterized protein	18,72	0.054953798716532
PADG_02909	Uncharacterized protein	14,92	0.00455833380773627
PADG_06699	Uncharacterized protein	14,25	0.000786530106643649

[a]Acession number - acession number of matched protein from *Paracoccidioides brasiliensis* Uniprot database

[b]Protein description - proteins annotation from *Paracoccidioides brasiliensis* database or by homology in Blast2GO or NCBI

[c]Score - score obtained from the MS Amanda 2.0

[d]p-value - statistically significant differences are considered with ≤ 0.05 (ANOVA)

[e]Biological process of differentially expressed proteins from MIPS (http://mips.helmholtz-muenchen.de/funcatDB) and Uniprot databases (http://www.uniprot.org/).

Table S5. Identified proteins from *Paracoccidioides brasiliensis* up-regulated in the mycelia-to-yeast transition compared to the mycelia phase and yeast cells

Acession number[a]	Protein description[b]	Score[c]	p-value[d]
Functional categories[e]			
METABOLISM			

Amino acid metabolism			
PADG_04487	chorismate synthase	22,9	0.0314909968419182
C-compound and carbohydrate metabolism			
PADG_01677	acetyl-coenzyme A synthetase	23,94	0.0413980013723899
ENERGY			
Glycolysis and gluconeogenesis			
PADG_08503	Phosphoenolpyruvate carboxykinase	71,43	0.0115249761276736
PADG_02411	Glyceraldehyde-3-phosphate dehydrogenase	554,25	0.0492052726676888
Electron transport and membrane-associated energy conservation			
PADG_06196	12-oxophytodienoate reductase	53,59	0.000130524968963367
PROTEIN FOLDING AND STABILIZATION			
Protein folding and stabilization			
PADG_08587	Peptidylprolyl isomerase	24,02	0.000635200628117717
PADG_01565	calnexin	82,6	0.0476035441549569
PADG_04034	Chaperone DnaJ	148,98	0.0070692227624351
PADG_02206	DnaJ domain protein Psi	62,1	0.0474842422073504
PADG_05229	chaperone protein dnaJ 3	20,67	0.00851844162738829
Protein/peptide degradation			
PADG_04167	aspartyl aminopeptidase	86,75	0.000221830754827111
CELLULAR TRANSPORT			
Transported compounds (substrates)			
PADG_03559	Cytochrome b5	28,87	0.0428430530059768
CELLULAR COMMUNICATION			
Cellular signalling			
PADG_07652	CAMK/CAMK1/CAMK1-CMK protein k	16,53	0.00982473505840494
CELL RESCUE			
Stress response			
PADG_08118	hsp72-like protein	959,26	0.00757422338032652
PADG_03963	30 kDa heat shock	138,26	0.000805454890924632
PADG_03654	hypothetical protein	19,31	0.000102412429082015
INTERACTION WITH THE ENVIRONMENT			
Cell adhesion			

PADG_07615	immunodominant antigen Gp43	22,2	0.00164042968040959
UNCLASSIFIED PROTEINS			
PADG_06699	Uncharacterized protein	14,25	0.000786530106643649
PADG_02909	Uncharacterized protein	14,92	0.00455833380773627

[a]Acession number - acession number of matched protein from *Paracoccidioides brasiliensis* Uniprot database

[b]Protein description - proteins annotation from *Paracoccidioides brasiliensis* database or by homology in Blast2GO or NCBI

[c]Score - score obtained from the MS Amanda 2.0

[d]p-value - statistically significant differences are considered with ≤ 0.05 (ANOVA)

[e]Biological process of differentially expressed proteins from MIPS (http://mips.helmholtz-muenchen.de/funcatDB) and Uniprot databases (http://www.uniprot.org/).

Table S6. Identified proteins from *Paracoccidioides brasiliensis* down-regulated in the mycelia-to-yeast transition compared to the mycelia and yeast cells

Acession number[a]	Protein description[b]	Score[c]	p-value[d]
Functional categories[e]			
METABOLISM			
Amino acid metabolism			
PADG_01488	thiol methyltransferase	16,36	0.00859584687713703
PADG_02214	4-aminobutyrate aminotransferase	146,62	0.000473697117025741
PADG_01621	aspartate aminotransferase	76,22	0.000603223867301128
PADG_05277	Serine hydroxymethyltransferase	84,56	0.00298066391122739
PADG_03627	2-oxoisovalerate dehydrogenase subunit beta	40,81	0.0373648418664289
PADG_08262	asparagine synthase (glutamine-hydrolyzing)	7,22	0.0374351680322741
PADG_03522	methylthioadenosine phosphorylase	61,07	0.00188671139057892
PADG_00888	Argininosuccinate synthase	54,79	0.0283905003634937
PADG_06252	1,2-dihydroxy-3-keto-5-methylthiopentene dioxygenase	29,88	0.00701338481935753
PADG_06144	saccharopine dehydrogenase	25,89	0.00527529557636022
PADG_01718	Saccharopine dehydrogenase [NADP+, L-glutamate-forming]	25,07	0.0221450392480064

PADG_08021	phospho-2-dehydro-3-deoxyheptonate aldolase	35,26	0.00034871632473159
PADG_05058	chorismate mutase	36,37	0.0226842449859004
PADG_01886	adenosylhomocysteinase	101,7	0.02113109868656
PADG_04603	spermidine synthase	34,69	0.0432103775062461
PADG_00210	glycine dehydrogenase	39,27	0.0105405077270114
PADG_08468	4-hydroxyphenylpyruvate dioxygenase	60,91	0.00549013636700336
PADG_08465	fumarylacetoacetase	57,67	0.0108038616369285
PADG_07366	methylcrotonoyl-CoA carboxylase subunit alpha	32,16	0.0509066885694793
Nucleotide/nucleoside/nucleobase metabolism			
PADG_04869	HIT domain-containing	27,59	0.00214233464281135
PADG_00780	ribose-phosphate pyrophosphokinase II	65,5	0.00949990061787514
PADG_08066	purine nucleoside phosphorylase I, inosine and guanosine-specific	14,82	0.00427473565670872
PADG_00322	xanthine-guanine phosphoribosyl transferase	29,21	0.00126429186045653
PADG_00621	Hydroxyisourate hydrolase	5,54	0.0195414250770774
PADG_04099	phosphoribosylaminoimidazolecarboxamide formyltransferase/IMP cyclohydrolase	105,74	0.0290343921451513
PADG_07970	dihydroorotase, homodimeric	36,69	0.000601494528361185
PADG_01100	uracil phosphoribosyltransferase	22,47	0.00342045544824264
PADG_07782	Deoxyuridine 5'-triphosphate nucleotidohydrolase	81,69	0.00385911777105953
PADG_01159	Uridylate kinase	25,89	0.0225226043444458
PADG_06054	deoxyribose-phosphate aldolase	14,93	0.0359382344610037
PADG_05321	DNA RNA non-specific nuclease	31,72	0.0499799223721024
PADG_02658	nucleoside-diphosphate-sugar epimerase	26,88	0.000440673349932956
Phosphate metabolism			
PADG_0417	Inorganic pyrophosphatase	101,62	0.00039648057603618
C-compound and carbohydrate metabolism			
PADG_03118	aldose 1-epimerase family	20,92	0.0473203607543561
PADG_00649	alcohol oxidase	99,63	0.000210018090153545
PADG_04687	short-chain dehydrogenase reductase family	63,12	0.00109994176880593
PADG_03859	NADP-dependent mannitol dehydrogenase	37,32	0.0016711614063246
PADG_00735	Lactam utilization protein lamB	19,26	0.00269083936760223
PADG_01372	mannitol-1-phosphate 5-dehydrogenase	98,2	0.00320014525763444
PADG_05855	lactonohydrolase	38,03	0.00734969612425638

PADG_00912	UDP-galactopyranose mutase	49,9	0.00775039746204842
PADG_07606	2,5-diketo-D-gluconic acid reductase A	77,45	0.010818881866288
PADG_06740	betaine aldehyde dehydrogenase	60,37	0.0325496051578872
PADG_04710	2-methylcitrate mitochondrial	179,9	0.00129368626044376
PADG_05081	Aldehyde dehydrogenase	222,22	0.000318428299089706
Lipid, fatty acid and isoprenoid metabolism			
PADG_12025	glutaryl- CoA dehydrogenase	11,75	0.0378176148991082
PADG_03492	phosphatidylserine decarboxylase	29,91	0.00185747080872941
PADG_01228	3-hydroxybutyryl-CoA dehydrogenase	26,98	0.00942493695792639
PADG_03449	Isopentenyl-diphosphate delta-isomerase	20,95	0.0209229087713661
PADG_00255	fatty acid synthase beta subunit dehydratase	97,69	0.0372553299870248
PADG_04718	2-methylcitrate dehydratase	162,21	0.000131666517534101
Metabolism of vitamins, cofactors, and prosthetic groups			
PADG_00443	Dihydropteroate synthase	75,47	0.00123800894548555
PADG_05822	Pyridoxine biosynthesis protein pyroA	89,63	0.00277034051507976
PADG_08457	biotin synthase	6,95	0.0395889417320599
Secondary metabolism			
PADG_08034	dienelactone hydrolase family protein	107,18	0.00108007819663931
PADG_01052	3-demethylubiquinone-9 3-methyltransferase	20,31	0.00572417440168868
PADG_00312	cytochrome c heme lyase	15,03	0.0179304699139903
ENERGY			
Glycolysis and gluconeogenesis			
PADG_00852	fructose-1,6-bisphosphate aldolase, class 2	18,6	0.0321261222174796
PADG_07950	glucokinase	34,61	0.0269789169774159
PADG_06906	Triosephosphate isomerase	155,73	0.00153813947318225
PADG_05109	2,3-bisphosphoglycerate-independent phosphoglycerate mutase	62,5	0.0117496849150458
PADG_01896	Phosphoglycerate kinase	134,19	0.000712735140039373
PADG_04059	Enolase	350,01	0.00541040257511781
Tricarboxylic-acid pathway (citrate cycle, Krebs cycle, TCA cycle)			
PADG_00246	pyruvate dehydrogenase E1 component subunit beta	71,06	0.0014620825618247
PADG_04993	ATP-citrate synthase subunit 1	69,17	0.0215948774017605
PADG_04165	pyruvate dehydrogenase complex component Pdx1	38,2	0.00131307433739174

PADG_07213	pyruvate dehydrogenase complex dihydrolipoamide acetyltransferase	103,07	0.006306183339428
PADG_11845	Aconitate hydratase, mitochondrial	207,07	0.0302112190508672
PADG_00317	succinyl-CoA ligase subunit beta	48,46	0.0126837599715285
PADG_02260	succinyl-CoA ligase subunit alpha	74,34	0.0326252304957893
PADG_01797	Dihydrolipoamide acetyltransferase component of pyruvate dehydrogenase	57,76	0.0128389547829813
PADG_04939	Succinyl-CoA:3-ketoacid-coenzyme A transferase	58,28	0.0201943831690541
PADG_08387	Citrate synthase	76,95	0.00379083047685583
Electron transport and membrane-associated energy conservation			
PADG_02561	ATP synthase subunit alpha, mitochondrial	327,16	0.00099703997320092
PADG_05436	Cytochrome b-c1 complex subunit Rieske	13,56	0.00954500862971618
PADG_03516	NADH-ubiquinone oxidoreductase 30.4 kDa subunit	15,29	0.00859471577854355
PADG_07749	NAD(P)H:quinone oxidoreductase, type IV	209,82	0.0488987573295302
Respiration			
PADG_05750	cytochrome c oxidase polypeptide VI	57,71	0.000329872995986405
PADG_07081	electron transfer flavo alpha subunit	85,34	0.0265951000485402
PADG_03039	MICOS complex subunit MIC60	52,1	0.0458991211511605
PADG_03872	mitochondrial import inner membrane translocase subunit tim1	28,08	0.0280037026658489
PADG_07042	ATP synthase F1, delta subunit	73,15	0.0514263542897544
PADG_07813	ATP synthase F1, gamma subunit	94,65	0.00320229579998738
PADG_08349	ATP synthase subunit beta, mitochondrial	526,17	0.0091913956997716
PADG_05403	NADH-ubiquinone oxidoreductase 21 kDa subunit	61,24	0.0252028231260988
PADG_02454	NADH-ubiquinone oxidoreductase	12,12	0.0505489922010667
PADG_05402	mitochondrial F1F0 ATP synthase subunit	32,02	0.0128065223457609
Fermentation			
PADG_11405	Alcohol dehydrogenase 1	181,54	0.000117667332982207
PADG_04701	Alcohol dehydrogenase	19,87	0.0398751128886334
Oxidation of fatty acids			
PADG_06805	acyl- dehydrogenase	93,54	0.00228164549110767
PADG_01209	enoyl-CoA hydratase	75,09	0.0158508402126517
PADG_07023	carnitine O-acetyltransferase	23,7	0.0299195036063134
PADG_01687	3-ketoacyl-CoA thiolase	148,38	0.000606823603773545
CELL CYCLE AND DNA PROCESSING			

DNA processing			
PADG_03459	replication factor-A protein	33,18	0.0149027131920101
PADG_05818	HLH DNA binding	11,19	0.0230078557563301
PADG_02683	UV excision repair protein Rad23	95,32	0.0101122103649832
PADG_05709	histone acetyltransferase type B subunit 2	27,36	0.00164234466516168
PADG_00656	Non-histone chromosomal protein 6	49,18	0.00349912944508594
Cell cycle			
PADG_04795	deubiquitination-protection protein dph1	66,45	0.00011583181867771
PADG_05683	cell division control protein 48	276,29	0.000330152297791995
PADG_07319	septin-1	30,11	0.000818895717889287
PADG_07515	NSFL1 cofactor p47	31,97	0.0143456926429943
TRANSCRIPTION			
RNA synthesis			
PADG_00814	branchpoint-bridging protein	22,78	0.000361519806372817
PADG_04307	mRNA binding post-transcriptional regulator	149,3	0.00322339287702619
PADG_02555	nucleic acid-binding protein	62,4	0.0101850714020848
PADG_01508	U1 small nuclear ribonucleoprotein C	9,16	0.0268581913593662
PADG_01455	KH domain RNA-binding protein	177,31	0.000544832339699319
PADG_08081	zinc knuckle domain	30,31	0.000727891867202843
PADG_00220	class 2 transcription repressor NC2	9,43	0.00304321420966517
PADG_04311	cellular nucleic acid-binding protein	21,89	0.0115271319353104
PADG_03869	HMG box	37,81	0.0149326260057446
PADG_00872	histone H4	71,3	0.0252015733715969
PADG_06182	transcriptional repressor	130,91	0.0323405291079937
RNA processing			
PADG_02783	RNA-binding La domain-containing protein	35,41	0.0252707765390186
PADG_07689	transformer-SR ribonucleoprotein	63,33	0.00285515817257463
PADG_00044	28 kDa ribonucleoprotein	51,51	0.0311052414112992
PADG_00576	RNA recognition domain-containing protein containing protein, variant	43,25	0.000366474914980045
PADG_05340	pre-mrna splicing factor	73,65	0.00567170230733727
PADG_04369	splicing factor U2AF 23 kDa subunit	7,35	0.0093556652043975
PADG_04301	WD repeat-containing protein	33,57	0.0304988927372442

PROTEIN SYNTHESIS

Ribosome biogenesis

PADG_11904	Ribosomal protein L1	36,56	0.0547556214196747
PADG_03856	60S ribosomal protein L15	31,71	0.000948265034607996
PADG_01026	60S ribosomal protein L43	48,71	0.00189393950236822
PADG_04848	60S ribosomal protein L8-B	58,13	0.00391393542396789
PADG_04862	50S ribosomal protein Mrp49	12,73	0.0046969426014565
PADG_05686	ribosome biogenesis protein	19,52	0.0171919284417786
PADG_05721	60S ribosomal protein L4	139	0.031687423620715
PADG_00784	40S ribosomal protein S0	43,43	0.038488765469723
PADG_00335	40S ribosomal protein S14	150,13	0.0009283171462339
PADG_02056	ribosomal protein L7	39,41	0.00101174747252608
PADG_01654	40S ribosomal protein S6-A	84,13	0.00128612006836141
PADG_07583	40S ribosomal protein S21	54,68	0.00321015987134523
PADG_00354	40S ribosomal protein S17	91,49	0.00512401922994533
PADG_01914	60S ribosomal protein L35	36,39	0.00595985342101163
PADG_00627	mitochondrial large ribosomal subunit L49, variant	5,15	0.00635571801442804
PADG_01387	60S ribosomal protein L7	35,88	0.00676476492288821
PADG_03781	60S ribosomal protein L30	65,22	0.00769160773234302
PADG_03778	60S ribosomal protein L10-A	56,25	0.0128434095495006
PADG_00995	ubiquitin-40S ribosomal protein S27a	80,68	0.0155770103199853
PADG_04106	60S ribosomal protein L11	47,97	0.0202870981819721
PADG_03873	60S ribosomal protein L20	18,21	0.0326173334051663
PADG_02249	60S ribosomal protein L2	50,71	0.049831342606761
PADG_06525	40S ribosomal protein S1	78,17	0.0498924638228775
PADG_05939	60S ribosomal protein L27a	92,23	0.00976778835723734
PADG_03326	40S ribosomal protein S9	28,36	0.0516200825998414
PADG_01427	40S ribosomal protein S12	55,94	0.00188255977619058
PADG_03315	40S ribosomal protein S4	84,65	0.00145057927925207
PADG_02888	60S ribosomal protein L6 O	64,61	0.00058696534564495
PADG_06838	40S ribosomal protein S5	81,11	0.0280593514265553
PADG_02828	Ribosomal protein	35,23	0.0319912825552141

PADG_06048	40S ribosomal protein S27	16,06	0.0441806922768012
PADG_11379	60S ribosomal protein L5	90,99	0.00947872658438146
Translation			
PADG_02759	ribosome recycling factor domain-containing protein	14,85	0.00717309135667122
PADG_02896	elongation factor 1-beta	55,72	0.000328396134515179
PADG_00692	elongation factor 1-alpha	229,91	0.0033049385655597
PADG_01079	translation initiation factor 4B	132,46	0.0305078072836169
PADG_07356	woronin body major protein	79,11	0.00055674974717756
PADG_01865	Eukaryotic translation initiation factor 3 subunit H	84,83	0.00217169449999158
PADG_00457	translation initiation factor 4G	97,39	0.0127112389368946
PADG_06110	translation initiation factor SUI1	25,21	0.0258640355371289
PADG_02691	eukaryotic translation initiation factor 6	19,22	0.0525198964080063
PADG_08125	Elongation factor 2	258,41	0.00977484226145031
PADG_06265	elongation factor 1-gamma	94,06	0.00245190358187735
Aminoacyl-tRNA-synthetases			
PADG_05848	glycine-tRNA ligase	29,33	0.0284549763738526
PROTEIN FOLDING AND STABILIZATION			
Protein folding and stabilization			
PADG_12323	peptidyl-prolyl cis-trans isomerase	46,01	0.000811310718754342
PADG_12329	prefoldin subunit 2	15,08	0.00122708938870604
PADG_02895	ATP-dependent Clp protease ATP-binding subunit ClpB	62,13	0.00276781772538938
PADG_07815	disulfide-isomerase domain	37,88	0.00378267127358446
PADG_04092	peptidyl-prolyl cis-trans isomerase B	109,77	0.00718691945820977
PADG_05628	Protein disulfide-isomerase domain	65,37	0.0189209329424933
PADG_06488	peptidyl-prolyl cis-trans isomerase D	139,23	0.0284592321370524
PADG_08048	T-complex protein 1 subunit beta	88,82	0.0435867936243462
PADG_01852	small glutamine-rich tetratricopeptide repeat-containing protein	61,51	0.0194408966072878
PADG_05203	Peptidyl-prolyl cis-trans isomerase	49,8	0.028957954112554
PADG_07953	Peptidyl-prolyl cis-trans isomerase	32,66	0.00239744249348738
Protein targeting, sorting and translocation			
PADG_02619	F-box domain-containing	45,73	0.0017688464217684
PADG_08188	vacuolar-sorting protein snf7	23,85	0.00562474527488371

PADG_08646	class E vacuolar -sorting machinery HSE1	22,48	0.0176936537439237
PADG_03274	mitochondrial import inner membrane translocase subunit tim9	36,03	0.0226626979060814
PADG_00240	SNF7 family protein Fti1/Did2	20,82	0.00561971799727414
Protein modification			
PADG_00809	ubiquitin-conjugating enzyme	17,71	0.00179716781257883
PADG_07925	ubiquitin-conjugating enzyme E2 N	24,77	0.00217641874973217
PADG_00569	5'/3'-nucleotidase SurE	7,3	0.0203490779710472
PADG_05929	protein-L-isoaspartate O-methyltransferase	8,5	0.000104293058688337
Protein/peptide degradation			
PADG_02637	ubiquitin-conjugating enzyme	47,99	0.00552046595228165
PADG_06290	proteasome component PRE5	48,18	0.0119003210880048
PADG_03221	thimet oligopeptidase	44,01	0.0152211653648595
PADG_05922	glutamate carboxypeptidase	62,82	0.018794315888034
PADG_05820	xaa-Pro aminopeptidase	60,96	0.0537361658754471
PADG_05160	Dipeptidyl peptidase 3	42,94	0.000553026709381306
PADG_08442	Proteasome subunit alpha type	30,72	0.00644585367629858
PADG_03967	proteasome component C5	45,24	0.012833799267322
PADG_00599	26S protease regulatory subunit 6A	58,13	0.0340488792956519
PADG_07190	Proteasome endopeptidase complex	37,56	0.0500129362578737
PADG_00634	vacuolar protease A	25,22	0.00276331930081985
PADG_06546	Aminopeptidase	59,91	0.018748446410497
CELLULAR TRANSPORT			
Transported compounds (substrates)			
PADG_07964	V-type proton ATPase subunit E	83,38	0.00770764690084264
PADG_06692	mitochondrial phosphate carrier protein	49,55	0.028478971205458
PADG_08176	phosphatidylinositol-phosphatidylcholine transfer protein	31,56	0.0103878866021587
PADG_01363	diazepam-binding inhibitor (GABA receptor acyl- -binding)	84,2	0.0170201896661536
PADG_01440	ADP,ATP carrier protein	185,6	0.00222386670540909
Transport facilities			
PADG_08263	mitochondrial outer membrane protein porin	144,86	0.00119131447896499
transport routes			
PADG_02022	clathrin light chain	84,07	0.00526327780889446

PADG_02924	G2/M phase checkpoint control protein Sum2	24,09	0.000640360610487575
PADG_07014	vesicular-fusion sec17	58,84	0.0410862235352565
CELLULAR COMMUNICATION			
Cellular signalling			
PADG_08191	cAMP-dependent kinase regulatory subunit	15,37	0.000153652216039725
PADG_02845	CORD and CS domain-containing	36,07	0.000230062222189261
PADG_04383	tricalbin-3	25,57	0.00157729548942107
PADG_08342	GTP-binding protein ypt1	36,58	0.0262887200043236
PADG_07287	WD repeat	13,98	0.0424886349236938
PADG_03219	myosin regulatory light chain cdc4	34,13	0.00245254380627877
CELL RESCUE			
stress response			
PADG_02981	ThiJ/PfpI family protein	71,14	0.0202700356111835
PADG_03170	serum paraoxonase/arylesterase 2	8,91	0.0049738065878992
PADG_01711	Hsp90 co-chaperone AHA1	85,65	0.00381621468774507
PADG_07715	hsp90-like protein	342,67	0.00592148500579047
PADG_02761	hsp75-like protein	294,38	0.0479601189854827
PADG_08369	hsp60-like protein	831,65	0.00127751244263923
PADG_03562	chaperone DnaK	355,03	0.00874116932727769
PADG_03163	cytochrome c peroxidase, mitochondrial	109,64	0.000593374880337985
PADG_04912	AhpC/TSA family protein	50,22	0.0170318717607415
PADG_07946	peroxisomal matrix protein	44,1	0.0297718977714577
PADG_00430	70 kDa heat shock protein	484,2	0.00660782723481957
PADG_02785	heat shock protein Hsp88	152,1	0.0223062727662165
PADG_00207	ribosome associated chaperone Zuotin	60,82	0.0439051277963011
PADG_05032	Hsp90 binding co-chaperone (Sba1)	39,31	0.0317768742306163
PADG_03423	glutathione S-transferase Gst3	28,83	0.000573696552796715
PADG_02764	thioredoxin-like protein	76,21	0.00495776661632139
PADG_05344	peroxiredoxin Q BCP	15,93	0.00309586826577796
PADG_05504	thioredoxin	106,67	0.0208911445460205
PADG_03095	mitochondrial peroxiredoxin PRX1	33,08	0.0351949640957963
Virulence, disease factors			

PADG_07422	serine proteinase	29,51	0.00264817902949662
Detoxification			
PADG_00073	SAM-dependent methyltransferase COQ5 family	35,14	0.000874824117092326
PADG_07418	superoxide dismutase [Cu-Zn] SOD1	101,1	0.00119250240482325
PADG_01755	Fe-Mn family superoxide dismutase SOD2	40,2	0.0191136606558536
CELL FATE			
Cell growth / morphogenesis			
PADG_05517	rho-gdp dissociation inhibitor	21,41	0.019945607030085
PADG_04559	progesterone binding	16,55	0.0378473693930494
Cell death			
PADG_06087	hypothetical protein	15,32	0.000495869192119841
INTERACTION WITH THE ENVIRONMENT			
Cell adhesion			
PADG_04440	14-3-3-like protein 2	109,53	0.0115304629233556
BIOGENESIS OF CELLULAR COMPONENTS			
Cell wall			
PADG_00994	chitinase class II	236,68	0.000152810421803673
PADG_03691	cell wall glucanase	9,66	0.000192529842468642
PADG_04499	cell wall protein ECM33 precursor	22,82	0.000415316082694873
PADG_05303	beta-1,6-glucan biosynthesis (Knh1)	5,13	0.013018510681609
PADG_02862	1,3-beta-glucosidase	9,17	0.0194863299097851
CELL TYPE DIFFERENTIATON			
Fungal/microorganismic cell type differentiation			
PADG_04260	NIMA-interacting protein TinC	29,3	0.000707300897920691
PADG_08091	cell polarity (Alp11)	11,88	0.0208774113534429
UNCLASSIFIED PROTEINS			
PADG_02604	hypothetical protein	33,89	0.00015844299425143
PADG_02181	HAD-superfamily hydrolase	36,51	0.000200997050975056
PADG_12447	hypothetical protein	102,27	0.000252966887635888
PADG_04907	hypothetical protein	47,96	0.000318705002215328
PADG_05157	cell surface protein, putative	27,81	0.000347601158886615
PADG_04343	short chain dehydrogenase/reductase	21,75	0.000645592053848837

PADG_01857	Uncharacterized protein	41,39	0.000735739746029736
PADG_02967	Uncharacterized protein	111,93	0.000954103076199105
PADG_06021	hypothetical protein	32,74	0.000987328858139613
PADG_06202	Arp2 3 complex subunit Arc16	66,98	0.00132807191136456
PADG_07670	SAP domain-containing protein	30,66	0.0013911862778064
PADG_11347	hypothetical protein	33,49	0.00197211084602885
PADG_00422	actin cytoskeleton protein (VIP1)	162,78	0.00207529238829785
PADG_04205	hypothetical protein	39,47	0.00267855755722755
PADG_01002	erythrocyte band 7 integral membrane protein	17,5	0.00271552290942387
PADG_02858	hypothetical protein	37,78	0.00310539167374307
PADG_11101	hypothetical protein	41,61	0.00317627875002816
PADG_12152	hypothetical protein	10,19	0.00345282888989835
PADG_00674	hypothetical protein	13,05	0.00394824311127837
PADG_11424	hypothetical protein	41,88	0.00515308641760238
PADG_02338	Uncharacterized protein	19,47	0.00599800759227989
PADG_12252	hypothetical protein	8,88	0.00737286242790404
PADG_08152	hypothetical protein	13,17	0.00772151473816209
PADG_08270	UBX domain-containing protein	8,33	0.00779498683485196
PADG_02944	hypothetical protein	23,01	0.00846113292689915
PADG_05356	isochorismatase domain-containing protein	80,89	0.00876062721083998
PADG_00921	Uncharacterized protein	35,19	0.00965739615783812
PADG_11487	hypothetical protein	17,57	0.0106368435907347
PADG_07225	Uncharacterized protein	24,59	0.0107115482507958
PADG_11950	hypothetical protein	122,48	0.0114196399407177
PADG_06136	related to mismatched base pair and cruciform dna recognition	21,36	0.0130031745279776
PADG_07506	hypothetical protein	44,27	0.0146863742665499
PADG_02118	Uncharacterized protein	16,96	0.016955093392485
PADG_04818	hypothetical protein	5,42	0.0170034848346801
PADG_00676	hypothetical protein	128,58	0.0225015189702146
PADG_04685	Uncharacterized protein	15,49	0.0233426763011714
PADG_03203	BAR domain-containing protein	88,17	0.0256785799658214
PADG_04215	DUF124 domain-containing protein	21,2	0.026961653931293

PADG_01688	DlpA domain-containing protein	12,4	0.030468175182578
PADG_02709	hypothetical protein	17,25	0.0373430897201166
PADG_05584	hypothetical protein	13,06	0.0507774717047346
PADG_02307	CUE domain-containing	12,64	0.052604670310913
PADG_04806	hypothetical protein	14,14	0.0526341547562164
PADG_06945	GYF domain-containing protein	26,02	0.0535146776162895
PADG_06080	hypothetical protein	17,63	0.00220468098930026
PADG_11413	hypothetical protein	19,14	0.0184217228588476
PADG_11832	hypothetical protein	18,79	0.0233063048763567
PADG_01128	hypothetical protein	11,22	0.0298111381892491
PADG_04439	Uncharacterized protein	18,72	0.054953798716532

[a]Acession number - acession number of matched protein from *Paracoccidioides brasiliensis* Uniprot database

[b]Protein description - proteins annotation from *Paracoccidioides brasiliensis* database or by homology in Blast2GO or NCBI

[c]Score - score obtained from the MS Amanda 2.0

[d]p-value - statistically significant differences are considered with ≤ 0.05 (ANOVA)

[e]Biological process of differentially expressed proteins from MIPS (http://mips.helmholtz-muenchen.de/funcatDB) and Uniprot databases (http://www.uniprot.org/).

Table S7. Identified proteins from *Paracoccidioides brasiliensis* up-regulated in the yeast phase compared to the mycelia-to-yeast transition and mycelia phases

Acession number[a]	**Protein description[b]**	**Score[c]**	**p-value[d]**
Functional categories[e]			
METABOLISM			
Amino acid metabolism			
PADG_01488	thiol methyltransferase	16,36	0.00859584687713703
PADG_01621	aspartate aminotransferase	76,22	0.000603223867301128
PADG_05277	Serine hydroxymethyltransferase	84,56	0.00298066391122739
PADG_03627	2-oxoisovalerate dehydrogenase subunit beta	40,81	0.0373648418664289
PADG_08262	asparagine synthase (glutamine-hydrolyzing)	7,22	0.0374351680322741

PADG_00888	Argininosuccinate synthase	54,79	0.0283905003634937
PADG_05058	chorismate mutase	36,37	0.0226842449859004
PADG_01886	adenosylhomocysteinase	101,7	0.02113109868656
PADG_00210	glycine dehydrogenase	39,27	0.0105405077270114
PADG_08468	4-hydroxyphenylpyruvate dioxygenase	60,91	0.00549013636700336
PADG_08465	fumarylacetoacetase	57,67	0.0108038616369285
PADG_07366	methylcrotonoyl-CoA carboxylase subunit alpha	32,16	0.0509066885694793
Nucleotide/nucleoside/nucleobase metabolism			
PADG_04099	phosphoribosylaminoimidazolecarboxamide formyltransferase/IMP cyclohydrolase	105,74	0.0290343921451513
PADG_01159	Uridylate kinase	25,89	0.0225226043444458
PADG_05321	DNA RNA non-specific nuclease	31,72	0.0499799223721024
C-compound and carbohydrate metabolism			
PADG_03118	aldose 1-epimerase family	20,92	0.0473203607543561
PADG_00912	UDP-galactopyranose mutase	49,9	0.00775039746204842
PADG_04710	2-methylcitrate synthase mitochondrial	179,9	0.00129368626044376
Lipid, fatty acid and isoprenoid metabolism			
PADG_12025	glutaryl- CoA dehydrogenase	11,75	0.0378176148991082
PADG_01228	3-hydroxybutyryl-CoA dehydrogenase	26,98	0.00942493695792639
PADG_00255	fatty acid synthase beta subunit dehydratase	97,69	0.0372553299870248
PADG_04718	2-methylcitrate dehydratase	162,21	0.000131666517534101
Metabolism of vitamins, cofactors, and prosthetic groups			
PADG_00443	Dihydropteroate synthase	75,47	0.00123800894548555
PADG_05822	Pyridoxine biosynthesis protein pyroA	89,63	0.00277034051507976
PADG_08457	biotin synthase	6,95	0.0395889417320599
ENERGY			
Glycolysis and gluconeogenesis			
PADG_01896	Phosphoglycerate kinase	134,19	0.000712735140039373
PADG_04059	Enolase	350,01	0.00541040257511781
Tricarboxylic-acid pathway (citrate cycle, Krebs cycle, TCA cycle)			
PADG_00246	pyruvate dehydrogenase E1 component subunit beta	71,06	0.0014620825618247
PADG_04993	ATP-citrate synthase subunit 1	69,17	0.0215948774017605
PADG_07213	pyruvate dehydrogenase complex dihydrolipoamide acetyltransferase	103,07	0.006306183339428

PADG_11845	Aconitate hydratase, mitochondrial	207,07	0.0302112190508672
PADG_00317	succinyl-CoA ligase subunit beta	48,46	0.0126837599715285
PADG_04939	Succinyl-CoA:3-ketoacid-coenzyme A transferase	58,28	0.0201943831690541
PADG_08387	Citrate synthase	76,95	0.00379083047685583
PADG_01797	Dihydrolipoamide acetyltransferase component of pyruvate dehydrogenase	57,76	0.0128389547829813
PADG_02260	succinyl-CoA ligase subunit alpha	74,34	0.0326252304957893
Electron transport and membrane-associated energy conservation			
PADG_02561	ATP synthase subunit alpha, mitochondrial	327,16	0.00099703997320092
PADG_05436	Cytochrome b-c1 complex subunit Rieske	13,56	0.00954500862971618
PADG_03516	NADH-ubiquinone oxidoreductase 30.4 kDa subunit	15,29	0.00859471577854355
Respiration			
PADG_05750	cytochrome c oxidase polypeptide VI	57,71	0.000329872995986405
PADG_07081	electron transfer flavo alpha subunit	85,34	0.0265951000485402
PADG_03039	MICOS complex subunit MIC60	52,1	0.0458991211511605
PADG_03872	mitochondrial import inner membrane translocase subunit tim1	28,08	0.0280037026658489
PADG_07042	ATP synthase F1, delta subunit	73,15	0.0514263542897544
PADG_07813	ATP synthase F1, gamma subunit	94,65	0.00320229579998738
PADG_08349	ATP synthase subunit beta, mitochondrial	526,17	0.0091913956997716
PADG_05402	mitochondrial F1F0 ATP synthase subunit	32,02	0.0128065223457609
Oxidation of fatty acids			
PADG_06805	acyl- dehydrogenase	93,54	0.00228164549110767
PADG_01209	enoyl-CoA hydratase	75,09	0.0158508402126517
PADG_07023	carnitine O-acetyltransferase	23,7	0.0299195036063134
PADG_01687	3-ketoacyl-CoA thiolase	148,38	0.000606823603773545
TRANSCRIPTION			
RNA synthesis			
PADG_02555	nucleic acid-binding protein	62,4	0.0101850714020848
PADG_00872	histone H4	71,3	0.0252015733715969
PROTEIN SYNTHESIS			
Ribosome biogenesis			
PADG_11904	Ribosomal protein L1	36,56	0.0547556214196747
PADG_03856	60S ribosomal protein L15	31,71	0.000948265034607996

PADG_04848	60S ribosomal protein L8-B	58,13	0.00391393542396789
PADG_04862	50S ribosomal protein Mrp49	12,73	0.0046969426014565
PADG_05721	60S ribosomal protein L4	139	0.031687423620715
PADG_00784	40S ribosomal protein S0	43,43	0.038488765469723
PADG_02056	ribosomal protein L7	39,41	0.00101174747252608
PADG_01654	40S ribosomal protein S6-A	84,13	0.00128612006836141
PADG_00354	40S ribosomal protein S17	91,49	0.00512401922994533
PADG_01914	60S ribosomal protein L35	36,39	0.00595985342101163
PADG_00627	mitochondrial large ribosomal subunit L49, variant	5,15	0.00635571801442804
PADG_01387	60S ribosomal protein L7	35,88	0.00676476492288821
PADG_03778	60S ribosomal protein L10-A	56,25	0.0128434095495006
PADG_04106	60S ribosomal protein L11	47,97	0.0202870981819721
PADG_03873	60S ribosomal protein L20	18,21	0.0326173334051663
PADG_06525	40S ribosomal protein S1	78,17	0.0498924638228775
PADG_05939	60S ribosomal protein L27a	92,23	0.00976778835723734
PADG_03326	40S ribosomal protein S9	28,36	0.0516200825998414
PADG_03315	40S ribosomal protein S4	84,65	0.00145057927925207
PADG_02888	60S ribosomal protein L6 O	64,61	0.00058696534564495
PADG_06838	40S ribosomal protein S5	81,11	0.0280593514265553
PADG_02828	Ribosomal protein	35,23	0.0319912825552141
PADG_06048	40S ribosomal protein S27	16,06	0.0441806922768012
PADG_11379	60S ribosomal protein L5	90,99	0.00947872658438146
translation			
PADG_02759	ribosome recycling factor domain-containing protein	14,85	0.00717309135667122
PADG_02896	elongation factor 1-beta	55,72	0.000328396134515179
PADG_00692	elongation factor 1-alpha	229,91	0.0033049385655597
PADG_08125	Elongation factor 2	258,41	0.00977484226145031
PADG_06265	elongation factor 1-gamma	94,06	0.00245190358187735
Aminoacyl-tRNA-synthetases			
PADG_05848	glycine-tRNA ligase	29,33	0.0284549763738526
PROTEIN FOLDING AND STABILIZATION			
Protein folding and stabilization			

PADG_02895	ATP-dependent Clp protease ATP-binding subunit ClpB	62,13	0.00276781772538938
PADG_07815	disulfide-isomerase domain	37,88	0.00378267127358446
PADG_08048	T-complex protein 1 subunit beta	88,82	0.0435867936243462
PADG_12323	peptidyl-prolyl cis-trans isomerase	46,01	0.000811310718754342
PADG_04092	peptidyl-prolyl cis-trans isomerase B	109,77	0.00718691945820977
PADG_05628	Protein disulfide-isomerase domain	65,37	0.0189209329424933
PADG_06488	peptidyl-prolyl cis-trans isomerase D	139,23	0.0284592321370524
Protein/peptide degradation			
PADG_00599	26S protease regulatory subunit 6A	58,13	0.0340488792956519
CELLULAR TRANSPORT			
Transported compounds (substrates)			
PADG_06692	mitochondrial phosphate carrier protein	49,55	0.028478971205458
PADG_01440	ADP,ATP carrier protein	185,6	0.00222386670540909
Transport facilities			
PADG_08263	mitochondrial outer membrane protein porin	144,86	0.00119131447896499
CELLULAR COMMUNICATION			
Cellular signalling			
PADG_02845	CORD and CS domain-containing	36,07	0.000230062222189261
PADG_08342	GTP-binding protein ypt1	36,58	0.0262887200043236
CELL RESCUE			
Stress response			
PADG_01711	Hsp90 co-chaperone AHA1	85,65	0.00381621468774507
PADG_07715	hsp90-like protein	342,67	0.00592148500579047
PADG_02761	hsp75-like protein	294,38	0.0479601189854827
PADG_08369	hsp60-like protein	831,65	0.00127751244263923
PADG_03562	chaperone DnaK	355,03	0.00874116932727769
PADG_00430	70 kDa heat shock protein	484,2	0.00660782723481957
PADG_02785	heat shock protein Hsp88	152,1	0.0223062727662165
PADG_04912	AhpC/TSA family protein	50,22	0.0170318717607415
PADG_03170	serum paraoxonase/arylesterase 2	8,91	0.0049738065878992
PADG_03163	cytochrome c peroxidase, mitochondrial	109,64	0.000593374880337985
PADG_07946	peroxisomal matrix protein	44,1	0.0297718977714577

PADG_00207	ribosome associated chaperone Zuotin	60,82	0.0439051277963011
INTERACTION WITH THE ENVIRONMENT			
Cell adhesion			
PADG_04440	14-3-3-like protein	109,53	0.0115304629233556
BIOGENESIS OF CELLULAR COMPONENTS			
Cell wall			
PADG_05303	beta-1,6-glucan biosynthesis (Knh1)	5,13	0.013018510681609
UNCLASSIFIED PROTEINS			
PADG_12152	hypothetical protein	10,19	0.00345282888989835
PADG_05356	isochorismatase domain-containing protein	80,89	0.00876062721083998
PADG_06080	hypothetical protein	17,63	0.00220468098930026
PADG_11413	hypothetical protein	19,14	0.0184217228588476
PADG_11832	hypothetical protein	18,79	0.0233063048763567
PADG_01128	hypothetical protein	11,22	0.0298111381892491
PADG_04439	Uncharacterized protein	18,72	0.054953798716532

[a]Acession number - acession number of matched protein from *Paracoccidioides brasiliensis* Uniprot database

[b]Protein description - proteins annotation from *Paracoccidioides brasiliensis* database or by homology in Blast2GO or NCBI

[c]Score - score obtained from the MS Amanda 2.0

[d]p-value - statistically significant differences are considered with ≤ 0.05 (ANOVA)

[e]Biological process of differentially expressed proteins from MIPS (http://mips.helmholtz-muenchen.de/funcatDB) and Uniprot databases (http://www.uniprot.org/).

Table S8. Identified proteins from *Paracoccidioides brasiliensis* down-regulated in the yeast phase compared to the mycelia-to-yeast transition and mycelia phases

Acession number[a]	**Protein description[b]**	**Score[c]**
Functional categories[e]		
METABOLISM		
Amino acid metabolism		
PADG_02214	4-aminobutyrate aminotransferase	146,62

PADG_03522	methylthioadenosine phosphorylase	61,07
PADG_06252	1,2-dihydroxy-3-keto-5-methylthiopentene dioxygenase	29,88
PADG_06144	saccharopine dehydrogenase	25,89
PADG_01718	Saccharopine dehydrogenase [NADP+, L-glutamate-forming]	25,07
PADG_08021	phospho-2-dehydro-3-deoxyheptonate aldolase	35,26
PADG_04603	spermidine synthase	34,69
Nucleotide/nucleoside/nucleobase metabolism		
PADG_04869	HIT domain-containing	27,59
PADG_00780	ribose-phosphate pyrophosphokinase II	65,5
PADG_08066	purine nucleoside phosphorylase I, inosine and guanosine-specific	14,82
PADG_00322	xanthine-guanine phosphoribosyl transferase	29,21
PADG_00621	Hydroxyisourate hydrolase	5,54
PADG_07970	dihydroorotase, homodimeric	36,69
PADG_01100	uracil phosphoribosyltransferase	22,47
PADG_07782	Deoxyuridine 5'-triphosphate nucleotidohydrolase	81,69
PADG_06054	deoxyribose-phosphate aldolase	14,93
PADG_02658	nucleoside-diphosphate-sugar epimerase	26,88
Phosphate metabolism		
PADG_0417	Inorganic pyrophosphatase	101,62
C-compound and carbohydrate metabolism		
PADG_00649	alcohol oxidase	99,63
PADG_04687	short-chain dehydrogenase reductase family	63,12
PADG_03859	NADP-dependent mannitol dehydrogenase	37,32
PADG_00735	Lactam utilization protein lamB	19,26
PADG_01372	mannitol-1-phosphate 5-dehydrogenase	98,2
PADG_05855	lactonohydrolase	38,03
PADG_07606	2,5-diketo-D-gluconic acid reductase A	77,45
PADG_06740	betaine aldehyde dehydrogenase	60,37
PADG_01677	acetyl-coenzyme A synthetase	23,94
PADG_05081	Aldehyde dehydrogenase	222,22
Lipid, fatty acid and isoprenoid metabolism		
PADG_03492	phosphatidylserine decarboxylase	29,91

PADG_03449	Isopentenyl-diphosphate delta-isomerase	20,95
Secondary metabolism		
PADG_08034	dienelactone hydrolase family protein	107,18
PADG_01052	3-demethylubiquinone-9 3-methyltransferase	20,31
PADG_00312	cytochrome c heme lyase	15,03
ENERGY		
Glycolysis and gluconeogenesis		
PADG_00852	fructose-1,6-bisphosphate aldolase, class 2	18,6
PADG_07950	glucokinase	34,61
PADG_08503	Phosphoenolpyruvate carboxykinase	71,43
PADG_06906	Triosephosphate isomerase	155,73
PADG_05109	2,3-bisphosphoglycerate-independent phosphoglycerate mutase	62,5
PADG_02411	Glyceraldehyde-3-phosphate dehydrogenase	554,25
Tricarboxylic-acid pathway (citrate cycle, Krebs cycle, TCA cycle)		
PADG_04165	pyruvate dehydrogenase complex component Pdx1	38,2
Electron transport and membrane-associated energy conservation		
PADG_06196	12-oxophytodienoate reductase	53,59
PADG_07749	NAD(P)H:quinone oxidoreductase, type IV	209,82
Respiration		
PADG_05403	NADH-ubiquinone oxidoreductase 21 kDa subunit	61,24
Fermentation		
PADG_11405	Alcohol dehydrogenase 1	181,54
PADG_04701	Alcohol dehydrogenase	19,87
CELL CYCLE AND DNA PROCESSING		
DNA processing		
PADG_03459	replication factor-A protein	33,18
PADG_05818	HLH DNA binding	11,19
PADG_02683	UV excision repair protein Rad23	95,32
PADG_05709	histone acetyltransferase type B subunit 2	27,36
PADG_00656	Non-histone chromosomal protein 6	49,18
Cell cycle		
PADG_04795	deubiquitination-protection protein dph1	66,45

PADG_05683	cell division control protein 48	276,29
PADG_07319	septin-1	30,11
PADG_07515	NSFL1 cofactor p47	31,97
TRANSCRIPTION		
RNA synthesis		
PADG_00814	branchpoint-bridging protein	22,78
PADG_04307	mRNA binding post-transcriptional regulator	149,3
PADG_01508	U1 small nuclear ribonucleoprotein C	9,16
PADG_01455	KH domain RNA-binding protein	177,31
PADG_08081	zinc knuckle domain	30,31
PADG_00220	class 2 transcription repressor NC2	9,43
PADG_04311	cellular nucleic acid-binding protein	21,89
PADG_03869	HMG box	37,81
PADG_06182	transcriptional repressor	130,91
RNA processing		
PADG_02783	RNA-binding La domain-containing protein	35,41
PADG_07689	transformer-SR ribonucleoprotein	63,33
PADG_00044	28 kDa ribonucleoprotein	51,51
PADG_00576	RNA recognition domain-containing protein containing protein, variant	43,25
PADG_05340	pre-mrna splicing factor	73,65
PADG_04369	splicing factor U2AF 23 kDa subunit	7,35
PADG_04301	WD repeat-containing protein	33,57
PROTEIN SYNTHESIS		
Ribosome biogenesis		
PADG_01026	60S ribosomal protein L43	48,71
PADG_05686	ribosome biogenesis protein	19,52
PADG_00335	40S ribosomal protein S14	150,13
PADG_07583	40S ribosomal protein S21	54,68
PADG_03781	60S ribosomal protein L30	65,22
PADG_00995	ubiquitin-40S ribosomal protein S27a	80,68
PADG_02249	60S ribosomal protein L2	50,71
PADG_01427	40S ribosomal protein S12	55,94

Translation		
PADG_01079	translation initiation factor 4B	132,46
PADG_07356	woronin body major protein	79,11
PADG_01865	Eukaryotic translation initiation factor 3 subunit H	84,83
PADG_00457	translation initiation factor 4G	97,39
PADG_06110	translation initiation factor SUI1	25,21
PADG_02691	eukaryotic translation initiation factor 6	19,22
PROTEIN FOLDING AND STABILIZATION		
Protein folding and stabilization		
PADG_12329	prefoldin subunit 2	15,08
PADG_08587	Peptidylprolyl isomerase	24,02
PADG_01852	small glutamine-rich tetratricopeptide repeat-containing protein	61,51
PADG_05203	Peptidyl-prolyl cis-trans isomerase	49,8
PADG_01565	calnexin	82,6
PADG_07953	Peptidyl-prolyl cis-trans isomerase	32,66
PADG_04034	Chaperone DnaJ	148,98
PADG_02206	DnaJ domain protein Psi	62,1
PADG_05229	chaperone protein dnaJ 3	20,67
Protein targeting, sorting and translocation		
PADG_02619	F-box domain-containing	45,73
PADG_08188	vacuolar-sorting protein snf7	23,85
PADG_08646	class E vacuolar -sorting machinery HSE1	22,48
PADG_03274	mitochondrial import inner membrane translocase subunit tim9	36,03
PADG_00240	SNF7 family protein Fti1/Did2	20,82
Protein modification		
PADG_00809	ubiquitin-conjugating enzyme	17,71
PADG_07925	ubiquitin-conjugating enzyme E2 N	24,77
PADG_00569	5'/3'-nucleotidase SurE	7,3
PADG_05929	protein-L-isoaspartate O-methyltransferase	8,5
Protein/peptide degradation		
PADG_04167	aspartyl aminopeptidase	86,75
PADG_02637	ubiquitin-conjugating enzyme	47,99

PADG_06290	proteasome component PRE5	48,18
PADG_03221	thimet oligopeptidase	44,01
PADG_05922	glutamate carboxypeptidase	62,82
PADG_05820	xaa-Pro aminopeptidase	60,96
PADG_05160	Dipeptidyl peptidase 3	42,94
PADG_08442	Proteasome subunit alpha type	30,72
PADG_03967	proteasome component C5	45,24
PADG_07190	Proteasome endopeptidase complex	37,56
PADG_00634	vacuolar protease A	25,22
PADG_06546	Aminopeptidase	59,91
CELLULAR TRANSPORT		
Transported compounds (substrates)		
PADG_07964	V-type proton ATPase subunit E	83,38
PADG_08176	phosphatidylinositol-phosphatidylcholine transfer protein	31,56
PADG_01363	diazepam-binding inhibitor (GABA receptor acyl- -binding)	84,2
PADG_03559	Cytochrome b5	28,87
Transport routes		
PADG_02022	clathrin light chain	84,07
PADG_02924	G2/M phase checkpoint control protein Sum2	24,09
PADG_07014	vesicular-fusion sec17	58,84
CELLULAR COMMUNICATION		
Cellular signalling		
PADG_08191	cAMP-dependent kinase regulatory subunit	15,37
PADG_04383	tricalbin-3	25,57
PADG_07652	CAMK/CAMK1/CAMK1-CMK protein k	16,53
PADG_07287	WD repeat	13,98
PADG_03219	myosin regulatory light chain cdc4	34,13
CELL RESCUE		
Stress response		
PADG_02981	ThiJ/PfpI family protein	71,14
PADG_08118	hsp72-like protein	959,26
PADG_03963	30 kDa heat shock	138,26

PADG_03654	hypothetical protein	19,31
PADG_05032	Hsp90 binding co-chaperone (Sba1)	39,31
PADG_03423	glutathione S-transferase Gst3	28,83
PADG_02764	thioredoxin-like protein	76,21
PADG_05344	peroxiredoxin Q BCP	15,93
PADG_05504	thioredoxin	106,67
PADG_03095	mitochondrial peroxiredoxin PRX1	33,08
Virulence, disease factors		
PADG_07422	serine proteinase	29,51
Detoxification		
PADG_00073	SAM-dependent methyltransferase COQ5 family	35,14
PADG_07418	superoxide dismutase [Cu-Zn] SOD1	101,1
PADG_01755	Fe-Mn family superoxide dismutase SOD2	40,2
CELL FATE		
Cell growth / morphogenesis		
PADG_05517	rho-gdp dissociation inhibitor	21,41
PADG_04559	progesterone binding	16,55
Cell death		
PADG_06087	hypothetical protein	15,32
INTERACTION WITH THE ENVIRONMENT		
Cell adhesion		
PADG_07615	immunodominant antigen Gp43	22,2
BIOGENESIS OF CELLULAR COMPONENTS		
Cell wall		
PADG_00994	chitinase class II	236,68
PADG_03691	cell wall glucanase	9,66
PADG_04499	cell wall protein ECM33 precursor	22,82
PADG_02862	1,3-beta-glucosidase	9,17
CELL TYPE DIFFERENTIATON		
Fungal/microorganismic cell type differentiation		
PADG_04260	NIMA-interacting protein TinC	29,3
PADG_08091	cell polarity (Alp11)	11,88

UNCLASSIFIED PROTEINS

PADG_02604	hypothetical protein	33,89
PADG_02181	HAD-superfamily hydrolase	36,51
PADG_12447	hypothetical protein	102,27
PADG_04907	hypothetical protein	47,96
PADG_05157	cell surface protein, putative	27,81
PADG_04343	short chain dehydrogenase/reductase	21,75
PADG_01857	Uncharacterized protein	41,39
PADG_02967	Uncharacterized protein	111,93
PADG_06021	hypothetical protein	32,74
PADG_06202	Arp2 3 complex subunit Arc16	66,98
PADG_07670	SAP domain-containing protein	30,66
PADG_11347	hypothetical protein	33,49
PADG_00422	actin cytoskeleton protein (VIP1)	162,78
PADG_04205	hypothetical protein	39,47
PADG_01002	erythrocyte band 7 integral membrane protein	17,5
PADG_02858	hypothetical protein	37,78
PADG_11101	hypothetical protein	41,61
PADG_00674	hypothetical protein	13,05
PADG_02909	Uncharacterized protein	14,92
PADG_11424	hypothetical protein	41,88
PADG_02338	Uncharacterized protein	19,47
PADG_12252	hypothetical protein	8,88
PADG_08152	hypothetical protein	13,17
PADG_08270	UBX domain-containing protein	8,33
PADG_02944	hypothetical protein	23,01
PADG_00921	Uncharacterized protein	35,19
PADG_11487	hypothetical protein	17,57
PADG_07225	Uncharacterized protein	24,59
PADG_11950	hypothetical protein	122,48
PADG_06136	related to mismatched base pair and cruciform dna recognition	21,36
PADG_07506	hypothetical protein	44,27

PADG_02118	Uncharacterized protein	16,96
PADG_04818	hypothetical protein	5,42
PADG_00676	hypothetical protein	128,58
PADG_04685	Uncharacterized protein	15,49
PADG_03203	BAR domain-containing protein	88,17
PADG_04215	DUF124 domain-containing protein	21,2
PADG_01688	DlpA domain-containing protein	12,4
PADG_02709	hypothetical protein	17,25
PADG_05584	hypothetical protein	13,06
PADG_02307	CUE domain-containing	12,64
PADG_04806	hypothetical protein	14,14
PADG_06945	GYF domain-containing protein	26,02
PADG_06699	Uncharacterized protein	14,25

[a]Acession number - acession number of matched protein from *Paracoccidioides brasiliensis* Uniprot database

[b]Protein description - proteins annotation from *Paracoccidioides brasiliensis* database or by homology in Blast2GO or NCBI

[c]Score - score obtained from the MS Amanda 2.0

[d]p-value - statistically significant differences are considered with ≤ 0.05 (ANOVA)

[e]Biological process of differentially expressed proteins from MIPS (http://mips.helmholtz-muenchen.de/funcatDB) and Uniprot databases (http://www.uniprot.org/).

Table S10. Identified phosphoproteins in TiO_2 enriched fraction of *Paracoccidioides brasiliensis* in the mycelia phase, mycelia-to-yeast transition and yeast cells

Acession number[a]	Protein description[b]	Coverage	# Peptides	# Protein Unique Peptides	# Unique Peptides	MW [kDa]	calc. pI	Modifications[c]	Tukey's test[d]		
Functional categories[e]											
METABOLISM									Yeast	Mycelium	Transition
Amino acid metabolism											

PADG_05301	cystathionine beta-synthase	5,816135	1	1	1	57,6	6,49	Phospho [S348(95.9)]	3,102419	2,768614	2,872892
PADG_03514	2-oxoisovalerate dehydrogenase E1 alpha subunit	3,104213	1	1	1	50,6	7,81	Phospho [S338(97)]	3,138558	3,098288	2,866981
Nitrogen, sulfur and selenium metabolism											
PADG_06490	formamidase	25,0646	6	6	6	42,3	6,09	Phospho [S280(100)]	5,945806	6,855969	6,537993
C-compound and carbohydrate metabolism											
PADG_00780	ribose-phosphate pyrophosphokinase II	12,11454	4	4	4	49	8,15	Phospho [Y124(84.1); T125(87.8); S167(98.8)]	4,94918	5,618977	5,198683
PADG_07217	ribose-phosphate pyrophosphokinase 1	2,692998	1	1	1	60,6	6,32	Phospho [S322(100)]	3,052182	3,298006	3,018495
Lipid, fatty acid and isoprenoid metabolism											
PADG_02299	choline-phosphate cytidylyltransferase	11,70213	3	3	3	61	8,88	Phospho [S18(99.9); S69(97)]	3,973515	4,517121	4,114901
ENERGY											
Glycolysis and gluconeogenesis											
PADG_11132	Phosphoglucomutase	3,23741	2	2	2	60,4	7,17	Phospho [T112(98.4)]	3,587329	3,732349	3,387184
PADG_05109	2,3-bisphosphoglycerate-independent phosphoglycerate mutase	9,213052	2	2	2	57,3	5,94	Phospho [S72(100)]	4,531219	4,047183	4,343606
CELL CYCLE AND DNA PROCESSING											
DNA processing											
PADG_06339	DNA topoisomerase 2	1,128784	1	1	1	216	8,51	Phospho [S1557(100)]	2,926207	1,997747	2,417284
PADG_08705	PHD finger domain-containing	3,289474	1	1	1	98,7	7,02	Phospho [S471(96.4)]	2,808023	3,494123	3,133677
cell cycle											
PADG_00085	arsenite resistance Ars2	1,260504	1	1	1	105,1	6,44	Phospho [S98(100)]	4,139722	3,91924	3,747664

PADG_07515	NSFL1 cofactor p47	8,673469	1	1	1	42,4	5,22	Phospho [S110(100); S114(100)]	5,281732	5,183344	4,953863
PADG_01028	sister chromatid cohesion	1,204056	1	1	1	173,4	6,51	Phospho [S317(100)]	2,570917	2,785402	2,435109
PADG_05893	nucleosome assembly	17,31707	4	4	4	46,6	4,54	Phospho [S318(100)]	4,419136	4,748355	4,369767
TRANSCRIPTION											
RNA synthesis											
PADG_01678	nucleoporin SONB	0,856855	1	1	1	211,3	6,23	Phospho [S810(98.5)]	2,866148	2,797013	2,69628
PADG_00814	branchpoint-bridging protein	7,615894	4	4	4	65,5	8,54	Phospho [S127(100); S129(99.9)]	4,557884	4,997641	4,537727
PADG_02315	RNA polymerase-associated protein LEO1	6,168224	3	3	3	60,1	4,58	Phospho [S140(100)]	3,881798	4,883672	4,339849
PADG_02652	RNP domain	26,12613	6	6	6	35	8,24	Phospho [S316(100)]	7,260518	7,33824	6,972037
PADG_07379	transcription factor	7,719298	1	1	1	32,1	6,81	Phospho [S122(100)]	3,698978	4,492681	3,647539
PADG_11651	transcription initiation factor TFIID subunit 1	2,043693	1	1	1	159	5,64	Phospho [S1214(99.9)]	2,166544	2,587685	2,261753
PADG_02622	CCR4-NOT transcription complex subunit	9,596929	2	2	2	55,9	7,03	Phospho [S371(98.6)]	2,90465	2,559746	2,451958
PADG_03515	CCR4-NOT transcription complex subunit 4	4,035309	2	2	2	170,1	8,72	Phospho [T391(98.7)]	2,670121	2,926809	2,680752
PADG_03869	HMG box	5,866667	1	1	1	39,7	8,57	Phospho [S117(100)]	2,340837	2,786426	2,515131
PADG_04730	nascent polypeptide-associated complex subunit alpha	28,22967	2	2	2	22,5	4,96	Phospho [S29(98.7)]	5,297625	5,94457	5,40916
PADG_07287	serine-threonine kinase receptor-associated protein	10,19737	1	1	1	32,7	6,52	Phospho [S91(96.5)]	2,416966	3,10709	2,747216
RNA processing											

PADG_11196	pinin SDK memA domain-containing	5,111111	1	1	1	49,8	5,99	Phospho [S329(100)]	2,473888	2,892355	2,524801
PADG_07689	transformer-SR ribonucleo	12,78689	3	3	3	34,3	9,38	Phospho [T152(100)]	4,761749	4,845409	4,463838
PADG_02899	nuclear mRNA splicing factor-associated	8,270677	2	2	2	45,4	4,84	Phospho [S22(99.2)]	4,712949	5,177192	4,769349
PADG_05340	pre-mRNA splicing factor	21,13402	5	5	5	23,1	9,79	Phospho [S121(100); S182(100)]	6,264775	6,255803	5,922197
PADG_02996	PAB1 binding	7,643885	5	5	5	120,5	9,47	Phospho [S724(93.8); S821(100)]	3,471296	3,721194	3,439953
PADG_00167	pre-mRNA-splicing factor	5,524862	1	1	1	39,6	6,92	Phospho [S67(100)]	2,55847	2,888766	2,745651
PROTEIN SYNTHESIS											
Ribosome biogenesis											
PADG_03778	60S ribosomal protein L10	9,865471	2	2	2	25,7	10,29	Phospho [S221(100)]	2,924283	2,539464	2,635543
translation											
PADG_04057	eukaryotic translation initiation factor 3 subunit J	23,15789	4	4	4	31,4	4,94	Phospho [S101(100)]	4,622483	5,615766	5,170419
PADG_02752	elongation factor 2	1,82002	1	1	1	110,6	5,24	Phospho [S38(100)]	2,500983	2,860576	2,44833
PADG_02896	elongation factor 1-beta	51,56951	6	6	1	25	4,84	Phospho [S93]	6,674853	6,317398	6,202431
PADG_05358	eukaryotic translation initiation factor 5	9,090909	2	2	2	47,8	5,24	Phospho [S47(100)]	4,896248	5,317287	4,719477
PADG_01250	WD repeat-containing protein JIP5	6,53753	1	1	1	43,9	5,45	Phospho [S351(100); S353(100)]	4,183511	4,536677	4,165468
PROTEIN FOLDING AND STABILIZATION											
Protein folding and stabilization											
PADG_02206	DnaJ domain protein Psi	7,629428	2	2	2	39,4	9,26	Phospho [T188(100)]	3,001708	1,240666	2,498676
Protein targeting, sorting and translocation											

PADG_06817	translocation SEC63	3,757225	1	1	1	77,5	6,18	Phospho [S633(100)]	3,151088	2,485279	2,611368
PADG_00011	actin binding	17,90123	7	7	7	86,6	5,11	Phospho [S455(97.3); S540(99.9); S559(100); S627(100)]	4,384566	4,700868	4,259884
Protein modification											
PADG_05366	SAGA complex component	7,280514	1	1	1	48,9	9,73	Phospho [S304(100)]	2,111369	2,274256	2,169323
Protein/peptide degradation											
PADG_02430	AAA family ATPase	1,292597	1	1	1	188,7	5,55	Phospho [S495(96.8)]	2,87433	2,781365	2,667517
CELLULAR TRANSPORT											
Transported compounds (substrates)											
PADG_01020	succinate:fumarate antiporter	5,538462	2	2	2	35,1	9,89	Phospho [S150(100)]	3,009416	2,908169	2,615264
PADG_03545	niemann-Pick C1 protein	2,431373	1	1	1	139,9	6,34	Phospho [S312(97.1)]	1,743632	1,329995	1,520132
Transport routes											
PADG_01191	nuclear export Yrb2	3,295311	1	1	1	84	4,96	Phospho [T319(98.3)]	1,059796	1,447115	1,198162
PADG_01114	importin subunit alpha-1	6,6787	1	1	1	60,7	5,03	Phospho [S84(92.5)]	1,452801	1,271282	1,220611
PADG_00061	peroxisomal biogenesis factor 6	1,69262	1	1	1	159,5	6,15	Phospho [S1457(100)]	1,178066	1,260667	1,208226
PADG_07659	transport sec9	6,651376	1	1	1	48	6,32	Phospho [S370(100)]	2,388188	2,055762	2,199313
PADG_06945	GYF domain-containing	3,005636	2	2	2	170,4	7,42	Phospho [S1225(98.3)]	3,626758	4,390126	3,969773
PADG_01152	actin cytoskeleton-regulatory complex protein PAN1	7,33945	4	4	4	165,2	6,24	Phospho [S919(94.7)]	1,397773	1,670157	1,377758
CELLULAR COMMUNICATION											

Cellular signalling											
PADG_03715	FK506-binding	21,0101	8	8	8	53,5	4,69	Phospho [S131(100); T270(100); S295(100)]	6,762602	6,540751	6,278808
CELL RESCUE											
Stress response											
PADG_01711	Hsp90 co-chaperone AHA1	6,811146	1	1	1	36	5,48	Phospho [S154(94.8)]	2,740702	2,878043	2,503326
PADG_00207	ribosome associated chaperone Zuotin	4,719101	2	2	2	50,6	8,95	Phospho [S82(100)]	4,847958	4,71884	4,525201
CELL FATE											
Cell growth / morphogenesis											
PADG_05959	hypothetical protein	11,61826	1	1	1	26,5	6,67	Phospho [S104(100)]	4,773336	4,950183	4,651108
UNCLASSIFIED											
PADG_00166	MGMT family	15,97222	1	1	1	16,1	5,31	Phospho [S129(100); S133(99.9)]	3,713882	4,282924	3,766512
PADG_00899	hypothetical protein	13,46154	1	1	1	23,2	5,41	Phospho [T153; S155; T157; T158; T166]	1,974433	2,582182	2,276036
PADG_01149	hypothetical protein	2,404526	1	1	1	76,4	6,87	Phospho [S289(99.9)]	2,325296	2,506974	2,223895
PADG_02076	hypothetical protein	1,264138	1	1	1	164,5	6,47	Phospho [S292(100)]	3,208983	2,474665	2,615864
PADG_02307	CUE domain-containing	14,28571	2	2	2	47,8	5,05	Phospho [S381(99.9)]	4,003074	4,063819	3,824686
PADG_02967	Uncharacterized protein	34,52381	18	18	1	61,9	5,49	Phospho [T484; S485]	5,1707	5,671596	5,326313
PADG_03822	Uncharacterized protein	31,70732	1	1	1	9	5,17	Phospho [S75(100)]	3,570318	3,961034	3,36203
PADG_03827	hypothetical protein	8,843537	1	1	1	14,6	11,39	Phospho [S22(99.4)]	4,128037	4,140261	4,006001

PADG_04006	hypothetical protein	7,692308	2	2	2	31,9	10,68	Phospho [S79(89.2)]	2,492957	2,440826	2,304749
PADG_04243	transcriptional regulator	8,762887	2	2	2	43,2	5,78	Phospho [S356(98.2)]	2,764076	2,520841	2,615695
PADG_04442	hypothetical protein	3,333333	1	1	1	62,2	5,03	Phospho [S79(100)]	2,574349	2,981064	2,754124
PADG_05112	hypothetical protein	7,978723	1	1	1	41,6	7,4	Phospho [S255(92.9); S258(92.9)]	3,230977	3,46201	3,038037
PADG_05935	spindle poison sensitivity Scp3	13,62984	4	4	4	73,7	9,19	Phospho [S118(98.8); S370(97.7)]	4,758374	5,080931	4,815578
PADG_07022	hypothetical protein	19,70149	3	3	3	36,3	7,03	Phospho [S115(97.6); S137(100)]	5,195515	5,12415	4,84574
PADG_08239	CBS and PB1 domain-containing	3,725782	1	1	1	72,6	6,21	Phospho [S462(100)]	1,399811	1,72896	1,503784
PADG_11936	apses transcription	7,637232	2	2	2	46,1	6,1	Phospho [S370(100)]	2,444898	2,898177	2,520452
PADG_11982	hypothetical protein	6,695157	2	2	2	78,4	8,54	Phospho [Y112(98.6); S565(99.9)]	3,485453	2,383411	2,756194
PADG_12447	hypothetical protein	25,04673	5	5	5	56,6	5,69	Phospho [S383(100)]	4,902494	5,855668	5,318341

[a]Accession number - acession number of matched protein from *Paracoccidioides brasiliensis* Uniprot database

[b]Protein description - proteins annotation from *Paracoccidioides brasiliensis* database or by homology in Blast2GO or NCBI identified in enriched fraction

[c]Modification- modification in the enriched fraction obtained from the MS Amanda 2.0

[d]Tukey's test- average of the Tukey test (of mycelia, mycelia-to-yeast transition and yeast)

[e] Biological process of differentially expressed proteins from MIPS (http://mips.helmholtz-muenchen.de/funcatDB) and Uniprot databases (http://www.uniprot.org/)

Table S11. Identified phosphoproteins in total fraction of *Paracoccidioides brasiliensis* in the mycelia phase, mycelia-to-yeast transition and yeast cells

Acession number[a]	Protein description[b]	Coverage	# Peptides	# Unique Peptides	# Protein Groups	MW [kDa]	calc. pI	Modifications[c]	Tukey's test[d]		
Functional categories[e]											
METABOLISM									Yeast	Mycelium	Transition
Amino acid metabolism											
PADG_05301	cystathionine beta-synthase	34,33396	13	13	1	57,6	6,49	Phospho [S348]	4,669516	4,573088	4,604525
PADG_07312	spermine spermidine synthase family	4,152249	1	1	1	63,5	7,61	Phospho [T316]; Methyl [E319]	1,3783	1,482255	1,684557
ENERGY											
Glycolysis and gluconeogenesis											
PADG_05109	2,3-bisphosphoglycerate-independent phosphoglycerate mutase	26,10365	9	9	1	57,3	5,94	Phospho [S58; S59; S72]	4,483192	4,697819	4,661476
CELL CYCLE AND DNA PROCESSING											
Cell cycle											
PADG_12492	SUMO-conjugating enzyme ubc9	7,211538	1	1	1	23,3	7,27	Phospho [T191; Y196]	1,347677	1,617028	1,594244
TRANSCRIPTION											
RNA processing											
PADG_05340	pre-mrna splicing factor	27,31959	6	6	1	23,1	9,79	Phospho [S182]	4,513186	4,732044	4,598566
PADG_04934	RNP domain-containing	49,26625	14	14	1	50,9	9,86	Phospho [S46; S48; S51]	4,531108	4,768104	4,522713
PADG_03236	DNA-binding protein creA	7,02403	1	1	1	58	9,69	Phospho [T374; S401]; Methyl [D372]	1,448436	1,600157	1,55319
PADG_06336	cell lysis protein cwl1	17,19298	3	3	1	32,2	6,62	Phospho [T14; S17]	2,881565	3,174896	3,140182
PROTEIN SYNTHESIS											
Translation											

PADG_04057	translation initiation factor 3 subunit J	40	7	7	1	31,4	4,94	Phospho [S101]	4,335911	4,789044	4,656223
PADG_01079	translation initiation factor 4B	36,69565	13	13	1	62,4	9,51	Phospho [S343; T345]	4,353437	4,808579	4,628514
PADG_02896	elongation factor 1-beta	51,56951	6	6	1	25	4,84	Phospho [S93]	4,902468	4,367075	4,505715
PROTEIN FOLDING AND STABILIZATION											
Protein targeting, sorting and translocation											
PADG_05074	exocyst complex component exo84	1,404056	1	1	1	71,7	9,22	Phospho [T362]	1,319824	1,64428	1,576151
PADG_00828	peroxisomal membrane protein receptor Pex19	6,132075	1	1	1	43,9	4,41	Phospho [S226; S227; S228; S229; T233]	2,502621	3,293574	3,186362
CELLULAR TRANSPORT											
Transport routes											
PADG_00945	actin like protein 2/3 complex, subunit 5	54,40415	5	5	1	20,5	6,1	Phospho [S141]	4,550736	4,696068	4,591444
PADG_03336	annexin ANXC4	2,567095	1	1	1	97,2	9,06	Phospho [S506; T508]	0,973755	1,743814	1,53129
CELLULAR COMMUNICATION											
Cellular signalling											
PADG_03715	FK506-binding protein	30,70707	10	10	1	53,5	4,69	Phospho [S131]	4,65136	4,5741	4,619937
PADG_04046	leucine Rich Repeat domain-containing protein	4,109589	1	1	1	87	9,67	Phospho [S366; S367; S369]	1,652733	1,389491	1,526106
CELL RESCUE											
Stress response											
PADG_00207	ribosome associated chaperone Zuotin	31,68539	10	10	1	50,6	8,95	Phospho [S82]	4,822792	4,487466	4,493959
BIOGENESIS OF CELLULAR COMPONENTS											
Cell wall											
PADG_03105	GPI-anchored cell surface glycoprotein	2,838221	1	1	1	114,4	7,37	Phospho [S135; S136; Y139]	1,386332	1,438175	1,703114

UNCLASSIFIED											
PADG_02863	hypothetical protein	0,778689	1	1	1	267,4	5,48	Phospho [S2091]	1,726674	1,34108	1,420022
PADG_12447	hypothetical protein	38,8785	10	10	1	56,6	5,69	Phospho [S383]	3,859343	4,914597	4,786712
PADG_05228	Uncharacterized protein	21,79487	1	1	1	17,2	7,52	Phospho [T125; T128; S131; S132; S136; S140]	0	0	0
PADG_02967	Uncharacterized protein	34,52381	18	18	1	61,9	5,49	Phospho [T484; S485]	3,980578	4,913309	4,729138

[a]Acession number - acession number of matched protein from *Paracoccidioides brasiliensis* Uniprot database

[b]Protein description - proteins annotation from *Paracoccidioides brasiliensis* database or by homology in Blast2GO or NCBI identified in enriched fraction

[c]Modification- modification in the enriched fraction obtained from the MS Amanda 2.0

[d]Tukey's test- average of the Tukey test (of mycelia, mycelia-to-yeast transition and yeast) used for statistical

[e] Biological process of differentially expressed proteins from MIPS (http://mips.helmholtz-muenchen.de/funcatDB) and Uniprot databases (http://www.uniprot.org/)

Produção científica durante o doutoramento

Artigo publicado

ARAÚJO, D. S; Lima, P. S; Baeza, L. C. [1]; Parente, A. F. A.; Bailão, A. M.; Borges, C. L.; Soares, C. M. A. Employing proteomic analysis to compare Paracoccidioides lutzii yeast and mycelium cell wall proteins. *Biochimica et Biophysica Acta - Proteins and Proteomics*, v. 1865, n. 11, p. 1304–1314, 2017. Disponível em: <http://dx.doi.org/10.1016/j.bbapap.2017.08.016>.

Trabalhos em publicação:

1. PHOSPHOPROTEOMIC ANALYSIS OF MEMBERS OF THE P*ARACOCCIDIOIDES* GENUS. Portis, I. G.; **Araújo, D**. **S.**; Santos Júnior, A. C. M.; Pontes, A. H., Fontes, W.; Paccez, J. D.; Ricart, C. A. O.; Soares, C. M. A.
2. PROTEOMIC ANALYSIS OF CELL WALL OF THE *Paracoccidioides brasiliensis* CRYTIC SPECIES *Pb*03 and *Pb*18. Ayda Luz Malaver Salamanca.
3. ANALYSIS OF *Paracoccidioides* HOMEOSTASIS IN RESPONSE TO HYPOXIC STRESS. Lucas Nojosa Oliveira.
4. PROTEOMIC ANALYSIS OF *Paracoccidioides brasiliensis* during infection of alveolar primed or not by interferon gamma. Edilânia G. A. Chaves[1], Lilian C. Baeza[1,2], Danielle S. Araújo[1], Clayton L. Borges[1], Juliana A. Parente-Rocha[1], Milton A. P. de Oliveira[3], Célia M. A. Soares[1*].

Referências

Adams, D. J. (2004). Fungal cell wall chitinases and glucanases. *Microbiology*, *150*(7), 2029–2035. https://doi.org/10.1099/mic.0.26980-0

Almeida, A. J., Cunha, C., Carmona, J. A., Sampaio-Marques, B., Carvalho, A., Malavazi, I., … Rodrigues, F. (2009). Cdc42p controls yeast-cell shape and virulence of Paracoccidioides brasiliensis. *Fungal Genetics and Biology*, *46*(12), 919–926. https://doi.org/10.1016/j.fgb.2009.08.004

Alonso, A., Sasin, J., Bottini, N., Friedberg, I., Friedberg, I., Osterman, A., … Mustelin, T. (2004). Protein tyrosine phosphatases in the human genome. *Cell*, *117*(6), 699–711. https://doi.org/10.1016/j.cell.2004.05.018

Andrade, R. V, Paes, H. C., Nicola, A. M., De, M. J. A., Fachin, A. L., Cardoso, R. S., … Felipe, S. S. (2006). Cell organisation , sulphur metabolism and ion transport-related genes are differentially expressed in Paracoccidioides brasiliensis mycelium and yeast cells. *BMC Genomics*, *7*(208), 1–13. https://doi.org/10.1186/1471-2164-7-208

Arantes, T. D., Theodoro, R. C., Teixeira, M. de M., Bosco, S. de M. G., & Bagagli, E. (2016). Environmental Mapping of Paracoccidioides spp. in Brazil Reveals New Clues into Genetic Diversity, Biogeography and Wild Host Association. *PLoS Neglected Tropical Diseases*, *10*(4), 1–18. https://doi.org/10.1371/journal.pntd.0004606

Araújo, D. S., de Sousa Lima, P., Baeza, L. C., Parente, A. F. A., Melo Bailão, A., Borges, C. L., & de Almeida Soares, C. M. (2017). Employing proteomic analysis to compare Paracoccidioides lutzii yeast and mycelium cell wall proteins. *Biochimica et Biophysica Acta - Proteins and Proteomics*, *1865*(11), 1304–1314. https://doi.org/10.1016/j.bbapap.2017.08.016

Bagagli, E., Franco, M., Bosco, S. D. M. G., Hebeler-Barbosa, F., Trinca, L. a, & Montenegro, M. R. (2003). High frequency of Paracoccidioides brasiliensis infection in armadillos (Dasypus novemcinctus): an ecological study. *Medical Mycology : Official Publication of the International Society for Human and Animal Mycology*, *41*(3), 217–223. https://doi.org/10.1080/13693780310001597368

Bagagli, E., Theodoro, R. C., Bosco, S. M. G., & McEwen, J. G. (2008). Paracoccidioides brasiliensis: Phylogenetic and ecological aspects. *Mycopathologia*, *165*(4–5), 197–207. https://doi.org/10.1007/s11046-007-9050-7

Baik, J. Y., Joo, E. J., Kim, Y. H., & Lee, G. M. (2008). Limitations to the comparative proteomic analysis of thrombopoietin producing Chinese hamster ovary cells treated with sodium butyrate. *Journal of Biotechnology*, *133*(4), 461–468. https://doi.org/10.1016/j.jbiotec.2007.11.008

Barbosa, S. M., Báo, S. N., Andreotti, P. F., Faria, F. P. De, Felipe, M. S. S., Feitosa, L. D. S., … Soares, C. M. D. A. (2006). Glyceraldehyde-3-Phosphate Dehydrogenase of *Paracoccidioides brasiliensis* Is a Cell Surface Protein Involved in Fungal Adhesion to Extracellular Matrix Proteins and Interaction with Cells. *Infection and Imunnity*, *74*(1), 382–389. https://doi.org/10.1128/IAI.74.1.382

Barbosa W, Daher R, O. A. F. (1968). Forma linfático-abdominal da blastomicose sul-americana. *Rev Inst Med Trop São Paulo*, *10*(1), 16–27.

Barrozo, L. V., Benard, G., Elisa, M., Silva, S., Bagagli, E., Alencar, S., & Mendes, R. P. (2010). First Description of a Cluster of Acute / Subacute Paracoccidioidomycosis Cases and Its Association with a Climatic Anomaly, *4*(3),

2–5. https://doi.org/10.1371/journal.pntd.0000643
Barrozo, L. V., Mendes, R. P., Marques, S. A., Benard, G., Siqueira Silva, M. E., & Bagagli, E. (2009). Climate and acute/subacute paracoccidioidomycosis in a hyper-endemic area in Brazil. *International Journal of Epidemiology*, *38*(6), 1642–1649. https://doi.org/10.1093/ije/dyp207
Bastos, K. P., Bailão, A. M., Borges, C. L., Faria, F. P., Felipe, M. S. S., Silva, M. G., … Soares, C. M. a. (2007). The transcriptome analysis of early morphogenesis in Paracoccidioides brasiliensis mycelium reveals novel and induced genes potentially associated to the dimorphic process. *BMC Microbiology*, *7*, 29. https://doi.org/10.1186/1471-2180-7-29
Batista, J., de Camargo, Z. P., Fernandes, G. F., Vicentini, A. P., Fontes, C. J. F., & Hahn, R. C. (2010). Is the geographical origin of a Paracoccidioides brasiliensis isolate important for antigen production for regional diagnosis of paracoccidioidomycosis? *Mycoses*, *53*(2), 176–180. https://doi.org/10.1111/j.1439-0507.2008.01687.x
Bayles, K. W., Wesson, C. A., Liou, L. E., Fox, L. K., Bohach, G. A., & Trumble, W. R. (1998). Intracellular Staphylococcus aureus Escapes the Endosome and Induces Apoptosis in Epithelial Cells. *Infect Immun.*, *66*(1), 336–342.
Beatrix, B., Sakai, H., & Wiedmann, M. (2000). The α and β subunit of the nascent polypeptide-associated complex have distinct functions. *Journal of Biological Chemistry*, *275*(48), 37838–37845. https://doi.org/10.1074/jbc.M006368200
Bellissimo-Rodrigues, F., Bollela, V. R., Da Fonseca, B. A. L., & Martinez, R. (2013). Endemic paracoccidioidomycosis: relationship between clinical presentation and patients' demographic features. *Medical Mycology*, *51*(3), 313–318. https://doi.org/10.3109/13693786.2012.714529
Bellissimo-Rodrigues, F., Machado, A. A., & Martinez, R. (2011). Paracoccidioidomycosis epidemiological features of a 1,000-cases series from a hyperendemic area on the southeast of Brazil. *American Journal of Tropical Medicine and Hygiene*, *85*(3), 546–550. https://doi.org/10.4269/ajtmh.2011.11-0084
Benschop, J. J., Mohammed, S., O'flaherty, M., Heck, A. J. R., Slijper, M., & Menke, F. L. H. (2007). Quantitative Phosphoproteomics of Early Elicitor Signaling in Arabidopsis. *Molecular & Cellular Proteomics*, *6.7*, 1198–1214. https://doi.org/10.1074/mcp.M600429-MCP200
Bookout, A. L., Cummins, C. L., Mangelsdorf, D. J., Pesola, J. M., & Kramer, M. F. (2006). High-throughput real-time quantitative reverse transcription PCR. *Current Protocols in Molecular Biology / Edited by Frederick M. Ausubel ... [et Al.]*, *Chapter 15*, Unit 15.8. https://doi.org/10.1002/0471142727.mb1508s73
Borges-walmsley, M. I., Chen, D., Shu, X., & Walmsley, A. R. (2002). The pathobiology of Paracoccidioides brasiliensis, *10*(2), 80–87.
Borges, C. L., Bailão, A. M., Báo, S. N., Pereira, M., Parente, J. A., & de Almeida Soares, C. M. (2011). Genes Potentially Relevant in the Parasitic Phase of the Fungal Pathogen Paracoccidioides brasiliensis. *Mycopathologia*, *171*(1), 1–9. https://doi.org/10.1007/s11046-010-9349-7
Borges, C. L., Parente, J. A., Barbosa, M. S., Santana, J. M., Báo, S. N., de Sousa, M. V., … De Almeida Soares, C. M. (2010). Detection of a homotetrameric structure and protein-protein interactions of *Paracoccidioides brasiliensis* formamidase lead to new functional insights. *FEMS Yeast Research*, *10*(1), 104–113. https://doi.org/10.1111/j.1567-1364.2009.00594.x
Brummer, E., Castaneda, E., & Restrepo, A. (1993). Paracoccidioidomycosis: an

update. *Clinical Microbiology Reviews*, *6*(2), 89–117. Retrieved from http://www.ncbi.nlm.nih.gov/pubmed/8472249

Brummer, E., Hanson, L. H., Restrepo, A., & Stevens, D. A. (1989). Intracellular multiplication of Paracoccidioides brasiliensis in macrophages: Killing and restriction of multiplication by activated macrophages. *Infection and Immunity*, *57*(8), 2289–2294.

Brummer, E., Sun, S. H., Harrison, J. L., Perlman, A. M., Philpott, D. E., & Stevens, D. A. (1990). Ultrastructure of phagocytosed Paracoccidioides brasiliensis in nonactivated or activated macrophages. *Infection and Immunity*, *58*(8), 2628–2636.

Buccheri, R., Khoury, Z., Barata, L. C. B., & Benard, G. (2016). Incubation Period and Early Natural History Events of the Acute Form of Paracoccidioidomycosis: Lessons from Patients with a Single Paracoccidioides spp. Exposure. *Mycopathologia*, *181*(5–6), 435–439. https://doi.org/10.1007/s11046-015-9976-0

Buchan, J. R., & Parker, R. (2009). Eukaryotic Stress Granules: The Ins and Outs of Translation. *Molecular Cell*, *36*(6), 932–941. https://doi.org/10.1016/j.molcel.2009.11.020

BURNETT G, K. E. (1954). The enzymatic phosphorylation of proteins. *J Biol Chem.*, *211*(2), 969–980.

C, N., & MU., S. (2000). Reactive oxygen and nitrogen intermediates in the relationship between mammalian host and microbial pathogens. *Proc Natl Acad Sci U S A.*, *1*(97), 8841–8848.

Cadavid, D., & Restrepo, a. (1993). Factors associated with Paracoccidiodes brasiliensis infection among permanent residents of three endemic areas in Colombia. *Epidemiology and Infection*, *111*(1), 121–133. https://doi.org/10.1017/S0950268800056740

Capra, E. J., & Laub, M. T. (2012). Evolution of Two-Component Signal Transduction Systems. *Annual Review of Microbiology*, *66*(1), 325–347. https://doi.org/10.1146/annurev-micro-092611-150039

Carpy, A., Krug, K., Graf, S., Koch, A., Popic, S., Hauf, S., & Macek, B. (2014). Absolute Proteome and Phosphoproteome Dynamics during the Cell Cycle of *Schizosaccharomyces pombe* (Fission Yeast). *Molecular & Cellular Proteomics*, *13*(8), 1925–1936. https://doi.org/10.1074/mcp.M113.035824

Carrero, L. L., Niño-Vega, G., Teixeira, M. M., Carvalho, M. J. A., Soares, C. M. A., Pereira, M., … San-Blas, G. (2008). New *Paracoccidioides brasiliensis* isolate reveals unexpected genomic variability in this human pathogen. *Fungal Genetics and Biology : FG & B*, *45*(5), 605–612. https://doi.org/10.1016/j.fgb.2008.02.002

Chaga, G., Hopp, J., & Nelson, P. (1999). Immobilized metal ion affinity chromatography on Cobalt - carboxymethylaspartate – agarose Superflow, as demonstrated by one-step purification of lactate dehydrogenase from chicken breast muscle. *Biotechnology and Applied Biochemistry*, *24*, 19–24. https://doi.org/10.1111/j.1470-8744.1999.tb01144.x

Chagas, R. F., Bailão, A. M., Pereira, M., Winters, M. S., Smullian, A. G., Deepe, G. S., & de Almeida Soares, C. M. (2008). The catalases of Paracoccidioides brasiliensis are differentially regulated: Protein activity and transcript analysis. *Fungal Genetics and Biology*, *45*(11), 1470–1478. https://doi.org/10.1016/j.fgb.2008.08.007

Chai, L. Y. A., Netea, M. G., Vonk, A. G., & Kullberg, B. (2009). Fungal strategies for overcoming host innate immune response. *Med Mycol.*, *47*(3), 227–236. https://doi.org/10.1080/13693780802209082

Chao, J. D., Wong, D., & Av-Gay, Y. (2014). Microbial protein-tyrosine kinases.

Journal of Biological Chemistry, *289*(14), 9463–9472. https://doi.org/10.1074/jbc.R113.520015

Chaves, A. F. A., Castilho, D. G., Navarro, M. V., Oliveira, A. K., Serrano, S. M. T., Tashima, A. K., & Batista, W. L. (2016). Phosphosite-specific regulation of the oxidative-stress response of Paracoccidioides brasiliensis: A shotgun phosphoproteomic analysis. *Microbes and Infection*, (August), 1–13. https://doi.org/10.1016/j.micinf.2016.08.004

Chaves, A. F. A., Navarro, M. V., Castilho, D. G., Calado, J. C. P., Conceição, P. M., & Batista, W. L. (2016). A conserved dimorphism-regulating histidine kinase controls the dimorphic switching in Paracoccidioides brasiliensis. *FEMS Yeast Research*, *16*(5), 1–10. https://doi.org/10.1093/femsyr/fow047

Chou, M. F., & Schwartz, D. (2011). Biological Sequence Motif Discovery Using *motif-x*. *Current Protocols in Bioinformatics*, 1–52. https://doi.org/10.1002/0471250953.bi1315s35

Cole, J. N., Aquilina, J. A., Hains, P. G., Henningham, A., Sriprakash, K. S., Caparon, M. G., … Walker, M. J. (2007). Role of group A Streptococcus HtrA in the maturation of SpeB protease. *Proteomics*, *7*(24), 4488–4498. https://doi.org/10.1002/pmic.200700626

Collart, M. A. (2016). The Ccr4-Not complex is a key regulator of eukaryotic gene expression. *Wiley Interdisciplinary Reviews: RNA*, *7*(4), 438–454. https://doi.org/10.1002/wrna.1332

Conesa, A., Götz, S., García-Gómez, J. M., Terol, J., Talón, M., & Robles, M. (2005). Blast2GO: A universal tool for annotation, visualization and analysis in functional genomics research. *Bioinformatics*, *21*(18), 3674–3676. https://doi.org/10.1093/bioinformatics/bti610

Corredor GG1, Peralta LA, Castaño JH, Zuluaga JS, Henao B, Arango M, Tabares AM, Matute DR, McEwen JG, R. A. (2005). The naked-tailed armadillo Cabassous centralis (Miller 1899): a new host to Paracoccidioides brasiliensis. Molecular identification of the isolate. *Med Mycol.*, *43*(3), 275–280.

Costa, A., Benard, G., Albuquerque, A., Fujita, C., Magri, A., Salge, J., … Carvalho, C. (2013). The lung in paracoccidioidomycosis: new insights into old problems. *Clinics*, *68*(4), 441–448. https://doi.org/10.6061/clinics/2013(04)02

Costa, M., Borges, C. L., Bailão, A. M., Meirelles, G. V., Mendonça, Y. A., Dantas, S. F. I. M., … Soares, C. M. A. (2007). Transcriptome profiling of Paracoccidioides brasiliensis yeast-phase cells recovered from infected mice brings new insights into fungal response upon host interaction. *Microbiology*, *153*(12), 4194–4207. https://doi.org/10.1099/mic.0.2007/009332-0

D, S., & Ehrt S, Voskuil MI, Liu Y, Mangan JA, Monahan IM, Dolganov G, Efron B, Butcher PD, Nathan C, S. G. (2003). Transcriptional Adaptation of Mycobacterium tuberculosis within Macrophages: Insights into the Phagosomal Environment. *J Exp Med.*, *198*.

Da Silva Cruz, A. H., Brock, M., Zambuzzi-Carvalho, P. F., Santos-Silva, L. K., Troian, R. F., Gões, A. M., … Pereira, M. (2011). Phosphorylation is the major mechanism regulating isocitrate lyase activity in Paracoccidioides brasiliensis yeast cells. *FEBS Journal*, *278*(13), 2318–2332. https://doi.org/10.1111/j.1742-4658.2011.08150.x

de Arruda Grossklaus, D., Bailão, A. M., Vieira Rezende, T. C., Borges, C. L., de Oliveira, M. A. P., Parente, J. A., & de Almeida Soares, C. M. (2013). Response to oxidative stress in *Paracoccidioides* yeast cells as determined by proteomic analysis. *Microbes and Infection / Institut Pasteur*, *15*(5), 347–364.

https://doi.org/10.1016/j.micinf.2012.12.002
de Carvalho, M. J. A., Amorim Jesuino, R. S., Daher, B. S., Silva-Pereira, I., de Freitas, S. M., Soares, C. M. A., & Felipe, M. S. S. (2003). Functional and genetic characterization of calmodulin from the dimorphic and pathogenic fungus Paracoccidioides brasiliensis. *Fungal Genetics and Biology : FG & B*, *39*(3), 204–210. https://doi.org/10.1016/S1087-1845(03)00044-6
de Castro LF, & Ferreira MC, da Silva RM, Blotta MH, Longhi LN, M. R. (2013). Characterization of the immune response in human paracoccidioidomycosis. *J Infect.*, *67*(5), 470–485.
De Groot, P. W. J., Ram, A. F., & Klis, F. M. (2005). Features and functions of covalently linked proteins in fungal cell walls. *Fungal Genetics and Biology*, *42*(8), 657–675. https://doi.org/10.1016/j.fgb.2005.04.002
De Souza Bonfim-Mendonça, P., Ratti, B. A., Da Silva Ribeiro Godoy, J., Negri, M., De Lima, N. C. A., Fiorini, A., … Svidzinski, T. I. E. (2014). β-Glucan induces reactive oxygen species production in human neutrophils to improve the killing of Candida albicans and Candida glabrata isolates from vulvovaginal candidiasis. *PLoS ONE*, *9*(9), 1–14. https://doi.org/10.1371/journal.pone.0107805
De Souza, C. P. C., Horn, K. P., Masker, K., & Osmani, S. a. (2003). NIMA Kinase in Aspergillus nidulans.
De Souza, C. P. C., Osmani, A. H., Wu, L. P., Spotts, J. L., & Osmani, S. A. (2000). Mitotic histone H3 phosphorylation by the NIMA kinase in Aspergillus nidulans. *Cell*, *102*(3), 293–302. https://doi.org/10.1016/S0092-8674(00)00035-0
De Souza, C. P., Hashmi, S. B., Osmani, A. H., Andrews, P., Ringelberg, C. S., Dunlap, J. C., & Osmani, S. A. (2013). Functional Analysis of the Aspergillus nidulans Kinome. *PLoS ONE*, *8*(3). https://doi.org/10.1371/journal.pone.0058008
Delom, F., & Chevet, E. (2006). Phosphoprotein analysis: from proteins to proteomes. *Proteome Science*, *4*, 15. https://doi.org/10.1186/1477-5956-4-15
Derengowski LS, Tavares AH, Silva S, Procópio LS, Felipe MS, S.-P. I. (2008). Upregulation of glyoxylate cycle genes upon Paracoccidioides brasiliensis internalization by murine macrophages and in vitro nutritional stress condition. *Med Mycol.*, *46*(2), 125–134. https://doi.org/10.1080/13693780701670509
Desjardins, C. A., Champion, M. D., Holder, J. W., Muszewska, A., Goldberg, J., Bailão, A. M., … Cuomo, C. A. (2011). Comparative genomic analysis of human fungal pathogens causing paracoccidioidomycosis. *PLoS Genetics*, *7*(10), e1002345. https://doi.org/10.1371/journal.pgen.1002345
Donofrio, F. C., Calil, A. C. A., Miranda, E. T., Almeida, A. M. F., Benard, G., Soares, C. M. de A. C. P., … Mendes Giannini, M. J. S. (2009). Enolase from Paracoccidioides brasiliensis: Isolation and identification as a fibronectin-binding protein. *Journal of Medical Microbiology*, *58*(6), 706–713. https://doi.org/10.1099/jmm.0.003830-0
Eymann, C., Becher, D., Bernhardt, J., Gronau, K., Klutzny, A., & Hecker, M. (2007). Dynamics of protein phosphorylation on Ser/Thr/Tyr in Bacillus subtilis. *Proteomics*, *7*(19), 3509–3526. https://doi.org/10.1002/pmic.200700232
Fabris LR, & Andrade UV, Dos Santos AF, Marques APC, de Oliveira SMVL, Mendes RP, et al. (2014). Decreasing prevalence of the acute/ subacute clinical form of paracoccidioidomycosis in Mato Grosso do Sul State, Brazil. *Rev. Inst. Med. Trop. Sao Paulo*, *56*(2), 121–125.
Fan W, & Kraus PR, Boily MJ, H. J. (2005). Cryptococcus neoformans gene expression during murine macrophage infection. *Eukaryot Cell.*, *4*(8), 1420–33.
Fang FC. (2004). Antimicrobial reactive oxygen and nitrogen species: concepts and

controversies. *Nat Rev Microbiol.*, *2*(10), 820–832.
Fassler, J. S., & West, A. H. (2013). Histidine phosphotransfer proteins in fungal two-component signal transduction pathways. *Eukaryotic Cell*, *12*(8), 1052–1060. https://doi.org/10.1128/EC.00083-13
Favreau, C., Worman, H. J., Wozniak, R. W., Frappier, T., & Courvalin, J. C. (1996). Cell cycle-dependent phosphorylation of nucleoporins and nuclear pore membrane protein Gp210. *Biochemistry*, *35*(24), 8035–8044. https://doi.org/10.1021/bi9600660
Felipe, M. S. S. (2005). Transcriptional Profiles of the Human Pathogenic Fungus Paracoccidioides brasiliensis in Mycelium and Yeast Cells. *Journal of Biological Chemistry*, *280*(26), 24706–24714. https://doi.org/10.1074/jbc.M500625200
Felipe, M. S. S. (2005). Transcriptional Profiles of the Human Pathogenic Fungus Paracoccidioides brasiliensis in Mycelium and Yeast Cells. *Journal of Biological Chemistry*, *280*(26), 24706–24714. https://doi.org/10.1074/jbc.M500625200
Felipe, M. S. S., Andrade, R. V., Petrofeza, S. S., Maranhão, A. Q., Torres, F. A. G., Albuquerque, P., … Brígido, M. M. (2003). Transcriptome characterization of the dimorphic and pathogenic fungus Paracoccidioides brasiliensis by EST analysis. *Yeast (Chichester, England)*, *20*(3), 263–271. https://doi.org/10.1002/yea.964
Fernandes, F. F., Oliveira, A. F., Landgraf, T. N., Cunha, C., Carvalho, A., Vendruscolo, P. E., … Roque-Barreira, M. C. (2017). Impact of paracoccin gene silencing on Paracoccidioides brasiliensis Virulence. *MBio*, *8*(4), 1–12. https://doi.org/10.1128/mBio.00537-17
Fernandes, L., Paes, H. C., Tavares, A. H., Silva, S. S., Dantas, A., Soares, M. A., … Felipe, M. S. S. (2008). Transcriptional pro ¢ le of ras1 and ras2 and the potential role of farnesylation in the dimorphism of the human pathogen Paracoccidioides brasiliensis. *FEMS Yeast Res.*, *8*(2), 300–310. https://doi.org/10.1111/j.1567-1364.2007.00317.x
Ferreira MS1, Freitas LH, Lacaz Cda S, del Negro GM, de Melo NT, Garcia NM, de Assis CM, Salebian A, H.-V. E. (1990). Isolation and characterization of a Paracoccidioides brasiliensis strain from a dogfood probably contaminated with soil in Uberlândia, Brazil. *J Med Vet Mycol*, *28*(3), 253–256.
Ferreira, S. D. P., Santos, S., Paula, L. B. De, & Adamski, A. (2012). Prevalência da Paracoccidioidomicose em pacientes diagnosticados no Hospital Araújo Jorge me Goiânia-Goiás, Brasil. *Revista Da Universidade Vale Do Rio Verde, Três Corações*, *10*(1), 167–177.
Ficarro, S. B., McCleland, M. L., Stukenberg, P. T., Burke, D. J., Ross, M. M., Shabanowitz, J., … White, F. M. (2002). Phosphoproteome analysis by mass spectrometry and its application to Saccharomyces cerevisiae. *Nature Biotechnology*, *20*(3), 301–305. https://doi.org/10.1038/nbt0302-301
Filler, S. G., & Sheppard, D. C. (2006). Fungal invasion of normally non-phagocytic host cells. *PLoS Pathog*, *2*(12). https://doi.org/10.1371/journal.ppat.0020129
Flory, M. R., Lee, H., Bonneau, R., Mallick, P., Serikawa, K., Morris, D. R., & Aebersold, R. (2006). Quantitative proteomic analysis of the budding yeast cell cycle using acid-cleavable isotope-coded affinity tag reagents. *Proteomics*, *6*(23), 6146–6157. https://doi.org/10.1002/pmic.200600159
Franco M, Montenegro MR, Mendes RP, Marques SA, Dillon NL, M. N. (1987). Paracoccidioidomycosis: a recently proposed classification of its clinical forms. *Revista Da Sociedade Brasileira de Medicina Tropical*, *20*(2), 129–132.
Franco, M., Bagagli, E., Scapolio, S., & da Silva Lacaz, C. (2000). A critical analysis of isolation of Paracoccidioides brasiliensis from soil. *Medical Mycology*, *38*(3), 185–

191. https://doi.org/10.1080/714030941
Franco M, & Mendes RP, Moscardi-Bacchi M, Rezkallah-Iwasso M, M. M. (1989). Paracoccidioidomycosis. *Baillière's Clinical Tropical Medicine and Communicable Diseases*, *4*, 185–220.
Fraser, J. A., Davis, M. A., & Hynes, M. J. (2001). The formamidase gene of Aspergillus nidulans: Regulation by nitrogen metabolite repression and transcriptional interference by an overlapping upstream gene. *Genetics*, *157*(1), 119–131. Retrieved from http://www.ncbi.nlm.nih.gov/pubmed/11139496
G, B., & Romano CC, Cacere CR, Juvenale M, Mendes-Giannini MJ, D. A. (2001). Imbalance of IL-2, IFN-gamma and IL-10 secretion in the immunosuppression associated with human paracoccidioidomycosis. *Cytokine.*, *13*(4), 248–252.
Gauthier, G., & Klein, B. S. (2010). Insights into Fungal Morphogenesis and Immune Evasion: Fungal conidia, when situated in mammalian lungs, may switch from mold to pathogenic yeasts or spore-forming spherules. *Microbe Wash DC.*, *3*(9), 416–423.
Gegembauer, G., Araujo, L. M., Pereira, E. F., Rodrigues, A. M., Mello, A., Paniago, M., … Camargo, Z. P. De. (2014). Serology of Paracoccidioidomycosis Due to Paracoccidioides lutzii, *8*(7). https://doi.org/10.1371/journal.pntd.0002986
Goldman, G. H., Marques, R., Luciano, A., Bernardes, D. S., Quiapin, C., Vitorelli, P. M., … Goldman, M. H. S. (2003). Expressed Sequence Tag Analysis of the Human Pathogen Paracoccidioides brasiliensis Yeast Phase : Identification of Putative Homologues of Candida albicans Virulence and Pathogenicity Genes. *Eukaryot Cell*, *2*(1), 34–48. https://doi.org/10.1128/EC.2.1.34
Gonzalez, A., Lenzi, H. L., Motta, E. M., Caputo, L., Sahaza, J. H., Cock, A. M., … Cano, L. E. (2005). Expression of adhesion molecules in lungs of mice infected with Paracoccidioides brasiliensis conidia. *Microbes Infect.*, *7*, 666–673. https://doi.org/10.1016/j.micinf.2005.01.004
Grasser, M., Lentz, A., Lichota, J., Merkle, T., & Grasser, K. D. (2006). The Arabidopsis Genome Encodes Structurally and Functionally Diverse HMGB-type Proteins. *Journal of Molecular Biology*, *358*(3), 654–664. https://doi.org/10.1016/j.jmb.2006.02.068
Grose E, T. J. (1965). Paracoccidioides brasiliensis recovered from the intestinal tract of three bats (Artibeus lituratus) in Colombia, S.A. *Sabouraudia*, *4*(2), 124–125.
Hahn, R. C., Macedo, A. M., Fontes, C. J. F., Batista, R. D., Santos, N. L., & Hamdan, J. S. (2003). Randomly amplified polymorphic DNA as a valuable tool for epidemiological studies of Paracoccidioides brasiliensis. *Journal of Clinical Microbiology*, *41*(7), 2849–2854. https://doi.org/10.1128/JCM.41.7.2849
Hayward, R. D., & Koronakis, V. (1999). Direct nucleation and bundling of actin by the SipC protein of invasive Salmonella. *EMBO J.*, *18*(18), 4926–4934.
Hernández O, Araque P, Tamayo D, Restrepo A, Herrera S, Mcewen JG, Pelaez C, A. A. (2015). Alternative oxidase plays an important role in Paracoccidioides brasiliensis cellular homeostasis and morphological transition. *Medical Mycology*, *53*(3), 205–214. https://doi.org/10.1093/mmy/myu091
JA, S., & SC., B. (1995). Phagocytosis by zippers and triggers. *Trends Cell Biol.*, *5*(3), 89–93.
Jensen, S. S., & Larsen, M. R. (2007). Evaluation of the impact of some experimental procedures on different phosphopeptide enrichment techniques. *Rapid Communications in Mass Spectrometry : RCM*, *21*(22), 3635–3645. https://doi.org/10.1002/rcm.3254
Jiang, P., Wei, W. F., Zhong, G. W., Zhou, X. G., Qiao, W. R., Fisher, R., & Lu, L.

(2017). The function of the three phosphoribosyl pyrophosphate synthetase (Prs) genes in hyphal growth and conidiation in Aspergillus nidulans. *Microbiology (United Kingdom)*, *163*(2), 218–232. https://doi.org/10.1099/mic.0.000427

Johnson, C., Kweon, H. K., Sheidy, D., Shively, C. A., Mellacheruvu, D., Nesvizhskii, A. I., … Kumar, A. (2014). The Yeast Sks1p Kinase Signaling Network Regulates Pseudohyphal Growth and Glucose Response. *PLOS Genetics*, *10*(3), e1004183. Retrieved from https://doi.org/10.1371/journal.pgen.1004183

JP, W. (2003). Knocking on the right door and making a comfortable home: Histoplasma capsulatum intracellular pathogenesis. *Curr Opin Microbiol.*, *6*(4), 327–331.

Juvvadi, P. R., Gehrke, C., Fortwendel, J. R., Lamoth, F., Soderblom, E. J., Cook, E. C., … Steinbach, W. J. (2013). Phosphorylation of Calcineurin at a Novel Serine-Proline Rich Region Orchestrates Hyphal Growth and Virulence in Aspergillus fumigatus. *PLoS Pathogens*, *9*(8). https://doi.org/10.1371/journal.ppat.1003564

Juvvadi, P. R., Ma, Y., Richards, A. D., Soderblom, E. J., Arthur Moseley, M., Lamoth, F., & Steinbach, W. J. (2015). Identification and mutational analyses of phosphorylation sites of the calcineurin-binding protein CbpA and the identification of domains required for calcineurin binding in Aspergillus fumigatus. *Frontiers in Microbiology*, *6*(MAR), 1–10. https://doi.org/10.3389/fmicb.2015.00175

Kanetsuna, F., & Carbonell, L. M. (1970). Cell wall glucans of the yeast and mycelial forms of Paracoccidioides brasiliensis. *Journal of Bacteriology*, *101*(3), 675–680.

Kanetsuna, F., Carbonell, L. M., Moreno, R. E., & Rodriguez, J. (1969). Cell wall composition of the yeast and mycelial forms of Paracoccidioides brasiliensis. *Journal of Bacteriology*, *97*(3), 1036–1041. Retrieved from http://www.ncbi.nlm.nih.gov/pubmed/5776517

Kaufmann, H., Bailey, J. E., & Fussenegger, M. (2001). Use of antibodies for detection of phosphorylated proteins separated by two-dimensional gel electrophoresis. *Proteomics*, *1*(2), 194–199. https://doi.org/10.1002/1615-9861(200102)1:2<194::AID-PROT194>3.0.CO;2-K

Kennelly, P. J. (2014). Protein Ser/Thr/Tyr phosphorylation in the archaea. *Journal of Biological Chemistry*, *289*(14), 9480–9487. https://doi.org/10.1074/jbc.R113.529412

Kosti, I., Mandel-Gutfreund, Y., Glaser, F., & Horwitz, B. A. (2010). Comparative analysis of fungal protein kinases and associated domains. *BMC Genomics*, *11*(1), 133. https://doi.org/10.1186/1471-2164-11-133

Kraus, P. R., Fox, D. S., Cox, G. M., & Heitman, J. (2003). The Cryptococcus neoformans MAP kinase Mpk1 regulates cell integrity in response to antifungal drugs and loss of calcineurin function. *Molecular Microbiology*, *48*(5), 1377–1387. https://doi.org/10.1046/j.1365-2958.2003.03508.x

Kummasook, A., Cooper, C. R., Sakamoto, A., Terui, Y., Kashiwagi, K., & Vanittanakom, N. (2013). Spermidine is required for morphogenesis in the human pathogenic fungus, Penicillium marneffei. *Fungal Genetics and Biology*, *58–59*, 25–32. https://doi.org/10.1016/j.fgb.2013.08.001

Kun Ping Lu, Kemp, B. E., & Means, A. R. (1994). Identification of substrate specificity determinants for the cell cycle- regulated NIMA protein kinase. *Journal of Biological Chemistry*, *269*(9), 6603–6607.

Lacaz, C. S. (1994). Historical Evolution of the knowledge on Paracoccidioidomycosis and its Etiolologic Agent, Paracoccidoides brasiliensis. In *Paracoccidioidomycosis* (pp. 1–7).

Lacaz CS, Porto E, M. J. (1984). Paracoccidioidomicose In: Lacaz CS, Porto E, Martins JEC, editors. *Micologia Medica.*, 189–216.

Lacerda Pigosso, L., Baeza, L. C., Vieira Tomazett, M., Batista Rodrigues Faleiro, M., Brianezi Dignani de Moura, V. M., Melo Bailão, A., … Soares, C. M. de A. (2017). Paracoccidioides brasiliensis presents metabolic reprogramming and secretes a serine proteinase during murine infection. *Virulence*, *8*(7), 1417–1434. https://doi.org/10.1080/21505594.2017.1355660

Lahari, T., Lazaro, J., & Schroeder, D. F. (2018). RAD4 and RAD23/HMR contribute to arabidopsis UV tolerance. *Genes*, *9*(1), 1–12. https://doi.org/10.3390/genes9010008

Lam, W. C., Gerik, K. J., & Lodge, J. K. (2013). Role of Cryptococcus neoformans Rho1 GTPases in the PKC1 signaling pathway in response to thermal stress. *Eukaryotic Cell*, *12*(1), 118–131. https://doi.org/10.1128/EC.05305-11

Lara-Lemus R, Alvarado-Vásquez N, Zenteno E, G. P. (2014). Effect of Histoplasma capsulatum glucans on host innate immunity. *Rev Iberoam Micol.*, *31*(1), 76–80.

Leitner, A. (2016). *Phospho-Proteomics*. (L. von Stechow, Ed.) (Vol. 1355). New York, NY: Springer New York. https://doi.org/10.1007/978-1-4939-3049-4

Leitner, A., Sturm, M., & Lindner, W. (2011). Tools for analyzing the phosphoproteome and other phosphorylated biomolecules: A review. *Analytica Chimica Acta*, *703*(1), 19–30. https://doi.org/10.1016/j.aca.2011.07.012

Levery, S. B., Toledo, M. S., Straus, A. H., & Takahashi, H. K. (1998). Structure elucidation of sphingolipids from the mycopathogen Paracoccidioides brasiliensis: An immunodominant β-galactofuranose residue is carried by a novel glycosylinositol phosphorylceramide antigen. *Biochemistry*, *37*(24), 8764–8775. https://doi.org/10.1021/bi9730083

Lewis, K. I. M. (2000). Programmed Death in Bacteria. *Microbiol Mol Biol Rev.*, *64*(3), 503–514.

Lim JP, & PA., G. (2011). Macropinocytosis: an endocytic pathway for internalising large gulps. *Immunol Cell Biol.*, *89*(8), 836–843.

Lin, M.-H., Sugiyama, N., & Ishihama, Y. (2015). Systematic profiling of the bacterial phosphoproteome reveals bacterium-specific features of phosphorylation. *Science Signaling*, *8*(394), rs10-rs10. https://doi.org/10.1126/scisignal.aaa3117

Loose, D. S., Stover, E. P., Restrepo, A., Stevens, D. A., & Feldman, D. (1983). Estradiol binds to a receptor-like cytosol binding protein and initiates a biological response in Paracoccidioides brasiliensis. *Proceedings of the National Academy of Sciences*, *80*(24), 7659–7663. https://doi.org/10.1073/pnas.80.24.7659

Lutz, A. (1945). Uma micose pseudococcídica localizada na boca e observada no Brasil . Contribuição ao conhecimento das. *Adolpho Lutz - Obra Completa*, 483–494.

Machado Filho J, M. J. & T. G. (1965). Das sequelas da blastomicose sul americana. *O Hospital*, *68*, 1346–1354.

Malanovic, N., Streith, I., Wolinski, H., Rechberger, G., Kohlwein, S. D., & Tehlivets, O. (2008). S-adenosyl-L-homocysteine hydrolase, key enzyme of methylation metabolism, regulates phosphatidylcholine synthesis and triacylglycerol homeostasis in yeast: Implications for homocysteine as a risk factor of atherosclerosis. *Journal of Biological Chemistry*, *283*(35), 23989–23999. https://doi.org/10.1074/jbc.M800830200

Manocha, M. (1980). Lipid composition of Paracoccidioides brasiliensis: comparison between the yeast and mycelial forms. *Sabouraudia*, *18*(4), 281–286.

Marques-da-Silva, S. H., Rodrigues, A. M., De Hoog, G. S., Silveira-Gomes, F., & De Camargo, Z. P. (2012). Case report: Occurrence of Paracoccidioides lutzii in the

Amazon Region: Description of two cases. *American Journal of Tropical Medicine and Hygiene*, *87*(4), 710–714. https://doi.org/10.4269/ajtmh.2012.12-0340

Martani, F., Marano, F., Bertacchi, S., Porro, D., & Branduardi, P. (2015). The Saccharomyces cerevisiae poly(A) binding protein Pab1 as a target for eliciting stress tolerant phenotypes. *Scientific Reports*, *5*(November), 1–13. https://doi.org/10.1038/srep18318

Martinez-Lopez, R., Monteoliva, L., Diez-Orejas, R., Nombela, C., & Gil, C. (2004). The GPI-anchored protein CaEcm33p is required for cell wall integrity, morphogenesis and virulence in *Candida albicans*. *Microbiology*, *150*(10), 3341–3354. https://doi.org/10.1099/mic.0.27320-0

Martinez-Lopez, R., Park, H., Myers, C. L., Gil, C., & Filler, S. G. (2006). *Candida albicans* Ecm33p is important for normal cell wall architecture and interactions with host cells. *Eukaryotic Cell*, *5*(1), 140–147. https://doi.org/10.1128/EC.5.1.140-147.2006

Martinez, R. (2017). New Trends in Paracoccidioidomycosis Epidemiology. *Journal of Fungi*, *3*(1), 1. https://doi.org/10.3390/jof3010001

Martins, V. P., Dinamarco, T. M., Soriani, F. M., Tudella, V. G., Oliveira, S. C., Goldman, G. H., … Uyemura, S. A. (2011). Involvement of an alternative oxidase in oxidative stress and mycelium-to-yeast differentiation in paracoccidioides brasiliensis. *Eukaryotic Cell*, *10*(2), 237–248. https://doi.org/10.1128/EC.00194-10

Masaki, S., Yamada, T., Hirasawa, T., Todaka, D., & Kanekatsu, M. (2008). Proteomic analysis of RNA-binding proteins in dry seeds of rice after fractionation by ssDNA affinity column chromatography. *Biotechnology Letters*, *30*(5), 955–960. https://doi.org/10.1007/s10529-007-9619-8

Matute, D. R., McEwen, J. G., Puccia, R., Montes, B. A., San-Blas, G., Bagagli, E., … Taylor, J. W. (2006). Cryptic speciation and recombination in the fungus Paracoccidioides brasiliensis as revealed by gene genealogies. *Molecular Biology and Evolution*, *23*(1), 65–73. https://doi.org/10.1093/molbev/msj008

MB, G., & PJ., S. (1993). Shigella subversion of the cellular cytoskeleton: a strategy for epithelial colonization. *Infect Immun*, *61*(12), 4941–4946.

McEwen JG, Bedoya V, Patiño MM, Salazar ME, R. A. (1987). Experimental murine paracoccidiodomycosis induced by the inhalation of conidia. *J Med Vet Mycol.*, *25*(3), 165–75.

Medoff, G., Painter, A., & Kobayashi, G. S. (1987). Mycelial- to Yeast-phase transitions of the dimorphic fungi Blastomyces dermatitidis and Paracoccidioides brasiliensis. *Journal of Bacteriology*, *169*(9), 4055–4060. https://doi.org/10.1128/jb.169.9.4055-4060.1987

Mendes-Giannini MJ, Hanna SA, da Silva JL, Andreotti PF, Vincenzi LR, Benard G, Lenzi HL, S. C. (2004). Invasion of epithelial mammalian cells by Paracoccidioides brasiliensis leads to cytoskeletal rearrangement and apoptosis of the host cell. *Microb Infect.*, *6*, 882–891. https://doi.org/10.1016/j.micinf.2004.05.005

Mendes-Giannini MJ, Monteiro da Silva JL, de Fátima da Silva J, Donofrio FC, Miranda ET, Andreotti PF, S. C. (2008). Interactions of Paracoccidioides brasiliensis with host cells : recent advances. *Mycopathologia.*, 237–248. https://doi.org/10.1007/s11046-007-9074-z

Mendes-Giannini MJ, Soares CP, da Silva JL, A. P. (2005). Interaction of pathogenic fungi with host cells : Molecular and cellular approaches. *FEMS Immunol Med Microbiol*, *45*, 383–394. https://doi.org/10.1016/j.femsim.2005.05.014

Mendes-Giannini MJ, Taylor ML, Bouchara JB, Burger E, Calich VL, Escalante ED,

Hanna SA, Lenzi HL, Machado MP, Miyaji M, Monteiro Da Silva JL, Mota EM, Restrepo A, Restrepo S, Tronchin G, Vincenzi LR, Xidieh CF, Zenteno E.Mendes-Giannini MJ1, Taylor ML, B, Z. E. (2000). Pathogenesis II : Fungal responses to host responses : interaction of host cells with fungi. *Med Mycol.*, *38*(1), 113–123.

Mendes, R. P., Cavalcante, R. de S., Marques, S. A., Marques, M. E. A., Venturini, J., Sylvestre, T. F., … Levorato, A. D. (2017). *Paracoccidioidomycosis: Current Perspectives from Brazil*. *The Open Microbiology Journal* (Vol. 11). https://doi.org/10.2174/1874285801711010224

Molinari-Madlum EE1, Felipe MS, S. C. (1999). Virulence of Paracoccidioides brasiliensis isolates can be correlated to groups defined by random amplified polymorphic DNA analysis. *Med Mycol.*, *37*(4), 269–276.

Montenegro MR, F. M. (1994). Paracoccidioidomycosis. *Pathology*, 131–150.

Moreira SF, Bailão AM, Barbosa MS, Jesuino RS, Felipe MS, Pereira M, de A. S. C. (2004). Monofunctional catalase P of Paracoccidioides brasiliensis : identification , characterization , molecular. *Yeast*, *21*(2), 173–182. https://doi.org/10.1002/yea.1077

Muñoz, J. F., Farrer, R. A., Desjardins, C. A., Gallo, J. E., Sykes, S., Sakthikumar, S., … Cuomo, C. A. (2016). Genome Diversity, Recombination, and Virulence across the Major Lineages of *Paracoccidioides*. *MSphere*, *1*(5), e00213-16. https://doi.org/10.1128/mSphere.00213-16

Nemecek, J. C. (2006). Global Control of Dimorphism and Virulence in Fungi. *Science*, *312*(5773), 583–588. https://doi.org/10.1126/science.1124105

Nilma Maciel GarciaI; Gilda Maria Barbaro Del NegroI; Elisabeth Maria Heins-VaccariI; Natalina Takahashi de MeloI; Cezar Mendes de. (1993). Paracoccidioides brasiliensis, nova amostra isolada de fezes de um pinguim (Pygoscelis adeliae). *Rev. Inst. Med. Trop. S. Paulo*, *35*(3). https://doi.org/http://dx.doi.org/10.1590/S0036-46651993000300003

Nogueira, S. V., Fonseca, F. L., Rodrigues, M. L., Mundodi, V., Abi-Chacra, E. A., Winters, M. S., … De Almeida Soares, C. M. (2010). Paracoccidioides brasiliensis enolase is a surface protein that binds plasminogen and mediates interaction of yeast forms with host cells. *Infection and Immunity*, *78*(9), 4040–4050. https://doi.org/10.1128/IAI.00221-10

Nunes, L. R., Costa de Oliveira, R., Leite, D. B., da Silva, V. S., dos Reis Marques, E., da Silva Ferreira, M. E., … Goldman, G. H. (2005). Transcriptome analysis of Paracoccidioides brasiliensis cells undergoing mycelium-to-yeast transition. *Eukaryotic Cell*, *4*(12), 2115–2128. https://doi.org/10.1128/EC.4.12.2115-2128.2005

Nunes, L. R., Oliveira, R. C. De, Batista, D., Schmidt, V., Marques, R., Eliana, M., … Goldman, G. H. (2005). Transcriptome Analysis of Paracoccidioides brasiliensis Cells Undergoing Mycelium-to-Yeast Transition Transcriptome Analysis of Paracoccidioides brasiliensis Cells Undergoing Mycelium-to-Yeast Transition. *Eukaryotic Cell*, *4*(12), 2115–2128. https://doi.org/10.1128/EC.4.12.2115

Olsen, J. V., Blagoev, B., Gnad, F., Macek, B., Kumar, C., Mortensen, P., & Mann, M. (2006). Global, In Vivo, and Site-Specific Phosphorylation Dynamics in Signaling Networks. *Cell*, *127*(3), 635–648. https://doi.org/10.1016/j.cell.2006.09.026

Olsen, J. V, Macek, B., Lange, O., Makarov, A., Horning, S., & Mann, M. (2007). Higher-energy C-trap dissociation for peptide modification analysis. *Nature Methods*, *4*(9), 709–712. https://doi.org/10.1038/nmeth1060

Parente-Rocha, J. A., Parente, A. F. A., Baeza, L. C., Bonfim, S. M. R. C., Hernandez, O., McEwen, J. G., … De Almeida Soares, C. M. (2015). Macrophage interaction

with *Paracoccidioides brasiliensis* yeast cells modulates fungal metabolism and generates a response to oxidative stress. *PLoS ONE*, *10*(9), 1–18. https://doi.org/10.1371/journal.pone.0137619

Park, S.-H., Kim, J.-W., Yun, S.-H., Leem, S. H., Kahng, H.-Y., & Kim, S. Il. (2006). Characterization of beta-ketoadipate pathway from multi-drug resistance bacterium, Acinetobacter baumannii DU202 by proteomic approach. *Journal of Microbiology (Seoul, Korea)*, *44*(6), 632–640. Retrieved from http://www.ncbi.nlm.nih.gov/pubmed/17205041

Pasricha, S., MacRae, J. I., Chua, H. H., Chambers, J., Boyce, K. J., McConville, M. J., & Andrianopoulos, A. (2017). Extensive Metabolic Remodeling Differentiates Non-pathogenic and Pathogenic Growth Forms of the Dimorphic Pathogen Talaromyces marneffei. *Frontiers in Cellular and Infection Microbiology*, *7*(August), 1–12. https://doi.org/10.3389/fcimb.2017.00368

Porath, J., Carlsson, J., Olsson, I., & Belfrage, G. (1975). Metal chelate affinity chromatography, a new approach to protein fractionation. *Nature*, *258*(5536), 598–599. https://doi.org/10.1038/258598a0

Posewitz, M. C., & Tempst, P. (1999). Immobilized Gallium (III) Affinity Chromatography of Phosphopeptides peptides , as a front end to mass spectrometric analysis , the use of an immobilized metal affinity chromatography. *Biosystems*, *71*(14), 29520–29529. https://doi.org/10.1021/ac981409y

Prado, M., da Silva, M. B., Laurenti, R., Travassos, L. R., & Taborda, C. P. (2009). Mortality due to systemic mycoses as a primary cause of death or in association with AIDS in Brazil: A review from 1996 to 2006. *Memorias Do Instituto Oswaldo Cruz*, *104*(3), 513–521. https://doi.org/10.1590/S0074-02762009000300019

Puttick, J., Baker, E. N., & Delbaere, L. T. J. (2008). Histidine phosphorylation in biological systems. *Biochimica et Biophysica Acta*, *1784*(1), 100–105. https://doi.org/10.1016/j.bbapap.2007.07.008

Ramsubramaniam, N., Harris, S. D., & Marten, M. R. (2014). The phosphoproteome of Aspergillus nidulans reveals functional association with cellular processes involved in morphology and secretion. *Proteomics*, *14*(21–22), 2454–2459. https://doi.org/10.1002/pmic.201400063

Rappleye, C. A., & Goldman, W. E. (2006). Defining virulence genes in the dimorphic fungi. *Annual Review of Microbiology*, *60*(1), 281–303. https://doi.org/10.1146/annurev.micro.59.030804.121055

Reinders, J., & Sickmann, A. (2005). State-of-the-art in phosphoproteomics. *Proteomics*, *5*(16), 4052–4061. https://doi.org/10.1002/pmic.200401289

Restrepo, a, McEwen, J. G., & Castañeda, E. (2001). The habitat of Paracoccidioides brasiliensis: how far from solving the riddle? *Medical Mycology : Official Publication of the International Society for Human and Animal Mycology*, *39*(3), 233–241. https://doi.org/10.1080/714031028

Rezende, T. C. V, Borges, C. L., Magalhães, A. D., de Sousa, M. V., Ricart, C. A. O., Bailão, A. M., & Soares, C. M. A. (2011). A quantitative view of the morphological phases of Paracoccidioides brasiliensis using proteomics. *Journal of Proteomics*, *75*(2), 572–587. https://doi.org/10.1016/j.jprot.2011.08.020

Ricci G1, Mota FT, Wakamatsu A, Serafim RC, Borra RC, F. M. (2004). Canine paracoccidioidomycosis. *Med Mycol.*, *42*(4), 379–383.

Riquelme, M. (2013). Tip growth in filamentous fungi: a road trip to the apex. *Annual Review of Microbiology*, *67*(June), 587–609. https://doi.org/10.1146/annurev-micro-092412-155652

Rooney, P. J., & Klein, B. S. (2002). Linking fungal morphogenesis with virulence. *Cellular Microbiology*, *4*(3), 127–137.

Rosenshine, I., Duronio, V., & Finlay, B. B. (1992). Tyrosine Protein Kinase Inhibitors Block Invasin-Promoted Bacterial Uptake by Epithelial Cells. *Infect Immun.*, (June), 2211–2217.

RP., M. (1994). The gamut of clinical manifestations. *Boca Raton: CRC Press*, 233–258.

S, B., & Pina A, Felonato M, Costa TA, Frank de Araújo E, Feriotti C, Bazan SB, Keller AC, Leite KR, C. V. (2013). TNF-α and CD8+ T cells mediate the beneficial effects of nitric oxide synthase-2 deficiency in pulmonary paracoccidioidomycosis. *PLoS Negl Trop Dis.*, *7*(8).

SA, C., & Peraçoli MT, Mendes RP, Marcondes-Machado J, Fecchio D, Marques SA, S. A. (2003). Effect of cytokines on the in vitro fungicidal activity of monocytes from paracoccidioidomycosis patients. *Microbes Infect.*, *5*(2), 107–113.

Salgado-Salazar, C., Jones, L. R., Restrepo, Á., & McEwen, J. G. (2010). The human fungal pathogen Paracoccidioides brasiliensis (Onygenales: Ajellomycetaceae) is a complex of two species: phylogenetic evidence from five mitochondrial markers. *Cladistics*, *26*(6), 613–624. https://doi.org/10.1111/j.1096-0031.2010.00307.x

San-Blas, G. (1982). The cell wall of fungal human pathogens: its possible role in host-parasite relationships. *Mycopathologia*, *79*(3), 159–184. Retrieved from http://www.ncbi.nlm.nih.gov/pubmed/6755258

San-Blas, G., & Niño-Vega, G. (2008). Paracoccidioides brasiliensis: Chemical and molecular tools for research on cell walls, antifungals, diagnosis, taxonomy. *Mycopathologia*, *165*(4–5), 183–195. https://doi.org/10.1007/s11046-007-9040-9

San-Blas, G., & San-Blas, F. (1977). *Paracoccidioides brasiliensis*: cell wall structure and virulence. A review. *Mycopathologia*, *62*(2), 77–86. Retrieved from http://www.ncbi.nlm.nih.gov/pubmed/340954

Santana, Lidiane Aparecida da Penha, M. H. V., Tomazett, P. K., Santo-silva, L. K., Góes, A. M., Schrank, A., & Célia Maria de Almeida Soares, M. P. (2012). Distinct chitinases are expressed during various growth phases of the human pathogen Paracoccidioides brasiliensis. *Mem Inst Oswaldo Cruz*, *107*(3), 310–316.

Santos, W. A. dos, Silva, B. M. da, Passos, E. D., Zandonade, E., & Falqueto, A. (2003). Association between smoking and paracoccidioidomycosis: a case-control study in the State of Espírito Santo, Brazil. *Caderno Saúde Pública*, *19*(1), 245–253.

Schneiter, R., Carter, A. T., Hernando, Y., Zellnig, G., Schweizer, L. M., & Schweizer, M. (2000). The importance of the five phosphoribosyl-pyrophosphate synthetase (Prs) gene products of Saccharomyces cerevisiae in the maintenance of cell integrity and the subcellular localization of Prs1p. *Microbiology*, *146*(12), 3269–3278. https://doi.org/10.1099/00221287-146-12-3269

Schwartz, D., & Gygi, S. P. (2005). An iterative statistical approach to the identification of protein phosphorylation motifs from large-scale data sets. *Nature Biotechnology*, *23*(11), 1391–1398. https://doi.org/10.1038/nbt1146

Selvan, L. D. N., Renuse, S., Kaviyil, J. E., Sharma, J., Pinto, S. M., Yelamanchi, S. D., … Harsha, H. C. (2014). Phosphoproteome of Cryptococcus neoformans. *Journal of Proteomics*, *97*, 287–295. https://doi.org/10.1016/j.jprot.2013.06.029

Shankar, J., Restrepo, A., Clemons, K. V., & Stevens, D. A. (2011). Hormones and the resistance of women to paracoccidioidomycosis. *Clinical Microbiology Reviews*, *24*(2), 296–313. https://doi.org/10.1128/CMR.00062-10

Shikanai-yasuda, M. A., Mendes, R. P., Colombo, A. L., Queiroz-telles, F. De, Satie,

A., Kono, G., … Bagagli, E. (2017). Consensus Brazilian guidelines for the clinical management of paracoccidioidomycosis. *Rev Soc Bras Med Trop*, *50*(June), 715–740. https://doi.org/10.1590/0037-8682-0230-2017

Shikanai-Yasuda, M. A., Telles Filho, F. de Q., Mendes, R. P., Colombo, A. L., & Moretti, M. L. (2006). [Guidelines in paracoccidioidomycosis]. *Revista Da Sociedade Brasileira de Medicina Tropical*, *39*(3), 297–310. https://doi.org/10.1590/S0037-86822006000300017

Silva, S. S., Paes, H. C., Soares, C. M. A., Fernandes, L., & Felipe, M. S. S. (2008). Insights into the pathobiology of Paracoccidioides brasiliensis from transcriptome analysis - Advances and perspectives. *Mycopathologia*, *165*(4–5), 249–258. https://doi.org/10.1007/s11046-007-9071-2

Simões, L. B., Marques, S. A., & Bagagli, E. (2004). Distribution of paracoccidioidomycosis: Determination of ecologic correlates through spatial analyses. *Medical Mycology*, *42*(6), 517–523. https://doi.org/10.1080/13693780310001656795

SJ, O., & Mamoni RL, Musatti CC, Papaiordanou PM, B. M. (2002). Cytokines and lymphocyte proliferation in juvenile and adult forms of paracoccidioidomycosis: comparison with infected and non-infected controls. *Microbes Infect.*, *4*(2), 139–144.

Smith, J. A., & Kauffman, C. A. (2012). Pulmonary fungal infections. *Respirology*, *17*(6), 913–926. https://doi.org/10.1111/j.1440-1843.2012.02150.x

Su, H.-C., Hutchison, C. A., Giddings, M. C., Hutchison III, C. A., Giddings, M. C., Hutchison, C. A., … Hutchison III, C. A. (2007). Mapping phosphoproteins in Mycoplasma genitalium and Mycoplasma pneumoniae. *BMC Microbiology*, *7*(1), 63. https://doi.org/10.1186/1471-2180-7-63

Su, Z., Li, H., Li, Y., & Ni, F. (2007). Inhibition of the Pathogenically Related Morphologic Transition in Candida albicans by Disrupting Cdc42 Binding to Its Effectors. *Chemistry and Biology*, *14*(11), 1273–1282. https://doi.org/10.1016/j.chembiol.2007.10.008

Tavares, A. H. F. P., Silva, S. S., Dantas, A., Campos, E. G., Andrade, R. V., Maranhão, A. Q., … Felipe, M. S. S. (2007). Early transcriptional response of Paracoccidioides brasiliensis upon internalization by murine macrophages. *Microbes and Infection*, *9*(5), 583–590. https://doi.org/10.1016/j.micinf.2007.01.024

Tavares, A. H., Fernandes, L., Bocca, A. L., Silva-Pereira, I., & Felipe, M. S. (2015). Transcriptomic reprogramming of genus Paracoccidioides in dimorphism and host niches. *Fungal Genetics and Biology*, *81*, 98–109. https://doi.org/10.1016/j.fgb.2014.01.008

Tavares, A. H., Silva, S. S., Bernardes, V. V., Maranhão, A. Q., Kyaw, C. M., Poças-Fonseca, M., & Silva-Pereira, I. (2005). Virulence insights from the Paracoccidioides brasiliensis transcriptome. *Genetics and Molecular Research : GMR*, *4*(2), 372–389. https://doi.org/Pb11 [pii]

Taylor, J. W., Jacobson, D. J., Kroken, S., Kasuga, T., Geiser, D. M., Hibbett, D. S., & Fisher, M. C. (2000). Phylogenetic species recognition and species concepts in fungi. *Fungal Genetics and Biology : FG & B*, *31*(1), 21–32. https://doi.org/10.1006/fgbi.2000.1228

Team, R. C. (2018). R: A language and environment for statistical computing. R Foundation for Statistical Computing, Vienna, Austria.

Teixeira, M. D. M., Theodoro, R. C., Oliveira, F. F. M. De, Machado, G. C., Hahn, R. C., Bagagli, E., … Felipe, M. S. S. (2013). *Paracoccidioides lutzii* sp. nov.:

biological and clinical implications. *Medical Mycology*, (June 2013), 1–10. https://doi.org/10.3109/13693786.2013.794311

Teixeira, M. M., Theodoro, R. C., de Carvalho, M. J. A., Fernandes, L., Paes, H. C., Hahn, R. C., … Felipe, M. S. S. (2009). Phylogenetic analysis reveals a high level of speciation in the Paracoccidioides genus. *Molecular Phylogenetics and Evolution*, *52*(2), 273–283. https://doi.org/10.1016/j.ympev.2009.04.005

Teixeira, M. M., Theodoro, R. C., Nino-Vega, G., Bagagli, E., & Felipe, M. S. S. (2014). Paracoccidioides species complex: ecology, phylogeny, sexual reproduction, and virulence. *PLoS Pathogens*, *10*(10), e1004397. https://doi.org/10.1371/journal.ppat.1004397

Terçarioli, G. R., Bagagli, E., Reis, G. M., Theodoro, R. C., Bosco, S. D. M. G., Macoris, S. A. da G., & Richini-Pereira, V. B. (2007). Ecological study of Paracoccidioides brasiliensis in soil: growth ability, conidia production and molecular detection. *BMC Microbiology*, *7*(1), 92. https://doi.org/10.1186/1471-2180-7-92

Theodoro, R. C., De Moraes Gimenes Bosco, S., Araújo, J. P., Candeias, J. M. G., Da Graça Macoris, S. A., Trinca, L. A., & Bagagli, E. (2008). Dimorphism, thermal tolerance, virulence and heat shock protein 70 transcription in different isolates of Paracoccidioides brasiliensis. *Mycopathologia*, *165*(6), 355–365. https://doi.org/10.1007/s11046-008-9091-6

Theodoro, R. C., Teixeira, M. de M., Felipe, M. S. S., Paduan, K. dos S., Ribolla, P. M., San-Blas, G., & Bagagli, E. (2012). Genus Paracoccidioides: Species recognition and biogeographic aspects. *PLoS ONE*, *7*(5). https://doi.org/10.1371/journal.pone.0037694

Theodoro RC, Candeias JM, Araújo JP Jr, Bosco Sde M, Macoris SA, Padula LO, Franco M, B. E. (2005). Molecular detection of Paracoccidioides brasiliensis in soil. *Med Mycol.*, *43*(8), 725–729.

Thewes, S., Kretschmar, M., Park, H., Schaller, M., Filler, S. G., & Hube, B. (2007). In vivo and ex vivo comparative transcriptional profiling of invasive and non-invasive Candida albicans isolates identifies genes associated with tissue invasion. *Molecular Microbiology*, *63*(6), 1606–1628. https://doi.org/10.1111/j.1365-2958.2007.05614.x

Thingholm, T. E., Jensen, O. N., & Larsen, M. R. (2009). Analytical strategies for phosphoproteomics. *Proteomics*, *9*(6), 1451–1468. https://doi.org/10.1002/pmic.200800454

Tobón, a M., Agudelo, C. a, Osorio, M. L., Alvarez, D. L., Arango, M., Cano, L. E., & Restrepo, a. (2003). Residual pulmonary abnormalities in adult patients with chronic paracoccidioidomycosis: prolonged follow-up after itraconazole therapy. *Clinical Infectious Diseases : An Official Publication of the Infectious Diseases Society of America*, *37*(7), 898–904. https://doi.org/10.1086/377538

Tuder RM, el Ibrahim R, Godoy CE, D. B. T. (1985). Pathology of the human pulmonary paracoccidioidomycosis. *Mycopathologia.*, *92*(3), 179–188.

Turissini, D. A., Gomez, O. M., Teixeira, M. M., McEwen, J. G., & Matute, D. R. (2017). Species boundaries in the human pathogen Paracoccidioides. *Fungal Genetics and Biology*, *106*(April), 9–25. https://doi.org/10.1016/j.fgb.2017.05.007

Valle ACF, Aprigliano FF, Moreira JS, W. B. (1995). Clinical and endoscopic findings in the mucosae of the upper respiratory and digestive tracts in post-treatment follow-up of paracoccidioidomycosis patients. *Rev Inst Med Trop São Paulo.*, *37*(5), 407–413.

VandenBerg, A. L., Ibrahim, A. S., Edwards, J. E., Toenjes, K. A., & Johnson, D. I.

(2004). Cdc42p GTPase regulates the budded-to-hyphal-form transition and expression of hypha-specific transcripts in Candida albicans. *Eukaryotic Cell*, *3*(3), 724–734. https://doi.org/10.1128/EC.3.3.724-734.2004

Vieira Gde D, & Alves Tda C, Lima SM, Camargo LM, S. C. (2014). Paracoccidioidomycosis in a western Brazilian Amazon State: clinical-epidemiologic profile and spatial distribution of the disease. *Rev Soc Bras Med Trop.*, *47*(1), 63–68.

Vieira Gde D, Alves Tda C, Lima SM, Camargo LM, S. C., Vieira, G. de D., Alves, T. da C., Lima, S. M. D. de, Camargo, L. M. A., & Sousa, C. M. de. (2014). Paracoccidioidomycosis in a western Brazilian Amazon State: clinical-epidemiologic profile and spatial distribution of the disease. *Rev Soc Bras Med Trop.*, *47*(1), 63–68. https://doi.org/10.1590/0037-8682-0225-2013

Villar LA, Salazar ME, R. A. (1988). Morphological study of a variant of Paracoccidioides brasiliensis that exists in the yeast form at room temperature. *J Med Vet Mycol.*, *26*(5), 269–276.

Voltan, A. R., Cassia, J. D. E., Sardi, O., Soares, C. P., Machado, M. P., Marisa, A. N. A., … Mendes-giannini, M. J. O. S. É. S. (2013). Early Endosome Antigen 1 (EEA1) decreases in macrophages infected with Paracoccidioides brasiliensis. *Med Mycol .*, *1*(October 2013), 759–764. https://doi.org/10.3109/13693786.2013.777859

Wheeler, R. T., & Diana Kombe, Sudeep D. Agarwala, G. R. F. (2008). Dynamic, Morphotype-Specific Candida albicans β-Glucan Exposure during Infection and Drug Treatment. *PLoS Pathog.*, *4*(12).

Willger, S. D., Liu, Z., Olarte, R. A., Adamo, M. E., Stajich, J. E., Myers, L. C., … Hogan, D. A. (2015). Analysis of the Candida albicans phosphoproteome. *Eukaryotic Cell*, *14*(5), 474–485. https://doi.org/10.1128/EC.00011-15

Wilson-Grady, J. T., Villén, J., & Gygi, S. P. (2008). Phosphoproteome Analysis of Fission Yeast. *Journal of Proteome Research*, *7*(3), 1088–1097. https://doi.org/10.1021/pr7006335

Xie, Z., Liu, S., Zhang, Y., & Wang, Z. (2004). Roles of Rad23 protein in yeast nucleotide excision repair. *Nucleic Acids Research*, *32*(20), 5981–5990. https://doi.org/10.1093/nar/gkh934

Xu, K.-P., & Yu, F.-S. X. (2007). Cross talk between c-Met and epidermal growth factor receptor during retinal pigment epithelial wound healing. *Investigative Ophthalmology & Visual Science*, *48*(5), 2242–2248. https://doi.org/10.1167/iovs.06-0560

Yamamoto, N., Bibby, K., Qian, J., Hospodsky, D., Rismani-yazdi, H., Nazaroff, W. W., & Peccia, J. (2012). Particle-size distributions and seasonal diversity of allergenic and pathogenic fungi in outdoor air. *The ISME Journal*, *6*(10), 1801–1811. https://doi.org/10.1038/ismej.2012.30

Zhang, Y. J., & Rubin, E. J. (2013). Feast or famine: The host-pathogen battle over amino acids. *Cellular Microbiology*, *15*(7), 1079–1087. https://doi.org/10.1111/cmi.12140

Zolnierowicz, S., & Bollen, M. (2000). Protein phosphorylation and protein phosphatasesDe Panne, Belgium, September 19–24, 1999. *The EMBO Journal*, *19*(4), 483–488. https://doi.org/10.1093/emboj/19.4.483

Anexo
Contribuição em artigo

Proteomic analysis of *Paracoccidioides brasiliensis* during infection of alveolar macrophages primed or not by interferon gamma

Edilânia G. A. Chaves[1], Lilian C. Baeza[1,2], **Danielle S. Araújo[1]**, Clayton L. Borges[1], Juliana A. Parente-Rocha[1], Milton A. P. de Oliveira[3], Célia M. A. Soares[1,*]

[1]Laboratório de Biologia Molecular, Instituto de Ciências Biológicas, Universidade Federal de Goiás, Goiânia, Brazil,

[2]Centro de Ciências Médicas e Farmacêuticas, Universidade Estadual do Oeste do Paraná, Cascavel, Brazil,

[3]Instituto de Patologia Tropical e Saúde Pública, Universidade Federal de Goiás, Goiânia, Brazil.

*Correspondence:
Célia M. de Almeida Soares
cmasoares@gmail.com

BBA - Proteins and Proteomics 1865 (2017) 1304–13 ll

Contents lists available ScienceDirec

BBA - Proteins and Proteomics

journal www.elsevier.com/locate/bbap

Employing proteomic analysis to compare Paracoccidioides lutzii yeast and mycelium cell wall proteins

Danielle Silva Araújo[a], Patrícia de Sousa Lima[a,b], Lilian Cristiane Baeza[a], Ana Flávia Alves Parente[c], Alexandre Melo Bailão[a], Clayton Luiz Borges[a], Célia Maria de Almeida Soares[a,*]

[a] Laboratório de Biologia Molecular, Instituto de Ciências Biológicas, ICB II, Campus II, Universidade Federal de Goiás, 74001-970 Goiânia, Goiás, Brazil [b] Laboratório Interdisciplinar de Biologia, Universidade Estadual de Goiás, Itapuranga, Goiás, Brazil

[c] Laboratório de Bioquímica e Química de Proteínas, Instituto de Biologia, Campus Universitário Darci Ribeiro, Brasília, DF, Brazil

ARTICLEINFO

Keywords:
Cell wall proteins
Paracoccidioides lutzii
Mycelia
Yeast cells
Proteomics
Paracoccidioidomycosis

ABSTRACT

Paracoccidioidomycosis is an important systemic mycosis caused by thermodimorphic fungi of the Paracoccidioides genus. During the infective process, the cell wall acts at the interface between the fungus and the host. In this way, the cell wall has a key role in growth, environment sensing and interaction, as well as morphogenesis of the fungus. Since the cell wall is absent in mammals, it may present molecules that are described as target sites for new antifungal drugs. Despite its importance, up to now few studies have been conducted employing proteomics in for the identification of cell wall proteins in Paracoccidioides spp. Here, a detailed proteomic approach, including cell wall-fractionation coupled to NanoUPLC-MS^E, was used to study and compare the cell wall fractions from Paracoccidioides lutzii mycelia and yeast cells. The analyzed samples consisted of cell wall proteins extracted by hot SDS followed by extraction by mild alkali. In summary, 512 proteins constituting different cell wall fractions were identified, including 7 predicted GPI-dependent cell wall proteins that are potentially involved in cell wall metabolism. Adhesins previously described in Paracoccidioides spp. such as enolase, glyceraldehyde-3-phosphate dehydrogenase were identified. Comparing the proteins in mycelium and yeast cells, we detected some that are common to both fungal phases, such as Ecm33, and some specific proteins, as glucanase Crf1. All of those proteins were described in the metabolism of cell wall. Our study provides an important elucidation of cell wall composition of fractions in Paracoccidioides, opening a way to understand the fungus cell wall architecture.

1. Introduction

During their life cycle, fungi have developed strategies to cope with environmental conditions such as changes in temperature and osmotic stress. Additionally they must subvert microbicide conditions they face when coming into contact with a host [1]. The cell wall is a key structure used by fungi to provide a protective barrier against adverse conditions imposed upon it, both environmentally and by host cells. During infection, the cell wall contributes directly to the host-parasite relationship, establishing initial contact between the fungus and the host cells. Processes such as adhesion, immune response, nutrient acquisition, virulence, host tissue damage, and morphogenesis give the cell wall relevance during the fungus' battle to establish disease in the host [2,3].

Although the composition of the cell wall varies between species of

fungi, it is basically composed of polysaccharides that include chitin and glucan, and a set of different proteins, often covered with carbohydrates and lipids [4–7]. Proteomic analyses of cell wall proteins of Candida albicans have categorized those molecules in four groups or fractions based on their linkage to cell wall components [8]. The first fraction contains proteins loosely associated by non-covalent and disulfide bounds with cell wall structure. These proteins are removed from the cell wall by treatment with denaturing and reducing agents at high temperature [9]. Proteins linked to the O-glycosyl side chains of β-1,3glucan (such as Pir proteins) or by other covalent alkaline sensitive linkage compose the second fraction and are obtained upon mild alkaline treatment [10]. Fraction three is obtained by removing the β-1,3glucan layer of the cell wall, which releases mannoproteins indirectly attached to β-1,3-glucan, via β-1,6-glucan, by a GPI anchor and other molecules anchored to β-1,3-glucan. This is achieved by cell wall treatment with glucanases. Finally, fraction four contains proteins attached to chitin by a glucanase resistant linkage and are extracted by exochitinase digestion [11,12]. Alternatively, the isolation of GPI-anchored proteins can be obtained by treating the cell wall with HFpyridine or trifluoromethanesulfonic acid (TMFS) [10,13,14].

The Paracoccidioides genus is composed of Paracoccidioides brasiliensis and Paracoccidioides lutzii species, which cause Paracoccidioidomycosis (PCM), a chronic granulomatous disease endemic in Latin America, [15–18]. Infection occurs by inhalation of infective propagules produced by mycelia in the soil that, upon reaching the lungs, differentiate into yeast cells due to the increase of body temperature (36–37 °C) [19].

Structurally, the cell wall of Paracoccidioides spp. is arranged in layers. Electron microscopy studies demonstrated that the mycelium cell wall has a layer with 80 to 150 nm thick, which consists of a microfibrillar network of β-1,3-glucan and in lesser amounts β-1,6-glucan that interconnect to chitin molecules located internally in the cell wall. In the yeast form, the cell wall has three layers 200 to 600 nm thick; two electron-dense zones and one electron-light zone alternating. The inner layer is formed by chitin and β-glucan and the outer layer by αglucan. Proteins are also found in both mycelium and yeast cell walls interconnected in the polysaccharides network [2,20,21].

The repertoire of proteins that constitute the cell wall have low solubility, hydrophobic nature, and are highly glycosylated [10]. Another important aspect that should be highlighted is the fact that proteins of the cell wall are synthesized and adjusted according to the growing conditions, environmental factors and developmental stage [22–24]. All these factors together, determine that the identification of these proteins can be complex.

Nevertheless, the total number and functions of cell wall proteins are still poorly understood in the genus Paracoccidioides. Published work has focused on the identification of mycelium and yeast proteins of two

* Corresponding author at: Laboratório de Biologia Molecular, Instituto de Ciências Biológicas II, Campus Samambaia, Universidade Federal de Goiás, 74690-900 Goiânia, Goiás, Brazil. E-mail address: celia@icb.ufg.br (C.M. de Almeida Soares).

http://dx.doi.org/10.1016/j.bbapap.2017.08.016
Received 25 January 2017; Received in revised form 17 August 2017; Accepted 21 August 2017 Available online 24 August 2017

isolates of P. brasiliensis [25]. The authors identified cell wall associated proteins, extractable with DTT, specific to morphological phases, as well as sequences exclusive to the isolates. A proteomic approach using NanoUPLC-MS^E was used to map the cell wall proteins in another species, P. lutzii, Pb01. To extract proteins bound to the cell wall by non-covalent or disulfide bonds, SDS and reducing agents were used. Proteins bound by alkali-labile bonds were obtained by NaOH extraction. This work allowed the identification of proteins from Pb01 cell wall in both mycelium and yeast phases. By using subcellular fractionation and NanoUPLC-MS^E we identified proteins present in cell wall that belong to several functional categories. Some of those proteins have been previously characterized in the cell wall of Paracoccidioides sp., playing important roles in cell wall biogenesis and organization as well as in virulence, adhesion, colonization, survival in hostile environments and evasion of the immune system thereby, allowing the establishment of the disease [26–32]. Results demonstrated that in addition to expected proteins containing signals for secretion, other proteins previously identified only in the cytosol or cell organelles are present in the cell wall extracts. By comparing proteins detected in mycelium and yeast cells, some are present in the cell wall fractions of both, including proteins related to cellular transport, cell rescue and biogenesis of components. Proteins were identified in just one fungus phase, that could reflect differential gene expression. These data in conjunction with previously published data can provide an integrated view of the cell wall in the genus Paracoccidioides. 2. Material and methods

2.1. Paracoccidioides strains and growth conditions

Paracoccidioides lutzii isolate Pb01 (ATCC MYA-826), was used in all experiments of this work. The fungus was cultivated in Fava Netto's solid medium containing 1% (w/v) peptone, 0.5% (w/v) yeast extract,

0.3% (w/v) protease peptone, 0.5% (w/v) beef extract, 0.5% (w/v) NaCl, 4% (w/v) glucose and 1% (w/v) agar, pH 7.2 at 36 °C and 22 °C for 7 and 15 days, for yeast cells and mycelia respectively. The yeast cells and mycelia were inoculated in Fava Netto's liquid medium for performing experiments as detailed below.

2.2. Isolation and purification of cell wall proteins (CWP) of P. lutzii

The protocol used for CWP extraction was based on literature data for C. albicans with some modifications [10]. Briefly, a total of 30 g of cells in 1800 mL of Fava Netto's liquid medium was incubated at 36 °C and 22 °C for 72 h (early-log phase growth). The cells were collected by centrifugation at 1200 ×g for 10 min, and washed 5 times with 40 mL of lysis buffer (10 mM Tris-HCl, 2 mM $CaCl_2$, pH 8.5, 1 mM PMSF). The cells were resuspended in 5 mL of 10 mM Tris-HCl, pH 8.0 with 1 mM PMSF and liquid nitrogen was added to the samples to keep the cells frozen. The cells were disrupted by maceration with mortar and pestle in the presence of liquid nitrogen until a very fine powder was obtained. The fine powder was resuspended in ice-cold lysis buffer then disrupted using glass beads and a beater apparatus (BioSepc, Oklahoma, USA) in 5 cycles of 30 s while on ice. This procedure was carried out, until complete disruption of the fungal cells, which was after verified by microscopy. After, the cells disruption a total of 8 g prepared from the cell wall was obtained. To reduce putative cytoplasmic contaminant proteins, the cell wall fraction was washed five times with 40 mL of icecold water and another five times with 40 mL each of the following icecold solutions: 5% (w/v) NaCl, 2% (w/v) NaCl, 1% (w/v) NaCl with 1 mM PMSF. The cell wall proteins were extracted by boiling with SDS extraction buffer [50 mM Tris-HCl, pH 7. 8, 100 mM EDTA, 2% (w/v) SDS, 10 mM DTT] for 10 min with 5 mL of extraction buffer added for each wet gram of cell walls. The material was centrifuged at 1200 ×g for 10 min and this step was performed twice. The supernatant constitutes the first fraction termed fraction 1 (F1). F1 was washed five times in 20 mL of ultrapure water and 50 mM ammonium bicarbonate, pH 8.5 by centrifugation using a 10-kDa molecular weight cut off in ultracel regenerated membrane (Amicon Ultra centrifugal filter, Millipore, Bedford, MA, USA). Subsequently, the material was concentrated to a final volume of 1 mL. To obtain alkaline sensitive proteins (Fraction 2- F2), the pellet from F1 was subjected to alkaline treatment. The pellet was subjected to washing steps with 40 mL each as follows: five times with ice-cold water and then further 10 further times with icecold 0.1 M sodium acetate, pH 5.5, 1 mM PMSF. This fraction was extracted with 30 mM NaOH overnight at 4

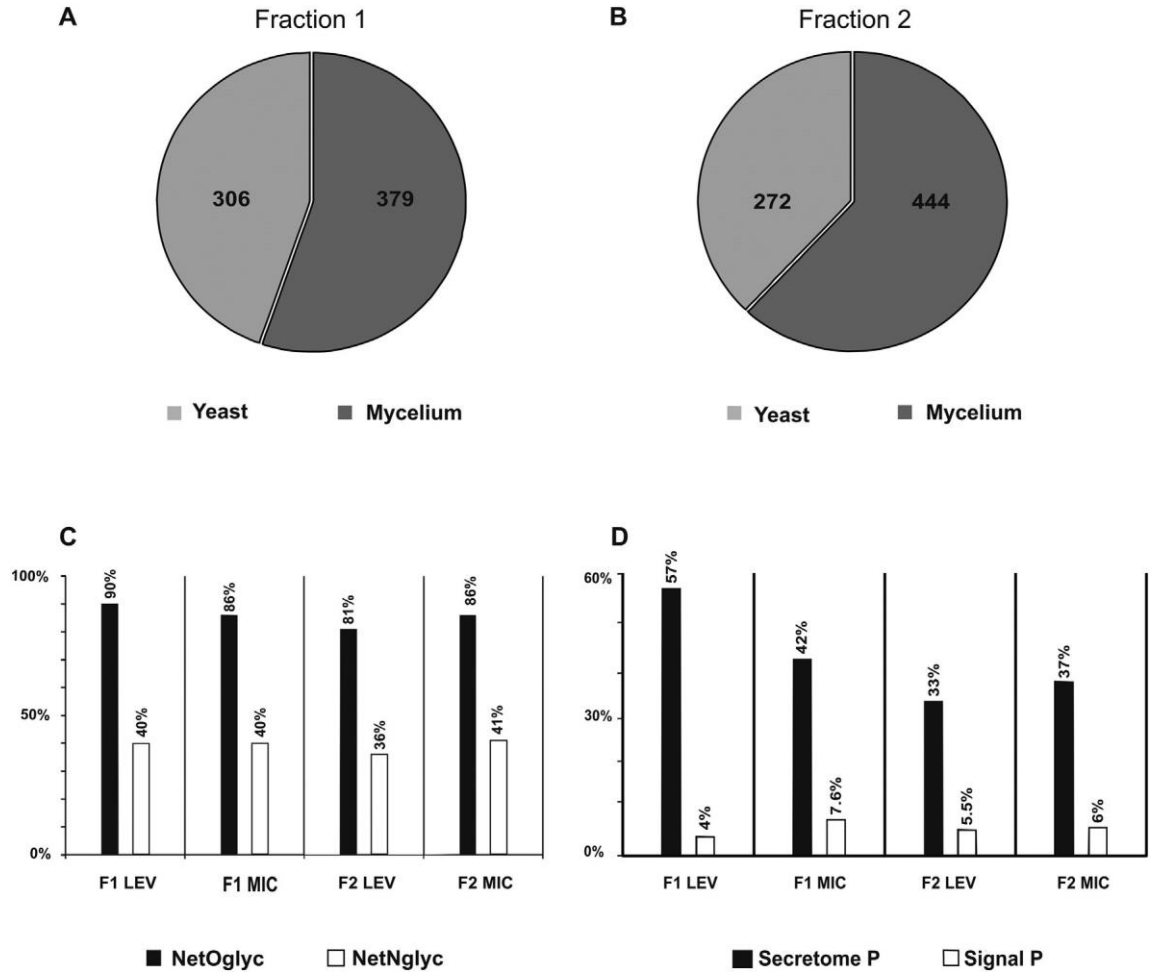

Fig. 1. Proteins in fractions 1 and 2, of yeast cells and mycelium. (A), (B) Total of identified proteins in yeast (diagrams in light gray) and mycelium (diagrams in dark gray) in the cell wall fractions 1 (F1) and 2 (F2), also including those proteins negative for secretion pathways (classical or not). (C) Potential glycosylation sites using the programs NetNGlyc or NetOGlyc. (D) Predicting secretion in accordance to the SignalP and SecretomeP programs.

°C; we added 4 mL of extraction solution NaOH for each wet gram of cell wall. Subsequently protein glycosylation was removed using the recombinant enzyme Nglycosidase F (Roche Applied Science). A total of 3 units of the enzyme was added to 300 μg of F2 fractions in solution [125 mM sodium phosphate, 25 mM EDTA, 1% nonidet P40 (w/v), 1% β-mercaptoethanol (v/v), 1% SDS (w/v)]. The mixture was incubated at 37 °C for 16 h and the reaction was quenched by boiling the mixture for 5 min. The sample was washed in the following sequence: 3 times with 20 mL of ultrapure water; once with 50 mM NH4HCO3 ammonium bicarbonate, pH 8.5. Both protein extracts (F1 and F2) were quantified using the Bradford method [33]. The concentration of proteins obtained for both yeast and mycelia of F1 was about 0.8 μg/μL, and for F2, yeast and mycelia it was about 0.6 μg/μL. Samples were obtained in biological triplicates. More details are depicted in Supplementary Fig. 1.

2.3. Tryptic digestion and sample preparation for analysis by NanoLC-MS/MS

Protein extracts were concentrated to a final volume of 50 μL and subjected to digestion with trypsin [34,35]. To 300 μg of protein extract, 150 μL of RapiGEST™ 0.2% (v/v) (Waters, USA) was added and the sample was vortexed and incubated at 80 °C for 15 min. Later, a reduction stage was carried out by addition of 5 μL of 100 mM dithiothreitol (DTT) and samples were incubated at 60 °C for 30 min. After,

5 μL of a 300 mM iodoacetamide solution was added, and samples were incubated in the dark at room temperature for 30 min. Then, 60 μL of trypsin

(Promega, Madison, WI, USA), prepared with 50 mM ammonium bicarbonate to 50 ng/μL, was added. The sample was digested at 37 °C for 16 h. RapiGEST™ precipitation was performed by adding 60 μL of a 5% (v/v) trifluoroacetic acid (TFA) solution, followed by incubation at 37 °C for 90 min. The samples were centrifuged at 13,000 ×g at 6 °C for 30 min. The supernatant was dried in a vacuum concentrator.

2.4. Data acquisition by NanoUPLC-MS^E

To allow quantification of peptides, Rabbit Phosphorylase B (Waters) was added to a final concentration of 200 fmol μL^{-1} as an internal standard. The tryptic peptides were separated by NanoUPLCMS^E on a nanoAcquity™ UPLC system (Waters Corporation, Manchester, UK) [36–39]. The first-dimension chromatography was carried out on an XBridge BEH130 C18 NanoEase column (5 μm, 300 μm × 50 mm;

Waters, USA) that allows the fractioning of the peptides. The first-dimension solvents were A: ammonium formiate (20 mM NH_4HCO_3, pH 10.0) and B: acetonitrile (100% ACN). The system was run at 2 $\mu L\ min^{-1}$ with an initial condition of 3% solvent B. The peptide mixture was fractionated ten times (F1–F10) by different solvent B concentrations ramps [8.7, 11.4, 13.2, 14.7, 16, 17.4, 18.9, 20.7, 23.4 and 65% of acetonitrile/0.1% (v/v) formic acid]. Second dimension chromatography was carried out by eluting each peptide fraction from the trapping column and separating them on a NanoAcquity UPLC column BEH 130 C18 (1.7 μm, 100 μm × 100 mm; Waters, USA). For the second dimension solvent A was H_2O and 0.1% (v/v) formic acid pH 2.4, and solvent B was ACN and 0.1% (v/v) formic acid, pH 2.4. The column was operated at 0.9 $\mu L\ min^{-1}$ at 35 °C. To increase the mass accuracy, precursor ion [Glu]^1-Fibrinopeptide B (GFP; Sigma) [([M + 2H]$^{2+}$ = 785.8486)] at 200 fmol μL^{-1} solution was delivered through the reference sprayer of the NanoLockSpray source and the MS/MS fragment ions of GFP were used to obtain the final instrument calibration. All samples were analyzed in three replicates. For spectrum processing and database searching, the Protein Lynx Global Server v.2.4 (PLGS) was used. The PLGS uses the following

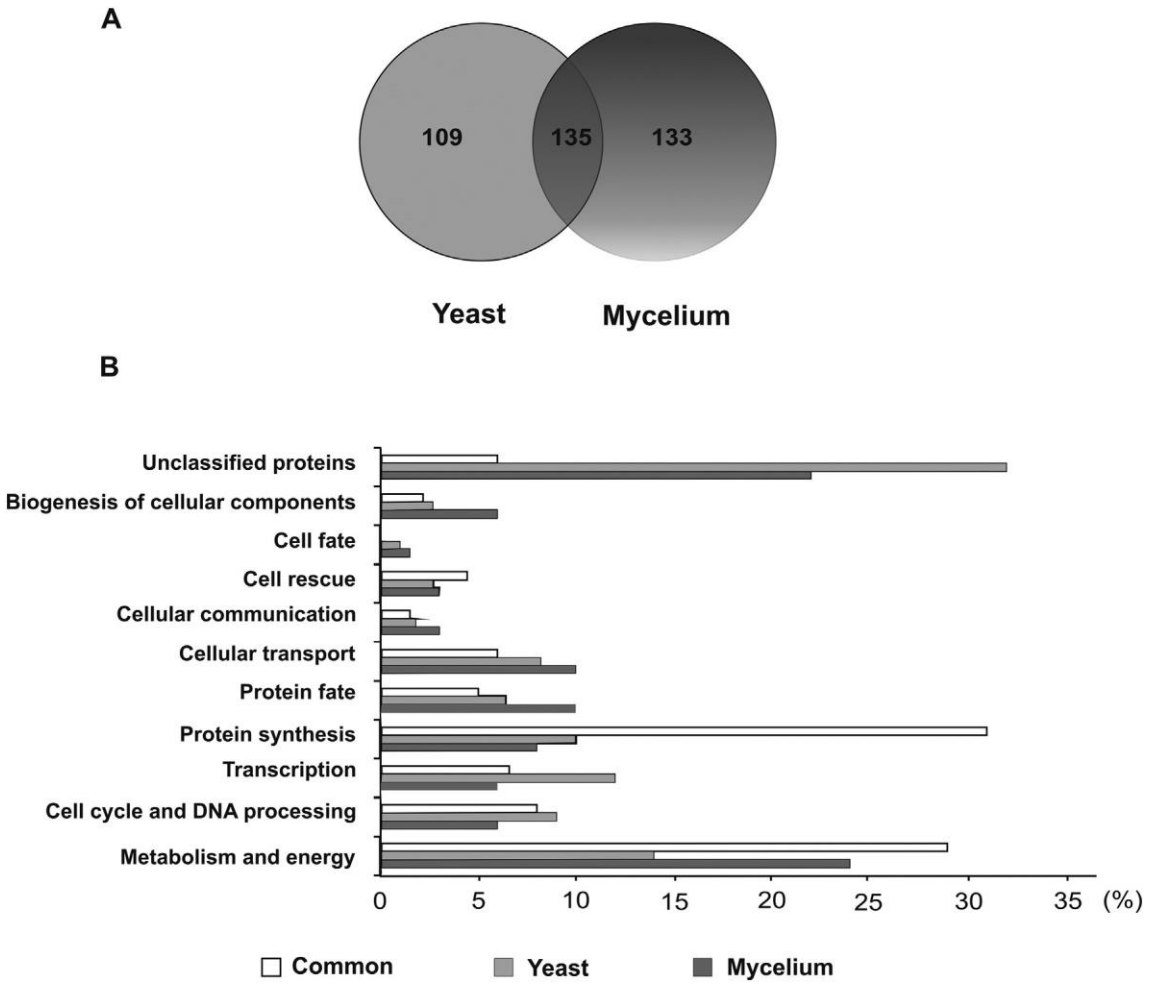

Fig. 2. Comparison of proteins in cell wall of P. lutzii mycelia and yeast cells. (A), Venn diagram shows the number of proteins exclusive or overlapping in yeast (diagrams in light gray) and mycelia (diagrams in dark gray). (B), Functional classification of differentially expressed and common cell wall proteins of yeast and mycelium.

strategy for peptide identification: first, only completely cleaved tryptic peptides are used for identification (PepFrag1). The second pass of the database algorithm (PepFrag2) is designed to identify peptide modifications and nonspecific cleavage products of proteins that were positively identified in the first pass. The mass error tolerance for peptide identification was under 50 ppm. Protein identifications were obtained by searching against the Paracoccidioides spp. genome database (http://www.broadinstitute.org/annotation/genome/paracoccidioides_brasiliensis/ MultiHome.html) together with reverse sequences. The parameters for protein identification included: the detection of at least 2 fragment ions per peptide; 5 fragments per protein; the determination of at least 1 peptide per protein; carbamidomethylation of cysteine as a fixed modification; phosphorylation of serine, threonine and tyrosine, and oxidation of methionine were considered as variable modifications; maximum protein mass (600 kDa); one missed cleavage site was allowed for trypsin; (maximum false positive ratio (FDR) of 4% was allowed [40]. The protein and peptides tables generated by PLGS were merged and the dynamic range of the experiment, peptides detection type, and mass accuracy were determined for each condition, as previously described [35,38].

2.5. Bioinformatics tools

The identified proteins were submitted to in silico analysis. The proteins sequences were examined for the presence of a signal peptide using the SignalP (http://www.cbs.dtu.dk/services/SignalP/). SecretomeP (http://www.cbs.dtu.dk/services/SecretomeP/) was used to identify non-classical protein secretion signals. Using the NetNGlyc (http://www.cbs.dtu.dk/services/NetNGlyc) and NetOGlyc (http:// www.cbs.dtu.dk/services/NetOGlyc/) programs, proteins glycosylation sites could be determined. In addition, the big-PI program (http://mendel.imp.ac.at/gpi/fungi_server.html) was used, to search for proteins GPI-anchoring sites.

3. Results and discussion

3.1. Isolation and identification of cell wall proteins

Proteins from yeast and mycelia were obtained by cell wall fractionation according to the type of interactions that they establish with cell wall components, as cited before. The fractionation was performed in steps that allowed the extraction of proteins by a SDS- boiling treatment to release proteins associated with the cell wall through noncovalent interactions or disulfide bridges. A second step included using an alkaline solution, to extract an enriched fraction of alkali-sensitive proteins or proteins that were attached to cell wall by covalent bonds (Fig. S1).

To assess the extract's quality, proteins were subjected to SDS-PAGE and silver stained as depicted in Fig. S2. Fractions F1 and F2 presented visible amount of proteins (Fig. S2A and B). To check the purity of the cell wall extract, the supernatant from the last wash (1% NaCl) was collected and subjected to SDS-PAGE (Fig. S2C). There were no visible cytoplasmic contaminants in the cell wall fraction.

The protein extracts were analyzed using nanoscale liquid chromatography coupled with tandem mass spectrometry, NanoUPLC-MS^{E}. The false positive rate obtained was 0% for F1, both yeast cells and mycelia, while it was 0.31 and 0.21% for corresponded to fraction F2 in yeast and mycelia, respectively (data not show). The experiments identified 3002 and 1525 identified peptides in fractions F1 in yeast and mycelium F1 fractions, respectively, while 3465 and 2732 identified peptides were identified in yeast and mycelium F2 fractions, respectively (data not show). Figs. S3–S7 showed the dynamic range of the experiments, peptide detection type, and mass accuracy determined for each condition.

Following proteomics global analysis, some filters were applied to the data. Proteins were admitted with one or more peptides found in the three replicates. Following those criteria, a total of 1401 proteins were identified. Fig. 1A and B depict the number of identified proteins as

Table 1
Common proteins in F1 and/or F2 of yeast cells and mycelia of Paracoccidioides lutzii identified by NanoUPLC-MS[E].

ID[a]	Annotation[b]	Cell wall fraction yeast[c]	Cell wall fraction mycelia[d]	SignalP/ SecretomeP[e]	NetOglyc[f]	NetNglyc[g]	Biological process[h]
	ort, transport facilities and transport routes						
PAAG_08620	ADP ATP carrier protein	1,2	1,2	Signal P	–	–	Nucleotide/nucleoside/ nucleobase transport
PAAG_01265	Cytochrome b5	2	2	Secretome P	+	+	Electron transport
PAAG_03161	GTP binding protein ypt5	2	2	Signal P	+	–	Vacuolar/lysosomal transport
PAAG_05680	NTF2 and RRM domain-containing protein	1	1	Secretome P	+	+	Nuclear transport
PAAG_07564	Outer mitochondrial membrane protein porin	1,2	1,2	Secretome P	–	–	Channel/pore class transport
PAAG_04276	Phosphatidylinositol transporter	1,2	2	Secretome P	+	–	Lipid/fatty acid transport
PAAG_07175	Vacuolar sorting-associated protein	2	1	Secretome P	+	–	Vacuolar/lysosomal transport
PAAG_06228	Translocation protein SEC62	1	2	Secretome P	+	–	Protein transport
Cellular communication/signal transduction mechanism							
PAAG_02973	Diploid state maintenance protein chpA 31	1	1	Secretome P	+	–	Cellular signalling
PAAG_02458	GTP binding protein ypt7	2	1,2	Secretome P	–	–	Small GTPase mediated signal transduction
Cell rescue, defense and virulence PAAG_03735							
	Chaperone protein dnaJ	1,2	2	Secretome P	+	–	Stress response
PAAG_03292	Cytochrome c peroxidase	2	1,2	Secretome P	+	–	Oxidative stress response
PAAG_07775	Heat shock protein SSB1	1,2	1,2	Secretome P	+	–	Stress response
PAAG_02116	Hsp70	2	2	Signal P	+	+	Stress response
PAAG_01262	hsp70 like protein	1,2	1,2	Signal P	+	–	Stress response
PAAG_02725	Superoxide dismutase 2	1,2	2	Secretome P	+	–	Superoxide metabolism
Biogenesis of cellular components PAAG_02990							
	Beta glucosidase	2	1,2	Signal P	+	+	Cell wall
PAAG_07670	Cell wall protein ECM33 precursor*	2	1,2	Signal P	+	+	Cell wall
PAAG_04829	Extracellular matrix protein*	1	1,2	Signal P	+	+	Cell wall

[a] Identification of proteins in the Paracoccidioides genome database (http://www.broadinstitute.org/annotation/genome/paracoccidioides_brasiliensis/MultiHome.html) using the ProteinLynx Global Server (PLGS) version 3.0 (Waters Corporation. Manchester. UK).

[b] Proteins annotation from Paracoccidioides genome database or by homology from NCBI database (http://www.ncbi.nlm.nih.gov/).

[c] Cell wall fraction yeast obtained by SDS and DTT (fraction 1), NaOH (fraction 2).

[d] Cell wall fraction mycelia obtained by SDS and DTT (fraction 1), NaOH (fraction 2).

[e] Prediction according SignalP 4.0 secretion, the corresponding number for the D-score must equal or exceed the value of 0.340 (D-score ≥ 0.340) (340) (http://www.cbs.dtu.dk/ services/SignalP/); or prediction according Secretome P 2.0, the corresponding number for the SecP-score must equal or exceed the value of 0.5 (SecP score ≥ 0.5) (http://www.cbs.dtu. dk/services/SecretomeP/). [f] Prediction secretion according NetOGlyc 4.0, the corresponding number for the discriminant score must equal or exceed the value of 0.5 (score ≥ 0.5) (http://www.cbs.dtu.dk/ services/NetOGlyc/). [g] Prediction secretion according NetNGlyc 1.0, the corresponding number for the discriminant score must equal or exceed the value of 0.5 (score ≥ 0.5) (http://www.cbs.dtu.dk/ services/NetNGlyc/). [h] Biological process of differentially expressed proteins from MIPS (http://pedant.helmholtz-muenchen.de/pedant3htmlview/pedant3view?Method=analysis&Db=p3_r48325_Par_brasi_Pb01) and Uniprot database (http://www.uniprot.org/).

* GPI-anchored protein prediction according big-PI (http://mendel.imp.ac.at/gpi/fungi_server.html).

follows: 306 (F1 yeast), 379 (F1 mycelium), 272 (F2 yeast), 444 (F2 mycelium). In synthesis, 685 and 716 proteins were identified in fractions F1 and F2, respectively (Supplemental Tables 1–4). Potential sites for N-glycosylation and O-glycosylation were predicted using the respective tools NetNGlyc and NetOGlyc, for all identified proteins in fractions F1 and F2, of mycelia and yeast cells (Fig. 1C). Fig. 1C demonstrates that of three hundred and six proteins listed in F1 fraction of yeast cells, 90% harbored potential O-glycosylation sites. Moreover, 40% also exhibited N-glycosylation sites. In the F1 fraction of mycelia, many proteins presented sites for O- and N- glycosylation, totaling 86% and 40% of proteins, respectively. Regarding the F2 fraction of yeast cells, 272 proteins were identified and of those, 81% presented sites for O- glycosylation and 36% for N- glycosylation. In the mycelium F2 fraction, among 444 identified proteins 86% and 41% presented sites for O- and N- glycosylation, respectively. The in silico analysis of the identified proteins revealed probable secretion pathways in accordance with the SignalP and SecretomeP (Fig. 1 D). Of special note, among 306 proteins in the F1 fraction of yeast cells, 61% presented a potential signal for a classical or non-classical secretion pathway. In the F1 fraction of mycelia, 187 proteins were putatively secreted by classical or non-classical secretion pathways, corresponding to 49.6% of the identified proteins in this

Table 2
Yeast cells stage-specific proteins of Paracoccidioides lutzii identified by NanoUPLC-MS[E].

ID[a]	Annotation[b]	Cell wall fraction yeast[c]	SignalP/ SecretomeP[d]	NetOglyc[e]	NetNglyc[f]	Biological process[g]
Cellular transport, transport facilities and transport routes						
PAAG_00782	Small COPII coat GTPase sar1	2	Signal P	–	–	Cellular export and secretion
PAAG_03054	G2/M phase checkpoint control protein Sum2	1	Secretome P	+	+	Cellular import
PAAG_04159	Phosphatidylinositol transporter	1	Secretome P	+	–	Cellular transport
PAAG_06249	Transport protein SEC31	1	Secretome P	+	+	ER to Golgi transport
PAAG_00326	Heavy metal ion transporter	1	Secretome P	+	–	Heavy metal ion transport (Cu+, Fe3+, etc.)
PAAG_01796	Vacuolar sorting receptor	1	Signal P	+	+	Vacuolar/lysosomal transport
PAAG_01602	Ras like GTP binding protein	2	Secretome P	+	–	Vesicle fusion
PAAG_08252	Clathrin light chain	1	Secretome P	+	–	Vesicular transport (Golgi network, etc.)
Cellular communication/signal transduction mechanism						
PAAG_03579	cAMP independent regulatory protein pac2	1	Secretome P	+	+	Cellular signalling
Cell rescue, defense and virulence						
PAAG_02364	Thioredoxin	1	Secretome P	+	+	Oxidative stress response
PAAG_06282	DnaJ domain protein	1	Secretome P	+	–	Stress response
PAAG_03334	Peptidyl prolyl cis trans isomerase D	1	Secretome P	+	+	Stress response
Biogenesis of cellular components						
PAAG_07373	Glucan synthesis regulatory protein	1	Secretome P	+	–	Cell wall
PAAG_04857	Beta glucosidase	2	Signal P	+	–	Cell wall
PAAG_05798	Golgi to endosome transporter	1	Secretome P	+	+	Cytoskeleton/structural proteins

[a] Identification of proteins in the Paracoccidioides genome database (http://www.broadinstitute.org/annotation/genome/paracoccidioides_brasiliensis/MultiHome.html) using the ProteinLynx Global Server (PLGS) version 3.0 (Waters Corporation. Manchester. UK).

[b] Proteins annotation from Paracoccidioides genome database or by homology from NCBI database (http://www.ncbi.nlm.nih.gov/).

[c] Cell wall fraction yeast obtained by SDS and DTT (fraction 1), NaOH (fraction 2).

[d] Prediction according SignalP 4.0 secretion, the corresponding number for the D-score must equal or exceed the value of 0.340 (D-score ≥ 0.340) (340) (http://www.cbs.dtu.dk/services/SignalP/)); or prediction according Secretome P 2.0, the corresponding number for the SecP-score must equal or exceed the value of 0.5 (SecP score ≥ 0.5) (http://www.cbs.dtu.dk/services/SecretomeP/). [e] Prediction secretion according NetOGlyc 4.0, the corresponding number for the discriminant score must equal or exceed the value of 0.5 (score ≥ 0.5) (http://www.cbs.dtu.dk/services/NetOGlyc/). [f] Prediction secretion according NetNGlyc 1.0, the corresponding number for the discriminant score must equal or exceed the value of 0.5 (score ≥ 0.5) (http://www.cbs.dtu.dk/services/NetNGlyc/).

[g] Biological process of differentially expressed proteins from MIPS (http://pedant.helmholtz-muenchen.de/pedant3htmlview/pedant3view?Method=analysis&Db=p3_r48325_Par_brasi_Pb01) and Uniprot database (http://www.uniprot.org/).

fraction. Regarding the F2 fraction of yeast cells, 106 proteins were predicted to be secreted, constituting 38.5% of the total. From the F2 fraction of mycelia, 193 proteins were putatively secreted, corresponding to 43% of the identified proteins in this fraction. In synthesis, the percentage of predicted secreted proteins in the analyzed fractions, mycelium and yeast cells, ranged from 38.5% to 61%.

3.2. Functional classification of proteins in cell wall of yeast cells and mycelia

Each protein was assigned to a specific functional group based on FUNCAT annotations. Supplementary Table 1 depicts the proteins in the F1 of yeast cells. The most abundant functional groups are involved in metabolism, energy production, and protein synthesis, as demonstrated in Supplementary Fig. 8A. The F1 mycelium proteins were also classified according to functional category, as depicted in Supplementary Table 2. The profile of functional categories, presented in Supplementary Fig. 8A indicates a very similar pattern when comparing to yeast cells.

Tables S3 and S4 list the proteins present in the F2 of yeast and mycelia, respectively. The number of identified proteins was 272 and 444 for yeast and mycelia, respectively. For both samples, the functional category of metabolism and energy were predominant as depicted in Supplementary Fig. 8B. Of relevance, the category of cellular transport was present among the identified functional classes. When comparing the proteins involved with carbohydrate metabolism in mycelium and yeast samples in F1/F2, it became evident that mycelium presents a higher number of proteins than the yeast. Our results are similar to those found for Pb3 and Pb18 in which proteins related to carbohydrate metabolism

were more expressed in mycelium. According to the study, it is supposed that mycelium need an extra energy for cell wall biosynthesis/remodeling [25].

3.3. Non-predicted cell wall proteins

Among the 1401 identified proteins in the F1 and F2 for both mycelia and yeast cells, 52% do not match when SignalP (classical secretion signal) or SecretomeP (non-classical secretion signal) were employed. Despite the absence of those signals, that could direct the proteins to the fungal surface, some atypical cell wall proteins (Tables S1–S4) were previously described in fungal cell wall, making clear the classification of those proteins at the cell wall. Among those proteins, enolase is present in fractions F1 and F2 from both, yeast and mycelia, and play role in pathogenesis and virulence of Paracoccidioides spp. [30,31]. Immunocytochemistry studies have demonstrated the localization of enolase at Paracoccidioides spp. cell surface, where it is able to recruiting plasminogen, activating the fibrinolytic system of plasmin which in turn degrades the extracellular matrix of the host and potentially promotes spread of the pathogen [30]. In addition, other atypical cell wall protein, formamidase, here identified, was detected in Paracoccidioides yeast and mycelium cell wall by immunomicroscopy; the protein can be related to resistance to acidic environments (Tables S2–S3) [41]. Additional metabolism related proteins, atypical cell wall proteins, such as malate synthase present in fraction F2 of mycelia, have already been described in Paracoccidioides cell wall. Malate synthase is an important adherence molecule binding to host extracellular matrix components such as fibronectin and type I and type IV collagen [42] (Table S4).

Additionally, studies often use different protocols to isolate cell wall proteins, and in almost all of them, some intracellular proteins were associated with this structure. Thus, some authors have suggested that those proteins, atypical cell wall proteins, perform dual or multiple roles depending on location [22,43]. Corroborating this result, a recent comparative study of the cell wall-associated proteins in yeast and mycelium of P. brasiliensis described known intracellular proteins associated with the cell wall [25]. Those proteins without signals for secretion, also highlight the importance of extracellular vesicles for the trans-cell wall transport of molecules to the extracellular space [44]. Cell wall-bound vesicles are described in diverse organism such as

Cryptococcus neoformans [45], Histoplasma capsulatum, C. albicans, Candida parapsilosis, Sporothrix schenckii, Saccharomyces cerevisiae [46] and P. brasiliensis [47]. Proteins that make up those are signal transduction regulators, heat shock proteins, chaperones, vesicle formation proteins, cell wall regulation molecules, cell growth proteins, sugar metabolism-related proteins, among others [44,47]. In addition, it has been inferred by some authors that those proteins may simply associate with the cell wall as a result of their release to the external environment due to the cell lysis process [48,49,50]. Another alternative explanation relates to the fact that as the cell wall is an elastic structure, it can stretch and shrink rapidly in response to osmotic changes of the environment, and consequently proteins in transit to the extracellular medium, may become attached to the cell wall [51].

Table 3
Mycelia stage specific proteins of Paracoccidioides lutzii identified by NanoUPLC-MS[E].

ID[a]	Annotation[b]	Cell wall fraction mycelia[c]	SignalP/ SecretomeP[d]	NetOglyc[e]	NetNglyc[f]	Biological process[g]
	ransport facilities and transport routes					
PAAG_01614	Sugar transporter	2	Secretome P	–	–	C-compound and carbohydrate transport
PAAG_04988	UDP N acetylglucosamine transporter	1	Secretome P	+	+	C-compound and carbohydrate transport
PAAG_06563	Succinate fumarate mitochondrial transport	2	Secretome P	+	+	C-compound and carbohydrate transport
PAAG_00136	Annexin	2	Secretome P	+	–	Cellular export and secretion
PAAG_04328	Endosomal cargo receptor Erp3	2	Signal P	–	–	Cellular export and secretion
PAAG_01111	Apolipoprotein O	1	Secretome P	–	–	Lipid transport
PAAG_03452	Carnitine acyl carnitine Carrier	1	Secretome P	+	+	Lipid/fatty acid transport
PAAG_03418	Mitochondrial precursor proteins import	1	Secretome P	+	+	Mitochondrial transport
PAAG_03644	Mitochondrial import receptor subunit tom	1,2	Secretome P	–	–	Mitochondrial transport
PAAG_00929	Transport protein sec61	1	Secretome P	+	–	Protein transport
PAAG_01473	Outer membrane protein	2	Secretome P	+	+	Transport routes
PAAG_04674	Translocation protein SEC66	2	Secretome P	+	–	Transport routes
PAAG_09048	Syntaxin family protein	2	Secretome P	+	–	Vesicle fusion
PAAG_03900	GTP-binding protein YPT52	2	Secretome P	+	–	Vesicular transport (Golgi network, etc.)
Cellular communication/signal transduction mechanism						
PAAG_06815	Tricalbin 3	1	Secretome P	+	+	Ca2+ mediated signal transduction
PAAG_02757	Serine threonine protein kinase cot 1	1	Secretome P	+	–	Cellular signalling
PAAG_07734	Adenylyl cyclase associated protein	2	Secretome P	+	–	Cellular signalling
PAAG_07740	Conserved hypothetical protein	2	Secretome P	+	+	GTPase activator (GAP)
Cell rescue, defense and virulence						
PAAG_04338	Interferon induced GTP binding protein Mx	2	Secretome P	+	+	Defense related proteins
PAAG_01454	Peroxisomal catalase	1,2	Secretome P	+	–	Oxidative stress response
PAAG_07444	Chaperone protein dnaK	2	Secretome P	+	+	Stress response
PAAG_07534	Chaperone protein dnaJ 3	1,2	Signal P	+	–	Stress response
Biogenesis of cell ılar components						
PAAG_00898	Conserved hypothetical protein*	1	Secretome P	+	+	Cell wall
PAAG_06779	Cell wall glucanase Utr2*	1,2	Secretome P	+	+	Cell wall
PAAG_04534	Mannan endo 1,6-alpha mannosidase DCW1*	1	Signal P	+	+	Cell wall
PAAG_04665	TOS1	1,2	Signal P	+	–	Cell wall
PAAG_04290	Neutral alpha_glucosidase AB	2	Signal P	+	–	Cell wall
PAAG_05245	1,3 Beta glucanosyltransferase gel2*	1,2	Signal P	+	+	Cell wall
PAAG_01139	Extracellular cell wall glucanase Crf1*	1,2	Signal P	+	–	Cell wall
PAAG_03849	Chitinase	2	Secretome P	+	+	Chitin anabolism

[a] Identification of proteins in the Paracoccidioides genome database (http://www.broadinstitute.org/annotation/genome/paracoccidioides_brasiliensis/MultiHome.html) using the ProteinLynx Global Server (PLGS) version 3.0 (Waters Corporation. Manchester. UK).

[b] Proteins annotation from Paracoccidioides genome database or by homology from NCBI database (http://www.ncbi.nlm.nih.gov/);

[c] Cell wall fraction mycelia obtained by SDS and DTT (fraction 1), NaOH (fraction 2).

[d] Prediction according SignalP 4.0 secretion, the corresponding number for the D-score must equal or exceed the value of 0.340 (D-score ≥ 0.340) (340) (http://www.cbs.dtu.dk/services/SignalP/); or prediction according Secretome P 2.0, the corresponding number for the SecP-score must equal or exceed the value of 0.5 (SecP score ≥ 0.5) (http://www.cbs.dtu.dk/services/SecretomeP/). [e] Prediction secretion according NetOGlyc 4.0, the corresponding number for the discriminant score must equal or exceed the value of 0.5 (score ≥ 0.5) (http://www.cbs.dtu.dk/services/NetOGlyc/). [f] Prediction secretion according NetNGlyc 1.0, the corresponding number for the discriminant score must equal or exceed the value of 0.5 (score ≥ 0.5) (http://www.cbs.dtu.dk/services/NetNGlyc/). [g] Biological process of differentially expressed proteins from MIPS (http://pedant.helmholtz-muenchen.de/pedant3htmlview/pedant3view?Method=analysis&Db=p3_r48325_Par_brasi_Pb01) and Uniprot database (http://www.uniprot.org/).

* GPI-anchored protein prediction according big-PI (http://mendel.imp.ac.at/gpi/fungi_server.html).

3.4. Proteins secreted by classical and non-classical routes in yeast cells and mycelia

Despite other pathways, as cited above, different from the classical and non-classical routes, we considered for further analysis just proteins that were putatively secreted according to SignalP and SecretomeP. The adopted criteria were based on studies demonstrating that many proteins bound to fungal cell wall, are characterized by having a classical signal peptide and of O- and N-glycosylation sites [5,22,52]. Also, we have included in our selection criteria proteins secreted by non-classical routes; proteins with values of SecPscore ≥0.5 were grouped in routes of non-classical secretion [53], once it has been described in Paracoccidioides spp. that most of the secreted proteins encoded in their genomes are predicted to be non-classically secreted [47,54]. The proteins secreted by non-classical routes

could reach the cell wall in extracellular vesicles, widely described in fungi as a protein transfer mechanism to the cell outside [55].

In this way, we analyzed proteins secreted by classical or nonclassical pathways in both fractions F1 and F2. Among the 1401 identified proteins, 244 from yeast cells and 268 from mycelia, corresponding to F1 and/or F2, were considered for further analysis as depicted in Fig. 2A. In addition, those proteins were classified into functional categories according to their biological processes, obtained using Pedant on MIPS (http://pedant.gsf.de/pedant3htmlview/pedant3view?Method=analysis&Db=p3_r48325_Par_lutzi) and the Uniprot database (http://www.uniprot.org/), as depicted in Fig. 2B for yeast and mycelia. Among the functional categories in this selection of proteins, the most abundant detected in fractions of both yeast and mycelia were metabolism and energy, followed by proteins synthesis and unclassified proteins. It is worth noting the detection of similar numbers of proteins in the fractions F1 and/or F2 from yeast and mycelia, as depicted in Fig. 2A. Also, the functional categorization of those proteins in F1 and/or F2 from yeast cells and mycelia presented very similar numbers, as depicted in Fig. 2B.

Table S5 depicts the proteins in yeast cells, putatively secreted by classical or non-classical pathways, present in both fractions F1 and F2. Enzymes related to several metabolic routes, such as the TCA cycle and methylcitrate cycle were present in addition to a high number of proteins belonging to protein synthesis. Table S6 depicts the proteins in mycelia presenting classical or non-classical secretion, present in both fractions F1 and F2. Cell metabolism and energy in addition to protein synthesis predominate in the fractions from mycelia. Another important consideration is that 127 proteins were found in both fractions, F1 and F2 (Tables S5 and S6). This result is consistent with other studies of cell wall proteome. It has been reported that one unique protein can be found throughout the cell wall, both in the outer and internal fractions [56]. Thus, we can suppose that those proteins can bind the cell wall by different types of linkages, and in this way can be obtained by different treatments.

Among the proteins identified in fractions of yeast and mycelia some related to metabolism and energy such as glyceraldehyde-3phosphate dehydrogenase (GAPDH) were identified, that presented signal for cell wall localization (Tables S5–S6). Although unexpected, such a protein had been described in the cell wall of Neisseria meningitidis, presumably facilitating colonization and invasion of host tissues by direct interaction with host proteins [57]. In P. lutzii, GAPDH is located in the cell wall, where it can bind laminin, collagen I and fibronectin, playing a role in the fungal adhesion [27]. Fructose 1,6bisphosphate aldolase, present in yeast F1, had been already been described in studies in Paracoccidioides cell wall as binding plasminogen and activating it to plasmin, therefore representing a potential virulence factor (Table S5) [58]. Corroborating our results, studies have shown that C. albicans presents eight plasminogen binding proteins including fructose-1,6-bisphosphate aldolase [59]. In N meningitidis studies demonstrated that fructose-1,6-bisphosphate aldolase might have a function related to adherence to host cells [60].

Again corroborating our findings, elongation factor 1 alpha, here identified in the cell wall of yeast and mycelia in both F1 and F2 (Table S5–S6), is also located in the cell wall of S. cerevisiae and C. albicans [22,56,61]. Moreover, translation elongation factors have been described on the cell surface of other organisms, such as Mycobacterium leprae, C. albicans and Staphylococcus aureus [62–64]. In an attempt to explain their location on the cell surface, it was proposed that elongation factors could be related to the adhesion process in tobacco cell walls [65]. Additionally the Leishmania elongation- factor 1 α is capable of activating multiple protein tyrosine phosphatases in the host which will downregulate interferon-γ signalling (INF-γ), impeding the effective expression of microbicide activity performed by macrophages, including TNF-α and nitric oxide (NO) production [66,67]. Additionally, regarding the cell cycle category, histones H2 and H3 were found in mycelium and yeast cells wall (Table S5–S6). Although those proteins are commonly associated with DNA, they were found on the cell surface of H. capsulatum [68]. Immunization of mice against H2B reduced the fungal burden, decreased pulmonary inflammation and prolonged mouse survival against histoplasmosis [68].

3.5. Common proteins in the cell wall of yeast cells and mycelia

Initially, we searched for proteins present in both, yeast cells and mycelia in F1 and F2. We believe that those proteins represent common processes for both fungal phases. Proteins numbering 135 were present in the fractions F1 and/or F2 of both phases, as depicted in Fig. 2A. We focused our analysis of common cell wall proteins on yeast and mycelia by analyzing functional categories that could be related to transport, cell communication, virulence and biogenesis of cellular components, as depicted in Table 1. We detected proteins related to cell rescue, defense and virulence, such as cytochrome c peroxidase, chaperone protein DnaJ and superoxide dismutase FeeMn family – SOD2. Cytochrome c peroxidase increases in yeast cells upon oxidative [69], and nitrosative stresses [70] in P. lutzii. Knock down of the gene encoding that protein results in increased sensitivity to oxidative and nitrosative agents [70,71] as well as decreased survival of P. brasiliensis in macrophages and in a murine model of infection [71], characterizing the protein as a virulence factor in this fungus. The mitochondrial chaperone DnaJ is localized at the P. brasiliensis cell surface, presenting an inferred function of adhesion [72]. Hsp70 has been described in cell wall of C. albicans [56,73–75], corroborating our finding. HSPs had also been associated with the maintenance of cell wall in Aspergillus fumigatus [75]. The heat shock protein SSB1, was also identified in the secretome of P. lutzii in mycelia and yeast cells [54]. In the group of proteins related to biogenesis of cellular components, we detected an extracellular matrix protein, a predicted structural GPI-anchored molecule that can be related to cell wall biosynthesis and remodeling. In addition, the identified proteins in this group include Ecm33, a GPIlinked cell wall protein important for cell wall integrity and architecture in C. albicans [76,77]. The absence of this protein from C. albicans affects the fungus morphology promoting an aberrant cell wall structure [76,77]. Beta glucosidase (PAAG_02990) here identified in F1 and/or F2 of yeast and mycelia may be involved in the remodeling of the fungal cell wall (Table 1).

3.6. Differentially expressed cell wall proteins in yeast and mycelia

One hundred and nine proteins were detected just in F1/F2 of yeast cells and 133 proteins were detected just in mycelia, (Fig. 2A). The biological processes according to GO classification are described in Fig. 2B. Specific proteins in fractions F1 and F2 of yeast cells were encompassed by categories of cellular transport (7% - 8 proteins), cellular communication (1% - 1 protein), cell rescue, defense and virulence (3% - 3 proteins) and biosynthesis of cellular components (3% - 3 proteins) as depicted in Fig. 2B and Table 2. The category of cell rescue, defense and virulence includes thioredoxin, (Table 2), a key protein for dealing with the antioxidant arsenal during oxidative stress, allowing the neutralization of H_2O_2 [69]. Proteins such as peptidylprolyl cis-trans isomerase D and thioredoxin described here were also exclusive to the yeast cells wall in Pb03 and Pb18 [25]. It was also possible to identify a beta glucosidase, most likely involved in remodeling and organization of the cell wall. The clathrin light chain here identified is required for trafficking of enzymes for cell wall synthesis/remodeling. In Schizosaccharomyces pombe, clathrin light chain is necessary for the origin of vesicles that transport some proteins to the cell surface such as β-glucan synthases and exoglucanases, both required for cell wall synthesis and remodeling [78].

The proteins identified just in the F1/F2 fractions of mycelia were mainly related to cellular transport (10% - 14 proteins), cellular communication (3% - 4 proteins), cell rescue, defense and virulence (3% - 4 proteins) and biosynthesis of cellular components (6% - 8 proteins) as depicted in Fig. 2B and Table 3. Some proteins related to cell rescue, such as DnaK and DnaJ, were identified only in mycelium cell wall. The chaperone DnaK is a major protein folding factor under stress conditions [79,80]. Loss of DnaK reduces the ability of Staphylococcus aureus to make biofilms and its adherence to eukaryotic cells [81]. Studies have provided evidence that the chaperone DnaK is localized at the surface of Mycobacterium tuberculosis [82], corroborating our analysis. Members of DnaJ are localized in the cell wall of Paracoccidioides [72]. In addition, GPI-anchored proteins involved in cell wall remodeling, were identified only in mycelia F1 and F2, as following: cell wall glucanase Utr2, extracellular cell wall glucanase Crf1, β-1,3 glucanosyltransferase gel2, mannan endo 1,6-alpha mannosidase DCW1 and a

putative GPI-anchored protein with unknown function (Table 3). Utr2 and Crf1 are transglycosylases members of the CRH family [83], that play role in linking chitin to β-glucans, both in vivo and in vitro [84–86].

Transglycosylases catalyze the cleavage of the β-(1,4) linkages of the donor chitin donor molecule and bind its reducing end in a sugar acceptor molecule by a β-(1,4) glycosidic bond [86,87]. In C. albicans a null mutant for UTR2 presents defects in filamentation, reduction in adherence, and loss of virulence [87,88]. In S. cerevisiae, the impairment of retrograde trafficking of proteins [89,90], affects cell wall integrity, since this impairment results in activation of the calcineurin signalling pathway [91], enhancing the expression of Chr11 and Utr2 transglycosylases. It was suggested that Utr2 plays role in cell wall remodeling and partially compensates for the cell wall defects when there is impaired retrograde trafficking [91].

The cell wall glucanase Crf1 belongs to glycosyl hydrolase family 16 and plays a role in cell wall organization since its homologue in S. cerevisiae (Crhl) has a transglycosidase activity that is involved in the crosslinking between polymers of chitin and β-1,6 glucan [85,92]. Proteins members of the glucanosyltransferase family operate in cleavage and joining of β-1,3-glucans to shorten or lengthen glucan polymers [93,94]. In this study, only the Gel2p was found (Table 3). Gel2p presents functional similarity with GAS/Phr and is member of the glycoside hydrolase family 72. Gel2p participates in cell wall integrity and maintenance in P. lutzii since it was able to restore the lack of Gas1p activity in a S. cerevisiae Gas1p mutant as indicated by complementation studies. Furthermore, Gel2p is associated mainly with the cell wall [32]. The protein DCW1 participates in Neurospora crassa cell wall biogenesis, incorporating glycoproteins into the cell wall. dcw1 mutants released large amounts of protein into the medium, including well-characterized cell wall proteins [95]. In C. albicans DCW1p is required for growth [96]. Dcw1p of S. cerevisiae is homologous to PbDfg5p of P. lutzii, a GPI β-glucan which can be related to interactions of P. lutzii with colonizing host tissues [97]. Proteins associated with cell wall remodeling, such as TOS1, were here described here [98]. Mutants for this protein, presents decreased levels of glycogen storage and susceptibility to the action of β-1,3-glucanase [43,99]. Neutral alpha glucosidase AB and chitinase were here found here in mycelia (Table 3). Chitinase cht3, member of the glycosyl hydrolase 18 family, is associated with the degradation of wall carbohydrates of the primary septum between mother and daughter cells [100,101]. Consistent with our results, Cht3 expression is higher in hyphae compared to yeast cells in C. albicans [102].

4. Conclusion

Sequential fractionation associated with a proteomic approach allowed the characterization of cell wall proteins of P. lutzii, which include proteins associated with the wall through non-covalent or disulfide bonds (F1) and proteins bound to the cell wall by alkali-labile bonds (F2). A high percentage of proteins without a classic signal peptide were identified, which is consistent with data in the literature. Proteins from both fractions, F1 and F2, were related to several biological processes, some of them classically related to the cell wall. When compared the proteins composition in mycelium and yeast, 135 proteins were common, such as Ecm33, beta glucosidase, protein DnaJ and superoxide dismutase. The total of 242 differentially expressed cell wall proteins in yeast and mycelia were identified. The specific proteins in yeast cells were composed by categories of cellular transport, cellular communication, cell rescue, defense and virulence and biosynthesis of cellular components. In mycelia, several proteins involved with carbohydrate metabolism were found such as GPI-anchored proteins. To our knowledge, up to now, this is the first work that describes, at the proteomic level, proteins in fractions of the cell wall in yeast cells and mycelia in the genus Paracoccidioides. Those proteins could be particularly valuable to search new specific targets for antifungal drugs.

Supplementary data to this article can be found online at http://dx. doi.org/10.1016/j.bbapap.2017.08.016.

Transparency document

The http://dx.doi.org/10.1016/j.bbapap.2017.08.016 associated with this article can be found, in online version.

Acknowldegments

This work at Universidade Federal de Goiás was supported by grants from Conselho Nacional de Desenvolvimento Científico e Tecnológico (CNPq) and Fundação de Amparo à Pesquisa do Estado de Goiás (FAPEG), grant numbers 407855/2013-0 and 465771/2014-9, respectively. This work is part of the National Institute of Science and Technology of the Strategies of Host-Pathogen Interaction (HPI).

References

[1] S.J. Free, Fungal cell wall organization and biosynthesis, Adv. Genet. 81 (2013) 33–82, http://dx.doi.org/10.1016/B978-0-12-407677-8.00002-6.

[2] G. San-Blas, F. San-Blas, Paracoccidioides brasiliensis: cell wall structure and virulence. A review, Mycopathologia 62 (1977) 77–86 http://www.ncbi.nlm.nih.gov/pubmed/340954.

[3] C.J. Heilmann, A.G. Sorgo, A.R. Siliakus, H.L. Dekker, S. Brul, C.G. Koster, L.J. de Koning, F.M. Klis, Hyphal induction in the human fungal pathogen Candida albicans reveals a characteristic wall protein profile, Microbiology 157 (2011) 2297–2307, http://dx.doi.org/10.1099/mic.0.049395-0.

[4] F.M. Klis, P. De Groot, K. Hellingwerf, Molecular organization of the cell wall of Candida albicans, Med. Mycol. 39 (2001) 1–8, http://dx.doi.org/10.1080/mmy.39.1.1.8-0.

[5] P.W.J. De Groot, A.F. Ram, F.M. Klis, Features and functions of covalently linked proteins in fungal cell walls, Fungal Genet. Biol. 42 (2005) 657–675, http://dx.doi.org/10.1016/j.fgb.2005.04.002.

[6] W.L. Chaffin, Candida albicans cell wall proteins, Microbiol. Mol. Biol. Rev. 72 (2008) 495–544, http://dx.doi.org/10.1128/MMBR.00032-07.

[7] X. Xie, P.N. Lipke, On the evolution of fungal and yeast cell walls, Yeast 27 (2010) 479–488, http://dx.doi.org/10.1002/yea.1787.

[8] P.W.J. de Groot, A.D. de Boer, J. Cunningham, H.L. Dekker, L. de Jong, K.J. Hellingwerf, C. de Koster, F.M. Klis, Proteomic analysis of Candida albicans cell walls reveals covalently bound carbohydrate-active enzymes and adhesins, Eukaryot. Cell 3 (2004) 955–965, http://dx.doi.org/10.1128/EC.3.4.955-965. 2004.

[9] J. Karkowska-Kuleta, A. Kozik, Cell wall proteome of pathogenic fungi, Acta Biochim. Pol. 62 (2015) 339–351, http://dx.doi.org/10.18388/abp.2015_1032.

[10] A. Pitarch, C. Nombela, C. Gil, Cell wall fractionation for yeast and fungal proteomics, Methods Mol. Biol. 425 (2008) 217–239, http://dx.doi.org/10.1007/9781-60327-210-0_19.

[11] M. Pittet, A. Conzelmann, Biosynthesis and function of GPI proteins in the yeast Saccharomyces cerevisiae, Biochim. Biophys. Acta 1771 (2007) 405–420, http://dx.doi.org/10.1016/j.bbalip.2006.05.015.

[12] J. Ruiz-Herrera, M. Victoria Elorza, E. Valentín, R. Sentandreu, Molecular organization of the cell wall of Candida albicans and its relation to pathogenicity, FEMS Yeast Res. 6 (2006) 14–29, http://dx.doi.org/10.1111/j.1567-1364.2005. 00017.x.

[13] M. Bernard, J.P. Latgé, Aspergillus fumigatus cell wall: composition and biosynthesis, Med. Mycol. 39 (Suppl. 1) (2001) 9–17, http://dx.doi.org/10.1128/mBio.00260-10.Updated.

[14] A. Maddi, S.M. Bowman, S.J. Free, Trifluoromethanesulfonic acid-based proteomic analysis of cell wall and secreted proteins of the ascomycetous fungi Neurospora crassa and Candida albicans, Fungal Genet. Biol. 46 (2009) 768–781, http://dx.doi.org/10.1016/j.fgb.2009.06.005.

[15] E. Brummer, E. Castaneda, A. Restrepo, Paracoccidioidomycosis: an update, Clin. Microbiol. Rev. 6 (1993) 89–117 http://www.ncbi.nlm.nih.gov/pubmed/ 8472249.

[16] L.L. Carrero, G. Niño-Vega, M.M. Teixeira, M.J.A. Carvalho, C.M.A. Soares, M. Pereira, R.S.A. Jesuino, J.G. McEwen, L. Mendoza, J.W. Taylor, M.S. Felipe, G. San-Blas, New Paracoccidioides brasiliensis isolate reveals unexpected genomic variability in this human pathogen, Fungal Genet. Biol. 45 (2008) 605–612, http://dx.doi.org/10.1016/j.fgb.2008.02.002.

[17] M.M. Teixeira, R.C. Theodoro, M.J.A. de Carvalho, L. Fernandes, H.C. Paes, R.C. Hahn, L. Mendoza, E. Bagagli, G. San-Blas, M.S.S. Felipe, Phylogenetic analysis reveals a high level of speciation in the Paracoccidioides genus, Mol. Phylogenet. Evol. 52 (2009) 273–283, http://dx.doi.org/10.1016/j.ympev.2009.04.005.

[18] D.R. Matute, J.G. McEwen, R. Puccia, B.A. Montes, G. San-Blas, E. Bagagli, J.T. Rauscher, A. Restrepo, F. Morais, G. Niño-Vega, J.W. Taylor, Cryptic speciation and recombination in the fungus Paracoccidioides brasiliensis as revealed by gene genealogies, Mol. Biol. Evol. 23 (2006) 65–73, http://dx.doi.org/10.1093/molbev/msj008.

[19] G. San-Blas, G. Niño-Vega, T. Iturriaga, Paracoccidioides brasiliensis and paracoccidioidomycosis: molecular approaches to morphogenesis, diagnosis, epidemiology, taxonomy and genetics, Med. Mycol. 40 (2002) 225–242, http://dx.doi.org/10.1080/714031110.

[20] L.M. Carbonell, J. Rodriguez, Mycelial phase of Paracoccidioides brasiliensis and Blastomyces dermatitidis: an electron microscope study, J. Bacteriol. 96 (1968) 533–543 http://www.ncbi.nlm.nih.gov/pubmed/5674059 (accessed August 3, 2016).

[21] G. San-Blas, The cell wall of fungal human pathogens: its possible role in hostparasite relationships, Mycopathologia 79 (1982) 159–184 http://www.ncbi.nlm.nih.gov/pubmed/6755258.

[22] L. Castillo, E. Calvo, A.I. Martínez, J. Ruiz-Herrera, E. Valentín, J.A. Lopez, R. Sentandreu, A study of the Candida albicans cell wall proteome, Proteomics 8 (2008) 3871–3881, http://dx.doi.org/10.1002/pmic.200800110.

[23] J.P. Latgé, The cell wall: a carbohydrate armour for the fungal cell, Mol. Microbiol. 66 (2007) 279–290, http://dx.doi.org/10.1111/j.1365-2958.2007.05872.x.

[24] G.P. Moran, D.C. Coleman, D.J. Sullivan, Comparative genomics and the evolution of pathogenicity in human pathogenic fungi, Eukaryot. Cell 10 (2011) 34–42, http://dx.doi.org/10.1128/EC.00242-10.

[25] L.V.G. Longo, J.P.C. da Cunha, T.J.P. Sobreira, R. Puccia, Proteome of cell wallextracts from pathogenic Paracoccidioides brasiliensis: comparison among morphological phases, isolates, and reported fungal extracellular vesicle proteins, EuPA Open Proteom. 3 (2014) 216–228, http://dx.doi.org/10.1016/j.euprot. 2014.03.003.

[26] C.L. Borges, M. Pereira, M.S.S. Felipe, F.P. de Faria, F.J. Gomez, G.S. Deepe, C.M. a Soares, The antigenic and catalytically active formamidase of Paracoccidioides brasiliensis: protein characterization, cDNA and gene cloning, heterologous expression and functional analysis of the recombinant protein, Microbes Infect. 7 (2005) 66–77, http://dx.doi.org/10.1016/j.micinf.2004.09.011.

[27] S.M. Barbosa, S.N. Báo, P.F. Andreotti, F.P. De Faria, M.S.S. Felipe, L.D.S. Feitosa, M.J.S. Mendes-Giannini, C.M.D.A. Soares, Glyceraldehyde-3-phosphate dehydrogenase of Paracoccidioides brasiliensis is a cell surface protein involved in fungal adhesion to extracellular matrix proteins and interaction with cells, Infect. Immun. 74 (2006) 382–389, http://dx.doi.org/10.1128/IAI.74.1.382.

[28] L.A. Pereira, S.N. Báo, M.S. Barbosa, J.L.M. Da Silva, M.S.S. Felipe, J.M. De Santana, M.J.S. Mendes-Giannini, C.M. De Almeida Soares, Analysis of the Paracoccidioides brasiliensis triosephosphate isomerase suggests the potential for adhesin function, FEMS Yeast Res. 7 (2007) 1381–1388, http://dx.doi.org/10.1111/j.1567-1364.2007.00292.x.

[29] N.D.S. Castro, K.P. de Castro, I. Orlandi, L.D.S. Feitosa, L.K. Rosa e Silva, M.H. Vainstein, S.N. Báo, M. Vai, C.M.D.A. Soares, Characterization and functional analysis of the beta-1,3-glucanosyltransferase 3 of the human pathogenic fungus Paracoccidioides brasiliensis, FEMS Yeast Res. 9 (2009) 103–114, http://dx.doi.org/10.1111/j.1567-1364.2008.00463.x.

[30] S.V. Nogueira, F.L. Fonseca, M.L. Rodrigues, V. Mundodi, E.A. Abi-Chacra, M.S. Winters, J.F. Alderete, C.M. De Almeida Soares, Paracoccidioides brasiliensis enolase is a surface protein that binds plasminogen and mediates interaction of yeast forms with host cells, Infect. Immun. 78 (2010) 4040–4050, http://dx.doi.org/10.1128/IAI.00221-10.

[31] A.M. Bailão, S.V. Nogueira, S.M. Rondon Caixeta Bonfim, K.P. De Castro, J. De Fátima da Silva, M.J.S. Mendes Giannini, M. Pereira, C.M. De Almeida Soares, Comparative transcriptome analysis of Paracoccidioides brasiliensis during in vitro adhesion to type I collagen and fibronectin: identification of potential adhesins, Res. Microbiol. 163 (2012) 182–191, http://dx.doi.org/10.1016/j.resmic.2012.01.004.

[32] P. De Sousa Lima, E.F.L.C. Bailão, M.G. Silva, N.D.S. Castro, S.N. Báo, I. Orlandi, M. Vai, C.M. De Almeida Soares, Characterization of the Paracoccidioides beta-1,3glucanosyltransferase family, FEMS Yeast Res. 12 (2012) 685–702, http://dx.doi.org/10.1111/j.1567-1364.2012.00819.x.

[33] M.M. Bradford, A rapid and sensitive method for the quantitation of microgram quantities of protein utilizing the principle of protein-dye binding, Anal. Biochem. 72 (1976) 248–254, http://dx.doi.org/10.1016/0003-2697(76)90527-3.

[34] A. Murad, Characterisation and quantitation expression analysis of recombinant proteins in plant complex mixtures using nanoUPLC mass spectrometry, Protoc. Exch. (2011) 1–17, http://dx.doi.org/10.1038/protex.2011.216.

[35] A.M. Murad, E.L. Rech, NanoUPLC-MSE proteomic data assessment of soybean seeds using the Uniprot database, BMC Biotechnol. 12 (2012) 82, http://dx.doi.org/10.1186/1472-6750-12-82.

[36] J.C. Silva, R. Denny, C. Dorschel, M.V. Gorenstein, G. Li, K. Richardson, D. Wall, S.J. Geromanos, Simultaneous qualitative and quantitative analysis of the Escherichia coli proteome, Mol. Cell. Proteomics 5 (2006) 589–607, http://dx.doi.org/10.1074/mcp.M500321-MCP200.

[37] J.C. Silva, Absolute quantification of proteins by LCMSE: a virtue of parallel ms acquisition, Mol. Cell. Proteomics 5 (2005) 144–156, http://dx.doi.org/10.1074/mcp.M500230-MCP200.

[38] P. de S. Lima, L. Casaletti, A.M. Baila, A.T. Ribeiro, Transcriptional and proteomic responses to carbon starvation in Paracoccidioides, PLoS Negl. Trop. Dis. 8 (2014), http://dx.doi.org/10.1371/journal.pntd.0002855.

[39] M.R. Schenauer, G.C. Flynn, A.M. Goetze, Identification and quantification of host cell protein impurities in biotherapeutics using mass spectrometry, Anal. Biochem. 428 (2012) 150–157, http://dx.doi.org/10.1016/j.ab.2012.05.018.

[40] G.-Z. Li, J.P.C. Vissers, J.C. Silva, D. Golick, M.V. Gorenstein, S.J. Geromanos, Database searching and accounting of multiplexed precursor and product ion spectra from the data independent analysis of simple and complex peptide mixtures, Proteomics 9 (2009) 1696–1719, http://dx.doi.org/10.1002/pmic.200800564.

[41] C.L. Borges, J.A. Parente, M.S. Barbosa, J.M. Santa, S.N. Báo, M.V. de Sousa, C.M. de Almeida Soares, Detection of a homotetrameric structure and proteinprotein interactions of Paracoccidioides brasiliensis formamidase lead to new functional insights, FEMS Yeast Res. 10 (2010) 104–113, http://dx.doi.org/10. 1111/j.1567-1364.2009.00594.x.

[42] B.R. da Silva Neto, J. de Fátima da Silva, M.J.S. Mendes-Giannini, H.L. Lenzi, C.M. de Almeida Soares, M. Pereira, The malate synthase of Paracoccidioides brasiliensis is a linked surface protein that behaves as an anchorless adhesin, BMC Microbiol. 9 (2009) 272, http://dx.doi.org/10.1186/1471-2180-9-272.

[43] A. Gil-Bona, C.M. Parra-Giraldo, M.L. Hernáez, J.A. Reales-Calderon, N.V. Solis, S.G. Filler, L. Monteoliva, C. Gil, Candida albicans cell shaving uncovers new proteins involved in cell wall integrity, yeast to hypha transition, stress response and host-pathogen interaction, J. Proteome 127 (2015) 340–351, http://dx.doi.org/10.1016/j.jprot.2015.06.006.

[44] M.L. Rodrigues, L. Nimrichter, D.L. Oliveira, J.D. Nosanchuk, A. Casadevall, Vesicular trans-cell wall transport in fungi: a mechanism for the delivery of virulence-associated macromolecules, Lipid Insights 2 (2008) 27–40, http://dx.doi.org/10.1038/jid.2014.371.

[45] M.L. Rodrigues, E.S. Nakayasu, D.L. Oliveira, L. Nimrichter, J.D. Nosanchuk, I.C. Almeida, A. Casadevall, Extracellular vesicles produced by Cryptococcus neoformans contain protein components associated with virulence, Eukaryot. Cell 7 (2008) 58–67, http://dx.doi.org/10.1128/EC.00370-07.

[46] P.C. Albuquerque, E.S. Nakayasu, M.L. Rodrigues, S. Frases, A. Casadevall, R.M. Zancope-Oliveira, I.C. Almeida, J.D. Nosanchuk, Vesicular transport in Histoplasma capsulatum: an effective mechanism for trans-cell wall transfer of proteins and lipids in ascomycetes, Cell. Microbiol. 10 (2008) 1695–1710, http:// dx.doi.org/10.1111/j.1462-5822.2008.01160.x.

[47] M.C. Vallejo, E.S. Nakayasu, A.L. Matsuo, T.J.P. Sobreira, L.V.G. Longo, L. Ganiko, I.C. Almeida, R. Puccia, Vesicle and vesicle-free extracellular proteome of Paracoccidioides brasiliensis: comparative analysis with other pathogenic fungi, J. Proteome Res. 11 (2012) 1676–1685, http://dx.doi.org/10.1021/pr200872s.

[48] P. Eroles, M. Sentandreu, M.V. Elorza, R. Sentandreu, The highly immunogenic enolase and Hsp70p are adventitious Candida albicans cell wall proteins, Microbiology 143 (Pt 2) (1997) 313–320, http://dx.doi.org/10.1099/00221287143-2-313.

[49] C.L. Madinger, S.S. Sharma, B.P. Anton, L.G. Fields, M.L. Cushing, J. Canovas, C.H. Taron, J.S. Benner, The effect of carbon source on the secretome of Kluyveromyces lactis, Proteomics 9 (2009) 4744–4754, http://dx.doi.org/10.1002/ pmic.200800915.

[50] A.J. Phillips, I. Sudbery, M. Ramsdale, Apoptosis induced by environmental stresses and amphotericin B in Candida albicans, Proc. Natl. Acad. Sci. U. S. A. 100 (2003) 14327–14332, http://dx.doi.org/10.1073/pnas.2332326100.

[51] F.M. Klis, C.G. de Koster, S. Brul, A mass spectrometric view of the fungal wall proteome, Future Microbiol 6 (2011) 941–951, http://dx.doi.org/10.2217/fmb.11.72.

[52] P.W.J. De Groot, E.A. Kraneveld, Y.Y. Qing, H.L. Dekker, U. Groß, W. Crielaard, C.G. De Koster, O. Bader, F.M. Klis, M. Weig, The cell wall of the human pathogen Candida glabrata: differential incorporation of novel adhesin-like wall proteins, Eukaryot. Cell 7 (2008) 1951–1964, http://dx.doi.org/10.1128/EC.00284-08.

[53] J.D. Bendtsen, L. Kiemer, A. Fausbøll, S. Brunak, Non-classical protein secretion in bacteria, BMC Microbiol. 5 (2005) 58, http://dx.doi.org/10.1186/1471-21805-58.

[54] S.S. Weber, A.F.A. Parente, C.L. Borges, J.A. Parente, A.M. Bailão, C.M. de Almeida Soares, Analysis of the secretomes of Paracoccidioides mycelia and yeast cells, PLoS One 7 (2012), http://dx.doi.org/10.1371/journal.pone.0052470.

[55] L. Nimrichter, M.M. de Souza, M. Del Poeta, J.D. Nosanchuk, L. Joffe, P.D.M. Tavares, M.L. Rodrigues, Extracellular vesicle-associated transitory cell wall components and their impact on the interaction of fungi with host cells, Front. Microbiol. 7 (2016) 1034, http://dx.doi.org/10.3389/fmicb.2016.01034.

[56] A. Pitarch, Sequential fractionation and two-dimensional gel analysis unravels the complexity of the dimorphic fungus Candida albicans cell wall proteome, Mol. Cell. Proteomics 1 (2002) 967–982, http://dx.doi.org/10.1074/mcp.M200062MCP200.

[57] S.A. Tunio, N.J. Oldfield, D.A.A. Ala'Aldeen, K.G. Wooldridge, D.P.J. Turner, The role of glyceraldehyde 3-phosphate dehydrogenase (GapA-1) in Neisseria meningitidis adherence to human cells, BMC Microbiol. 10 (2010) 280, http://dx.doi.org/10.1186/1471-2180-10-280.

[58] E.G.A. Chaves, S.S. Weber, S.N. Báo, L.A. Pereira, A.M. Bailão, C.L. Borges, C.M. de A. Soares, Analysis of Paracoccidioides secreted proteins reveals fructose 1,6-bisphosphate aldolase as a plasminogen-binding protein, BMC Microbiol. 15 (2015) 53, http://dx.doi.org/10.1186/s12866-015-0393-9.

[59] J.D. Crowe, I.K. Sievwright, G.C. Auld, N.R. Moore, N.A.R. Gow, N.A. Booth, Candida albicans binds human plasminogen: identification of eight plasminogenbinding proteins, Mol. Microbiol. 47 (2003) 1637–1651, http://dx.doi.org/10.1046/j.1365-2958.2003.03390.x.

[60] S.A. Tunio, N.J. Oldfield, A. Berry, D.A.A. Ala'Aldeen, K.G. Wooldridge, D.P.J. Turner, The moonlighting protein fructose-1, 6-bisphosphate aldolase of Neisseria meningitidis: surface localization and role in host cell adhesion, Mol. Microbiol. 76 (2010) 605–615, http://dx.doi.org/10.1111/j.1365-2958.2010. 07098.x.

[61] C. Nombela, C. Gil, W.L. Chaffin, Non-conventional protein secretion in yeast, Trends Microbiol. 14 (2006) 15–21, http://dx.doi.org/10.1016/j.tim.2005.11. 009.

[62] M. Angela, D.M. Marques, S. Mahapatra, D. Nandan, T. Dick, E. Nunes, P. Joseph, M. Cristina, V. Pessolani, Bacterial and host-derived cationic proteins bind α 2laminins and enhance Mycobacterium leprae attachment to human Schwann cells, Microbes Infect. (2000) 1407–1417, http://dx.doi.org/10.1016/S1286-4579(00) 01294-6.

[63] V. Maneu, A.M. Cervera, J.P. Martínez, D. Gozalbo, Molecular cloning and characterization of a Candida albicans gene (EFB1) coding for the elongation factor EF-1 beta, FEMS Microbiol. Lett. 145 (1996) 157–162 http://www.ncbi.nlm.nih.gov/pubmed/8961551.

[64] V.K. Singh, R.K. Jayaswal, B.J. Wilkinson, Cell wall-active antibiotic induced proteins of Staphylococcus aureus identified using a proteomic approach, FEMS Microbiol. Lett. 199 (2001) 79–84 http://www.ncbi.nlm.nih.gov/pubmed/ 11356571.

[65] J. Zhu, B. Damsz, A.K. Kononowicz, R.A. Bressan, P.M. Hasegawaai, A higher plant extracellular vitronectin-like adhesion s related to the translational elongation factor-I a protein 1, Plant Cell 6 (1994) 393–404, http://dx.doi.org/10.1105/tpc.6.3.393.

[66] J.M. Silverman, J. Clos, E. Horakova, A.Y. Wang, M. Wiesgigl, I. Kelly, A. Lynn, W.R. Mcmaster, L.J. Foster, K. Megan, N.E. Reiner, Leishmania exosomes modulate innate and adaptive immune responses through effects on monocytes and dendritic cells, J. Immunol. 185 (2010) 5011–5022, http://dx.doi.org/10.4049/ jimmunol.1000541.

[67] J.M. Silverman, N.E. Reiner, Leishmania exosomes deliver preemptive strikes to create an environment permissive for early infection, Front. Cell. Infect. Microbiol. 1 (2012) 1–8, http://dx.doi.org/10.3389/fcimb.2011.00026.

[68] J.D. Nosanchuk, J.N. Steenbergen, L. Shi, G.S. Deepe, A. Casadevall, Antibodies to a cell surface histone-like protein protect against Histoplasma capsulatum, J. Clin. Invest. 112 (2003) 1164–1175, http://dx.doi.org/10.1172/JCI200319361.

[69] D. de Arruda Grossklaus, A.M. Bailão, T.C. Vieira Rezende, C.L. Borges, M.A.P. de Oliveira, J.A. Parente, C.M. de Almeida Soares, Response to oxidative stress in Paracoccidioides yeast cells as determined by proteomic analysis, Microbes Infect. 15 (2013) 347–364, http://dx.doi.org/10.1016/j.micinf.2012.12.002.

[70] A.F.A. Parente, P.E.C. Naves, L.L. Pigosso, L. Casaletti, J.G. McEwen, J.A. Parente-Rocha, C.M.A. Soares, The response of Paracoccidioides spp. to nitrosative stress, Microbes Infect. 17 (2015) 575–585, http://dx.doi.org/10.1016/j.micinf.2015.03. 012.

[71] J.A. Parente-Rocha, A.F.A. Parente, L.C. Baeza, S.M.R.C. Bonfim, O. Hernandez, J.G. McEwen, A.M. Bailão, C.P. Taborda, C.L. Borges, C.M. De Almeida Soares, Macrophage interaction with Paracoccidioides brasiliensis yeast cells modulates fungal metabolism and generates a response to oxidative stress, PLoS One 10 (2015) 1–18, http://dx.doi.org/10.1371/journal.pone.0137619.

[72] W.L. Batista, A.L. Matsuo, L. Ganiko, T.F. Barros, T.R. Veiga, E. Freymüller, R. Puccia, The PbMDJ1 gene belongs to a conserved MDJ1/LON locus in thermodimorphic pathogenic fungi and encodes a heat shock protein that localizes to both the mitochondria and cell wall of Paracoccidioides brasiliensis, Eukaryot. Cell 5 (2006) 379–390, http://dx.doi.org/10.1128/EC.5.2.379-390.2006.

[73] R. Matthews, C. Wells, J.P. Burnie, Characterisation and cellular localisation of the immunodominant 47-Kda antigen of Candida albicans, J. Med. Microbiol. 27 (1988) 227–232.

[74] J.L. López-Ribot, H.M. Alloush, B.J. Masten, W.L. Chaffin, Evidence for presence in the cell wall of Candida albicans of a protein related to the hsp70 family, Infect. Immun. 64 (1996) 3333–3340 http://www.ncbi.nlm.nih.gov/pubmed/8757872.

[75] F. Lamoth, P.R. Juvvadi, J.R. Fortwendel, W.J. Steinbach, Heat shock protein 90 is required for conidiation and cell wall integrity in Aspergillus fumigatus, Eukaryot. Cell 11 (2012) 1324–1332, http://dx.doi.org/10.1128/EC.00032-12.

[76] R. Martinez-Lopez, L. Monteoliva, R. Diez-Orejas, C. Nombela, C. Gil, The GPIanchored protein CaEcm33p is required for cell wall integrity, morphogenesis and virulence in Candida albicans, Microbiology 150 (2004) 3341–3354, http://dx.doi.org/10.1099/mic.0.27320-0.

[77] R. Martinez-Lopez, H. Park, C.L. Myers, C. Gil, S.G. Filler, Candida albicans Ecm33p is important for normal cell wall architecture and interactions with host cells, Eukaryot. Cell 5 (2006) 140–147, http://dx.doi.org/10.1128/EC.5.1.140-147. 2006.

[78] N. de León, M.R. Sharifmoghadam, M. Hoya, M.-Á. Curto, C. Doncel, M.H. Valdivieso, Regulation of cell wall synthesis by the clathrin light chain is essential for viability in

Schizosaccharomyces pombe, PLoS One 8 (2013) e71510, , http://dx.doi.org/10.1371/journal.pone.0071510.

[79] A.T. Large, M.D. Goldberg, P. a Lund, Chaperones and protein folding in the archaea, Biochem. Soc. Trans. 37 (2009) 46–51, http://dx.doi.org/10.1042/ BST0370046.

[80] a Muga, F. Moro, Thermal adaptation of heat shock proteins, Curr. Protein Pept. Sci. 9 (2008) 552–566, http://dx.doi.org/10.2174/138920308786733903.

[81] V.K. Singh, M. Syring, A. Singh, K. Singhal, A. Dalecki, T. Johansson, An insight into the significance of the DnaK heat shock system in Staphylococcus aureus, Int. J. Med. Microbiol. 302 (2012) 242–252, http://dx.doi.org/10.1016/j.ijmm.2012.05. 001.

[82] T.B.M. Hickey, L.M. Thorson, D.P. Speert, M. Daffé, R.W. Stokes, Mycobacterium tuberculosis Cpn60.2 and DnaK are located on the bacterial surface, where Cpn60.2 facilitates efficient bacterial association with macrophages, Infect. Immun. 77 (2009) 3389–3401, http://dx.doi.org/10.1128/IAI.00143-09.

[83] G. Pardini, P.W.J. De Groot, A.T. Coste, M. Karababa, F.M. Klis, C.G. de Koster, D. Sanglard, The CRH family coding for cell wall glycosylphosphatidylinositol proteins with a predicted transglycosidase domain affects cell wall organization and virulence of Candida albicans, J. Biol. Chem. 281 (2006) 40399–40411, http://dx.doi.org/10.1074/jbc.M606361200.

[84] E. Cabib, Two novel techniques for determination of polysaccharide cross-links show that Crh1p and Crh2p attach chitin to both beta(1-6)- and beta(1-3)glucan in the Saccharomyces cerevisiae cell wall, Eukaryot. Cell 8 (2009) 1626–1636, http://dx.doi.org/10.1128/EC.00228-09.

[85] E. Cabib, N. Blanco, C. Grau, J.M. Rodríguez-Peña, J. Arroyo, Crh1p and Crh2p are required for the cross-linking of chitin to beta(1-6)glucan in the Saccharomyces cerevisiae cell wall, Mol. Microbiol. 63 (2007) 921–935, http://dx.doi.org/10.1111/j.1365-2958.2006.05565.x.

[86] E. Cabib, V. Farkas, O. Kosík, N. Blanco, J. Arroyo, P. McPhie, Assembly of the yeast cell wall: Crh1p and Crh2p act as transglycosylases in vivo and in vitro, J. Biol. Chem. 283 (2008) 29859–29872, http://dx.doi.org/10.1074/jbc.M804274200.

[87] M. Mazáň, N. Blanco, K. Kováčová, Z. Firáková, P. Rehulka, V. Farkaš, J. Arroyo, A novel fluorescence assay and catalytic properties of Crh1 and Crh2 yeast cell wall transglycosylases, Biochem. J. 455 (2013) 307–318, http://dx.doi.org/10.1042/BJ20130354.

[88] C. Alberti-Segui, A.J. Morales, H. Xing, M.M. Kessler, D.A. Willins, K.G. Weinstock, G. Cottarel, K. Fechtel, B. Rogers, Identification of potential cell-surface proteins in Candida albicans and investigation of the role of a putative cell-surface glycosidase in adhesion and virulence, Yeast 21 (2004) 285–302, http://dx.doi.org/10.1002/yea.1061.

[89] E. Conibear, Vps51p mediates the association of the GARP (Vps52/53/54) complex with the late Golgi t-SNARE Tlg1p, Mol. Biol. Cell 14 (2003) 1610–1623, http://dx.doi.org/10.1091/mbc.E02-10-0654.

[90] J.H. Stack, Vesicle-mediated protein transport: regulatory interactions between the Vps15 protein kinase and the Vps34 PtdIns 3-kinase essential for protein sorting to the vacuole in yeast, J. Cell Biol. 129 (1995) 321–334, http://dx.doi.org/10.1083/jcb.129.2.321.

[91] Y. Liu, N.V. Solis, C.J. Heilmann, Q.T. Phan, A.P. Mitchell, F.M. Klis, S.G. Filler, Role of retrograde trafficking in stress response, host cell interactions, and virulence of Candida albicans, Eukaryot. Cell 13 (2014) 279–287, http://dx.doi.org/10.1128/EC.00295-13.

[92] J.M. Rodriguez-Peña, C. Rodriguez, A. Alvarez, C. Nombela, J. Arroyo, Mechanisms for targeting of the Saccharomyces cerevisiae GPI-anchored cell wall protein Crh2p to polarised growth sites, J. Cell Sci. 115 (2002) 2549–2558 http://www.ncbi.nlm.nih.gov/pubmed/12045225.

[93] R. Hurtado-Guerrero, A.W. Schüttelkopf, I. Mouyna, A.F.M. Ibrahim, S. Shepherd, T. Fontaine, J.P. Latgé, D.M.F. van Aalten, Molecular mechanisms of yeast cell wall glucan remodeling, J. Biol. Chem. 284 (2009) 8461–8469, http://dx.doi.org/10.1074/jbc.M807990200.

[94] I. Mouyna, T. Fontaine, M. Vai, M. Monod, W. a Fonzi, M. Diaquin, L. Popolo, R.P. Hartland, J. Latge, Play an active role in the biosynthesis of the fungal cell wall *, Biochemistry 275 (2000) 14882–14889.

[95] A. Maddi, C. Fu, S.J. Free, The Neurospora crassa dfg5 and dcw1 genes encode α1,6-mannanases that function in the incorporation of glycoproteins into the cell wall, PLoS One 7 (2012) e38872, , http://dx.doi.org/10.1371/journal.pone. 0038872.

[96] E. Spreghini, D.A. Davis, R. Subaran, M. Kim, A.P. Mitchell, Roles of Candida albicans Dfg5p and Dcw1p cell surface proteins in growth and hypha formation, Eukaryot. Cell 2 (2003) 746–755, http://dx.doi.org/10.1128/EC.2.4.746-755. 2003.

[97] N. da Silva Castro, M.S. Barbosa, Z.A. Maia, S.N. Báo, M.S.S. Felipe, J.M. Santana, M.J. Soares Mendes-Giannini, M. Pereira, C.M. de Almeida Soares, Characterization of Paracoccidioides brasiliensis PbDfg5p, a cell-wall protein implicated in filamentous growth, Yeast 25 (2008) 141–154, http://dx.doi.org/10. 1002/yea.1574.

[98] Q.Y. Yin, P.W.J. De Groot, H.L. Dekker, L. De Jong, F.M. Klis, C.G. De Koster, Comprehensive proteomic analysis of Saccharomyces cerevisiae cell walls: Identification of proteins covalently attached via glycosylphosphatidylinositol remnants or mild alkali-sensitive linkages, J. Biol. Chem. 280 (2005) 20894–20901, http://dx.doi.org/10.1074/jbc.M500334200.

[99] K. Steczkiewicz, L. Knizewski, L. Rychlewski, K. Ginalski, TOS1 is circularly permuted 1,3-beta-glucanase, Cell Cycle 9 (2010) 201–204, http://dx.doi.org/10.4161/cc.9.1.10510.

[100] F.M. Klis, S. Brul, Adaptations of the secretome of Candida albicans in response to host-related environmental conditions, Eukaryot. Cell 14 (2015) EC.00142-15 http://dx.doi.org/10.1128/EC.00142-15.

[101] C.J. Heilmann, A.G. Sorgo, S. Mohammadi, G.J. Sosinska, C.G. de Koster, S. Brul, L.J. de Koning, F.M. Klis, Surface stress induces a conserved cell wall stress response in the pathogenic fungus Candida albicans, Eukaryot. Cell 12 (2013) 254–264, http://dx.doi.org/10.1128/EC.00278-12.

[102] S. Selvaggini, C.A. Munro, S. Paschoud, D. Sanglard, N.A.R. Gow, Independent regulation of chitin synthase and chitinase activity in Candida albicans and Saccharomyces cerevisiae, Microbiology 150 (2004) 921–928, http://dx.doi.org/10.1099/mic.0.26661-0.